ЖУРНАЛ
ПРИКЛАДНОЙ ХИМИИ

Volume 31 No. 11

November 1958

JOURNAL OF
APPLIED CHEMISTRY
OF THE USSR

(ZHURNAL PRIKLADNOI KHIMII)

IN ENGLISH TRANSLATION

CONSULTANTS BUREAU, INC.

Volume 31 No. 11

November 1958

JOURNAL OF
APPLIED CHEMISTRY
OF THE USSR

(ZHURNAL PRIKLADNOI KHIMY)

A publication of the Academy of Sciences of the USSR

IN ENGLISH TRANSLATION

Year and issue of first translation:
Vol. 23, No. 1 January 1950

	U. S. and Canada	*Foreign*
Annual subscription	*$60.00*	*$65.00*
Annual subscription for libraries of non-profit academic institutions	*20.00*	*25.00*
Single issue	*7.50*	*7.50*

Copyright 1959

CONSULTANTS BUREAU, INC.
227 W. 17th St., NEW YORK 11, N.Y.

Editorial Board
(ZHURNAL PRIKLADNOI KHIMII)

P. B. Budnikov, S. I. Vol'fkovich, A. F. Dobrianskii,
O. E. Zviagintsev, N. I. Nikitin (Editor in Chief),
G. V. Pigulevskii, M. E. Pozin, L. K. Simonova
(Secretary), S. N. Ushakov, N. P. Fedot'ev

Note: The sale of photostatic copies of any portion of this copyright translation is expressly prohibited by the copyright owners.

Printed in the United States of America

JOURNAL OF APPLIED CHEMISTRY OF THE USSR

Volume 31, Number 11 November 1958

CONTENTS

	PAGE	RUSS. PAGE
Chemical "Aging" of Precipitated Basic Nickel Carbonate, and the Mechanism of Sodium Carbonate Utilization in the Precipitation Process. I. M. Vasserman and Kh. Z. Brainina	1605	1617
Investigation of the Rate of Absorption of Hydrogen Sulfide by Arsenical Soda Solutions. M. I. Gerber, V. P. Teodorovich, and A. D. Shusharina	1612	1624
Influence of Various Factors on the Structure of Surface Films on Silicate Glasses. L. S. Iastrebova and V. S. Molchanov	1615	1628
Applications of the Theory of Similarity to Certain Processes in Chemical Technology. S. Bretsznajder	1623	1636
Kinetics of Heat and Mass Transfer in a Foam Layer. I. P. Mukhlenov and E. S. Tumarkina.	1635	1647
Laboratory Column for Microfractionation. A. I. Levin	1643	1655
Investigation of Bright Nickel-Plating Baths. T. A. Mechkovskaia	1649	1661
Influence of Chloride-Ion Admixtures on the Deposition of Copper by Periodically-Reversed Current. V. V. Ostroumov and I. F. Plotnikova	1655	1668
Mechanism of Alkaline Surface Oxidation of Steel. A. V. Shreider and A. G. Arakelov	1660	1673
Kinetics of the Gas-Phase Corrosion of EI-437B Alloy in Air and in Nitrogen – Hydrogen Mixture. I. A. Makolkin, N. P. Petrov, and V. F. Faiman.	1665	1678
Synthesis of Copolymers of Vinyl Acetate with Crotonic Acid and its Derivatives. S. N. Ushakov and E. M. Lavrent'eva.	1673	1686
Sulfonic Ion-Exchange Resins Based on Polystyrene and Formaldehyde. A. A. Vasil'ev and A. A. Vansheidt	1678	1692
Study of the Chemical Structure of SKB Sodium Divinyl Rubber (Made by the Rod Process). A. I. Iakubchik, S. K. Zykova, and S. P. Goncharuk	1683	1697
Component Ratio in the Synthesis of Vinyl Acetate by Heterogeneous Catalysis. I. A. Arbuzova, S. N. Ushakov, and E. N. Rostovskii	1691	1704
Herbicides from Phenols in Tar Obtained by Pyrolysis of Wood. V. Kovalev and D. Tishchenko	1695	1708
Hydrofluorination of Vinylacetylene with a Suspended Catalyst. I. I. Dolgopol'skii, I. M. Dobromil'skaia, and B. A. Byzov.	1702	1716
Influence of Used Catalyst on the Acidity Increase of Hydrogenated Fat. V. P. Golendeev, K. G. Bogareva, E. I. Bobkova, and O. N. Dobrynina	1708	1722

CONTENTS (continued)

	PAGE	RUSS. PAGE
Upgrading of Straight-Run Gasolines by Low-Temperature Dehydrogenation Over Platinized Carbon. N. I. Shuikin, Kh. M. Minachev, S. S. Novikov, N. F. Kononov, and I. L. Garanin.	1717	1732
Brief Communications		
A New Cooling Brine for Condensation of Nitrogen Oxides from Nitrous Gases. M. A. Miniovich, A. L. Shneerson, and V. A. Klevke	1724	1739
Aluminate – Borate Anomaly of the Optical Properties of Silicate Glasses. E. I. Galant and A. A. Appen.	1727	1741
Influence of Frit Crystallization on the Properties of Ground-Coat Enamel. G. N. Beliaev and N. F. Smakota.	1730	1744
Investigation of the Reaction Products of Certain Organosilicon Compounds with Aqueous Alkaline Solutions of Aluminates, Stannates, and Plumbites by Means of Infrared Absorption Spectroscopy. A. P. Kreshkov, Iu. Ia. Mikhailenko, L. V. Myshliaeva, and L. M. Khananashvili.	1733	1746
Electrical Conductivity of the System NaOH – Na_2CO_3 – NaCl. A. F. Alabyshev, M. F. Lantratov, and L. I. Sokolova	1737	1749
Electrochemical Polishing of Zinc in Sulfuric Acid. G. P. Maitak	1741	1752
Electrolysis with a Mercury Cathode Flowing Over a Vertical Metallic Surface. G. I. Volkov and E. I. Kus'kina	1744	1755
Preparation of Ethylene Glycol Diacetate in Presence of Cation-Exchange Resins. N. S. Rabovskaia and V. N. Kucherovskaia	1747	1757
Binary Compounds of Glucose with Mineral Salts. V. I. Sharkov and V. Guzhavina	1749	1759
Thermooxidative Decomposition of Benzylcellulose. O. P. Koz'mina and V. I. Kurliankina	1752	1761
Study of the Composition of the Turpentine and the Properties of Rosin from the Oleoresin of the Sudak Pine (Pinus Pithyusa Var. Stankewiczii Suk., Pinus Stankewiczii Fom.) I. I. Bardyshev and L. V. Roman	1754	1762
Preparation of Toluene Concentrates from Petroleum Fractions by Low-Temperature Dehydrogenation Over Platinized Carbon. N. I. Shuikin, Kh. M. Minachev, I. L. Garanin, S. S. Novikov, and N. F. Kononov	1757	1765
"High Polymers" – a New Journal of the Academy of Sciences, USSR	1760	1768

CHEMICAL "AGING" OF PRECIPITATED BASIC NICKEL CARBONATE, AND THE MECHANISM OF SODIUM CARBONATE UTILIZATION IN THE PRECIPITATION PROCESS*

I. M. Vasserman and Kh. Z. Brainina

The formation of sparingly soluble salts by double decomposition of aqueous solutions of two salts, of the general type

$$MeA + Me_1A_1 \rightarrow MeA_1 + Me_1A,$$

where Me_1A is the precipitate, involving ions common with the precipitate and also other ions, is of considerable practical interest. Studies of such reactions are also of interest from the theoretical standpoint.

A particular case of the formation of sparingly soluble salts is the precipitation of carbonates, with the use of sodium carbonate as the practical precipitant. The salts formed may be neutral or basic, depending on the precipitated cation. Unfortunately, no attention is being devoted in chemical technology to the development of a theory and practical studies of separation of substances from solutions by chemical precipitation. This is shown by the fact that instructional courses do not deal with processes and equipment used for chemical precipitation, although this type of process is very common inchemical technology. Not enough attention is being devoted to the theory of precipitation processes by chemists, either [1-8].

The present paper deals with the mechanism of sodium carbonate utilization in the formation of a basic salt, and the chemical "aging" of the precipitate during precipitation and in contact with the mother liquor. The experimental work consisted of a physicochemical study of the formation of basic nickel carbonate, the purpose being to develop a method for automatic regulation of the industrial process.

EXPERIMENTAL

Basic nickel carbonate was prepared by the interaction of nickel nitrate and sodium carbonate solutions. The precipitation was carried out by the usual heterogeneous** method. The sodim carbonate solution being added to the nickel nitrate solution. The course of precipitation was studied by potentiometric titration at 60, 87, and 89° in a TS-15M thermostat, for different durations of the process (20, 60, and 180 minutes). The pH variations of the medium were recorded by means of a system consisting of an antimony and a saturated calomel electrode immersed in the solution. The e. m. f. was measured by the compensation method with the aid of the PPTV-1 potentiometer and the M-21 mirror galvanometer. The CO_2 liberated during the reaction was absorbed in tubes packed with askarit and calcium chloride. Air free from CO_2 was drawn through the whole system during the experiment by means of an aspirator. For elucidation of the mechanism of sodium carbonate utilization, the liquid phase of the system $Ni(NO_3)_2 - Na_2CO_3 - H_2O$ was studied. For this, the mother liquors obtained in the experiments were titrated potentiometrically with hydrochloric acid at 20°. The pH was measured by means of the LLPU-1 electronic potentiometer designed by the Ural Chemical Scientific Research Institute, with the aid of a glass and a saturated calomel electrode.

Solutions of $Ni(NO_3)_2$ and Na_2CO_3 were prepared from exactly-weighed samples of the salts. In addition,

*Communication I in the series on the technology of separation of substances from solution by chemical precipitation.

**Translation of Russian – Publisher's note.

TABLE 1

Potentiometeric Titration of the Mother Liquors from Basic Nickel Carbonate Prepared Under Different Conditions

Experiment No.	$Ni(NO_3)_2$ (meq)	Added (meq)		Ratio of meq of Na_2CO_3 to meq of $Ni(NO_3)_2$	Found (meq)		$NaHCO_3$ formed during the reaction (meq)	Degree of carbonate utilization (%)	Basicity of precipitate*	Temperature (°C)	pH at 20°	Duration of precipitation (minutes)
		Na_2CO_3	$NaHCO_3$		Na_2CO_3	$NaHCO_3$						
1	10.0	4.75	0.79	0.55	0.0	1.99	1.2	64.2	—	60	7.65	—
2	10.0	10.23	1.70	1.19	0.0	4.12	2.42	65.3	—	60	8.09	—
3	10.0	10.75	1.79	1.25	0.0	4.57	2.78	64.5	—	60	8.05	—
4	10.0	13.0	2.16	1.52	0.0	6.07	3.91	60.0	—	60	8.43	—
5	10.0	14.75	0.79	0.55	0.0	0.61	—0.1	87.5	—	87	7.7	—
6	10.0	10.23	1.70	1.19	0.0	1.13	—0.56	91.0	—	87	8.0	—
7	10.0	13.0	2.16	1.52	0.0	5.54	3.38	—	—	87	9.2	—
8	10.0	10.0	0.0	1.0	0.0	2.56	2.56	74.4	0.3	89	7.7	—
9	5.0	6.81	0.0	1.36	0.4	1.3	1.3	76.0	0.2	89	9.05	145
10	10.0	14.2	0.0	1.42	0.0	4.3	4.3	68.0	0.4	89	8.05	—
11	5.0	7.55	0.0	1.51	0.0	2.64	2.64	65.0	0.5	89	8.85	25
12	5.0	8.35	0.0	1.67	1.12	2.0	2.0	63.0	0.4	89	9.5	120
13	5.0	8.35	0.0	1.67	0.56	2.97	2.97	58.0	0.6	89	9.3	20
14	5.0	8.35	0.0	1.67	0.87	2.66	2.66	57.5	0.5	89	9.3	60
15	5.0	8.35	0.0	1.67	7.8	0.87	0.87	55.0	0.2	89	>10	180
16	5.0	9.86	0.0	1.97	0.9	4.0	4.0	51.0	0.8	89	9.5	rapid

* The basicity of the precipitate is the ratio of the number of equivalents of OH to the number of equivalents of Ni^{2+} in the precipitate (in the present instance it is the ratio of the number of equivalents of $NaHCO_3$ formed to the number of equivalents of Ni^{2+} with complete precipitation of Ni^{2+}).

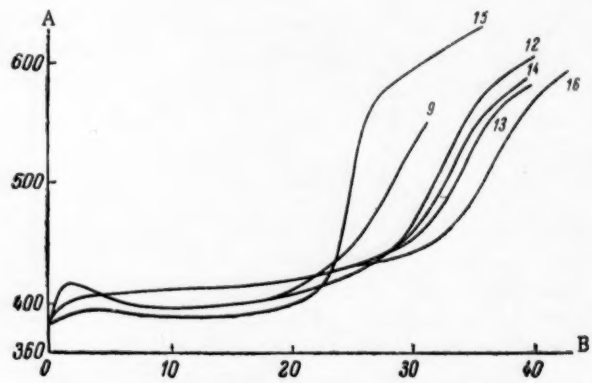

Fig. 1. Potentiometric titration of $Ni(NO_3)_2$ solution by sodium carbonate. 0.209 N $NaCO_3$ solution, temperature 89°.
A) Potential of the antimony electrode (mv), B) amount of Na_2CO_3 (ml). The numbers of the curves correspond to the experiment numbers.

the Na_2CO_3 solution was titrated potentiometrically in order to determine the presence of any $NaHCO_3$ present as an impurity.

In each experiment 25 ml of 0.1 M $Ni(NO_3)_2$ solution and 400 ml of water, or 50 ml of the $Ni(NO_3)_2$ solution

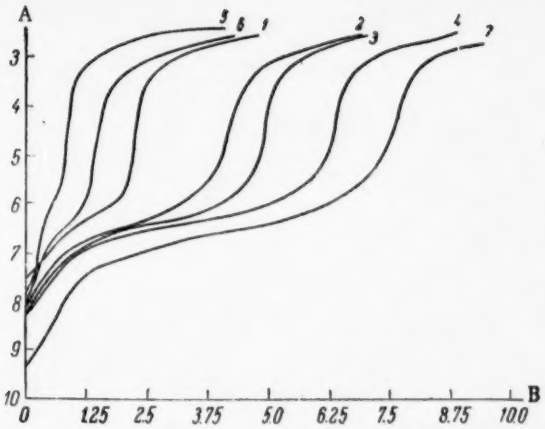

Fig. 2. Potentiometric titration of mother liquors from basic nickel carbonate by 0.1 N hydrochloric acid, K = 1.1002.
A) pH, B) amount of HCl (ml). The numbers of the curves correspond to the experiment numbers.

and 800 ml of water, was put into reaction vessel, and after the system had reached the required temperature sodium carbonate was added gradually from a buret. Samples of the precipitates formed during the experiments were analyzed as necessary. The results of the experiments are given in Table 1 and Figs. 1-5.

The curves in Fig. 1 represent the potential of the antimony electrode (which is a measure of the pH) as a function of the amount of sodium carbonate added; it is seen that after the initial ascent of the curves to the potential (pH of the medium) at which precipitation begins, there is an extensive buffer region in which basic nickel salts are precipitated. The curves begin to ascend only when sodium carbonate is added in excess over the stoichiometric quantity; the ascent begins with different amounts of added carbonate, and the curves differ in slope, according to the duration of the experiment. These results show that not all the sodium carbonate consumed is utilized for precipitation. This is not because an excess of sodium carbonate must be present in solution in order to create the required pH. The course of Curves 1, 2, 3, 4, 5, 6, and 7 (Fig. 2) and 8, 10, and 11 (Fig. 3) indicates that the mother liquors formed during precipitation at 60° contain definite amounts of unutilized soda in the form of sodium bicarbonate. Sodium bicarbonate is formed by hydrolysis of the carbonate in solution

$$Na_2CO_3 + H_2O \rightleftharpoons NaOH + NaHCO_3.$$

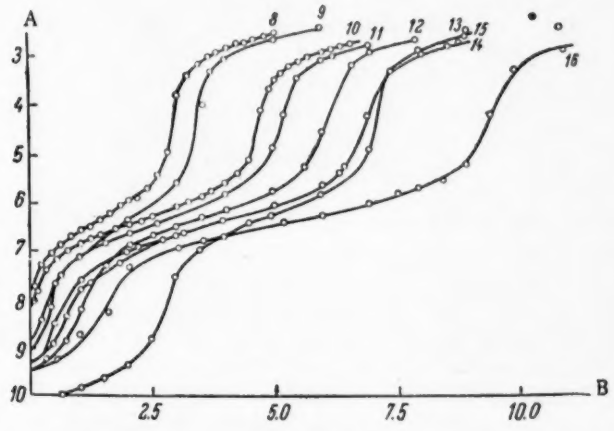

Fig. 3. Potentiometric titration of mother liquors from basic nickel carbonate by 0.1 N hydrochloric acid, K = 1.1002.
A) pH, B) amount of HCl (ml). The numbers on the curves correspond to the experiment numbers.

The low degree of utilization of the sodium carbonate, about 65% at 60°, is due to accumulation of sodium bicarbonate in the mother liquors. If the precipitation is carried out at higher temperatures (~90°), the potentiometric titration curves of the mother liquors show two regions in which the potential of the glass electrode increases corresponding to the reactions:

$$Na_2CO_3 + HCl \rightarrow NaHCO_3 + NaCl,$$
$$NaHCO_3 + HCl \rightarrow NaCl + H_2O + CO_2.$$

Sodium carbonate appears in the mother liquors together with sodium bicarbonate, probably as the result of secondary reactions in the system.

At higher temperatures the useful conversion of sodium carbonate increases to 91% under the same conditions. The results (Fig. 3; compare Experiments 13 and 14, and 12 and 16 in Table 1) show that useful conversion of sodium carbonate also depends on the duration of the precipitation process, and is associated with decrease of the sodium bicarbonate content of the mother liquors with increase of the precipitation time (Fig. 4), and the corresponding increase of the carbonate content. Variations of the composition of the mother liquor must be correlated with possible secondary chemical reactions in the system mother liquor – precipitate, between the basic salt in the precipitate and the acid salt $NaHCO_3$ in the mother liquor. The following experiment was carried out to clarify this point. Into a reaction flask containing sodium bicarbonate solution at 60° there was put a precipitate of basic nickel carbonate previously made by rapid precipitation (Table 2) and the flask was kept in a thermostat for 3 hours (Table 3).

The results of this experiment show that the basicity of the precipitate fell from 0.54 to 0.24 as the result of

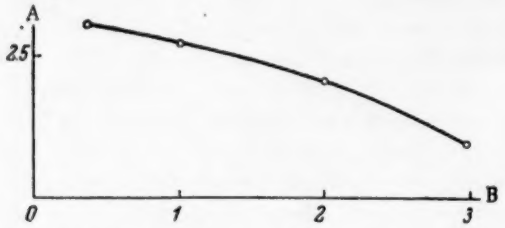

Fig. 4. Effect of the precipitation time on the amount of bicarbonate ions in the mother liquor, at constant temperature and with the same amount of utilized sodium carbonate.
A) Amount of $NaHCO_3$ (meq), B) time (hours).

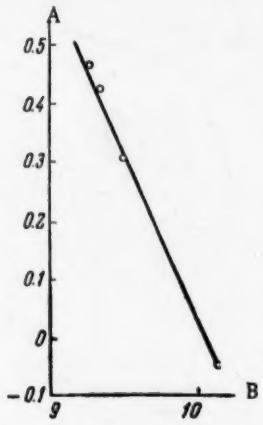

Fig. 5. Variation of the salt basicity with solution pH at constant sodium carbonate consumption.
A) log α, B) pH.

TABLE 2

Conditions for the Formation of the Original Precipitate

Taken for experiment (meq)		Found after experiment (meq)		Temperature (°C)	Duration of experiment (minutes)	pH at 20°	Basicity of the precipitate OH^- equiv/ Ni^{2+} equiv
$Ni(NO_3)_2$	Na_2CO_3	Na_2CO_3	$NaHCO_3$				
5.0	7.55	0.00	2.64	89	20	8.85	0.53

TABLE 3

Reaction Between Precipitate and Solution

Original $NaHCO_3$ content of solution (meq)	Found in solution after experiment (meq)		Amount of of CO_2 evolved	Temperature (°C)	Basicity of the precipitate OH^- equiv/ Ni^{2+} equiv
	Na_2CO_3	$NaHCO_3$			
5.0	1.2	3.8	0.0	60	0.24

a chemical reaction between the basic salt (basic nickel carbonate) and the acid salt ($NaHCO_3$); the composition of the solution changed accordingly.

DISCUSSION OF RESULTS

It follows from the experimental results that the interaction of solutions of a nickel salt (such as the nitrate) and sodium carbonate is complex in character, and consists of the following principal processes.

Primary formation of a precipitate. As the result of hydrolysis

$$Na_2CO_3 + H_2O \rightleftharpoons NaOH + NaHCO_3 \qquad (1)$$

a sodium carbonate solution simultaneously contains CO_3^{2-}, HCO_3^-, OH^- ions, which may form $Ni(OH)_2$, $NiCO_3$ by reaction with a soluble nickel salt. Comparison of the solubility products of $Ni(OH)_2$ and $NiCO_3$ (at 25° shows that the basic salt should be precipitated. This reaction occurs homogeneously in solution at a high rate:

$$\begin{aligned}&(a + b)Ni(NO_3)_2 + bNa_2CO_3 + 2aNaOH \rightarrow \\ &\rightarrow aNi(OH)_2 \cdot bNiCO_3 + 2(a + b)NaNO_3.\end{aligned} \qquad (2)$$

The sodium bicarbonate formed by hydrolysis of the sodium carbonate does not take part in the precipitation, and accumulates in the mother liquor.

At constant pH and temperature the basicity of the freshly formed precipitate depends on the amount of sodium carbonate introduced. If CO_2 is not liberated (if $NaHCO_3$ is not decomposed), the number of equivalents of bicarbonate present in solution is equal to the number of equivalents of alkali bound in the precipitate.

The aim in industry is to obtain precipitates with the best properties and structure by carrying out precipitation under optimum conditions.

With this object in view, various methods are often used to lower the high rate of separation of a substance from a homogeneous solution. For example, the concentrations of the reacting substances is lowered by the use of dilute solutions (which is disadvantageous in practice), or a solution of the precipitant is added gradually in small amounts to the other substance, or both solutions are poured gradually and simultaneously with stirring into a small volume of water or electrolyte solution, etc. In the last two cases the forming precipitate is in contact with the mother liquor for some time during the precipitation.

Interaction of the precipitate with the mother liquor. It is known [9] that a freshly-formed precipitate in contact with the mother liquor undergoes a process, known as "aging," in which its physical properties change. As a rule the total particle surface decreases, the crystal form becomes more perfrect, and adsorption of impurities from the solution by the precipitate decreases. This process may be described as physical "aging" of the precipitate. Because of the favorable effects of the "aging" process, it is often used in practice to improve the properties of precipitates. The precipitate is left for some time after its formation in contact with the mother liquor for this purpose.

In the process under investigation, in which solutions of two salts react by double decomposition to form a sparingly soluble basic carbonate, the system precipitate – mother liquor is formed, in which the constituent salts differ in chemical character; the precipitate contains a basic salt (basic nickel carbonate), while the solution contains an acid salt (sodium bicarbonate). Therefore conditions exist in the system for the occurrence of the chemical reaction

$$aNi(OH)_2 \cdot bNiCO_3 + 2xNaHCO_3 \rightarrow (a - x)Ni(OH)_2 \cdot (b + x)NiCO_3 + xNa_2CO_3 + 2xH_2O. \qquad (3)$$

Irrespectively of the course of this reaction, at higher temperatures (> 70°) some of the bicarbonate undergoes thermal decomposition

$$2NaHCO_3 \rightarrow Na_2CO_3 + CO_2 + H_2O \qquad (4)$$

with evolution of bubbles of carbon dioxide.

As the result of Reaction (3) the composition of the precipitate changes, it becomes less basic and approaches to the composition of a neutral salt, while the reacting bicarbonate is replaced by an equivalent amount of carbonate in the solution; as a result, the pH of the solution changes (increases).

In fact, the precipitates formed in our experiments were metastable and changed not only in physical properties but also in chemical composition in the course of precipitation.

Consequently, if a precipitate of basic carbonate is in contact for some time with the mother liquor, either during precipitation by sodium carbonate or after precipitation, the chemical Reaction (3) is a secondary reaction which, together with the Reaction (2) in which the precipitate is formed, constitutes the chemical aspect of the separation of the substance from solution by chemical precipitation. This reaction decreases the initial chemical activity of the precipitate and at the same time alters the curface properties of the particles, including such an important property as the adsorption of impurities. In the chemical sense, the precipitate undergoes a peculiar process of chemical "aging". It might perhaps be termed "chemiaging" to distinguish it from the usual (physical) "aging" of the precipitate. Whereas ordinary "aging" makes the form, dimensions, and surface properties of the precipitated particles more stable, in "chemiaging" the chemical composition of the precipitate becomes more stable, while the surface properties, dimensions, and form of the particles become unstable. The two processes take place simultaneously and their mutual influence determines the final properties of the precipitate. The process of "aging" as a whole, when ordinary "aging" is complicated by chemical reactions between the precipitate and the mother liquor, may be termed anomalous "aging".

The secondary chemical process in precipitation, "chemiaging," differs sharply in character from the primary process of precipitate formation. The precipitate is formed from a homogeneous solution in a rapid reaction of double decomposition between two salts. "Chemiaging" is heterogeneous in character, as it is a process which occurs between two salts present in different phases, at the boundary between these phases. The interaction is slow, is diffusion-controlled, and its rate depends on a number of factors: the degree of perfection of the precipitate, i. e., the method and conditions of precipitation, and here not only the surface area of the precipitate but also its "instability," i. e., structure, is important; the conditions of contact between the precipitate and the mother liquor – the degree of stirring of the suspension (renewal of the interphase area), temperature, and the contact time. Therefore it can be regulated easily and within wide limits, and the composition and properties of the precipitate can thereby be influenced. The course of the curves for the potentiometric titration of nickel nitrate by sodium carbonate indicates that, when a definite pH is reached, precipitation of basic salts begins; with rapid precipitation, a more basic salt is formed, unreacted sodium bicarbonate accumulates in the solution, and therefore the buffer region is wider and the ascent of the curve (sharp increase of the pH of the medium) occurs later. The amount of sodium carbonate required for precipitation increases.

In experiments of considerable duration there is time for the sodium bicarbonate to react with the basic precipitate, the solution contains mainly sodium carbonate, the buffer region is narrower, the ascent of the curve corresponding to complete precipitation of Ni^{2+} occurs earlier, and the consumption of Na_2CO_3 decreases considerably.

In experiments in which equal amounts of sodium carbonate were used for precipitation, but of different duration, the logarithm of the basicity of the precipitate is a linear function of the solution pH (Fig. 5).

If the precipitation is performed at a lower temperature, the degree of useful conversion of the sodium carbonate decreases because of the slower reaction between the solution and the precipitate, only bicarbonate is found in the solution, and the precipitates are more basic.

SUMMARY

1. The precipitation of basic nickel carbonate was studied as an example of the double decomposition of two salts in solution, one being an alkali-metal carbonate and the other containing a cation which gives rise to a sparingly soluble basic carbonate; it was found that the precipitate of basic carbonate is chemically metastable and its composition is a function of the temperature, precipitation time, and pH of the medium.

2. Two main chemical reactions take place during precipitation: a) the rapid formation of a primary precipitate of the basic carbonate from a homogeneous solution, and accumulation of sodium bicarbonate in the mother liquor; b) chemical "aging" ("chemiaging") of the precipitate as the result of a seondary interaction between the precipitate and the mother liquor, or, more correctly, a heterogeneous reaction between the basic carbonate in the precipitate and the bicarbonate in the mother liquor; this reaction proceeds at a low rate which depends on the technological precipitation conditions. At higher temperatures the bicarbonate undergoes thermal decomposition with evolution of bubbles of carbon dioxide.

3. The known "aging" of a freshly-formed precipitate in contact with its mother liquor is complicated by the simultaneous process of "chemiaging" in the case of the formation of a sparingly soluble basic carbonate by the action of an alkali-metal carbonate, and is anomalous in character.

4. The useful conversion of an alkali-metal carbonate (such as sodium carbonate) depends on the precipitation conditions; "chemiaging" of the precipitate increases the degree of useful conversion of the precipitant.

LITERATURE CITED

[1] H. T. S. Britton, J. Chem. Soc. 127, 2115 (1925).

[2] W. Feitknecht, et al. Helv. Chim. Acta. 19, 831 (1936).

[3] W. Feitknecht, et al. Helv. Chim. Acta. 23, 180 (1940).

[4] P. Dechamps, C. r. 220, 693 (1945).

[5] Geloso and P. Dechamps, C. r. 224, 1163 (1947).

[6] I. V. Tananaev, I. B. Mizetskaia, and A. D. Vinogradova, J. Anal. Chem. 7, 1, 14 (1952).*

[7] A. K. Babko, J. Anal. Chem. 7, 1, 3 (1952).*

[8] W. J. Singley and J. T. Carriel, J. Am. Chem. Soc. 75, 4, 778 (1953).

[9] I. M. Kolthoff, and E. B. Sandell, Quantitative Analysis (GONTI, 1938) [Russian translation].

Received February 22, 1957.

* Original Russian pagination. See C. B. Translation.

INVESTIGATION OF THE RATE OF ABSORPTION OF HYDROGEN SULFIDE BY ARSENICAL SODA SOLUTIONS*

M. I. Gerber, V. P. Teodorovich, and A. D. Shusharina

(The Leningrad Scientific Research Institute of Petroleum Processing and Production of Synthetic Liquid Fuel)

In order to obtain information on the course of absorption of hydrogen sulfide by solutions of arsenic compounds under conditions resembling those used in industrial practice, experiments on the influence of various factors on the absorption rate were carried out.

The experimental procedures and syntheses of the oxythioarsenate compounds were described previously [1, 2].

EXPERIMENTAL

Absorption of hydrogen sulfide by a solution containing a mixture of Na_2HAsS_3O and $Na_2HAsS_2O_2$. In works arsenical soda liquors the atomic ratio of sulfur to arsenic after regeneration is usually close to 2.5. We therefore prepared a solution containing a mixture of the salts Na_2HAsS_3O and $Na_2HAsS_2O_2$, in which this ratio was 2.48.

Experimental data on the absorption of hydrogen sulfide by this solution are presented in Table 1.

TABLE 1

Effect of Solution pH on the Rate of Absorption of Hydrogen Sulfide by a Solution of Na_2HAsS_3O and $Na_2HAsS_2O_2$. Atomic ratio of sulfur to arsenic 2.48 at 40°, As concentration of solution 0.05 g-atom/liter

Composition of solution	H_2S content of gas (%)	Solution pH		Amount of H_2S absorbed in 3 minutes (ml)	Time in which the S/As ratio in solution increased by 0.5 (minutes)
		original	after 3 minutes		
$Na_2HAsS_{2.48}O_{1.52}$ + NaOH	4.8	10.5	—	68.3	70
$Na_2HAsS_{2.48}O_{1.52}$	4.45	8.2	7.05	26.3	46
$Na_2HAsS_{2.48}O_{1.52}$ + H_2SO_4	4.65	7.2	6.55	30.9	48

As in the experiments described in the preceding paper [2], addition of alkali retards the replacement of oxygen by sulfur. However, addition of sulfuric acid has almost no effect on the absorption rate in this case. The probable explanation is that although a decrease of pH raises the reaction rate, there are certain factors which lower the HS^- ion concentration in solution, and thereby decrease the reaction rate. It is possible that one such factor is the lower degree of hydrolysis of the salt Na_2HAsS_3O, relative to that of the salt $Na_2HAsS_2O_2$, described earlier.

Absorption of hydrogen sulfide by Na_2HAsS_3O solution. The rate of absorption of hydrogen sulfide by Na_2HAsS_3O solutions was studied in two ways: the partial pressure of hydrogen sulfide was varied in one series of experiments, and the concentration of sodium oxythioarsenate was varied in the other. The experiments were carried out at 20°.

* This work was performed under the guidance of V. V. Ipat'ev.

TABLE 2

Variation of the Rate of Absorption of Hydrogen Sulfide by a Solution of $Na_2HAsS_3O + H_2SO_4$ with the Partial Pressure of Hydrogen Sulfide in the Gas at 20°. As concentration of solution 0.05 g-atom/liter

H_2S content of gas (%)	Solution pH		Amount of H_2S absorbed in 3 min (ml)			Time in which the S/As ratio increased by 0.5 (minutes)
	original	after 3 minutes	physically dissolved	by rapid chemical reaction	total	
2.1	7.30	7.20	5.4	3.3	8.7	242
5.0	7.25	6.85	12.9	11.0	23.9	138
10.0	7.30	6.60	25.8	21.3	47.1	115
15.0	7.30	6.45	38.7	36.7	75.4	—

TABLE 3

Variation of the Rate of Absorption of Hydrogen Sulfide by a Solution of $Na_2HAsS_3O + H_2SO_4$ with the Solution Concentration at 20°

Solution concentration (mole/liter)	H_2S content of gas (%)	Solution pH		Amount of H_2S absorbed in 3 min (ml)			Time in which the S/As ratio in solution increased by 0.5 (minutes)
		original	after 3 minutes	physically dissolved	by rapid chemical reaction	total	
0.026	5.0	7.30	6.55	12.9	5.5	18.4	93
0.051	5.0	7.25	6.85	12.9	11.0	23.9	138
0.079	5.0	7.30	6.90	12.9	15.5	28.4	119
0.105	5.0	7.25	7.20	12.9	21.5	34.4	135

TABLE 4

Effect of Temperature on the Rate of Absorption of Hydrogen Sulfide by $Na_2HAsO_4 + H_2SO_4$ Solution. As concentration of solution 0.45 g-atom/liter

Temperature (°C)	H_2S content (%)	Solution pH		Amount of H_2S absorbed in 3 minutes (ml)	Time in which the S/As ratio in solution increased by 0.5 (min)
		original	after 3 minutes		
20	15.6	6.9	6.35	58.8	55
40	16.8	6.9	6.35	40.7	24
50	15.5	6.9	—	44.5	14

The results, presented in Tables 2 and 3, show that, at the first and second stages, the rate of absorption of hydrogen sulfide by 0.5 M Na_2HAsS_3O solution is directly proportional to the concentration of hydrogen sulfide in the gas phase, and the concentration of the absorbent.

Effect of temperature on the absorption rate. Table 4 contains the results of experiments on absorption of hydrogen sulfide by Na_2HAsO_4 solution at various temperatures. It is seen that the rate of the slow reaction of substitution of sulfur for oxygen greatly depends on the temperature. For example, the time required to increase the sulfur – arsenic ratio by 0.5 in the saturation of Na_2HAsO_4 by hydrogen sulfide at 40° is one half of the time required at 20°.

Absorption of hydrogen sulfide by Na_2HAsO_4 solution with intermittent supply of hydrogen sulfide into the reaction vessel. A special experiment was performed in order to confirm the views put forward in the previous

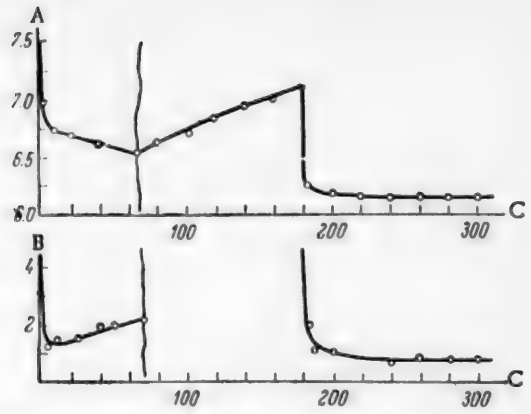

Variations of the rate of absorption of hydrogen sulfide and of solution pH with time, in an experiment with intermittent supply of hydrogen sulfide into the reaction vessel.
A) pH, B) H_2S content (ml H_2S/minute), C) time (minutes).

paper [2] on the mechanism of the absorption of hydrogen sulfide by sodium oxythioarsenate solutions. The solution pH was measured continuously during the experiment, while the supply of hydrogen sulfide into the reaction vessel was stopped at intervals. The experiment was carried out as follows.

The absorption of hydrogen sulfide by 0.05 M solution of Na_2HAsO_4(pH = 8.5) was studied; the gas contained 17% of hydrogen sulfide. The solution pH was measured during absorption of hydrogen sulfide. As in all the preceding experiments, the pH decreased with time. After some time the hydrogen sulfide supply was discontinued and the vessel was stopped, but the pH measurement was continued; the pH gradually rose. The buret with hydrogen sulfide was then connected again, the motor which moved the vessel was switched on, and the experiment was continued.

The results of this experiment are plotted in the graph. The course of the curves indicates that during the time interval when the experiment was interrupted and the supply of hydrogen sulfide was stopped, a slow reaction between hydrosulfide and sodium oxythioarsenate continued in the solution. This is shown by the continuous increase of the solution pH. Hydrogen sulfide was gradually absorbed from the gas phase by the solution, and the pressure in the vessel was reduced somewhat. When the motor was switched on and the buret with hydrogen sulfide was connected, hydrogen sulfide was again dissolved with formation of sodium hydrosulfide, and the process went on, a large amount of hydrogen sulfide being absorbed at once.

This experiment confirms the foregoing views concerning the chemical reactions which occur in the absorption of hydrogen sulfide by the solutions studied. Moreover, this experiment demonstrates that it is advisable to increase the time during which the arsenical soda liquor remains in the absorber, as not only the alkaline capacity of the absorbent but also its chemical capacity due to its arsenic content can then be utilized.

SUMMARY

1. The rate of replacement of oxygen by sulfur in sodium oxythioarsenate (stage III) depends on the partial pressure of hydrogen sulfide in the gas, the solution pH, and the solution temperature.

2. It is shown experimentally that the time during which the arsenical soda liquor remains in the absorber should be increased.

LITERATURE CITED

[1] N. I. Brodskaia, M. I. Gerber, V. P. Teodorovich, and A. D. Shusharina, J. Appl. Chem. 30, 11, 1588 (1957).•

[2] M. I. Gerber, V. P. Teodorovich, and A. D. Shusharina, J. Appl. Chem. 31, 10, 1478 (1958).•

Received October 25, 1956.

• Original Russian pagination. See C. B. Translation.

INFLUENCE OF VARIOUS FACTORS ON THE STRUCTURE OF SURFACE FILMS ON SILICATE GLASSES

L. S. Iastrebova and V. S. Molchanov

It is known that the surface of every silicate glass is always coated with a very thin film (a few tens of angstroms thick), consisting mainly of hydrated silica [1]. The presence of this film determines the surface properties of the glass, and, in particular, its chemical resistance. By treatment of glass with dilute acid solutions the thickness of the silica surface film can be increased to several hundreds or even thousands of angstroms. Such artificially-formed films are now extensively used for clarification of optical components [2] and for protection of the latter against chemical attack [3]. The clarifying and especially the protective effect of the silica surface films depend on their thickness and porosity, i. e., on the number and dimensions of the pores. Therefore for the production of films with desirable properties for some particular purpose it is necessary to have information on the film thickness and porosity. When our investigation was started, only the first part of the problem had been adequately studied – the influence of various factors on film thickness [2, 4, 5] (or, more accurately, on the time required for the formation of a film of standard thickness at which the reflection coefficient of the glass surface reached a minimum). With regard to porosity, only a few exploratory experiments had been carried out*.

For example, Schroder [7, 8] studied the nature of the porosity of a film formed on glass specimens of the heavy-crown type by treatment with dilute nitric acid. According to his calculations, the pores were from 8 to 100 A in diameter, with 60 A the predominant diameter. Zhdanov [9], who determined the sorption of water and alcohol by films on certain optical glasses, merely reported that the pores in these films are less than 8 A in radius. Neither of these authors presents any data on the effects of formation conditions on the porosity of the surface films.

We studied the effects of the etching conditions on the porosity of films formed by the action of acids on silicate glasses, and also the influence of the composition and the thermal history of the glass. The materials studied were powdered glasses of the optical type; the composition is given in Table 1. The average grain size of the powders was about 60μ**. The powders were treated in the etching solutions until films about 1000 A thick (by calculation) were formed. The conditions for the formation of films of this thickness were determined with the aid of polished specimens (made from the same pieces of glass as were subsequently used for grinding to powders) by an optical method; the specimens were kept in the etching solution (which was stirred) until a film of a blue-violet interference color was formed. A film of this type has an optical thickness of about 1375 A. If variations of the refractive index of the film substance on glasses of different composition are disregarded and if it is assumed that the refractive index is 1.4, then the geometrical thickness of the blue-violet film has the required value (about 1000 A).

The film porosity was estimated by the sorption method in a vacuum volumetric apparatus in which pressure changes could be measured to an accuracy of 0.05 mm, which corresponds to the absorption of 3.5-4 mm^3 of water vapor at standard temperature and pressure (STP). The adsorbed substance was water; because of the small size of its molecules it can penetrate into even very fine pores. It was also taken into account that water is a most important corrosive medium for glasses, and therefore the film porosity estimated from water sorption would be a good measure of the protective properties. All the isotherms were determined at 15°. The sorption

*Apart from studies of the product formed by the destruction of certain alkali borosilicate glasses, known as porous glass, which cannot be regarded as the complete analog of the protective films on silicate glasses [6].

**The powders were sifted in the range of 230-270 mesh.

TABLE 1

Glass Compositions

Glasses	Chemical composition (molar %)							
	SiO_2	B_2O_3	Al_2O_3	ZnO	BaO	CaO	PbO	R_2O
No. 1	64.5	15.6	—	3.2	9.6	—	—	7.1
No. 2	62.4	—	—	—	—	—	33.5	3.9
No. 3	61.3	—	—	—	—	—	35.2	3.3
No. 4	57.8	5.1	1.8	11.7	8.5	—	6.2	8.9
No. 5	52.5	12.2	5.4	—	28.3	1.6	—	—
No. 6	52.3	7.3	1.6	11.3	22.1	—	—	—
No. 7	43.2	9.4	2.3	6.7	29.4	4.4	4.4	—

TABLE 2

Film Characteristics

Glass	Conditions for formation of films of different thickness		Film characteristics	
	temperature (°C)	time	pore volume · 10^3 (in m^2/cc of glass)	pore volume · (in m^2/cc of glass)
No. 1	25	3 hrs	2.7	6.3
	50	15 min	3.4	7.3
	80	2 min	3.5	7.9
No. 2	25	2 hrs	2.9	6.3
	50	14 min	3.0	7.0
	80	3.5 min	3.2	6.7

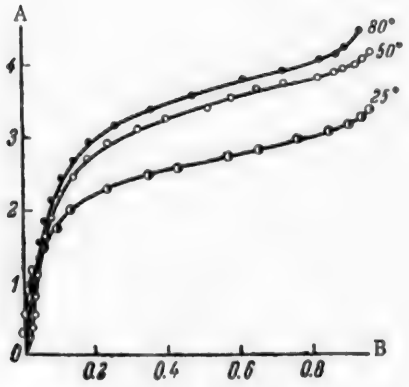

Fig. 1. Isotherms of water adsorption on glass No. 1.
A) Amount of water vapor adsorbed (a), reduced to standard temperature and pressure (in cc H_2O (STP)/cc glass), B) relative pressure of water vapor p/p_s.

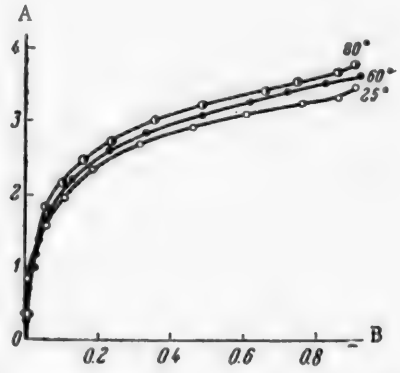

Fig. 2. Isotherms of water adsorption on glass No. 1. Designations as in Fig. 1.

isotherm invariably exhibited irreversible hysteresis (the curve for the desorption of water was always above the adsorption curve; this is primarily due to the special features of the fine-pore structure of the films), and therefore only the adsorption isotherms are shown in all the diagrams.

TABLE 3

Effect of Solution pH on Film Porosity

pH of acetic acid solution	Time for formation of films of equal thickness at 25° (minutes)	Film characteristics (glass No 5)	
		pore volume · 10^3 (cc/cc of glass)	pore area (m^2/cc of glass)
3.83	29-30	1.35	1.65
3.35	15-16	1.90	2.41
2.83	5-5.5	5.96	6.57
2.29	3	10.70	8.93

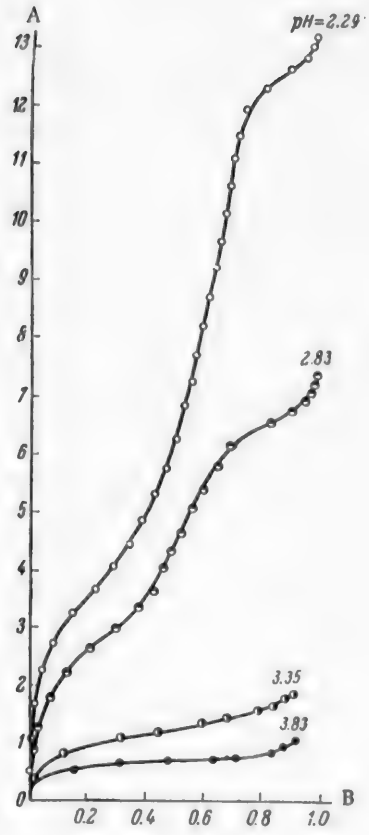

Fig. 3. Effect of hydrogen-ion concentration on the porosity of films on glass No. 5 in CH_3COOH solution at 25°. Designations as in Fig. 1.

The amount of water vapor absorbed (a), reduced to standard temperature and pressure, is plotted against the relative pressure of water vapor (p/p_s). Because of the irreversible hysteresis it was not possible to calculate the average pore radii with sufficient relaibility, or to plot the pore-size distribution curves. We therefore confined ourselves to calculations of the total pore volume (from the final value of the adsorption at pressures close to saturation) and the pore area (from the Brunauer – Emmett – Teller equation). All the calculations were made for 1 cc of glass powder, with the same macrogeometric surface area, nominally 100 cm^2 in each case (for the given grain size, on the assumption that all the grains are cubic in form).

Effect of Formation Conditions on Film Porosity

The effects of the following factors on film porosity were studied: temperature of the etching solution, its hydrogen-ion concentration, nature of the acid, and presence of organic solvents in the etching solution.

Figs. 1 and 2 show isotherms for adsorption of water on films of glasses Nos.1 and 2 (Table 1), formed at 25, 50, and 80° by the action of decinormal aqueous acetic acid solution. The sequence of the isotherms in the two diagrams, and the film characteristics calculated from the isotherms, given in Table 2, show that increase of the acid-treatment temperature leads to a very slight increase of film porosity with a sharp increase in the film-formation rate.

Data on the effect of hydrogen-ion concentration of the etching solution on film porosity are presented in Fig. 3 and Table 3. The isotherms in Fig. 3 are for films on glass No 5 at 25°, formed in aqueous acetic acid solutions of the following pH: 3.83, 3.35, 2.83, 2.29.

The growth rate and the sorption capacity of the films increase with increasing hydrogen-ion concentration (Column 2, Table 3). Further, beyond a certain pH value the increase of pore volume is accompanied by changes in the character of the porosity. The isotherms in Fig. 3 are grouped in pairs. Two of them, for films formed in acid solutions of pH 3.83 and 3.35, indicate that these films have a low sorption capacity and a finely porous

TABLE 4

Effect of the Nature of the Acid on Film Characteristics

Acid	Dissociation constant	Solution pH	Time for formation of films of equal thickness at 25° (minutes)	Film characteristics (glass No 4)	
				pore volume · 10^3 (cc/cc of glass)	pore area (m^2/cc of glass)
Acetic	$1.8 \cdot 10^{-5}$	3.33	10	1.23	2.81
Oxalic	$6.0 \cdot 10^{-2}$	3.40	7.5	1.34	1.54
Hydrochloric	Completely dissociated	3.36	7	1.41	1.40

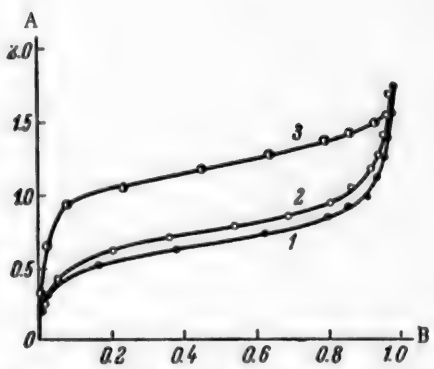

Fig. 4. Effect of the nature of the acid on the porosity of films on glass No. 4. Designations as in Fig. 1. Curves: 1) HCl, pH = 3.36; 2) $H_2C_2O_4$, pH = 3.40; 3) CH_3COOH, pH = 3.33.

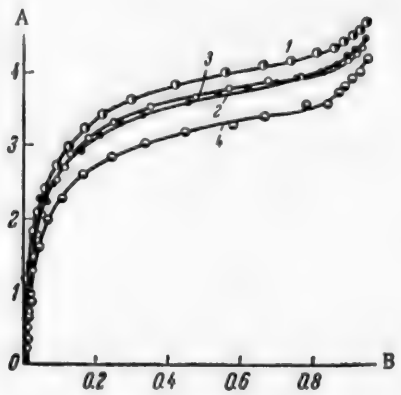

Fig. 5. Effects of the presence of various solvents in the solution on the porosity of films on glass No.6. Designations as in Fig. 1. Films made in CH_3COOH solutions containing: 1) alcohol, 2) acetone, 3) dioxane, 4) water only.

TABLE 5

Effects of Added Solvents on Film Characteristics

Characteristics of acetic acid solution used for etching		Time for formation of films of equal thickness at 25°(minutes)	Film characteristics (glass No 6)	
organic solvent added	solution pH		pore volume · 10^3 (cc/cc of glass)	pore area (m^2/cc of glass)
Ethanol	3.42	6	3.8	8.6
Acetone	3.29	6	3.6	7.7
Dioxane	3.46	11.5	3.5	7.8
Aqueous solution .	3.53	3 – 3.5	3.3	7.4

structure. The other two isotherms, corresponding to films made in solutions of pH 2.29 and 2.83, not only lie considerably higher than the other two (which shows that these films have a considerably higher sorption capacity), but also differ sharply from them in character. The continuous steep ascent of these isotherms over the entire range of relative pressures can be due only to the presence of pores ranging very widely in size, including relatively large pores.

TABLE 6

Effect of Tempering on Film Characteristics

Heat treatment	Time for formation of films of equal thickness at 25°(minutes)	Film characteristics (glass No.5)	
		pore volume · 10^3 (cc/cc of glass)	pore area (m^2/cc of glass)
Annealing	~6	4.6	5.8
Tempering in lump form.	~5	6.2	9.1
Tempering in powder form.	~5	6.7	10.9

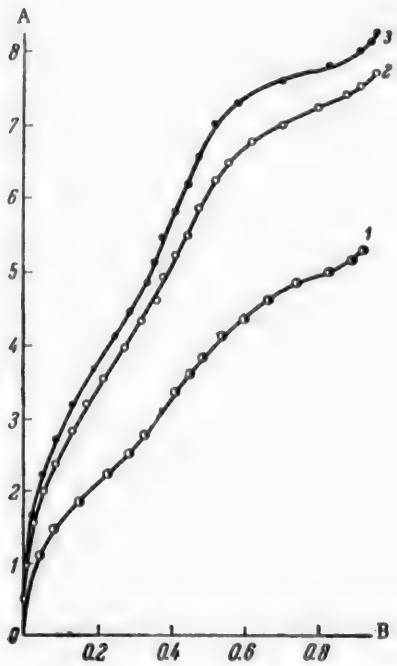

Fig. 6. Effect of tempering on the porosity of films on glass No. 5. Etching on 0.1 N CH_3COOH at 25°. Designations as in Fig. 1. Glass: 1) annealed, 2) tempered in lump form, 3) tempered in powder form.

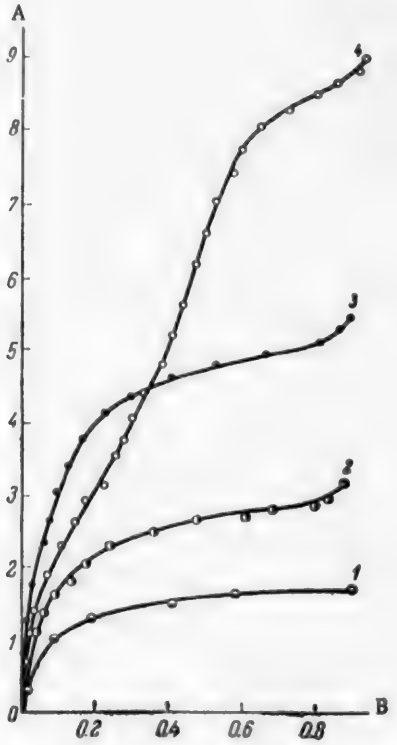

Fig. 7. Effect of chemical composition of the glass on film porosity. Designations as in Fig. 1. Glass: 1) No.3, 2) No 4, 3) No.6, 4) No.7.

It follows from the data in Table 3 that with a decrease of pH from above 3 to below 3 the pore volume increases 3.7 to 6.7-fold, and the pore area, 3.3 to 4.5-fold. A similar variation of film porosity with pH of the etching solution was found by us earlier in the case of TK6 optical glass [3]. The hydrogen-ion concentration of the etching solution is therefore one of the decisive factors determining the structure of surface silica films.

The influence of the nature of the etching acid is illustrated by data for glass No.4 (Table 1), films on which were made by the action of solutions of three acids: acetic, oxalic, and hydrochloric; the pH values of the solutions were almost identical. The isotherms for these films are given in Fig. 4, and the film characteristics calculatedfrom them, in Table 4.

TABLE 7

Effect of the Chemical Composition of Glass in Film Characteristics

Glass	Film characteristics	
	pore volume · 10^3 (cc/cc of glass)	pore area (m^2/cc of glass)
No.3	1.3	2.5
No.4	2.5	5.5
No.6	4.2	10.9
No.7	7.2	8.9

Fig. 4 shows that the isotherm for the film formed in acetic acid differs sharply in character from the isotherms for films formed in a solution of a strong acid (hydrochloric) or an acid of moderate strength (oxalic). All three films are roughly equivalent with regard to the total amount of sorbed water. In the first case, the steep rise of the isotherm begins in the region of low relative pressures; this shows that the film has a finely porous structure. In the second case, the isotherm begins to rise steeply only when the relative pressure has reached 0.8-0.9, and the shape of the isotherms indicates that the films contain predominantly large pores, which become filled at water-vapor pressures close to saturation. Accordingly, the transition from acetic to oxalic and hydrochloric acids is accompanied by a slight increase of the total pore volume and an appreciable decrease of pore area (Table 4).

It follows from these results that, at equal pH of the etching solutions, weak acids give rise to finely porous, and strong acids to coarsely porous films; the pore size appears to increase with increasing degree of dissociation of the acid. Therefore the nature of the acid is the second important factor determining the structure of surface silica films.

In view of the fact that a common practical procedure in the formation of surface films on unstable glasses is dilution of the etching liquid with alcohol (whereby the etching rate may be regulated), it was of interest to determine the influence of various organic solvents in the solution on film porosity. The experiments were performed with powders of glass No.6, treated in acetic acid solutions with addition of equal volumes of ethanol, acetone, or dioxane, and also in pure aqueous solutions of the same acid at similar pH values*. The isotherms for these films are presented in Fig. 5, and the film characteristics calculated from them, in Table 5. It follows from these results that the presence of organic solvents in the etching solutions has a strong influence on the rate of film formation (see Column 3), but has virtually no effect on film structure.

Effect of the Thermal History of the Glass on Film Porosity

In addition to studies of the effects of various external factors on the structure of the surface films on the glass described above, it was of interest to determine how far the structure of the films depends on the internal state of the glass itself, determined by its thermal history. The experiments were performed with glass No.5 (Table 1). The annealed glass used was factory-made pot glass. It was tempered in air down from 660° after preliminary exposure at that temperature for 1 hour. Some of the glass was tempered in the form of separate lumps, and some in powder form. It was etched in decinormal aqueous acetic acid at 25°. The isotherms for the films are plotted in Fig. 6. Comparison of these isotherms shows that tempering causes appreciable changes in the structure of the surface films, the effect increasing with increasing degree of tempering**. Thus, the total pore volume is 1.3-2.5 times greater for tempered than for annealed glass, according to the degree of tempering, and the pore area is 1.5-1.9 times greater (Table 6). However, there is little difference between the rates of film growth.

The steeper ascent of the isotherms for the tempered glasses in the region of low relative pressures suggests that the observed change in the character of the porosity should be attributed to an increase of the relative proportion of the finer pores in the film formed on tempered glass, with a simultaneous increase of the total number of pores. In any event, there can be no doubt that the thermal history of the glass is a factor which has a strong influence on film structure. It must be emphasized once again that it has a stronger influence on porosity than on the time of film formation.

Effect of Chemical Composition of the Glass in Film Porosity

This effect was studied in experiments on glasses Nos.3, 4, 6, and 7, which form a series with decreasing silica contents (Table 1).

* The solutions were prepared from equal volumes of decinormal acetic acid, water, and organic solvent; the pure aqueous solution of the acid (pH = 3.53) was 0.005 N.

** The degree of tempering of glass powders is undoubtedly higher than that of lumps.

The glass powders were treated in decinormal aqueous acetic acid at 25°. The porosity differences between the films formed can be deduced from the isotherms in Fig. 7 and the data in Table 7.

With decrease of the silica content of the glass, the shape of the isotherms changes from one similar to the Langmuir type (for glass No.3) to S-shaped (for glass No.7). The total sorption capacity of the pores and the pore area increase accordingly (Table 7).

The smaller pore area for the film on glass No.7, as compared with glass No 6, together with the larger pore volume, is due to the fact that in the film on the former glass a large part of the volume is accounted for by the larger pores. In fact, whereas the form of the isotherm for glass No.6 indicates that the film on it has a finely porous structure, the steady rise of the isotherm for glass No.7 over a wide range of relative pressures (up to nearly unity) indicates that the film on this glass contains pores of a wide range of sizes. Therefore the chemical composition of the glass, and especially its silica content, has a decisive influence on the structure of the surface films. Films formed on glasses of different composition by the action of acids may differ not only in total pore volume, but also in the nature of the porosity.

General Conclusions

In the light of the foregoing experimental data, the factors influencing the structure of silica surface films may be divided into two groups. The first comprises the factors associated with the internal structure of the glass itself, namely: the chemical composition and the thermal history. They determine the film structure to a considerable extent; the film porosity increases with decreasing silica content in the glass and with increasing degree of tempering. The first fact is a natural consequence of the loosening of the glass structure with decrease of its silica content. The most general hypothesis as to the causes of a more developed film structure in the case of tempered glasses (in comparison with annealed glasses) can be based on considerations of the lower energetic stability of the cations in tempered glass, and of the smaller dimensions of the microregions in which the silicate molecules are aggregated, and which are the first to be influenced by the etching solution. This, on the one hand, should facilitate leaching of the cations, and on the other, it should increase the relative proportions of the small pores in the film. The second group of factors operative in the formation of surface films consists of the conditions of film formation. These, which we term the external factors, can in their turn be grouped as follows. Two of them, namely: the hydrogen-ion concentration of the etching solution, and the nature of the acid used for etching, have appreciable effects both on the film porosity and on the rate of film formation. The other two factors of this group – the temperature of the etching solution and the presence of organic solvents in it – have a strong influence on the rate of film formation, but have hardly any effect on the film structure.

The increase in the porosity of surface films with increasing hydrogen-ion concentration of the etching solution must be attributed to changed conditions for the hydration of silica which comprises the glass framework, and for the peptization of the silicic acid formed in the decomposition of silicates constituting the glass.

The causes of the structural differences between films formed in solutions of different acids with the same pH must be sought in the specific effects of different anions on these same processes of hydration and peptization of the silicon – oxygen structural elements of the glass.

The reason why the etching temperature has little effect on film porosity is probably that the action of this factor largely reduces to the usual temperature dependence of chemical reaction rates, and does not affect the reaction mechanism.

The retardation of the rate of film growth in presence of organic solvents in the etching solution is most probably due to adsorption of organic molecules on the reactive centers of the glass surface, which hinders access of hydrogen ions to them. However, the latter soon displace the organic molecules from the active centers (because of their high affinity to the glass surface), and the main factor determining the film structure comes into operation – the hydrogen-ion concentration of the etching acid solution. This explains why films formed in solutions containing different organic solvents (but of the same pH) are of approximately the same porosity.

In conclusion, it is our pleasant duty to thank Professor K. S. Evstrop'ev for interest in this work and for active participation in discussion of the results.

LITERATURE CITED

[1] I. V. Grebenshchikov, Bull. Acad. Sci. USSR, OTN 1, 3 (1937).

[2] I. V. Grebenshchikov, et al., Clarification of Optical Material (State United Press, 1946). [In Russian]

[3] L. S. Iastrebova, Trans. State Optical Inst. 24, 145, 172 (1956).

[4] E. Berger, Glastechn. Ber. 12, 6, 189 (1934).

[5] O. S. Molchanova, Optico-Mechanical Ind. 8 (1937) and 6-7 (1940).

[6] S. P. Zhdanov, Dissertation (State Optical Inst., 1949).

[7] H. Schroder, Glastechn. Ber. 20, 6, 161 (1942).

[8] H. Schroder, Z. Techn. Phys. 23, 8, 196 (1942).

[9] S. P. Zhdanov, Trans. State Optical Inst. 24, 145, 210 (1956).

Received September 28, 1957.

APPLICATIONS OF THE THEORY OF SIMILARITY TO CERTAIN PROCESSES IN CHEMICAL TECHNOLOGY

S. Bretsznajder

(Chair of Technological Planning, the Warsaw Polytechnic Institute)

The methods of the similarity theory are not being used widely enough in the modeling of processes in chemical technology. The cause lies in the difficulties associated with the use of these methods for complex processes involving chemical reactions.

Therefore, in contrast to such physical processes as heat and mass transfer, filtration, agitation, etc., where in most cases criterial equations derived with the aid of the similarity theory are used to describe the effects, in chemical processes there have been only some isolated attempts at analytical generalization of reaction thermodynamics and kinetics.

At the present time practical problems in technology are solved mainly by means of investigations in pilot units with subsequent empirical increase of the production scale. A wider utilization of the methods of the similarity theory would undoubtedly shorten the route to the solutions of such problems [1].

Determination of the Flow Regimes of Liquids (or Gases), and of Heat- and Mass-Transfer Coefficients in Complex Systems by Modeling Methods

For solution of technological problems by modeling methods, it is necessary to develop a procedure whereby it is possible to determine the flow regimes of liquids or gases, and the heat- and mass-transfer coefficients, at selected points in a complex model.

Among the earliest efforts in this direction, mention must be made of the work of Rubinshtein [2], who based his determinations of heat-transfer coefficients at different points of a boiler furnace on the analogy of the heat- and mass-transfer processes. He used a model to determine the quantity of ammonia diffusing from a moving ammonia – air mixture to the wall surface; at the points in the walls where it was necessary to determine the heat-transfer coefficients, he placed pieces of filter paper soaked in acid, and calculated the heat-transfer coefficients from the amounts of ammonia absorbed by the acid.

Djurdjevic [3] recently described a method in which a dye solution was passed through a model. The inner walls of the apparatus were coated with a colorless adsorbent (powdered silica gel) which became colored by adsorbing the dye. The color intensity can be determined colorimetrimetrically, and the results can be used to estimate the mass-transfer (and, by analogy, the heat-transfer) coefficients.

Qualitative results are also given by the method described long ago by Thoma [4], and applied to investigations of boiler furnaces. Pieces of filter paper soaked in concentrated hydrochloric acid are placed on the surfaces of a model; when a gaseous mixture containing ammonia is introduced into the model, a mist of ammonium chloride is formed from which conclusions may be drawn concerning heat-transfer processes (the effect was photographed).

In some cases the dissolution of metals is suitable for modeling diffusional and thermal processes [5].

Several of our own investigations are concerned with the problem under discussion [6].

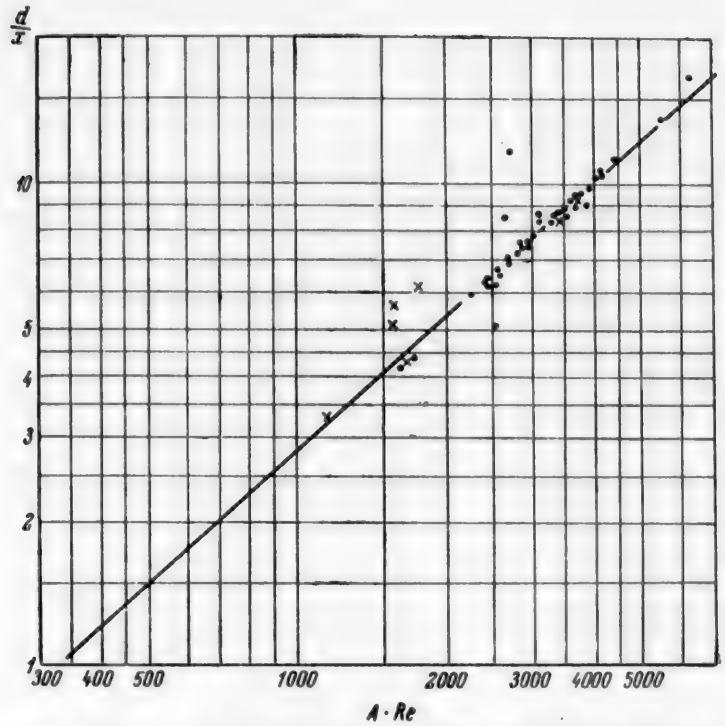

Fig. 1. Absorption of ammonia by acid soaked in a strip of filter paper (transition region, Reynolds numbers 500-2300).
A) Degree of absorption of ammonia, d) tube diameter, x) thickness of boundary layer, $\frac{d}{x} \cong Nu'$.

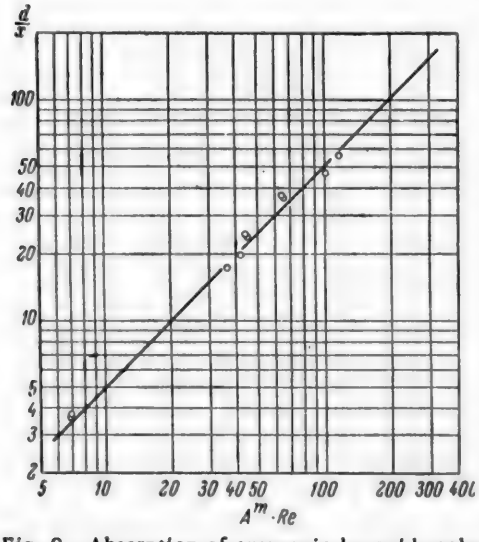

Fig. 2. Absorption of ammonia by acid soaked in a strip of filter paper (laminar and transition regions, Reynolds numbers 8-1000). Notations as in Fig. 1.

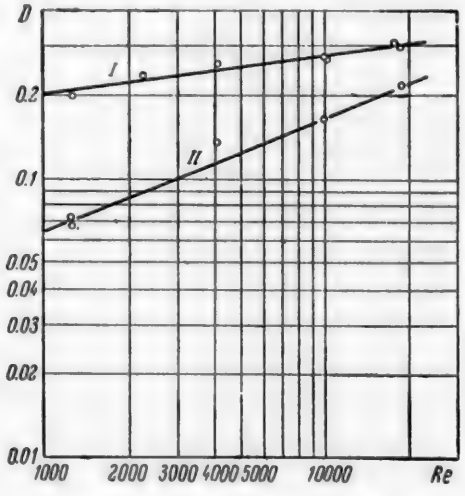

Fig. 3. Variation of the degree of blackening D of photosensitive paper with the Reynolds number Re. Explanation in text.

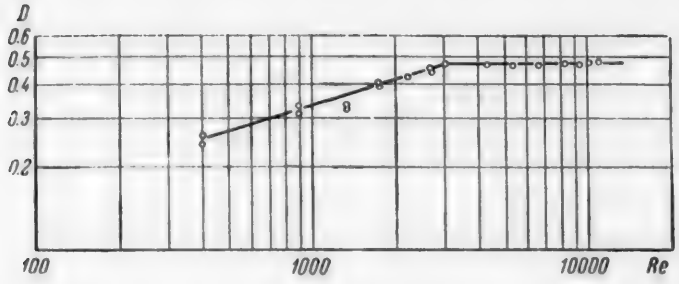

Fig. 4. Variation of the blackening D of photosensitive paper with the Reynolds number Re. Explanation in text.

Fig. 5. Model consisting of three tubes of different diameters.

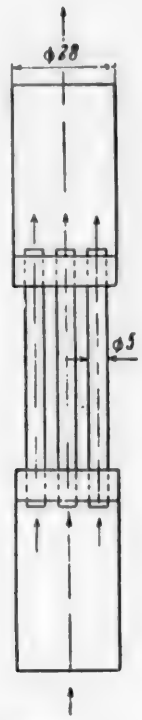

Fig. 6. Model of heat exchanger.

Absorption of Ammonia by Acid

At the first stage, out aim was to apply the method described above, in which ammonia is absorbed from a gas by acid in filter paper, to determination of the flow regimes of gases in models; it was desired to determine the dependence of the amount of ammonia diffusing to the inner surface of a tube wall on the Reynolds number, which determines the flow regime of a gaseous mixture, and to test the reproducibility of the experiments *.

*L. Lesnevich, I. Moschitska, M. Kaspshitski, and V. Batsiia took part in this work.

If a satisfactory solution to this problem is found, further work is simplified considerably; the relationships between the Reynolds number and the mass- and heat transfer criteria for flow in pipes are known. The results of measurements performed in a model may be used to determine the Reynolds numbers and to calculate the mass- and heat-transfer coefficients at different points of the system under investigation.

A ring made from a strip of filter paper soaked in sulfuric acid solution was placed in a glass tube, and a mixture of air and ammonia was passed through the tube for a definite time. The amount of ammonia absorbed by the acid was then determined by titration.

Dimensional analysis yields the relationship

$$\frac{d}{x} = \text{const}\, Re^a \cdot Sc^b \cdot \left(\frac{l}{d}\right)^c, \qquad (1)$$

where $\frac{d}{x}$ is the diffusional analog of the Nusselt criterion, and d is the tube diameter; x is the thickness of the hypothetical laminar boundary layer; l is the width of the strip of filter paper; Re is the Reynolds number; Sc is the diffusional analog of the Prandtl criterion (Pr'); a, b, and c are indices.

The gas mixtures used in our experiments differed little from air in properties; Sc can therefore assumed to be constant. It also follows from the experimental data that $(l/d)^c \cong \text{const}$ (c is small, about 0.1).

The experimental conditions were: tube diameter 8-72 mm, width of the strip of filter paper 10-135 mm, concentration of sulfuric acid 5 N or 10 N, ammonia concentration 0.005-4.3%. The determinations lasted from 10 seconds to 1 hour.

This method would be satisfactory provided that nearly all the ammonia which diffuses from the gas phase to the surface of the filter paper is absorbed by the acid.

However, this is possible only during the first, short period of the experiment – as the acid becomes neutralized by ammonia, the absorption conditions deteriorate.

Our experiments showed that, for reproducible results, the amounts of neutralized ammonia and acid, the determination time, and the dimensions of the filter paper should all be kept to a minimum, while the amount of acid used for absorption should be as large as possible. In our experiments from 5 to 15% of the acid was neutralized.

It was rather difficult to conform to all these conditions, as the analytical error in the determination of the absorbed ammonia is then large. Moreover, it is impossible to eliminate the influence of changes in the ammonia concentration during the determinations.

This influence can be taken into account with sufficient accuracy by the introduction of an empirical factor (the extraction coefficient A) into the equation; the value of A depends on the amount of ammonia absorbed.

For the transition region, in the range of Re = 500-2300, we obtained the expression

$$\frac{d}{x} = 0.0757 \cdot (Re \cdot A^{1.37})^{0.814} \qquad (2)$$

or, approximately

$$\frac{d}{x} = 0.075 \cdot A \cdot Re^{0.8}. \qquad (2a)$$

The relationship between $(\frac{d}{x})$ and $(Re \cdot A^{1.37})$ is plotted in Fig. 1.

In these experiments the amount of ammonia absorbed (extraction coefficient A) was, on the average, 0.3-0.5 (over 0.8 in some instances).

Despite the wide range of A, the points on the graph (plotted in logarithmic coordinates) lie close to a straight line corresponding to the relationship $\log d/x - \log (Re \cdot A^{1.37})$, in accordance with Equation (2).

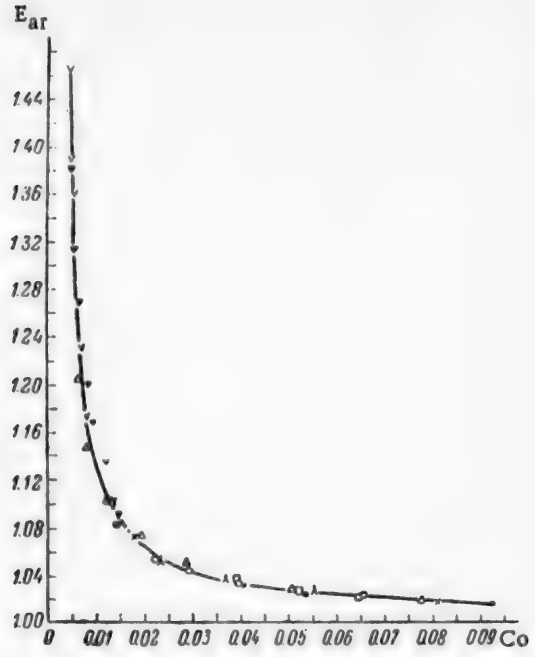

Fig. 7. The relationship between the criterion of thermodynamic equilibrium Eq and the contact criterion Co for a reaction of the type $A_{solid} \rightleftharpoons B_{solid} + C_{gas}$.

The investigation showed that for laminar and transitional flow in the range of Re from 8 to 1000 the index m of the coefficient A^m depends on the extraction coefficient A and on the ratio of the tube diameter d to the width l of the strip of filter paper

$$m \cong \left(\frac{d}{l}\right)^{0.16} - A^{0.4}.$$

The relationship between $\frac{d}{x}$ and the Reynolds number becomes

$$\frac{d}{x} = 0.485 \cdot A^m \cdot Re. \qquad (3)$$

In this case, when $\frac{d}{x}$ is plotted against $Re \cdot A^m$ (in logarithmic coordinates) (Fig. 2), the experimental points lie around a straight line represented by Equation (3).

These observations show that the method in question gives reproducible results, and that it can be used for determinations of heat- and mass-transfer coefficients in the modeled systems. However, the amounts of acid and ammonia neutralized should be small, and approximately the same at different points in the model. For comparison of the heat- and mass-transfer coefficients in the model with the values found from the standard graphs (Figs. 1, 2) it is necessary to take into account the values of the extraction coefficient A at the different points in the model.

The necessity of conforming to the conditions described introduces difficulties and complications into determinations of heat- and mass-transfer coefficients in models by the ammonia-absorption method.

We used this method to check our calculations of the amounts of ammonia diffusing to the surface of a platinum gauze in industrial contact units.

Similar calculations had been performed earlier by Apel'baum and Temkin [7], and by Buben [8].

In an earlier investigation [9] we calculated the mass-transfer coefficients [11] and checked the results experimentally. For this, ammonia was absorbed by a thread gauze impregnated with sulfuric acid, and the amount of ammonia absorbed was determined. The gauze was made of threads 0.18 mm thick, and had 25 holes per cm^2.

For the region of laminar flow, the following expression was found:

$$\frac{d}{x} = 0.698 \cdot A^m \cdot Re \cdot \frac{R-r}{R}, \qquad (4)$$

where $m = 1.74\ A^{0.19}$.

The radii R and r determine the dimensions of the part of the gauze impregnated with acid.

The results confirm the validity of the assumptions made in the calculations in the paper cited [9].

Action of Ammonia on Photosensitive Paper

Because of the difficulties in the use of absorption of ammonia by acids as a method for the modeling of various processes, we tested a new method, dependent on the action of ammonia on photosensitive paper containing diazo compounds * [6]. The unexposed regions of such paper are blackened by ammonia, and the intensity

*L. Lesnevich, D. Khomich, and I. Moschitska took part in the development of the method.

of the blackening depends on the ammonia concentration and the duration of its action.

For investigations of the process, a sample of the paper was placed in a model of the apparatus, a stream of gas containing ammonia was passed through it, and the blackening of different samples was determined photometrically.

The degree of blackening D is defined as the logarithm of the ratio of the coefficient of reflection of unused photosensitive paper, i_0, to the coefficient of reflection of the paper subjected to the action of ammonia in the model, i:

$$D = \lg \frac{i_0}{i}.$$

The very first experiments showed that by comparison of the degree of blackening of the paper with a standard scale it is possible to determine the Reynolds number, which characterizes the flow regime and hence the conditions of mass or heat transfer at different points of the model.

The experiments were performed under isothermal conditions at room temperature; a gas mixture containing ammonia was allowed to act on photosensitive paper placed in a tube (with the sensitive layer inward).

The ammonia concentration of the gas mixture depends on the type of paper and on the Reynolds numbers characterizing flow in the process in question. The ammonia concentration was varied from 0.15 to 14.4 vol. %.

The degree of blackening D also depends on the time during which the ammonia acts; we obtained the following expression for two different types of paper:

$$D = \text{const}\, \tau^{1/3}. \tag{5}$$

In a study of the effect of aging time of the paper on the degree of blackening it was found that the blackening increases with the time between the action of ammonia on the paper and development of the paper (for example, D determined photometrically was approximately 45% higher when the paper was left in darkness until the next day after the action of ammonia, than the values of D for specimens developed 10 minutes after the experiment). In the subsequent experiments an aging time of 90 minutes was adopted. When a moist gas was passed through, it was not necessary to take the aging time into account.

The degree of blackening is greatly influenced by the moisture content of the gaseous mixture which contains, in addition to ammonia and neutral gases, a certain amount of water vapor. When the gaseous mixture was saturated with water vapor at room temperature, the degree of blackening was 20-30% higher than that given by a dry gas; if the gas was saturated with water vapor at 40°, the degree of blackening increased 7-fold over that produced by a dry gas.

The moisture content of the photosensitive paper is also significant – if the paper is humidified before the experiment, for example, by being left for 1 hour in a desiccator containing water (at 16°), the degree of blackening increases by 30-50%.

These observations lead to the conclusion that the main condition for reproducible results is maintenance of a constant and definite humidity of the gaseous mixture and paper.

It should be noted that the paper absorbs very small amounts of ammonia, so that the ammonia concentration of the gas alters very little during the experiment.

The relationship between the degree of blackening D and the Reynolds number, plotted in logarithmic coordinates, is represented by straight lines the slopes of which depend on the experimental conditions.

In Fig. 3, the Line I represents D as a function of Re under the following conditions: ammonia concentration in the gaseous mixture 0.15 vol. %, gas not humidified, paper normally humidified, duration of experiment 10 minutes, Reynolds numbers varied in the range Re 1000-18700.

This relationship may be represented by the equation

$$D = \text{const}\, Re^{0.15}. \tag{6}$$

Line II represents the analogous relationship for the following conditions: time 1 minute, gas humidified, paper not humidified (the remaining conditions as before). The line represented by the equation

$$D = \text{const}\, Re^{0.40}. \quad (7)$$

In some of the experiments air was passed through an aqueous ammonia solution for preparation of the gaseous mixture. This gaseous mixture was saturated with water vapor, and contained 10.4% NH_3. The time of action of the ammonia on the paper was 1 minute. For these conditions the D – Re relationship is represented by the equation

$$D = 0.044 Re^{0.29}. \quad (8)$$

This relationship (Fig. 8) was tested over the range of Re = 400-3040. At higher values of Re the paper becomes saturated with ammonia, and D is constant. The maximum possible blackening was obtained at Reynolds numbers above 3000.

Thus, Fig. 4 is a standard blackening scale. To check its accuracy, we measured the blackening of photosensitive paper in order to determine the type of flow in simple models of equipment, so chosen that the experimental results could be verified by calculation [6].

The first such apparatus consisted of three pipes of different diameters, connected in series (Fig. 5).

The following deviations were found between the calculated values of Re and values found by the photosensitive-paper method: ~3% (d = 8 mm), ~5.8% (d = 10 mm), and ~0.6% (d = 16 mm).

Another model (a heat exchanger) is shown in Fig. 6.

In this case the Reynolds numbers were determined in the wide parts of the model and in the heat-exchanger tubes it was 0.9, 12.2, and 7% respectively.

These experiments showed that measurement of the blackening of photosensitive paper is a suitable method for investigations of heat- and mass-transfer coefficients in process equipment.

Modeling of a Process Involving a Chemical Reaction

The use of the similarity theory for characterization of processes involving chemical reactions has been studied by Damkohler [11], Johnstone [12], Traustel [13], and, almost simultaneously with these workers, by D'iakovon [14]. The latter performed a thorough analysis of the problem as a whole and criticized earlier work; in particular, he drew attention to the limitations in the application of Damkohler's criteria to diffusion processes. D'iakonov introduced the contact criterion Co and the criterion of thermodynamic equilibrium Eq for characterization of the course of processes involving chemical reactions. Traustel proposed the use of the Gulberg – Waage number GW [15], which is less convenient to use.

In the first part of the investigation our aim was to test experimentally* whether it is possible to increase the scale of a process in a homogeneous system with retention of approximate similarity (affined systems) in conformity with the similarity principle. It was not easy to choose a reaction suitable for the investigation, as the reaction should have a large heat effect, should involve a liquid phase, but should not be accompanied by gas formation.

The reaction used in our experiments consisted of the action of an aqueous solution of sodium dichromate and sulfuric acid on a suspension of zinc dust in water.

The similarity theory leads to the conclusion that if it is desired to obtain, by a homogeneous reaction in two affined systems (for example, in tubular reactors) equal amounts of product in unit time per unit volume V of the equipment, geometrical and hydrodynamic similarity of the systems cannot be maintained [1, 11]. However, similarity of the course of the reaction should be retained; i. e., the reaction yields should be the same in both systems, which would correspond to equal degrees of conversion at corresponding points of the reactors, or

*The work was performed jointly with R. Martsinkovskii.

to equality of the criteria I [11]. For similarity of the systems, the temperature increments Δt in the specimen (subscript w) and the model (subscript m) must be maintained equal. Therefore similarity must be maintained between the heat-transfer processes through the reactor walls; i. e., the ratios of the quantity of heat formed in the reaction to the quantity of heat transferred through the reactor walls should be equal for the two systems.

If the amount of material to be converted in the model reactor is to be n times the amount converted in the specimen reactor, the following conditions must be satisfied [11].

The condition for an n-fold scale increase

$$nd_w^2 \cdot w_w = d_m^2 \cdot w_m, \tag{9}$$

where n is the scale ratio, d is the diameter of the reactor tube, and w is the linear velocity of the reagent mixture in the reactor.

The condition for equality of the heat ratios or equality of the criteria IV [11]

$$IV = \frac{Q \cdot U_w \cdot d_w^2}{\lambda \cdot \Delta t_w \cdot Nu_w} = \frac{Q \cdot U_m \cdot d_m^2}{\lambda \cdot \Delta t_m \cdot Nu_m}, \tag{10}$$

where Q is the heat of reaction, U is the reaction rate, λ is the heat-conductivity coefficient of the reagent mixture, Δt is the temperature increase in the system, and Nu is the Nusselt number.

For example, for turbulent flow we have

$$Nu = \text{const } Re^{0.8}, \tag{11}$$

where $Re = \frac{w \cdot d \cdot \rho}{\mu}$.

The condition for equal percentage conversion in the two reactors

$$I = \frac{U' \cdot L_w}{w_w} = \frac{U' \cdot L_m}{w_m}, \tag{12}$$

where U' is a measure of the conversion rate, proportional to U; L is the length of the reactor tube.

Since the chemical reaction is identical, the heat of reaction Q, the heat-conductivity coefficient λ, the density ρ, and the viscosity μ must all be the same for the two systems.

The dimensions of the systems and the flow rates must be so chosen as to satisfy the condition

$$U_w = U_m, \text{ and also } U'_w = U'_m, \tag{13}$$

$$\Delta t_w = \Delta t_m. \tag{14}$$

From the equality of the criteria IV (Equation (10)), with Conditions (13) and (14) taken into account, it follows that

$$\frac{d_w^{1.2}}{w_w^{0.8}} = \frac{d_m^{1.2}}{w_m^{0.8}} \tag{15}$$

and from the equality of the criteria I (Equation (12))

$$\frac{L_w}{w_w} = \frac{L_m}{w_m}. \tag{16}$$

Solving the system of Equations (9), (15), and (16), we finally have [11]:

$$\left.\begin{aligned} d_m &= d_w n^{0.286}, \quad C_d = n^{0.286}, \\ L_m &= L_w \cdot n^{0.428}, \quad C_L = n^{0.428}, \\ w_m &= w_w \cdot n^{0.428}, \end{aligned}\right\} \tag{17}$$

where C_d and C_L are the geometrical affinity factors of the affined systems of the specimen and model.

The experimental unit consisted of two glass tubular reactors of the following dimensions, calculated in accordance with (17), corresponding to a 5-fold scale increase:

reactor I (specimen): L_w = 48.8 cm, d_w = 0.68 cm,

reactor II (model): L_m = 98.5 cm, d_m = 1.10 cm.

The reaction used was the dissolution of zinc dust by sodium dichromate and sulfuric acid.

In one experiment the volume rates were:

reactor I: V_w = 0.81 liters/min (Re_I = 2630),

reactor II: V_m = 4.16 liters/min (Re_{II} = 8350)

with scale ratio n = 5.15.

If our considerations, expressed in the form of Equations (9), (10), and (12), are correct, then the degree of conversion (Y) should be the same in both reactors (Equation (13)), with equal temperature increases Δt at corresponding points of the reactors (Equation (14)).

To test the validity of our reasoning, based on the principle of modeling of chemical processes, these temperature increases, Δt_w and Δt_m, were measured.

For this, 8 thermistors were placed in each of the two tubular reactors, at corresponding points and at equal distances apart. The reactors were cooled externally with water; the difference between the final and initial temperatures of the water was very small, so that the conditions for heat transfer from the side walls of the reactors were the same for both systems.

The experiments showed that in cases when the degree of conversion Y at the reactor exit is 73-74%, the deviations of this value at the separate corresponding points do not exceed 2%.

In the first series of experiments the temperature increases were: in the first reactor Δt_I = 17.2°, in the second reactor Δt_{II} = 17.4°; the deviations between the measured temperatures at corresponding points of the reactors varied from 0.1 to 0.9° (average 0.4°).

In the second series of experiments, conducted in the same reactors, the reagent concentrations were increased by 50% while the remaining conditions were the same as before. For example, in one experiment the scale ratio was n = 5.30, the volume rate V_w = 0.79 liter/minute, and V_m = 4.19 liters/minute.

The temperature increases in the reactors were correspondingly greater than in the experiments of the first series, and were Δt_I = 23.6°, Δt_{II} = 24.1°.

The temperature-variation curves were almost the same for the two reactors (as in the first series of experiments), and the temperature deviations at corresponding points of the reactors were 0.3-1.0° (average 0.5°).

In view of the fact that the measurements cannot be very accurate under the conditions described, it may be concluded that the experimental results provided approximate confirmation, for the example under consideration, of the validity of the model theory as applied to processes involving chemical reactions.

Kinetic processes may be described with the aid of the theory of similarity.

According to D'iakonov [11], for a reaction of the type

$$m_1A_1 + m_2A_2 \rightleftarrows n_1B_1 + n_2B_2 \tag{18}$$

we can derive the criterial equation

$$\frac{1}{\mathrm{Co}} = 1 - Pa, \tag{19}$$

where $\mathrm{Co} = \frac{V_1}{W}$ is the contact criterion, which characterizes the conversion rate; $E_q = \frac{\frac{C_{B_1}^{n_1} \cdot C_{B_2}^{n_2} \cdot \ldots}{C_{A_1}^{m_1} \cdot C_{A_2}^{m_2} \cdot \ldots}}{K_C}$ is the criterion of thermodynamic equilibrium, which is a measure of the deviation of the system from a state of equilibrium.

In these criteria, V_1 is the partial internal velocity of the restoration of thermodynamic equilibrium in Equation (18) from left to right; W is the resultant conversion rate; C is the reagent concentration; K_C is the equilibrium constant, expressed in terms of equilibrium concentrations.

Assuming, on the basis of formal kinetics, that

$$V_1 = K_1 \cdot C_{A_1}^{m_1} \cdot C_{A_2}^{m_2}, \tag{20}$$

and introducing partial pressures P instead of the concentrations C, we have

$$\mathrm{Co} = \frac{K_1 \cdot P_{A_1}^{m_1} \cdot P_{A_2}^{m_2} \cdot \ldots}{W (RT)^{\Sigma m}}, \tag{21}$$

$$E_q = \frac{\frac{P_{B_1}^{n_1} \cdot P_{B_2}^{n_2} \cdot \ldots}{P_{A_1}^{m_1} \cdot P_{A_2}^{m_2} \cdot \ldots}}{K_P}. \tag{22}$$

The validity of Equations (19), (21), and (22) was tested for a generalized criterial equation for a reaction of reversible thermal dissociation, of the type

$$A_{\text{Solid}} \rightleftharpoons B_{\text{Solid}} + C_{\text{gas}}. \tag{23}$$

Use was made of the results of our kinetic studies, conducted jointly with Zawadzki [16], [17], [18], of the reactions

$$\begin{aligned} &CaCO_3 \rightarrow CaO + CO_2, \\ &CaO + CO_2 \rightarrow CaCO_3, \\ &CdCO_3 \rightarrow CdO + CO_2, \\ &CdO + CO_2 \rightarrow CdCO_3. \end{aligned} \tag{24}$$

Introducing into Equations (19), (21), and (22) the partial pressures P_A, P_B, P_C of the reactants in the thermal-dissociation reaction (23), and indicating these pressures by the subscript "O" at equilibrium we may write

$$\frac{\frac{1}{K_1 \cdot P_A}}{\frac{W \cdot RT}{}} = 1 - \frac{\frac{P_B \cdot P_C}{P_A}}{\frac{P_{B_0} \cdot P_{C_0}}{P_{A_0}}}. \tag{25}$$

A reaction of the type of (23) must conform to our relationship [17]*

$$W = \pm K (P_C - P_{C_0}).* \tag{26}$$

*Here the minus sign represents dissociation, and the plus sign, the reverse reaction.

This expression is valid if the pressure of the gaseous component P_C is close to the equilibrium pressure P_{C_0}.

For reactions involving solids, the partial vapor pressures of these solids are constant.

$$P_A = P_{A_0} = \text{const},$$
$$P_B = P_{B_0} = \text{const}. \tag{27}$$

From Equation (25), in conjunction with (26) and (27), we have

$$\frac{1}{\frac{K'}{W}} = 1 - \frac{P_C}{P_{C_0}}, \tag{28}$$

where $K' = \frac{K_1 \cdot P_A}{RT}$ is constant at constant temperature.

It follows that

$$Co = \frac{K'}{W} \tag{29}$$

and

$$E_q = \frac{P_C}{P_{C_0}}. \tag{30}$$

Equation (28) is the general criterial equation for a reaction of thermal dissociation.

From the results of kinetic studies of the four Reactions (24), we calculated the corresponding values of the criteria Eq and Co, and plotted the relationship between the criterion of thermodynamic equilibrium Eq and the contact criterion Co.

In Fig. 7 the points corresponding to the values of Co and Eq for four different reactions are grouped around the same common curve, thereby confirming that Equation (28) is the general criterial equation for reactions of thermal dissociation and reactions proceeding in the reverse direction. By the condition defined for Equation (26), this equation is valid if the reaction proceeds at pressures not far from the pressure of the equilibrium system.

LITERATURE CITED

[1] S. Bretsznajder, Planning of Processes in the Chemical Industry, III (Warsaw, 1956), 213-377.

[2] Ia. M. Rubinshtein, Collected Papers on Steam Turbines (Moscow, 1937). [In Russian]

[3] S. K. Djurdjevic, Genie Chim. 75, 5, 195 (1956).

[4] H. Thoma, Hochleistungskessel (1921).

[5] D. A. Frank-Kamenetskii, Problems of Kinetics and Catalysis 6 (1949), 363. [In Russian]

[6] S. Bretsznajder, and L. Lesniewicz, Przemyst Chemiczny 35 (12), 315 (1956).

[7] A. Apel'baum and M. Temkin, J. Phys. Chem. 22, 179, 195 (1948).

[8] N. Ia. Buben, Collected Papers on Physical Chemistry (AN SSR, 1947), 123 [In Russian]

[9] S. Bretsznajder, Przemyst Chemiczny, 34, 13, 17 (1955).

[10] T. H. Chilton, and A. P. Colburn, Ind. Eng. Ch. 26, 1183 (1935); B. W. Gamson, G. Thodos, and O. A. Hougen, Trans. Am. Inst. Chem. Eng. 39, 1 (1943).

[11] G. Damkohler, Z. Elektroch; 42, 846 (1936); 43, 1 (1937); 46 (1940).

[12] R. E. Johnstone, Trans. Inst. Chem. Eng. 17, 129 (1939); R. E. Johnstone and M. W. Thring, Pilot Plants, Models, and Scale-Up Methods in Chemical Engineering (McGraw-Hill, N. Y. 1957).

[13] S. Traustel, Feuerungstechnik 29, 1, 25, 49, 152 (1941); 31, 1 (1943); Modellgesetze der Vergasung und Verhuttung. Berlin (1949).

[14] G. K. D'iakonov, Proc. Acad. Sci. USSR 39, 4, 143 (1943); 57, 7, 701 (1947); Bull. Acad. Sci. USSR, OTN 78, 473 (1944); Problems of the Similarity Theory in Physicochemical Processes (Moscow, 1956). [In Russian]

[15] S. Bretsznajder, Nowa technika 11, 9-64 (1957).

[16] S. Bretsznajder, Roczniki Chemii, 12, 799 (1932); Kataliza i katalizatory (Catalysis and Catalysts) (Warsaw, 1952).

[17] J. Zawadzki, and S. Bretsznajder, Z. Phys. Chem. 22, 79 (1933); 40, 158 (1938); Z. Elektroch. 41, 215 (1935).

[18] S. Bretsznajder, Roczniki Chemii, 12, 551 (1932); J. Zawadzki, and S. Bretsznajder, Z. Physikal. Chem. 22, 60 (1933).

Received February 5, 1958.

KINETICS OF HEAT AND MASS TRANSFER IN A FOAM LAYER*

I. P. Mukhlenov and E. S. Tumarkina

(The Lensoviet Technological Institute, Leningrad)

It was shown in the preceding communication [1] that processes of heat and mass transfer in a layer of mobile foam, governed by diffusion in the gas phase, may be represented by analogous criterial equations:

$$\frac{k_H}{w_G \cdot c_G \cdot \gamma_G} = A\left(\frac{w_G \cdot D_e}{\nu_G}\right)^m \cdot \left(\frac{H}{h_0}\right)^n \cdot \left(\frac{\nu_G}{a}\right)^q \cdot \left(\frac{h_0}{D_e}\right)^r \cdot \left(\frac{m}{d_0}\right)^s, \quad (1)$$

$$\frac{k_M}{w_G} = B\left(\frac{w_G \cdot D_e}{\nu_G}\right)^m \cdot \left(\frac{H}{h_0}\right)^n \cdot \left(\frac{\nu_G}{D}\right)^q \cdot \left(\frac{h_0}{D_e}\right)^r \cdot \left(\frac{m}{d_0}\right)^s, \quad (2)$$

where A and B are constants; $a = \frac{\lambda}{c_G \cdot \gamma_G}$ is the coefficient of temperature conductivity (in m^2/hour), c_G is the heat capacity of the gas (in kcal/kg. degree); D is the coefficient of diffusion (mx in m^2/hour); D_e is the equivalent diameter (in m), and in the criteria D_e = 1.13 m; d_0 is the diameter of the grid orifices (in m); H is the height of the foam layer (in m); h_0 is the height of the original liquid layer from which the foam on the grid is formed (in m); $w_{G,L}$ is the linear velocity (of the gas or liquid) in the apparatus (in m/second); γ is the density (in kg/m^3); λ is the coefficient of thermal conductivity (in kcal/m · hour · degree); $\nu_{G,L}$ is the coefficient of kinematic viscosity (of the gas or liquid) (in m^2/second or m^2/hour); m is the distance between the orifice centers (in m); k_M is the mass-transfer coefficient; k_H is the heat-transfer coefficient, in kcal · hour · degree per m^2 of grid area (in kcal · m^2 · hour · degree).

It was shown experimentally that k_H and k_M are independent of the geometrical parameters D_e, m, d_0, and that k_H and k_M are proportional to the height of the foam layer, H.

In this paper we consider the influence, on the heat- and mass-transfer coefficients (k_H and k_M), of the other parameters in Equations (1) and (2), namely: the gas velocity w_G, the height of the original liquid layer h_0, and the physical parameters of the system, represented by the Prandtl numbers

$$\left(Pr = \frac{\nu_G}{a} \text{ and } Pr' = \frac{\nu_G}{D}\right).$$

The influence of the gas velocity w_G on k_H and k_M has been studied by many workers [2-12] for different hydrodynamic conditions. Two types of formulas have been proposed for evaluation of the relationship $k = f(w_G)$; particular formulas for a proportionality of the type

$$k = A_1 \cdot w_G + B_1 \quad (3)$$

or formulas of the following type, more convenient for inclusion as factors in general equations:

$$k = A_2 \cdot w_G^n. \quad (4)$$

*Communication II. The experiments were performed jointly with M. E. Pozin and E. Ia. Tarat.

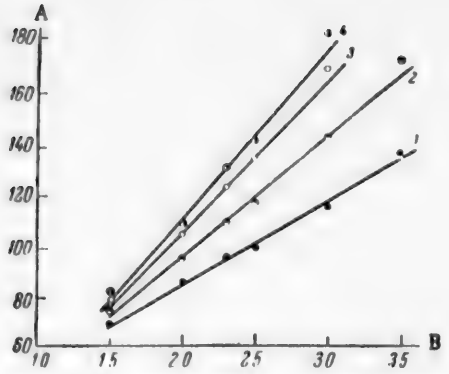

Fig. 1. Effect of air velocity on the coefficient of condensation of water vapor. A) Coefficient of condensation k_a (in kg/m^2· hour· kg/m^3), B) air velocity w_G (m/second). System: moist air – water. Height of foam layer H (mm): 1) 100, 2) 200, 3) 300, 4) 350.

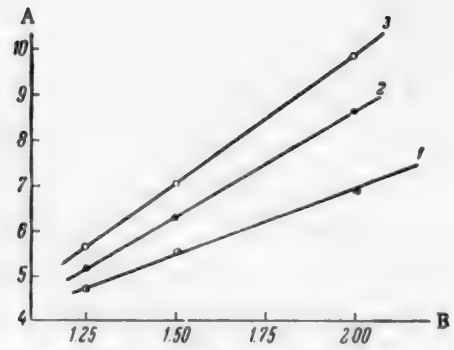

Fig. 2. Effect of air velocity on the coefficient of absorption of ammonia. A) Coefficient of absorption k_a (in kg/m^2· ·hour· kg/m^3), B) gas velocity w_G (m/second). System: air – ammonia mixture and water; grids of m/d_0 (mm/mm) of: 5/2, 6/3 and 6/4. Height of foam later H (mm): 1) 50, 2) 100, 3) 150.

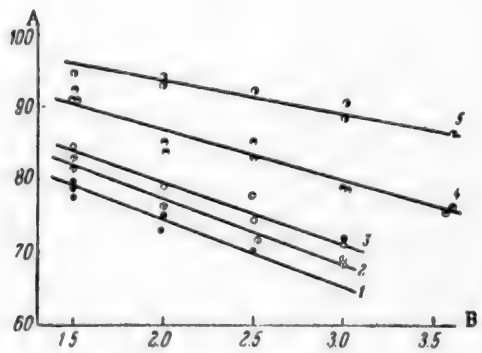

Fig. 3. Variation of the efficiency of a foam layer with the gas velocity in heat transfer from moist air to water. A) Efficiency (%), B) air velocity w_G (m/second). Grids of m/d_0 (mm/mm): 6/3 and 6/4. Height of foam layer H (mm): 1) 100, 2) 120, 3) 140, 4) 200, 5) 300.

In formulas of type (4), values of n vary from 0.625 to 1.8 for investigations carried out under different conditions. However, in most cases, for packed towers and for sieve and bubble-cap towers, n varies between 0.7 and 0.9, and the average value of n is 0.8 [2-8].

In the case of a suspended liquid layer (foam layer), the gas velocity in the apparatus is one of the main factors determining the height and the turbulence of the foam layer, and therefore the rates of mass and heat transfer. In our earlier papers [13, 14] we considered the influence of the gas velocity on k_H and k_M at constant weir height h_w and liquid flow rate i in the apparatus; in this case increase of the gas velocity resulted in changes of the height of the foam layer, foam density, and turbulence of the foam, and therefore the relationship $k = f(w_G)$ was represented by complex curves.

In the present investigation, for determination of the index m in Equations (1) and (2) the relationship between k and w_G should be considered at constant foam height H (independently of h_w and i), and with all the other parameters in Equations (1) and (2) constant. These conditions are satisfied by the experimental data plotted in Figs. 1 and 2.

Experiments showed that the relationships between coefficicients of heat transfer, absorption, and desorption, and the gas velocity at constant foam height are all of the same type, and can be represented by particular equations of the type of Equation (3), where the coefficients A_1 and B_1 are functions of the foam height. In equations of type (4), the average value of the index n, both from the experiental data in Figs. 1 and 2, and from other experimental data (on heat transfer and desorption) is equal to 1. It follows from a comparison of Equations (1) and (2) with (4) that the index of the Reynolds number $m = n - 1$. Therefore, for mass and heat transfer in a foam layer, $m = 0$ in Equations (1) and (2), i. e., the Margules number is independent of the Reynolds number. This is quite understand-

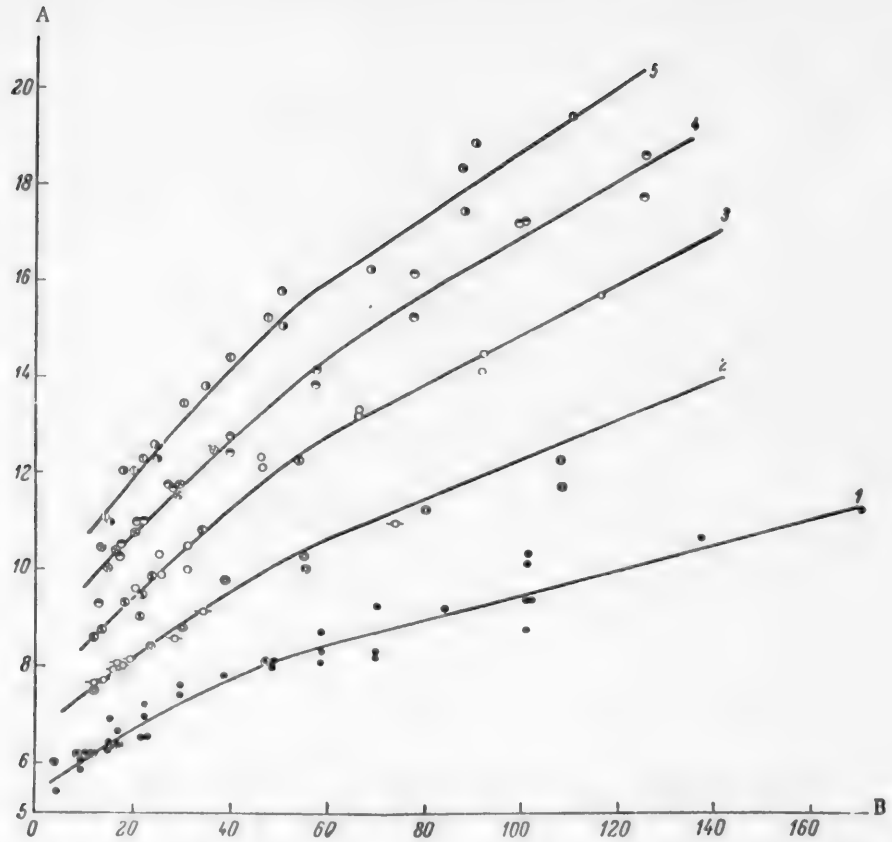

Fig. 4. Variation of heat-transfer coefficient with the height of the original liquid layer.
A) Heat-transfer coefficient $k_H \cdot 10^{-3}$ (kcal/ $m^2 \cdot$ hour $\cdot$ degree), B) Original height of liquid layer $h_0 \cdot 10^3$ (m). System: moist air – water; grids of m/ d_0 (mm/ mm): 6/ 3 and 6/ 4. Air velocity w_G (m/ second): 1) 1.5, 2) 2.0, 3) 2.5, 4) 3, 5) 3.5.

able, as the influence of hydrodynamic factors (including the gas velocity) on the Margules number in Equations (1) and (2) is represented by the criterion of the specific foam height $H_{SP} = H/h_0$ [1, 15].

We now consider the influence of the gas velocity on the efficiency of the foam layer. It was shown in the preceding papers [13, 14] that in heat-transfer and absorption processes involving readily soluble gases the gas velocity does not have any significant influence on the tray efficiency of the foam apparatus at constant weir height, liquid rate, and physical and chemical properties of the system. Under these conditions the decrease of the residence time of the gas in the intertray space is almost balanced by the increase in the height and turbulance of the foam layer. In this respect the foam apparatus differs advantageously from many other types of equipment, in which the extent of the process falls sharply with increasing gas velocity. If the efficiency is determined at constant foam height, it is always found to decrease with increasing gas velocity, as illustrated by the example in Fig. 3. Therefore to increase the efficiency it is necessary to increase the foam height by increase of the original layer of the clear liquid from which the foam is formed.

The effect of the height of the original liquid layer on the heat- and mass-transfer coefficients can be represented by two criteria in Equations (1) and (2).

It was shown earlier [15] that the height h_0 of the original liquid layer on the grid is a function of the weir height h_w, the liquid rate i, and the support of the liquid at the overflow orifice. In our earlier papers [13, 14] the influence of the weir and accumulation of foam, i. e., increase of h_0 as the result of support on the foam in the overflow orifice, was not considered accurately enough. Therefore an "anomalous increase of k_H" was observed in precisely those instances where there was considerable foam support.

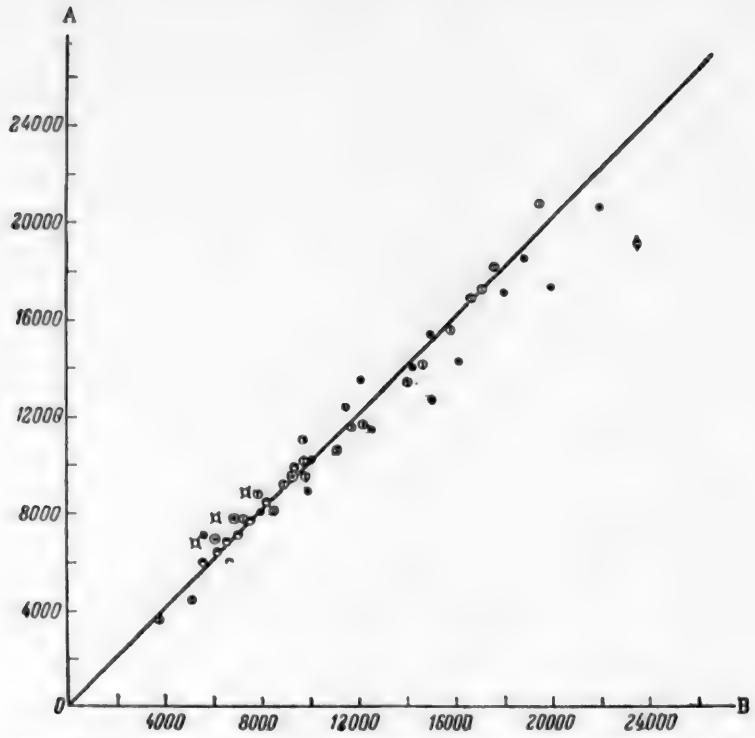

Fig. 5. Comparison of experimental and calculated values of heat- and mass-transfer coefficients in foam equipment.
A) Values of k_{expt} (in kcal/m^2·hour·degree or kg/m^2·hour·kg/m^3), B) values of k calculated from Equations (5) and (6) (in kcal/m^2·hour·degree or kg/m^2·hour·kg/m^3).

The relationship $k_H = f(h_0)$ is plotted in Fig. 4, which is typical not only for heat transfer but also for absorption of soluble gases. This relationship is similar to the relationship between H and h_0, considered in our previous papers [14, 16]. It therefore seemed likely that the influence of h_0 on k is completely represented by the relationship k = f(H), found prviously [1]. In fact, determination of the values of n and r in Equations (1) and (2) by graphical analysis of the experimental data showed [16] that for heat transfer r = n − 0.003, and for absorption r = n − 0.005. Since $n \geq 0.3$, for technical calculations it may be assumed that r = n. Therefore the influence of h_0 in the two criteria of Equations (1) and (2) is mutually compensated, i. e., it is expressed completely by H.

The effect of the physical properties of the liquid and gas on the rates of heat and mass transfer, for readily soluble gases, should be represented mainly by the height of the foam layer H and the Prandtl number in Equations (1) and (2).

Comparison of experimental data on the transfer of heat from moist air to water, NaCl solution, and various liquors of the soda industry [14] showed that the heat-transfer coefficients for different liquids differ in accordance with the heights of the foam formed by the different liquids. Mass transfer of readily soluble gases, like heat transfer, is controlled by diffusion (turbulent or molecular) in the gas phase, and therefore the physical and (within certain limits) even the chemical properties of the liquid cannot influence the mass-transfer coefficients. Therefore the influence of physical properties on the coefficients of heat and mass transfer in the systems in question is determined by the Prandtl number for the gas phase [1, 16].

The values of the index q of the Prandtl criterion in Equations (1) and (2) should not depend on the hydrodynamics of the gas − liquid interaction. In fact, a survey of extensive literature data showed [16] that the great majority of workers found the same value of q in formulas of the type $K = A_3 \cdot Pr^q$; q = 0.33. Large deviations in the values of q obtained by some investigators can be attributed to experimental error or to incorrect derivation

of the criterial equations. It was found that the influence of Pr and Pr' on heat transfer and absorption in our experiments fully corresponds to the formula

$$k = A_3 \cdot Pr^{0.33}.$$

Equations for calculation of k_H and k_M are derived by substitution of the values found for the indices into Equations (1) and (2), and determination of the constants A and B from experimental data.

In the present and preceding [1] communications it is shown how our own experimental data and literature information were used to find the indices in Equations (1) and (2): m = 0, n = r = 0.3 – 0.4, q = 0.33, s = 0. Taking average values of the indices from the results of different series of experiments, we used the method of averages to calculate the constants A and B in Equations (1) and (2) from extensive experimental data [16]. As a result, the following calculation formulas were derived.

For heat transfer

$$\frac{k_H}{w_G \cdot c_G \cdot \gamma_G} = 9.58 \left(\frac{H}{h_0}\right)^{0.33} \left(\frac{\nu_G}{a}\right)^{0.33} \left(\frac{h_0}{D_E}\right)^{0.33} = 9.58 \sqrt[3]{H_{S_p} \cdot Pr \cdot \Gamma} \qquad (5)$$

or

$$k_H = 9.20 w_G H^{0.33} \cdot \nu_G^{0.33} \cdot a^{-0.33} \cdot c_G \gamma_G \text{ kcal/m}^2 \cdot \text{hr} \cdot \text{degree}, \qquad (5a)$$

where $9.20 = 9.58 \cdot D_e^{-0.33} = 9.58 : \sqrt[3]{1.13}\ 1/\text{m}^{0.33}$.

For the absorption of readily soluble gases (and condensation of water vapor)

$$\frac{k_a}{w_G} = 2.76 \left(\frac{H}{h_0}\right)^{0.33} \left(\frac{\nu_G}{D}\right)^{0.33} \left(\frac{h_0}{D_e}\right)^{0.33} = 2.76 \cdot \sqrt[3]{H_{S_p} \cdot Pr' \cdot \Gamma} \qquad (6)$$

or

$$k_a = 2.65 \cdot w_G H^{0.33} \cdot \nu_G^{0.33} \cdot D^{-0.33} \text{ kg} / \text{m}^2 \cdot \text{hr} \cdot \text{kg} / \text{m}^3 \qquad (6a)$$

where

$$2.65 = 2.76 : \sqrt[3]{D_e}\ 1/\text{m}^{0.33};$$

$H_{SP} = \frac{H}{h_0}$ is the specific foam height; $Pr = \frac{\nu_G}{a}$ is the Prandtl thermal criterion; $Pr' = \frac{\nu_G}{D}$ is the Prandtl diffusion criterion; $G = \frac{h_0}{D_e}$ is the geometrical term representing the ratio of the height and length of the original liquid layer on the grid; k_a is the over-all gas-phase mass-transfer coefficient in absorption, m/hour (kg/m^2 · hour · kg/m^3 of gas).

The validity of Equations (5) and (6) was tested for various gas – liquid systems over a wide range of conditions: w_G from 1.5 to 3.5 m/second, H from 50 to 400 mm, k_H from 5,000 to 20,000 kcal/m^2 · hour · degree, and k_M over the same range.

The experimental values of the heat- and mass-transfer coefficients are compared with the values calculated from Equations (5) and (6) in Fig. 5. Points based on experimental data on heat transfer from air and other gases to production liquors, on absorption of ammonia by water and of nitrogen oxides by sulfuric acid, on condensation of water vapor and evaporation of water under industrial conditions are plotted. Fig. 5 shows that the equations are sufficiently accurate for technical calculations.

For many practical calculations, Equations (5a) and (6a) are simplified considerably. For example, it is known that the values of Pr and Pr' for a given gas – liquid system remain virtually constant over a wide range of temperatures; for example, Pr for air remains almost unchanged between 10 and 500° [17]. In all our experiments on heat transfer from air and from gases highly diluted with air, at atmospheric pressure, Pr = 0.716, and Equation (5a) becomes

$$k_H = 2.37 \cdot w_G \cdot H^{0.33} \text{ kcal/m}^2 \cdot \text{hr} \cdot \text{deg} \quad (7)$$

or

$$M = \frac{2.37}{c_G \cdot \gamma_G} \cdot \sqrt[3]{H}, \quad (7a)$$

where $M = \frac{k_G}{w_G \cdot c_G \cdot \gamma_G}$ is the Margules thermal criterion.

For condensation of water vapor at atmospheric pressure

$$Pr^1_{H_2O} = 0.669 \text{ and } k_a = 2.32 \cdot w_G \cdot H^{0.33} \text{ kg/m}^3 \cdot \text{hr} \cdot \text{kg/m}^3 \quad (8)$$

or

$$M' = 2.32 \sqrt[3]{H}, \quad (8a)$$

where $M' = \frac{ka}{w_G}$, the Margules diffusion criterion (or the D'iakonov criterion Di).

For absorption of ammonia by water at an average NH_3 concentration of 1.5% in the gas (average between the values at the entry and exit of the gas from the foam layer), $Pr_{NH_3} = 0.765$,

$$k_a = 2.43 \cdot w_G \cdot H^{0.33} \text{ kg/m}^2 \cdot \text{hr} \cdot \text{kg/m}^3 \quad (9)$$

or

$$M' = 2.43 \sqrt[3]{H}. \quad (9a)$$

Equations (7) - (9) show that in the experimental conditions used the magnitude of the Margules criterion is determined entirely by the foam height. To increase the operating rate it is necessary to increase the height of the foam layer and the gas velocity w_G. However, increase of H above 400 mm is generally unsuitable [1], while increase of the velocity above 3.5 m/second (and in some cases above 2.5 m/second) results in much spray loss.

Comparison of Equations (5) and (6) shows that only equality of the coefficients is lacking for complete analogy between heat-transfer processes in gas – liquid systems and absorption of readily soluble gases. However, the inequality $9.58 \neq 2.76$ is purely formal, and is the consequence of differences in the structure of the Margules criterion in these equations. For example, in many of our experiments on heat transfer from air at 20° $c_G = 0.24$ kcal/kg · degree and $\gamma_G = 1.2$ kg/m^3. Substitution of these values of c and γ_G into Equation (5) gives

$$\frac{k_H}{w_G} = 2.76 \left(\frac{H}{h_0}\right)^{0.33} \cdot \left(\frac{\nu_G}{a}\right)^{0.33} \cdot \left(\frac{h_0}{D_e}\right)^{0.33}, \quad (5b)$$

which is identical to Equation (6), but has the dimensional coefficient 2.76 kcal/m^3 · degree.

The identity of Equations (5b) and (6) confirms that there is an analogy between the processes, and verifies the validity of the original criterial Equations (1) and (2). This analogy makes it possible to use experimental data obtained in one process for approximate calculations relating to any analogous process.

Analysis of experimental data on desorption of gases [16, 17] showed that an equation of the type of (6) does not fully describe the desorption process. It was shown for the desorption of ammonia from filtration liquors* in the soda industry [16] that an equation of the following type can be used for desorption calculations:

$$\frac{k_d}{w_G} = B_d \left(\frac{H}{h_0}\right)^{0.33} \cdot \left(\frac{i}{\nu_L}\right)^{0.4} \cdot \left(\frac{\nu_G}{D_G}\right)^{0.33} \cdot \left(\frac{h_0}{D_e}\right)^{0.33}. \quad (10)$$

* The synthetic filtration liquor used was an aqueous solution of the following composition (in g/liter): NH_4Cl 160, NaCl 70, NH_4HCO_3 45, $(NH)_2CO_3$ 30.

where k_d is the over-all mass-transfer coefficient in desorption (in m/hour), $\underline{i}$ is the liquor flow rate in m^3/hour per meter length of the overflow orifice ($m^3/m \cdot hour = m^2/hour$), $Re_L = \frac{w_L \cdot h_0}{\nu_L} = \frac{\underline{i}}{\nu_L}$ is the Reynolds number for the liquid on the grid of the apparatus.

The criterion Re_L represents the influence of the rate at which the desorbed component enters into the zone of liquid – gas interaction, on the desorption coefficient k_d.

Therefore there is not a complete analogy between absorption and desorption.

SUMMARY

1. The rates of heat and mass transfer in a foam layer of a given gas – liquid system are determined mainly by the height of the foam layer and the gas velocity in the apparatus. The heat- and mass-transfer coefficients of readily soluble gases are proportional to the height of the foam layer and the gas velocity.

2. The heat- and mass-transfer efficiency of a tray of the foam apparatus increases with increasing height of the foam layer. The efficiency does not depend to any significant extent on the gas velocity in the apparatus if the other hydrodynamic conditions (height of the weir, liquid flow rate, properties of the gas and liquid) are constant. The efficiency determined at constant foam height falls regularly with increase of the gas velocity.

3. The influence of the physical properties of the liquid and gas on the rates of heat transfer and absorption of readily soluble gases is expressed in terms of foam height and the Prandtl number in Equations (5) and (6).

4. Generalization and graphical analysis of our experimental data and literature information yielded the general Equations (5) and (6), suitable for calculations of heat- and mass-transfer coefficients or other process parameters (included in these equations) over a wide range of conditions.

5. Simple particular equations (7-9) have been derived for calculations of heat-transfer, water-vapor condensation, and ammonia absorption coefficients.

6. There is shown to be an analogy between heat-transfer processes and absorption of readily soluble gases; it is therefore possible to utilize experimental data, determined for one process, for approximate calculation of the parameters in an analogous process.

7. It is shown that desorption of readily soluble gases is not fully analogous to absorption. Equation (10) is proposed to represent the desorption process; it was verified for the desorption of ammonia from Solvay filtration liquor.

LITERATURE CITED

[1] I. P. Mukhlenov, J. Appl. Chem. 31, 9, 1342 (1958).*

[2] V. M. Ramm, Heat-Transfer Equipment (Goskhimizdat, 1948). [In Russian]

[3] V. M. Ramm, Absorption Processes in Chemical Industry (Goskhimizdat, 1951). [In Russian]

[4] L. D. Berman, Evaporative Cooling of Circulation Water (Gosenergoizdat, 1949). [In Russian]

[5] N. M. Zhavoronkov, Hydraulic Principles of the Scrubber Process and Heat Transfer in Scrubbers (Soviet Science Press, 1944). [In Russian]

[6] A. G. Kasatkin, Fundamental Processes and Equipment in Chemical Technology (Goskhimizdat, 1955).

[7] S. S. Kutateladze, Heat Transfer in Condensation and Evaporation (Mashgiz, 1952).

[8] I. N. Kuz'minykh et al., Chem. Ind. 2, 86 (1954).

[9] D. W. Van Krevelen, and P. Y. Hoftijzer, Rec. Trav. Cheim. 66, 1-2, 49, 67 (1947); 7-8, 513 (1947); Chem. Eng. Progr. 44, 7, 529 (1948).

[10] W. H. McAdams, I. B. Pohlens, and R. John, Chem. Eng. Progr. 45, 4, 241 (1949).

[11] T. K. Sherwood, and R. L. Pigford, Absorption and Extraction (1952).

* Original Russian pagination. See C. B. Translation.

[12] F. West, W. Gilbert, and T. Shimizu, Ind. Eng. Chem. 44, 10, 2470 (1952).

[13] I. P. Mukhlenov and E. S. Tumarkina, J. Appl. Chem. 28, 2, 135; 4, 346 (1955).*

[14] M. E. Pozin, I. P. Mukhlenov, E. S. Tumarkina, and E. Ia. Tarat, The Foam Method for Treatment of Gases and Liquids (Goskhimizdat, 1955).

[15] I. P. Mukhlenov. J. Appl. Chem. 31, 1, 45 (1958).*

[16] I. P. Mukhlenov, Dissertation, Leningrad (1955). [In Russian]

[17] N. M. Zhavoronkov, Hydraulic Principles of the Scrubber Process and Heat Transfer in Scrubbers (Soviet Science Press, 1944). [In Russian]

Received August 20, 1957.

* Original Russian pagination. See C. B. Translation.

LABORATORY COLUMN FOR MICROFRACTIONATION

A. I. Levin

(All-Union Scientific Research Institute of Petrochemical Processes)

In analytical fractionation, a very important characteristic of the column is the minimum volume of the substance to be fractionated.

How can the minimum volume of the substance for fractionation be determined? It is evident that the volume of the substance put in must be greater than the holdup of the reflux in the column. However, it is not yet clear how much greater it must be. Quite often certain authors give volumes of still charges for their columns which hardly exceed the reflux holdup.

We consider it desirable to introduce the concept of the minimum charge volume, which is taken to be 10 times the total reflux holdup under standard operating conditions. Despite its arbitrary nature (for which there is some measure of experimental support) this criterion helps to clarify the issue and may therefore be useful.

Another unsolved question is, what is to be regarded as microfractionation. Some authors consider microfractionation to refer to volumes of tenths of a milliliter, and others, to tens of milliliters.

In view of the level of modern laboratory rectification techniques and of the requirements of control and research laboratories, the following classification may be suggested: microfractionation – up to 2 ml, semimicrofractionation, from 2 to 10 ml, small-scale fractionation, 10 to 50 ml, and normal fractionation, more than 50 ml.

The literature contains relatively few publications on the design and testing of columns for micro- and semimicrofractionation.

For semimicrofractionation, concentric-tube columns and small spiral columns have proved the most suitable. Among the best apparatus of this type is the Irlin – Bruns column [1], which can be used for fractionation of about 10 ml lots of material, with a column efficiency of up to 50 theoretical plates. The columns described by Weston [2], Selker et al. [3], and many others cannot be described as microcolumns, as the normal charge for them is 10-50 ml. The microcolumn of Shrader and Ritzer [4] is a simple reflux column 7-15 cm high, without a condenser and without temperature recording, differing little in efficiency from a distillation flask. Similarly, the Tidcke apparatus [5] hardly has an efficiency higher than 1-2 theoretical plates. Other microcolumn designs are no better. In general, one must agree with the views of Weygand [6]: "All attempts to make it possible to separate fractions in the distillation of very small amounts of liquids . . . fail . . . Therefore we shall not describe the numerous complex fractionation units which have been proposed for distillation of a few cubic centimeters of liquid."

It is quite evident that the trend in the design of microfractionation apparatus should be the use wetted-wall columns, with maximum increase of the contact area and improvement of the interphase mass-transfer conditions.

Our aim was to design a column with efficiency of not less than 25 theoretical plates, for fractionation of 2-5 ml of liquid.

EXPERIMENTAL

In a search for the optimum design, a series of preliminary tests was carried out on different types of pack-

TABLE 1

General Characteristics of Columns 2, 4, and 6 mm in Diameter, with Different Packings and without Packing

Column No.	Column dimensions		No. theoret. plates	Height equal to a theoret. plate (cm)	Reflux holdup (ml)	Maximum flow rate (ml/min)
	diameter (mm)	height (cm)				
9a *	6	18	1.5	12.0	—	—
9	6	18	9.0	2.0	0.7	1.4
10	6	18	8.0	2.3	0.8	1.6
11	6	18	20.5	0.9	1.0	1.2
3a	4	25	7.5	3.3	—	—
3	4	21	7.5	2.8	0.4	0.8
4	4	25	8.0	3.1	0.6	0.3
5	4	23	9.0	2.6	0.5	0.5
6	4	25	7.5	3.3	0.6	0.9
7	4	15	10.5	1.4	0.7	0.4
8	4	20	17.5	1.1	0.6	0.7
1	2	20	10.0	2.0	0.1	1.6
2	2	100	18.5	5.4	0.5	1.6

* The subscript "a" corresponds to the same columns but without packing (empty tubes).

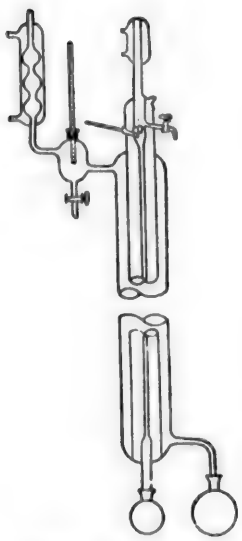

Fig. 1. Wetted-wall microfractionation column.

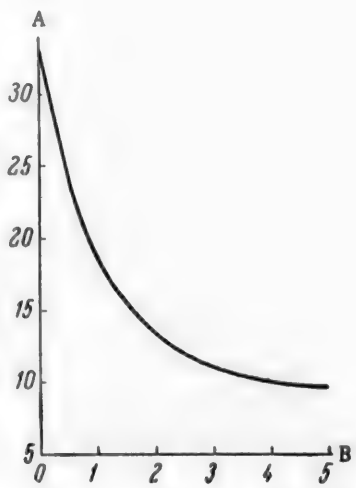

Fig. 2. Efficiency of the microcolumn at different collection rates.
A) Number of equivalent plates,
B) collection rate (ml/hour).

ing and columns of small diameter. Brief descriptions and dimensions of these columns are given below.

Column No.1. Without packing, diameter 2 mm, height 20 cm; the top and bottom ends of the tube widened to 6 mm; the refluxing liquid flows down the tube walls.

Column No.2. A similar column, but 100 cm high.

Column No. 3. Diameter 4 mm, height of the packing section 21 cm; a round glass rod 2.8 mm in diameter is inserted in the tube, to leave an annular gap of 0.6 mm.

TABLE 2

Efficiency of Wetted-Wall Column No 12 under Various Operating Conditions

Reflux (ml/minute)	Collection rate (ml/hour)	Number of equivalent plates	Reflux (ml/minute)	Collection rate (ml/hour)	Number of equivalent plates
0.17	0	33.0	0.17	0.5	25.0
0.33	0	20.5	0.17	1.0	18.5
0.67	0	12.0	0.17	2.0	13.5
1.00	0	10.5	0.17	3.0	11.0
1.00	0.5	7.5	0.17	4.0	10.5
0.67	0.5	9.5	0.17	5.0	9.5

TABLE 3

General Characteristics of Wetted-Wall Column No. 12

Characteristics	Values	Characteristics	Values
Maximum number of theoretical plates at equilibrium (TP)	33.0	Maximum possible reflux (ml/minute)	1.7
Height equivalent to a theoretical plate (cm)	3.0	Reflux holdup in column: total (ml)	0.5*
Number of equivalent plates under operating conditions (EP)	25.0	specific (ml/TP)	0.01
Height corresponding to an equivalent plate (cm)	4.0	Minimum volume of charge (ml)	5.0
Nominal efficiency of colum (EP/TP)	0.76	Time to reach equilibrium (hours)	1.0
		Resistance in column (mm H_2O)	9

*Including 0.3 ml in the overflow chamber and stopcock.

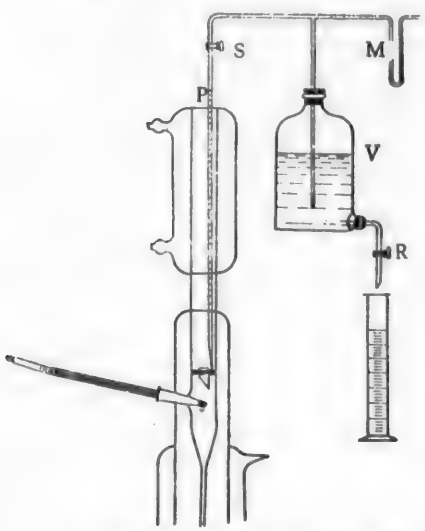

Fig. 3. System for distillate collection from the microcolumn.

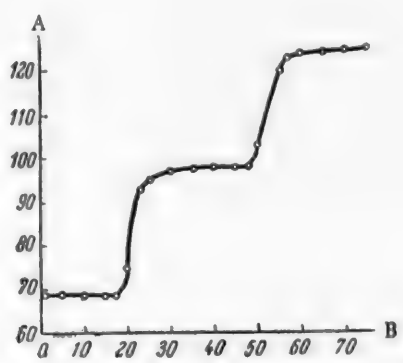

Fig. 4. Distillation curve for an alkane mixture with the use of the microcolumn.
A) Temperature (°C), B) distillate yield (%).

Column No.4. Diameter 4 mm, height 25 cm; rod 2.8 mm in diameter is inserted in the tube, with copper wire 0.6 mm in diameter wound spirally around the rod with 2 mm between the spiral turns; the rod and spiral fit closely into the column.

Column No.5. Diameter 4 mm, height 23 cm; the inner wall of the tube carries a wire spiral as in Column No 4, but the inner rod is 1.8 mm in diameter; the annular gap between the rod and the spiral turns is 0.5 mm.

Column No.6. Diameter 4 mm, height 25 cm; packing consists of 4 slightly extended and intercoiled 3-sided spirals.

Column No. 7. Diameter 4 mm, height 15 cm; packing of single-turn spirals 1.0 mm in diameter made from copper wire 0.2 mm in diameter.

Column No. 8. Diameter 4 mm, height 20 cm; packing of 3-sided spirals [7].

Column No. 9. Diameter 6 mm, height of the packing section 18 cm; packing consists of a glass rod 2 mm in diameter, with a 3-sided spiral wound closely, turn to turn, around it. The size of the spiral is so chosen that the rod and spiral fit closely into the column.

Column No. 10. Same dimensions; packing consists of three slightly extended 3-sided spirals twisted together.

Column No. 11. Same dimensions; loose packing as in Column No. 8. The columns were tested under equilibrium conditions for a mixture of benzene + dichloroethane. The results of the tests are given in Table 1.

These results show that all the columns tested have relatively high holdup and low efficiency.

The most promising were the wetted-wall columns 2 mm in diameter. Further work was directed at improving their efficiency.

The following experiments were carried out in order to study the effect of the state of the glass surface on the flow of the liquid film. Two glass plates of equal size were taken; one with a smooth and the other with a frosted surface. Both plates were thoroughly cleaned, washed, and dried. Experiments on drop spreading were performed on the plates placed horizontally, and experiments on the motion of liquid streams, on the plates in inclined and vertical positions. All the experiments were performed under the same conditions, simultaneously on both plates.

Visual observations of the spreading and flow of liquids over smooth and frosted glass surfaces, and the necessary calculations, showed that on a smooth horizontal surface the spreading area of a drop of isooctane is approximately one half, and the time of complete evaporation (drying) is 1.5 times, the corresponding values for a frosted surface. With the plates in a vertical position, benzene flowed along the smooth surface in a fine stream, thicker along the axis and thin at the edges; on the smooth surface the stream spread in an even film, and formed a broad band. When the liquid flow was discontinued, the trail on the surface disappeared immediately, but persisted for more than 3 minutes on the frosted glass.

Calculations showed that the area of the liquid film on the frosted glass is treble that on the smooth glass, and the thickness is correspondingly one third. Despite the fact that the film on the frosted glass is thinner, it is retained much better. Therefore in a column with a frosted surface the active contact area is greater and the mass-transfer conditions are better.

This formed the principle of a new type of wetted-wall column for microfractionation.

A general view of the column is shown in Fig. 1.

The column (No 12) consists of a distillation tube 2 mm in diameter and 100 cm high, with a rough (etched) inner surface. The inner surface of the tube is roughened by means of hydrofluoric acid, by blasting with fine sand, or by means of a piston with a grinding disk on the end. The upper and lower ends of the tube are widened to 6 mm to prevent flooding. A flask 5-10 ml in capacity is fitted to the bottom end by means of a ground-glass joint. In the upper widened end there is a plate with an overflow spout 4 mm in diameter. A capillary stopcock for collection of the distillate is fitted above the overflow plate. The lower end of the chamber is drawn out so that the drops formed should be as small as possible and should flow onto the wall of the distillation tube. The condenser is fitted directly at the top of the tube. A ground-glass joint for a special thermometer is provided below

the overflow spout. The distillation tube is sealed in a vacuum jacket in which the residual pressure is 10^{-6} mm Hg. The column is equipped with a vapor heating system. A substance of suitable boiling point is put into the flask of the vapor heating system. The vapor of this substance heats the column jacket.

The column was tested at equilibrium and under operating conditions, with benzene – dichloroethane mixture*.

The test results are presented in Tables 2 and 3.

The data in Table 2 show that the efficiency of this column decreases sharply with increasing reflux, both at equilibrium and under operating conditions. This is the consequence of worsening of the mass-transfer conditions caused by increases of the film thickness and vapor speed.

With increase of the collection rate at constant reflux the column efficiency falls sharply (Fig. 2), and therefore the rate of distillate collection should be maintained at not over 0.5 ml/hour.

Comparison of the efficiencies of Columns No 2 and No 12 shows that as the result of the proposed treatment (frosting) of the inner tube surface the separating power of the column is almost doubled.

The efficiency of Column No.12 is 33 theoretical plates at equilibrium, and 25 equivalent plates at a collection rate of 0.5 ml/hour.

Because of the relatively large amount of liquid held in the overflow spout and stopcock, this column is suitable for distillation of 5 ml quantities, i. e., for semimicrofractionation.

A second column (No.13) for microfractionation was constructed similarly to the one described above. The height of this column is 50 cm; the vacuum jacket is silvered, while the vapor jacket is detachable and can be easily replaced by an ordinary electrically-heated jacket. The projecting portion of the overflow spout was eliminated in order to decrease the holdup. If less than 2 ml of material is distilled, the collecting stopcock is covered from above with mercury, and the distillate is collected by means of a micropipet graduated in 0.01 ml divisions. If it is necessary to collect the distillate by fractions, the collection is carried out at intervals, each fraction being drawn into a separate micropipet by small portions. If the purpose of the distillation is to determine the boiling-temperature curve of a mixture, the distillate is collected continuously and uniformly into the same pipet, and the boiling point is recorded for definite volumes collected in the pipet (for example, at intervals of 0.05 ml). The system shown schematically in Fig. 3 was used for this purpose.

The capillary micropipet P with a stopcock S is fixed vertically; its lower end rests on the overflow plate, and the upper end is connected to a water manometer M and a vessel V filled with water. When the required conditions have been reached, the stopcock S is opened and water is run out of the vessel V, so that the distillate is sucked into the pipet. The collection rate is regulated by means of a precision stopcock R through which the water is let out. The purpose of the manometer is to ensure a constant vacuum in the system.

It must be pointed out that this collection system is somewhat complicated, and a high degree of skill is needed to operate it. Therefore the collecting stopcock should be used whenever conditions allow.

Tests of Column No.13 showed that its efficiency reaches 23 TP, and the holdup does not exceed 0.2 ml.

In order to decrease reflux holdup in Column No 12, described above, the collecting stopcock and the projecting portion of the overflow spout were filled with mercury, and the distillate was collected by the method just described. The reflux holdup was then 0.2 ml, and the column was suitable for microfractionation.

The distillation curve for 3 ml of a ternary mixture of alkanes is shown in Fig. 4. The characteristic feature here is not the effective separation (which is easily achieved with an ordinary column) but the small amount of substance fractionated.

It follows from these results that this column design fully conforms to the original requirements, both with regard to the volume of the liquid fractionated, and to the effectiveness of separation.

For comparison, it may be noted that the wetted-wall column described by Rose [8], 3 mm in diameter, had an efficiency of 9.5 TP; moreover, its operation was so difficult that the author himself did not recommend the use of columns less than 6 mm in diameter.

* The tests were conducted by L. O. Semeniuk.

SUMMARY

A wetted-wall column has been designed, suitable for microfractionation, with an etched (frosted) inner surface of the distillation tube; the efficiency of a wetted-wall tube is approximately doubled by such treatment of the inner surface.

LITERATURE CITED

[1] A. L. Irlin, and B. P. Bruns, J. Anal. Chem. 1 (1950).

[2] P. Weston, Ind. Eng. Chem. 5, 179 (1933).

[3] M. L. Selker, R. E. Burk, and H. P. Lankelma, Ind. Eng. Chem. 12, 352 (1940).

[4] S. Shrader, and I. Ritzer, Ind. Eng. Chem. 11, 54 (1939).

[5] C. Tidcke, Ind. Eng. Chem. 51, 81 (1943).

[6] C. Weygand, Experimental Methods in Organic Chemistry, I (IL, 1950) [Russian translation].

[7] A. I. Levin, Petroleum Economy 10 (1949).

[8] A. Rose, Ind. Eng. Chem. 28, 1210 (1936).

Received March 15, 1957.

INVESTIGATION OF BRIGHT NICKEL-PLATING BATHS

T. A. Mechkovskaia

The question of bright electrolytic nickel plating now occupies an important place in electroplating technology. A considerable number of publications deal with bright nickel-plating baths and the mechanism of bright deposit formation. The book of Kudriavtsev and Fedurkin [1] contains the principal characteristics of bright nickel plating, descriptions of the properties of the deposits, electrolysis conditions, and an account of the process. The literature on bright nickel plating is cited in Springer's paper [2].

Despite the considerable number of papers in this field, the question of the mechanism of formation of bright nickel deposits is still not clear, as the available experimental data are not yet adequate for the formulation of a precise theory of the formation of bright deposits. These data are supplemented to some extent by the material presented in this paper.

A study was made of the effects of electrolysis conditions and electrolyte composition on the reflectance of the deposits, current efficiency, and cathode polarization. The brightening additives used were sulfonated naphthalene (the technical product [3]) and the sodium salts of 2,6- and 2,7-disulfonaphthalic acids [4]).

EXPERIMENTAL

The reflectance of nickel deposits* was measured by means of a reflectometer with a selenium photocell, to an accuracy of 0.5-1.0%. The nickel deposits were formed on flat polished steel and brass plates 25 mm in diameter and 5 mm thick. The bath was of the simplest composition (Bath IV, Table 1) and contained no metal cations other than nickel. Introduction of small amounts of sulfonated naphthalene lowers the reflectance coefficient somewhat (Fig. 1, Curves 1 and 2) rather than raising it. Bright deposits of the maximum reflectance coefficient obtainable for nickel, irrespectively of the thickness, are formed only when the sulfonated naphthalene content exceeds 0.20 g/liter. When pure sodium salts of disupfonaphthalic acids were used as brighteners, the reflectance coefficient was lowered at lower concentrations (0.02-0.05 g/liter).

The electrolyte acidity has a significant influence on the reflectance of nickel deposits. The reflectance decreases with increasing pH for baths without additives. In a bath containing sulfonated naphthalene increase of pH up to 6.3 results in a considerable increase of the reflectance coefficient, but at pH above 6.3 the luster decreases sharply and rough deposits are formed.

The effect of electrolyte composition on the reflectance of nickel deposits was studied for the electrolytes the composition of which is given in Table 1. All the electrolytes contained 2 g of sulfonated naphthalene per liter.

The reflectance coefficients of deposits, 20μ thick, formed in these baths under various deposition conditions are given in Table 2.

Bright deposits of high reflectance were formed from all the baths studied, over fairly narrow ranges of pH (5.8-6.3), current density (1-3 amps/dm^2), and temperature (20-40°). The best results were obtained with Bath IV. Bath V (containing ammonium sulfate) gave deposits of poor reflectance.

The effects of additions of zinc and iron to the electrolyte on the reflectance of the deposits were studied.

*I. F. Plokhotnikova took part in this section of the work.

TABLE 1

Electrolyte Compositions

Components	Bath composition (g/liter)				
	I	II	III	IV	V
$NiSO_4 \cdot 7H_2O$	170	170	170	170	170
H_3BO_3	30	30	30	25	—
KCl	5	5	—	—	8
KF	—	6	—	—	—
NaCl	—	—	15	—	—
$NiCl_2 \cdot 6H_2O$	—	—	—	30	—
$(NH_4)_2 \cdot SO_4$	—	—	—	—	21

TABLE 2

Reflectance Coefficients (1)

Bath		I		II		III		IV		V	
t°	pH	Current density (amps/dm²)									
		1	3	1	3	1	3	1	3	1	3
20	4.0	43.0	35.5	50.0	53.6	30.5	32.0	40.5	52.0	39.5	27.0
20	6.0	58.5	41.5	60.5	48.0	54.0	28.5	48.0	60.0	48.0	53.0
40	4.0	55.0	57.0	57.0	58.0	48.0	51.5	45.0	60.5	55.0	54.0
40	6.0	59.0	61.5	61.0	61.5	52.0	55.0	62.0	62.0	55.5	60.0

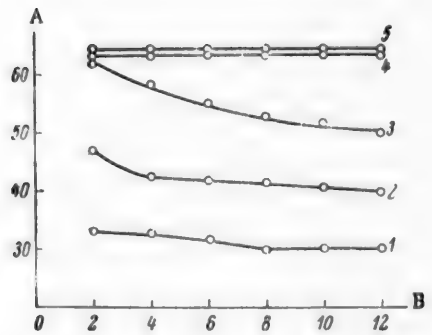

Fig. 1. Effect of the concentration of sulfonated naphthalene in the electrolyte on the reflectance of nickel deposits.
A) Reflectance coefficient (%), B) thickness of nickel deposit (%). Concentration of sulfonated naphthalene (g/liter): 1) 0.03, 2) 0.10, 3) without additive, 4) 6.60, 5) 0.30 and 1.7

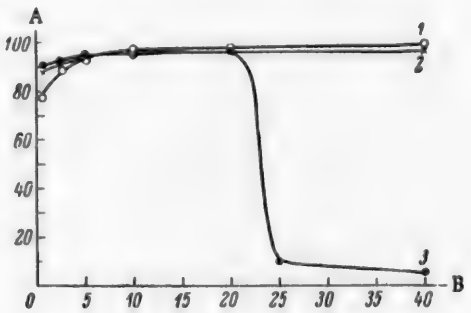

Fig. 2. Effect of current density on the current efficiency for nickel, in baths with and without added sulfonated naphthalene.
A) Current efficiency (%), B) current density (ma/cm²). Concentration of sulfonated naphthalene (g/liter): 1) without additive, 2) 1.7, 3) 3.3.

In baths containing disulfonaphthalene the luster of the deposits deteriorates with zinc contents above 0.15 g/liter, and with iron contents above 0.4 g/liter, whreas in the ordinary nickel bath these additives begin to have a harmful effect at concentrations above 0.1 g/liter.

Current efficiency for nickel. All the determinations of current efficiency were performed with electrolyte IV at 20°.

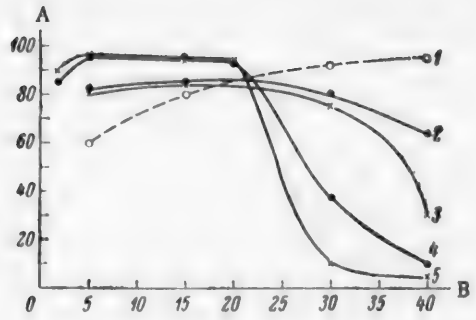

Fig. 3. Effect of stirring on the current efficiency for nickel.
A) Current efficiency (%), B) current density (ma/cm^2). Concentration of sulfonated naphthalene (in g/liter): 1) without additive, 2) 10, 3) 20, 4) 10, 5) 20. 1, 2, 3) With stirring; 4, 5) without stirring.

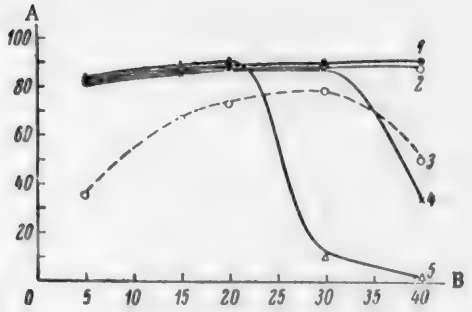

Fig. 4. Effect of electrolyte acidity on the current efficiency for nickel, in a bath containing 1 g of sulfonated naphthalene per liter.
A) Current efficiency (%), B) current density (ma/cm^2). pH values: 1) 3, 2) 5, 3) 2, 4) 5.7, 5) 6.2.

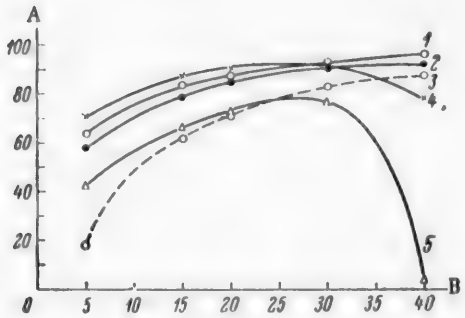

Fig. 5. Effect of acidity on current efficiency for nickel, in a bath without additive.
A) Current efficiency (%), B) current density (ma/cm^2). pH values: 1) 5, 2) 3, 3) 2, 4) 5.7, 5) 6.2.

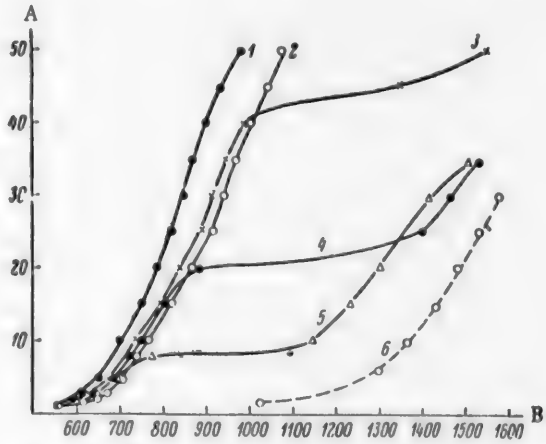

Fig. 6. Effect of additions of sulfonated naphthalene on cathode polarization in nickel electrolytes.
A) Current density (ma/cm^2), B) cathode potential E_c (mv). Concentration of sulfonated naphthalene (g/liter): 1) without additive, 2) 1.7, 3) 3.3, 4) 6.6, 5) 17, 6) electrolyte without nickel, with added sulfonated naphthalene.

As the current density is increased from 1 to 40 ma/cm^2, the current efficiency rises somewhat, both in the bath without additive (Fig. 2, Curve 1), and in bath containing a small amount of additive (Fig. 2, Curve 2). At low current densities (1-5 ma/cm^2) the current efficiency is somewhat higher in the bath with the additive. This difference vanishes with increase of current density. At an additive content of 3.3 g/liter, the form of the current-efficiency curve changes – the current efficiency begins to drop sharply, and intensive evolution of hydrogen takes place at current densities exceeding 20 ma/cm^2 (Fig. 2, Curve 3). This effect is seen very distinctly if electrolysis is performed simultaneously in two baths, with and without additive, connected in series. In the bath without additive the deposition proceeds without visible changes, whereas in the bath containing sulfonated naphthalene gas is evolved vigorously at the cathode, with spattering of the electrolyte. A rough, dull deposit is formed, and the cathode becomes coated with nickel hydroxide. The character of the deposition does not alter substantially with further increase of the amount of additive from 3.3 to 60 g/liter – in all cases the current efficiency begins to drop sharply at current densities above 20 ma/cm^2.

Agitation of the electrolyte at low current densities lowers the current efficiency by 5-10%. A decrease of

current efficiency is even more pronounced in baths without additive. The influence of the additive on the current efficiency is more distinct if the electrolyte is stirred, because stirring results in a continuous supply of the brightener to the cathode, and the concentration of the additive in the cathode layer therefore does not decrease. Whereas, at low current densities, the additive increased the current efficiency only very slightly in absence of stirring (Fig. 2), this increase was quite appreciable with stirring (Fig. 3, Curve 1). The decrease of current efficiency begins at higher current densities if the electrolyte is stirred vigorously than in absence of stirring, and with a higher content of the additive (Fig. 3).

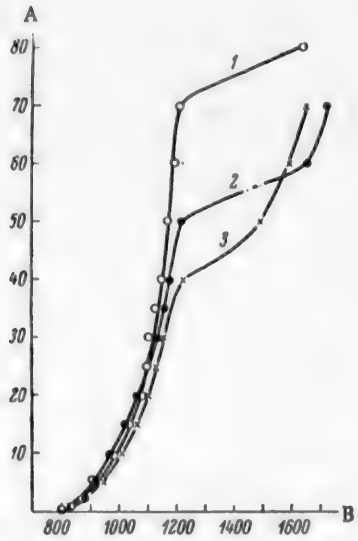

Fig. 7. Effect of the sodium salts of 2,6- and 2,7-disulfonaphthalic acids on cathode polarization in nickel electrolytes.
A) Current density (ma/cm^2), B) cathode potential E_c (mv). 1) Without additive; 2) 5 g of 2,7-disulfonaphthalene salt per liter, 3) 5 g of 2,6-disulfonaphthalene salt per liter.

The electrolyte was stirred in determinations of the current efficiency at different acidities. The bath contained 3.3 g of the additive per liter.

In considerations of the influence of electrolyte acidity on current efficiency, two current-density regions in which this influence differs considerably must be distinguished. In the region of low current densities (up to 20 ma/cm^2) in presence of additive, pH variations from 3 to 6.2 have almost no effect on the current efficiency (Fig. 4), whereas in absence of additive the current efficiency rises appreciably with increase of pH (Fig. 5).

In the region of high current densities (above 20 ma/cm^2), the higher the pH the sooner does the current efficiency begin to decrease. In an electrolyte without additive an appreciable decrease of the current efficiency is found even at low current density at pH 6.2.

Cathode polarization in the deposition of nickel. The cathode polarization was measured by the potentiometric method at increasing cathodic current density. The cathode potential was measured 10 minutes after a steady current density was established. The reference electrode was a saturated calomel half cell. The determinations were performed at 20° in unstirred electrolytes.

Fig. 6 shows polarization curves for different contents of sulfonated naphthalene in the electrolyte. With a low content of the additive, the potential is shifted by 100-150 mv in the negative direction in the current-density range from 1 to 50 ma/cm^2 (Fig. 6, Curve 2). Increase of the concentration of sulfonated naphthalene leads to a sharp increase of cathode polarization at a certain definite current density; the value of this current density decreases with increasing concentration of sulfonated naphthalene. After the sharp increase of polarization, the cathode potential approaches the potential of nickel polarized in an electrolyte free from nickel salts (Fig. 6, Curve 6). In the latter case the cathode potential is wholly determined by the discharge of hydrogen ions. The increased polarization in the electrolyte containing sulfonated naphthalene is associated with the almost complete cessation of nickel deposition. This is confirmed by the current efficiency data presented above.

Fig. 7 shows polarization curves for electrolytes to which the pure sodium salts of 2,6- and 2,7-disulfonaphthalic acids had been added. In this case the change of potential is observed at higher current densities than in electrolytes with added sulfonated naphthalene. The limiting current is reached considerably later in the electrolyte without additives (Fig. 7, Curve 1).

DISCUSSION OF RESULTS

The experimental results indicate that the deposition of nickel is retarded considerably in presence of sul-

fonated naphthalene. This is shown both by the polarization measurements and the determinations of current efficiency. The retardation of metal deposition is probably caused by formation of a dense adsorbed layer of the surface-active substance. The presence of such a layer is associated with a special character of the deposition process, leading to the formation of bright deposits. The following hypothesis is advanced to account for the formation of bright deposits. The dense adsorption film on the cathode surface retards growth of the deposits at right angles to the cathode. Therefore the deposit grows in a tangential direction, in layers spreading along the cathode. All the current passing through the cathode is thus distributed over a very small area, representing the growth front of one layer. The real current density in this case is considerably higher than the current density calculated from the geometrical cathode dimensions, so that a fine structure is formed, which ensures a high luster of the deposit. This hypothesis explains the layer structure often observed in bright deposits formed in presence of surface-active substances [5,6]. It has been shown that the dark bands observed in cross sections of bright copper deposits are layers of metal enriched with the organic substance adsorbed at the cathode surface and incorporated in the galvanic deposit [7]. In the formation of bright deposits the adsorbed film of surface-active substance prevents the continued growth of individual crystallites as the thickness of the deposits increases; therefore in each new layer the crystallites remain of the same size as in the preceding layer. Therefore the reflectance remains constant with increase of the thickness of a bright layer. The increase of the actual current density in the deposition of nickel in presence of a passivating additive probably accounts for the increase of current efficiency at low current densities, and the very sharp decrease of current efficiency at high current densities (Fig. 2). The current efficiency in an electrolyte without additives apparently begins to decrease at current densities above 70 ma/cm^2, as shown by the course of the polarization curve for the solution without brightener (Fig. 7, Curve 1). Stirring naturally favors a more rapid supply of metal ions into the catholyte layer, and the sharp drop of current efficiency is observed at higher current densities (Fig. 3).

The increase of current efficiency with decreasing acidity of electrolytes without additives (Fig. 5) can be attributed by incorporation of nickel hydroxide or its basic salts, in increasing amounts with increase of pH, in the deposit. The codeposition of nickel hydroxide in such cases has been demonstrated by a number of workers [8]. Zhurin and Shoikhet [9] showed that there are two stages of hydroxide formation in the electrodeposition of nickel. At the first stage particles of colloidal dimensions appear (at pH 3 to 5); in this range increase of pH does not lead to any appreciable increase of particle size until the second stage is reached (pH ~ 6.7), when rapid coagulation of the colloidal particles takes place. This same effect probably causes the sharp fall in current efficiency observed at pH = 6.2 (Fig. 5, Curve 5). In presence of sulfonated naphthalene, acidity has almost no effect on the current efficiency until the critical pH is reached (Fig. 4). This indicates that the additive suppresses the formation of nickel hydroxide at the first stage, but the second stage with formation of large hydroxide particles begins earlier, and the subsequent fall of current efficiency is sharper. It is significant that the additive has very little influence on the current efficiency at pH = 2, as at this pH the formation of hydroxide does not yet begin.

The suppressing effect of disulfonaphthalene on hydroxide formation is also seen in changes of the reflectance of nickel deposits with increase of pH. Incorporation of nickel hydroxide in the deposit must inevitable lead to a decrease of reflectance, and this is observed in the deposition of nickel from ordinary electrolytes without additives. However, when nickel is deposited in presence of sulfonated naphthalene the reflectance of the deposits does not diminish, but even increases with decrease of acidity; this also indicates that adsorption of this additive and the strength of the adsorption film increase with decrease of acidity. This occurs only until the second stage of hydroxide formation is reached. The influence of the additive then ceases, as the formation of large particles of nickel hydroxide disturbs the continuity of the surface-active film.

The weakening of the effects of zinc and iron impurities in presence of sulfonated naphthalene can probably also be attributed to the suppressing effect of the brightener on the formation of hydroxides of these metals.

The cause of the decreased reflectance of nickel deposits formed in presence of small amounts of sulfonated naphthalene (Fig. 1) is still not clear. It must be pointed out that this is not an accidental effect, as it has been repeatedly observed that the effects of small amounts of surface-active substance are directly opposite to its effects at high concentrations. For example, the internal stresses in nickel deposits formed at low contents of disulfonaphthalene are of the opposite sign to the stresses in nickel deposited from solutions with a high content of the additive [10].

SUMMARY

1. The influence of electrolysis conditions and electrolyte composition in bright nickel plating on the reflectance of the nickel deposits has been studied, and it is shown that in presence of sulfonated naphthalene the reflectance of the nickel deposits is independent of the thickness of the deposits, and increases with increasing current density and electrolyte pH. The reflectance is lowered by additions of less than 0.2 g of brightener per liter.

2. In presence of brighteners the current efficiency at low current densities is independent of the acidity in the pH range from 3 to 6.2. At current densities above 20 ma/cm^2 the current efficiency drops rapidly; the lower the electrolyte acidity, the sooner does this drop occur. The results lead to the hypothesis that the presence of sulfonated naphthalene suppresses the first stage of nickel hydroxide formation.

3. Addition of sulfonated naphthalene to the nickel electrolyte leads to a sharp increase of cathode polarization at a certain definite current density, which is lower at higher concentrations of the additive. The considerable retardation of nickel deposition indicates the existence of a dense adsorption layer on the cathode surface.

In conclusion, I thank Professor A. G. Samartsev for his interest and valuable advice.

LITERATURE CITED

[1] N. T. Kudriavtsev and V. V. Fedurkin, Bright Nickel Plating (State Local Light Industries Press, Moscow, 1951). [In Russian]

[2] R. Springer, Metalloberflache 5 (A), 7 (1951).

[3] D. V. Stepanov and I. P. Liashchenko, J. Appl. Chem. 14, 3 (1941).

[4] H. E. Fierz- David and A. Hasler, Helv. Chim. Acta 6, 1142 (1923).

[5] J. Henriks, Trans. Electroch. Soc. 82, 113 (1942).

[6] A. Hothersall and G. Gardam, Met. Ind. 55, 21 (1939).

[7] Iu. V. Lyzlov, T. A. Mechkovskaia, and A. G. Samartsev, J. Phys. Chem. 31, 12, 2720 (1957).

[8] D. I. Macnaughtan, G. E. Gardam, and R. A. I. Hammond, Trans. Far. Soc. 29, 729 (1935).

[9] A. I. Zhurin and N. G. Sholkhet, J. Appl. Chem. 29, 4, 583 (1956).*

[10] A. G. Samartsev and Iu. V. Lyzlov, J. Phys. Chem. 29, 2, 374 (1955).

Received February 22, 1957.

* Original Russian pagination. See C. B. Translation.

INFLUENCE OF CHLORIDE-ION ADMIXTURES ON THE DEPOSITION OF COPPER BY PERIODICALLY-REVERSED CURRENT

V. V. Ostroumov and I. F. Plotnikova

It was already pointed out in the previous paper [1] that in the deposition of copper by means of periodically-reversed current, deposits with a mirror-bright surface cannot be obtained from acid electrolytes in presence of about 10 mg of chloride ions per liter. The influence of chloride ions was studied in considerable detail, as they are a most likely impurity in water and in reagents used for electrolyte preparation.

The practical application of the process in the production of bright copper deposits may involve difficulties caused by the use of unpurified water used for washing articles after nickel plating, if such water contaminates the copper electrolyte. The method of removing chloride ions from electrolytes is therefore important.

EXPERIMENTAL

The surface state of the copper deposits was, as before, investigated by reflectance measurements in a beam of white light. These measurements were supplemented by microscopical studies of the deposit surfaces.

For purification of the electrolyte (2-3 liters in volume) if the impurity content was low, the electrolyte was boiled with metallic copper and the copper crystals deposited from the cooled solution were separated off (by filtration through a glass filter). Another method was used for purification of 70-100 liter volumes of electrolyte. Excess of silver sulfate solution was added to the electrolyte, and the precipitated silver chloride was filtered off. The filtration was effected with the aid of a small gear pump made from organic glass and driven by an electric motor. The filter was a vinyl resin cylinder filled with quartz sand.

An electrolyte containing 200 g of copper sulfate and 100 g of sulfuric acid per liter was used for most of the investigations. The cathode surface was always coated with a layer of bright electrolytic nickel, upon which the copper was then deposited. The electrolyte temperature was maintained at 18-20°. The cathode period of the current was 4 seconds, and the anode period, 1 second. Copper layers 25μ thick were deposited. The electrolyte was usually stirred during electrolysis.

At first, copper deposits with a consistent and high reflectance coefficient could not be obtained from different electrolytes. The lack of reproducibility of the results was caused by the presence of chloride ions in the electrolyte, in variable amounts in different cases. The source of the contamination was copper sulfate; "chemically pure" samples were found to contain chloride, as shown by the reaction with silver nitrate solution. Single or repeated purification of the electrolyte by means of boiling with copper ensured the formation of electrolytic deposits of high reflectance.

Fig. 1 illustrates the consecutive improvement of deposit quality on repeated purification. After purification there was a distinct decrease of the chloride concentration (as shown by the silver nitrate reaction), but chloride was not eliminated completely. It was also found that the introduction of chloride ions (in the form of very dilute hydrochloric acid or sodium chloride solution) into the purified electrolyte invariably leads to an appreciable decrease in the reflectance of the copper deposits (Fig. 2). For example, in the presence of 10 mg of chloride per liter the reflectance of the deposits falls to 12%. The copper surface becomes rough and scatters light strongly, owing to the appearance of microscopic pyramidal projections (Fig. 3). At a chloride-ion concentration of about 20 mg/liter these projections almost disappear, but the whole surface of the deposit becomes uneven, and its reflectance deteriorates (down to about 7%). The pyramidal projections are especially prominent at low current

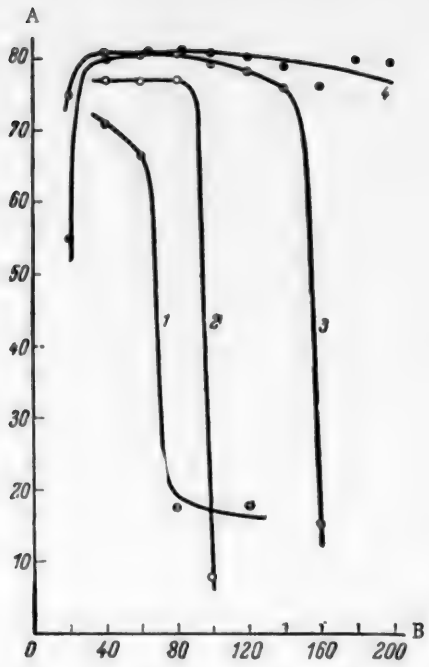

Fig. 1. Reflectance of copper deposits before and after purification of the electrolyte by boiling with metallic copper.
A) Reflectance (%), B) current density (ma/cm^2). Curves: 1) Original electrolyte; single purification; 3) 2-fold purification; 4) after prolonged use of the electrolyte.

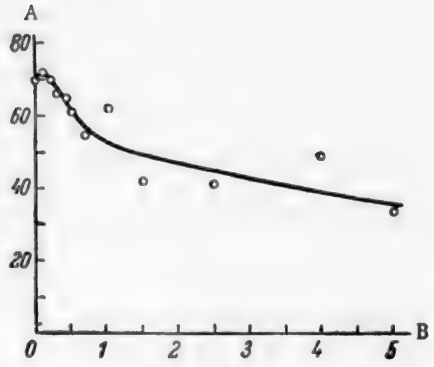

Fig. 2. Effect of chloride ions added to purified electrolyte on the reflectance of copper deposits at current density 80 ma/cm^2. A) Reflectance (%), B) chloride-ion concentration (mg/liter).

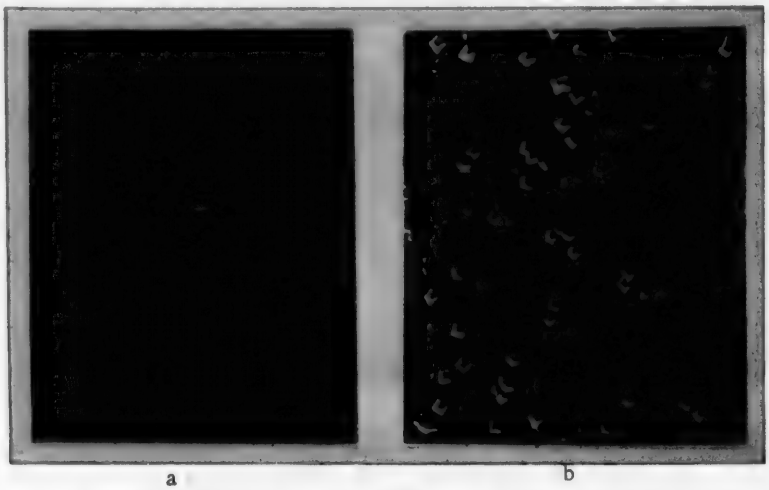

Fig. 3. Effect of chloride ions on the nature of copper deposits at current density 60 ma/cm^2. Chloride-ion content (g/liter) and reflectance (%) respectively:
a) 0.0005 and 71, b) 0.010 and 12. Dark ground. Magnification 320.

densities (Fig. 4). They gradually disappear with increase of current strength, and the reflectance of the deposits increases somewhat.

An attempt was first made to remove chloride ions by means of activated carbon. To remove any volatile organic impurities and soluble substances, the carbon was first heated strongly and boiled for a long time in 10%

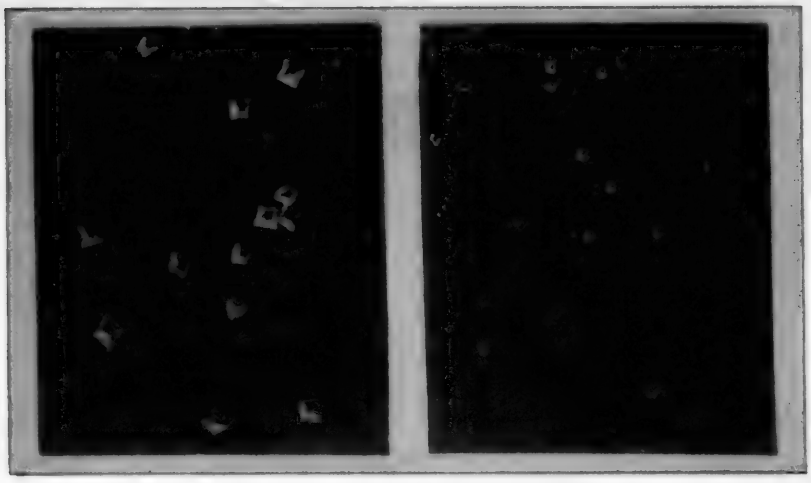

a b

Fig. 4. Effect of current density on the nature of copper deposits in presence of chloride ions (20 mg/liter) in the electrolyte. Current density (ma/cm^2) and reflectance (%) respectively:
a) 20 and 5; b) 60 and 7. Dark ground. Magnification 320.

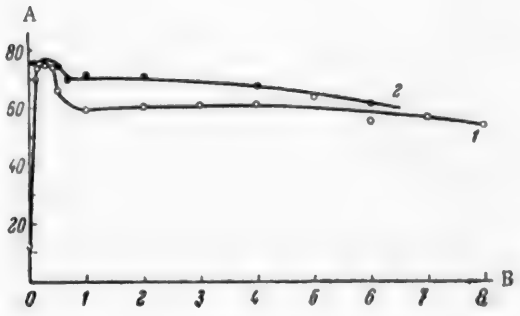

Fig. 5. Effect of chloride ions on the reflectance of copper deposits formed from electrolytes purified by means of silver sulfate.
A) Reflectance (%), B) chloride-ion concentration (mg/liter). Stirring: 1) moderate, 2) vigorous.

sulfuric acid solution. Electrolytes treated with carbon always yielded copper deposits of very low reflectance (2-3%), although chloride ions could not be detected in the purified electrolytes. Addition of dilute solution of hydrochloric acid to the electrolyte produced a distinct increase of the reflectance of the deposits (up to 55%), in contrast to the effect observed when chlorides were added to electrolytes purified by boiling with copper.

In the light of the foregoing observations, the following hypothesis, completely confirmed later, was put forward: the electrolyte must contain a very low concentration of chloride ions to ensure the formation of bright deposits. It is shown below that this concentration is in the range of 0.2-0.3 mg of chloride ions per liter. Therefore the chloride ion acts as a brightener effective at very low concentrations.

The removal of chloride ions by means of silver sulfate was completed as follows. After addition of excess of silver sulfate and removal of the precipitate by filtration, the excess reagent was removed from the electrolyte; for this, two copper electrodes of large area were immersed in the solution and a low direct current was passed; the electrolyte was stirred. The silver which partially separated out on the anode in the form of a loose deposit was removed mechanically at intervals in a stream of water. The electrolysis was continued for some time after a separate sample of the solution gave a negative reaction for silver ions with hydrochloric acid.

After purification by means of silver sulfate, the electrolytes always yielded copper deposits of very low reflectance (12%) with the use of periodically-reversed current. Introduction of hydrochloric acid into the electrolyte to a concentration of 0.25 mg/liter sharply raised the reflectance of the deposits; as Fig. 5 shows, it reached almost 80%. Further increase of the chloride concentration to 10 mg/liter resulted in the formation of dull deposits. Increase of the stirring rate of the electrolytes produced the usual increase in the reflectance of the deposits (Fig. 5, Curve 2).

Further tests were performed with an electrolyte purified free from chloride and then "contaminated" by the addition of 0.3 mg of chloride per liter. The variations of reflectance of the deposits with current density in stirred and stationary electrolytes are plotted in Fig. 6. The curves are of the same form as those obtained for an

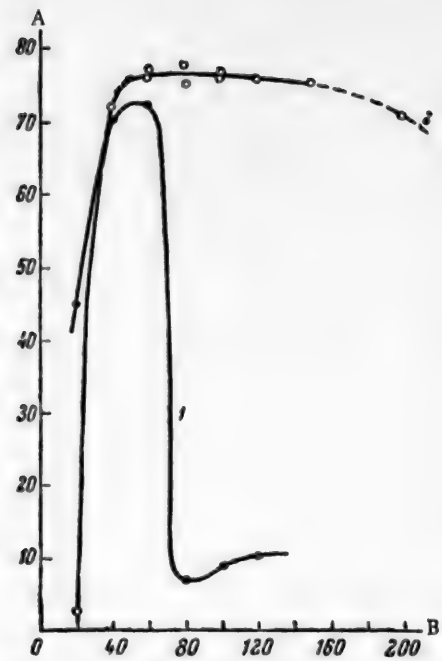

Fig. 6. Effects of current density and stirring on the reflectance of copper deposits formed from an electrolyte containing 0.3 mg of chloride ions per liter.
A) Reflectance (%), B) current density (ma/cm^2). Curves: 1) static electrolyte, 2) stirred electrolyte.

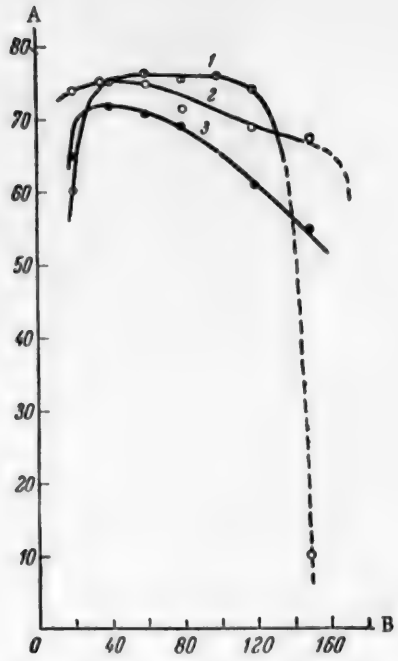

Fig. 7. Effect of chloride-ion concentration in the electrolyte on the reflectance of copper deposits formed from a stirred electrolyte.
A) Reflectance (%), B) current density (ma/cm^2). Chloride-ion concentration (mg/liter): 1) 0.3, 2) 0.6, 3) 1.2.

electrolyte boiled with copper to purify it [1]. As chloride ions accumulate in the electrolyte, the nature of the curves changes – the reflectance of the deposits decreases (Fig. 7).

DISCUSSION OF RESULTS

It has long been known that chloride ions influence the nature of copper deposits formed by the action of direct current. For example, in the refining of copper, addition of 10-50 mg of chloride per liter, in the form of chloride or hydrochloric acid, is recommended. This results in a decrease of grain size, increased hardness, and changes in the color of the copper deposits. The chloride-ion content of the electrolyte falls fairly rapidly during the electrolysis, and chloride can be detected by analysis in the copper deposits. At higher chloride contents in the electrolyte, a flocculent precipitate of cuprous chloride appears, first near the anode and then in the volume of the solution [2, 3].

The appearance of this precipitate is attributed to accumulation of cuprous ions in the solution, so that the solubility product of cuprous chloride is reached.

According to Luther's data [4], at 25°

$$[Cu^+] \cdot [Cl^-] = 2.2 \cdot 10^{-7} \text{ g-equiv/liter.}$$

A solution containing 200 g of copper sulfate per liter, acidified with sulfuric acid and at equilibrium with metallic copper at 20°, contains about $0.62 \cdot 10^{-3}$ g-equivalent of cuprous copper per liter [5]. Hence the concentration of chloride ions in the solution may reach $3.5 \cdot 10^{-4}$ g-equiv/liter*, or 12 mg/liter. This is close to the value given above (10 mg/liter), which is the critical value at which the reflectance of copper deposits falls sharply.

*The calculations are approximate, as the activities of the other ions are not taken into account.

The cause of this similarity is probably adsorption of cuprous chloride on the surfaces of the growing crystallites, with consequent disturbance of their growth and changes in the structure of the deposit.

It is appropriate at this stage to consider the purification of the electrolyte when it is boiled with metallic copper.

At 101° the content of cuprous copper in the electrolyte may reach $25.3 \cdot 10^{-3}$ g-equiv/liter [5]. After the solution is cooled, this concentration persists for some time, until copper crystals begin to form. The presence of chloride ions in such an electrolyte results in the formation of cuprous chloride, which is deposited on the surface of the forming copper crystals, and is thus removed with the precipitate. In the surrounding solution the chloride-ion concentration can only correspond to the solubility product of cuprous chloride:

$$[Cl^-] = \frac{2.2 \cdot 10^{-7}}{25.3 \cdot 10^{-3}} = 0.87 \cdot 10^{-5} \text{ g-equiv/liter}$$

or 0.23 mg/liter. This values is very close to the chloride-ion concentration (0.25-0.3 mg/liter) needed in the electrolyte for the formation of deposits of the maximum reflectance (Fig. 5). This explains why the electrolyte can be purified effectively if it is boiled with metallic copper.

The foregoing data indicate that we are concerned here with an electrolyte containing an inorganic brightener. The constant presence of an impurity difficult to control – chloride ions – in acid copper electrolytes is probably one of the reasons why many workers have failed to obtain bright copper deposits by means of periodically-reversed current. Another likely reason for such failures is that no attempts were made to use under layers of bright nickel in electrolysis.

It may be noted in conclusion that other substances apart from chloride may be used as brighteners in the process, but we have no definite information on this subject as yet.

SUMMANRY

1. Acid copper electrolytes should contain about 0.3 mg of chloride ions per liter to ensure the formation of bright copper deposits in electrolysis by means of periodically-reversed current.

2. Concentrations of about 10 mg of chloride ions per liter prevent the formation of bright copper deposits.

LITERATURE CITED

[1] V. V. Ostroumov and I. F. Plokhotnikova, J. Appl. Chem. 31, 10, 1520 (1958).••

[2] W. H. Gauvin and C. A. Winkler, J. Electroch. Soc. 99, 2, 71 (1952).

[3] L. Mandelcorn, W. B. McConnell, W. Gauvin, and C. A. Winkler, J. Electroch. Soc. 99, 2, 84 (1952).

[4] R. Luther, Z. Phys. Ch. 36, 385 (1901).

[5] E. Heinerth, Z. Electroch. 37, 2, 61 (1931).

Received March 28, 1957.

• As in original-Publisher's note.

•• Original Russian pagination. See C. B. Translation.

MECHANISM OF ALKALINE SURFACE OXIDATION OF STEEL

A. V. Shreider and A. G. Arakelov

Alkaline surface oxidation (black oxide finishing) is extensively used for protection of steel articles against corrosion. One of the advantages of the process is that the original surface quality and dimensions are retained (the lateral change of dimensions in the formation of the coating does not exceed 0.125μ [1]).

The formation mechanism of oxide films in the surface oxidation of steel is not fully understood. There is no doubt that the process is one of uniform corrosion of a thin surface layer of the metal, accompanied by the formation of a fairly compact film of corrosion products, firmly attached to the basis metal and having protective properties.

Samartsev [2] regards the surface-oxidation process as a reaction of secondary deposition of magnetite, Fe_3O_4, which forms a compact film on the metal surface. Magnetite is formed by the reaction of hypoferrite, Na_2FeO_2, with its oxidation product, ferrite, $Na_2Fe_2O_4$. Hypoferrite is formed by the corrosion of iron in strong alkaline solutions.

The alkaline corrosion of iron yields loose and powdery corrosion products which have the composition of magnetite [3, 4]. Studies of alkaline corrosion in steam boilers have shown that this form of metal attack is characterized by deposition of the corrosion product – magnetite – at considerable distances from the zone of corrosive attack. This is consistent with the mechanism of formation of alkaline-corrosion products by secondary deposition (crystallization) from solution. It is in harmony with the fact that the films formed in treatment baths of excessively high alkali content and a deficiency of oxidizing agent are loose and have poor adherence to the basis metal [2, 5]. Hence it may be concluded that in the formation of such films a considerable proportion of the oxidation products is formed by crystallization of magnetite from solution.

However, studies of the normal process of alkaline surface oxidation of steel reveal a number of features which cannot be satisfactorily explained in terms of a chemical mechanism of film formation. These include the increase of the rate at which the oxide coating is formed with increasing carbon content of the steel [6]; the significant differences between the properties of films formed on low-alloy steels, cast iron, and carbon steels; the very similar properties of films formed by chemical and electrochemical oxidation; and the effect observed by Zvereva [7], of the formation of an oxide film on steel previously coated with thin galvanic coatings of gold or silver.

Doubt may also be cast on the assertion [5] that oxygen is involved in the formation of ferrite within the bulk of the solution (oxygen is virtually insoluble in the boiling treatment baths, and therefore oxidation by oxygen can occur only at the solution – air interface, and ferrite is transferred into the bulk of the solution as the result of agitation due to boiling).

In 1946 Zabyvaev put forward a hypothesis of an electrochemical mechanism of alkaline surface oxidation [5]. Vigorous depolarizing agents, NO_2^- and NO_3^- ions, are involved in the steel treatment; their presence should therefore raise the oxidation – reduction potential of the solution considerably. This gives rise to conditions in which the oxidation proceeds mainly as a microelectrochemical process. An anodic reaction in which iron ions are formed giving rise to magnetite, takes place in the pores of the growing film. As the entire steel surface becomes covered by a magnetite film, the anodic process is retarded; this accounts for the damping of the "film thickness – oxidation time" curves, observed by Shvarts [8].

The action of anodic polarization is similar to the action of strong oxidizing agents. However, anodic

Activities of Solution and Metal Samples in Surface Oxidation

Iron-plated specimen	Treatment Solution	Pulses per minute over background level
Radioactive	Inactive,* 700 g/liter NaOH, 200 g/liter $NaNO_2$, 50 g/liter $NaNO_3$	13-30
The same	The same 1000 g/liter NaOH	3-19
Inactive	Radioactive** 700 g/liter NaOH, 200 g/liter $NaNO_2$, 50 g/liter $NaNO_3$	14-16
The same	The same 1000 g/liter NaOH	Over 3500

*Exposures of 15, 20, 25, 30, 35 and 40 minutes.

**Exposure of 40 minutes.

polarization in electrochemical oxidation confers a higher anode potential to the iron that the equilibrium potential which becomes established in a solution containing oxidizing agents, used for surface oxidation without application of current. Therefore under conditions of electrochemical oxidation (in an alkaline solution without additions of strong oxidizing agents) fairly complete oxidation of Fe^{++} is achieved; this is confirmed by the higher content of Fe_3O_4 in oxide films formed electrochemically [7].

The presence of some magnetite, formed by chemical precipitation, within the film has an adverse effect on the compactness and continuity of the oxide coatings. A much more compact and continuous film is formed by electrochemical oxide coating of steel [7]; this is because in the latter instance the whole process of film formation takes place without chemical precipitation of magnetite – the oxide can be formed, for example, by direct oxidation of the metal by the active oxygen liberated at the anode.

Krotov [9], as the result of his thermographic observations, also considers that alkaline surface oxidation is an electrochemical process, but he also assumes that the film may be formed partially by crystallization of magnetite from solution.

In a later investigation, Hurd and Hackerman [10] showed by the use of chemical kinetics that the proportion of the film formed during oxide coating by secondary precipitation of iron from solution can only be very small. The proportion of precipitated ferrite increases only if the technological process conditions are disturbed (for example, if the bath temperature is increased).

Whereas in the case of alkaline corrosion of iron in absence of air (in boilers) the concept of hydrogen depolarization has been put forward [3], in the oxidation of iron in strong alkaline solutions without added oxidants, but in contact with air, depolarization may take place through the agency of oxygen carriers – Fe^{++} and Fe^{+++} ions, which are in this case present as the complex anions $(FeO_2)^-$ and $(FeO_4)^=$. The microelectrochemical process of alkaline oxidation is characterized by reduction of NO_2^- and NO_3^- ions at the cathodic regions, with formation of reduction products as far as ammonia [9].

Krotov [9] put forward equations for the cathodic and anodic reactions in the microelectrochemical process of alkaline oxidation. However, it is difficult to understand why, in the cathode process, he considers that nitrate can be reduced to nitrite:

$$3H_2O+3NO_3^-+6e^-\rightarrow 6\ (OH)^-+3NO_2^-,$$

while in the anode process, not only can iron be oxidized to Fe_3O_4, but nitrate is reduced to ammonia:

$$3Fe+5^3/_4OH^-+{}^1/_4NO_3^--6e^-\rightarrow Fe_3O_4+2\tfrac{1}{2}H_2O+{}^1/_4NH_3.$$

If the concept of a homogeneous electrochemical mechanism of the corrosion process [11] is accepted, it would be more correct to consider the oxide-coating process statistically, i. e., as a microelectrochemical corrosion process which proceeds as a series of conjugate acts of metal oxidation and reduction of the oxidizing agent taking place simultaneously at different points on the metal surface. Because of the differences in the potential of the metal at different points of the surface, different reduction products of the oxidizing agents may be formed at such points. This need not necessarily involve the migration of electrons between such points, as is postulated in Krotov's mechanism of the process.

Krotov's mechanism also fails to conform to the fundamental principle of a heterogeneous electrochemical corrosion mechanism, which requires spatial separation of the anodic process of metal oxidation from the cathodic process of reduction of the depolarizer [12].

We used the radioactive-isotope method to show that whereas the principal route of film formation on iron in boiling strong alkaline solutions (containing 500-1000 g NaOH/liter) is by precipitation (crystallization) of magnetite, when strong oxidizing agents are introduced into such solutions, or in anodic polarization, the route is by direct oxidation to Fe_3O_4.

EXPERIMENTAL

The specimens for the investigation were prepared by galvanic iron plating of brass plates, 5 cm^2 in area, in an electrolyte containing 450 g of $FeCl_2 \cdot 4H_2O$, 500 g of NaCl, 750 g of water, and HCl to pH = 1.8, at 90-110° and D_C = 10 amps/dm^2 [13]. Some of the specimens were coated with an inactive iron deposit, while the rest covered with radioactive iron. For preparation of the radioactive deposit, an amount of powdered Fe^{59} corresponding to an activity of 10 millicuries was dissolved in warm HCl. The $Fe^{59}Cl_2$ solution was added to 750 ml of the prepared electrolyte. The iron was deposited in a quartz vessel from 150 ml of electrolyte, the activity of which was about 2 millicuries.

Both the inactive and the active iron deposits were formed during an exposure time of 15 minutes, and were about 34 ± 3μ thick. The activity of the specimens was 20,000-30,000 pulses/minute. Because of the relatively short half life of Fe^{59} (T = 46 days), the duration of the experiments from the preparation of the Fe^{59} solution to the end of all the operations with radioactive specimens and the activity determinations was restricted to 3 days.

The active and inactive specimens were subjected to surface oxidation in solutions of two types. One solution had the composition of the oxide-coating bath proposed by Zabyvaev in 1932 and widely used in industry: 700 g NaOH, 200 g $NaNO_2$, and 50 g $NaNO_3$ per liter. The other solution contained 1000 g NaOH per liter. The treatment temperature was 140° and the exposure time 45 minutes in both solutions.

Two types of each bath (with and without oxidizing agents) were prepared – active and inactive. For preparation of the active bath, powdered Fe^{59} isotope in a quantity corresponding to 2 millicuries was dissolved in 50 ml of 15% HNO_3. The solution was divided into two equal parts, and each was evaporated down to 1-2 cc in a quartz vessel. The evaporated portions of the radioactive nitrate $Fe^{59}(NO_3)_2$ were added to the normal treatment bath and to the bath with NaOH but without oxidizing agent. The treatment baths were made from quartz glass, and were 150 ml each in volume.

Before the alkali treatment, the iron-coated specimens were cleaned with emery and pickled in 15% HCl for 30 seconds. Each time, 10 samples were treated simultaneously in the bath. The exposures in the alkali treatment were 15, 20, 25, 30, 35 and 40 minutes.

In treatment of radioactive specimens in the inactive bath, 0.5 ml samples were taken from the solutions every 5 minutes by means of a micropipet, and placed on pieces of filter paper 15-25 mm in size. The paper was dried, wrapped in tracing cloth, and the activity was determined in the ordinary counting by means of an end-type counter [14].

After treatment of inactive specimens in the active bath, the plates were subjected to repeated 10-minute washings in boiling 5% soap solution, and the activity was determined after each washing; so long as the activities differed by more than 5% after consecutive washings, the washings (and the subsequent activity determinations) were repeated until the active solution had been removed almost completely from the film pores. The metallic specimens, were also wrapped in tracing cloth before the activity determinations.

The average results of 10 parallel determinations for each point were used in assessment of the results.

As the result of treatment of active specimens in the inactive bath, samples of the solution showed a small increase of activity over the background level (see table). The increase of activity over the background level became appreciable only when the active specimens had been held for 15 minutes in these solutions.

The increases of solution activity found in both baths are due not so much to isotope exchange as to dissolution of radioactive iron – a process which accompanies film formation on steel in alkaline media with and without oxidizing agents. In the experimental conditions used (small electrode area, brief exposure (40 minutes), absence of dissolved oxygen in the electrolyte, tendency of the metal to become passive in the given medium, and the presence of iron in both solutions in the form of complex anions), isotope exchange would be quite negligible in practice [15-19]. These results confirm the passage of iron into solution; an effect which accompanies the formation both of compact and smooth films, firmly attached to the iron surface, in the oxide-coating bath, and of thin, loose, discontinuous, and smeary films in pure alkaline baths.

The treatment of inactive specimens in the active bath was accompanied by a very slight increase in the activity of the electrodeposited iron – the activity increased by only 15 pulses/minute over the background level after treatment. In view of the very thorough washing of the treated specimens, this slight increase of activity should be ascribed, not to adsorption of the the treatment solution by the porous film, but to some participation of the chemical process of magnetite precipitation in film formation. The role of isotope exchange in this case is negligible, as apart from the factors already mentioned; it is also opposed by the very low concentration of iron in solution.

On the other hand, exposure in an active pure alkali solution without oxidizing agent resulted in a very sharp increase (60 to 70-fold) or activity over the background level. After very thorough (10-fold) washing, the specimens which were initially inactive but had been treated in the alkaline active bath had activities of about 3500 pulses/minute over the background level. This experiment demonstrates the important role played by precipitation of iron oxides from solution in the surface oxidation of steel in alkaline solutions in absence of strong oxidizing agents (but containing a small amount of iron dissolved in the bath when it was made radioactive).

Any possible suspicions that the strong increase of activity in specimens with thin, loose, smeary films formed from radioactive alkaline solutions may be caused by physical adsorption are dispelled by the following considerations. In the preparation of 150 ml of the active alkaline solution, half a portion of radioactive iron with an activity of 2 millicuries (i. e., $2 \cdot 3.7 \cdot 10^7$ pulses/minute [14]) was used. Hence the activity of 1 ml of the alkaline solution was $3.7 \cdot 10^7 : 150 = 2.5 \cdot 10^5$ pulses/minute. To confer stable radioactivity of the order of 3500 pulses/minute, undiminished by the most thorough repeated washing (with the use of a surface-active agent, soap), on the specimen, irreversible adsorption of not less than $3.5 \cdot 10^3 : 2.5 \cdot 10^5 = 1.4 \cdot 10^{-2}$ ml of solution is necessary. Since the film formed on the specimen, 5 cm^2 in area, in this case is thin (in any event not thicker than 0.2μ), and consists of magnetite (sp. gr. 5.2 [20]), its weight is small (not greater than $0.2 \cdot 5 \cdot 5.2 \cdot 10^{-4}$ g), and any suggestion that the high activity is caused by physical adsorption must be rejected. Factors opposing physical adsorption of iron ions from solution are the short exposure to the alkaline solution containing radioactive iron ions (the adsorption of electrolytes is a slow process), high temperature, and the negative-adsorption effect resulting from repeated washings by a liquid of very low surface tension (soap solution).

The hypothesis that chemisorption of iron compounds by the film formed by treatment in an alkaline solution without strong oxidizing agents takes place simultaneously should not lead to any objections; this process leads to virtually the same results as the formation of magnetite by separation of iron compounds from solution. The only difference is that in chemisorption the film substance is formed not in the liquid phase [2] but at the phase boundary.

This conclusion is not contradicted by the absence of any significant increase in the activity of a pure alkaline solution (without strong oxidizing agents) after treatment of a radioactive iron-plated specimen, if one takes into account the slight dissolution of iron (about 1 mg/cm^2) in oxide coating [14], the relatively large volume (150 ml) of the solution as compared with the small area (5 cm^2) of the treated specimen, and the very small volume of the sample taken for radioactivity tests (0.2 ml).

SUMMARY

1. It was shown by the tracer atom method that the formation of oxide films in the alkaline – nitrite oxide coating of steel occurs mainly by direct oxidation of the iron. Iron oxides formed by crystallization from solution form a totally insignificant part of the oxide film.

2. If the oxidizing power of the alkaline solution is decreased (for example, in absence of nitrites and nitrates), the role played by precipitation of secondary products of iron corrosion in the formation of oxidation products on the metal surface increases considerably.

LITERATURE CITED

[1] A. J. Mitchell, Materials and Methods 35, 3, 92 (1952).

[2] A. G. Samartsev, Oxide Coatings on Metals (Moscow, Izd. AN SSSR, 1944). [In Russian]

[3] A. P. Mamet, Corrosion of Heat and Power Equipment in Electrical Power Stations (Gosenergoizdat, 1952). [In Russian]

[4] B. N. Kabanov and D. A. Leites, Proc. Acad. Sci. USSR 58, 8 (1947).

[5] E. N. Zabyvaev, Candidate's Dissertation (Central Scientific Research Institute of Heavy Machinery, Moscow, 1946). [In Russian]

[6] P. K. Lavorko, Surface Oxidation of Metal (Mashgiz, 1951). [In Russian]

[7] V. N. Zvereva, Candidate's Dissertation, The Bauman Higher Tech. School, Moscow (1953). [In Russian]

[8] I. A. Shvarts, Candidate's Dissertation (1950). [In Russian]

[9] I. V. Krotov, J. Phys. Chem, 18, 7, 1327 (1954).

[10] R. M. Hurd and V. Hackerman, J. Electroch. Soc. 104, 8, 482 (1957).

[11] V. V. Skorcheletti, Metal Corrosion; Appendix II to the book by G. A. Kashchenko: Principles of Metal Science (Leningrad – Moscow, Metallurgy Press, 1950) 582. [In Russian]

[12] N. D. Tomashov, Theory of Metal Corrosion (Metallurgy Press, 1952). [In Russian]

[13] V. I. Lainer and N. T. Kudriavtsev, Principles of Electroplating, vol. 2, 2nd Edn. (Moscow, Metallurgy Press, 1946). [In Russian]

[14] V. N. Spitsyn, P. N. Kadochigov, et al. Techniques of the Use of Radioactive Tracers (Izd. AN SSR, 1954). [In Russian]

[15] N. B. Miller and V. A. Pleskov, Proc. Acad. Sci. USSR 74, 2, 233 (1950).

[16] H. Haissinsky and M. Cottin, J. Chim. Phys. 46, 9, 476 (1949).

[17] P. Dandel, La Radioactivitée. Presses universitaires de France, Paris (1955).

[18] M. Cottin, C. r. 251, 14, 697 (1950).

[19] M. DoCarmo Anta and M. Cottin, C. r. 242, 17, 1686 (1942).

[20] Chemist's Companion, vol. 2 (Goskhimizdat, 1953). [In Russian]

Received April 15, 1957.

KINETICS OF THE GAS-PHASE CORROSION OF EI-437B ALLOY IN AIR AND IN NITROGEN – HYDROGEN MIXTURE

I. A. Makolkin, N. P. Petrov, and V. G. Faiman

The high-temperature oxidation of EI-437B alloy was studied by Davidovskaia and Kestel' [1], and by Preece and Lucas [2].

Our experiments showed that at 700-750° the oxidation of the alloy in air is so slight that the corrosion effect cannot be determined by methods such as the usual gravimetric method. The experiments were therefore performed in the 800-1080° range. The corrosion effect (in mg/cm^2) was determined by periodic weighings of the specimens, without removal from the furnace, on an analytical balance, as shown in Fig. 1.

The results of the experiments are given in Table 1.

TABLE 1

Calculations of the Weight Increase m by Equations (6) - (10)

Temperature of experiment (°C)									
800		900		1000		1080		1080	
Rate constant K									
0.0347		0.293		0.352		0.373		0.396	
Weight increase (mg/cm^2)									
by Equation (6)	experimental	by Equation (7)	experimental	by Equation (8)	experimental	by Equation (9)	experimental	by Equation (10)	experimental
0.0000	0.0000	0.0000	0.0000	0.0000	0.0000	0.0000	0.0000	0.0000	0.0000
0.00979	0.01518	0.0787	0.1123	0.2265	0.3324	0.3425	0.4698	0.5059	0.7738
0.01801	0.02237	0.0993	0.1488	0.3889	0.4156	0.5830	0.6214	0.8480	0.8988
0.02668	0.02904	0.1813	0.1725	0.4973	0.4729	0.7340	0.7003	1.0775	1.0250
0.03505	0.03381	0.2140	0.2034	0.5757	0.5357	0.8447	0.7960	1.2235	1.1179
0.04312	0.03716	0.2382	0.2274	0.6252	0.5602	0.9210	0.8809	1.3359	1.2179
0.05071	0.0 523	0.2566	0.2437	0.6481	0.6480	0.9730	0.9423	1.4060	1.3022
0.05824	0.05286	0.2701	0.2643	0.6934	0.6752	1.0104	1.0000	1.4505	1.4298
0.06552	0.06428	0.2803	0.2801	0.7167	0.7113	1.0348	1.0307	1.4849	1.4857

The variations of the average weight increase m (Table 1) with temperature and duration of the process are plotted in Fig. 2.

Analysis of the curves (Fig. 2) shows that they are of the saturation type, and in the 800-1100° range correspond satisfactorily to the equation

$$\frac{dm}{dt} = k\,(M - m), \qquad (1)$$

where M is the weight increase of the specimen (in mg/cm^2) after complete oxidation; m is the weight increase (in mg/cm^2) as a function of time (an independent variable) and temperature (as a parameter); k is the oxidation rate constant.

Integration of Equation (1) gives:

$$\frac{dm}{M-m}=k\,dt,\quad -\int_0^m -\frac{dm}{M-m}=\int_0^t k\,dt,$$

$$\int_0^m -\frac{dm}{M-m}=-k\int_0^t dt,\quad \ln(M-m)\Big|_0^m=-kt,$$

$$\ln(M-m)-\ln M=-kt, \tag{2}$$

$$\ln\frac{M-m}{M}=-kt,\quad \frac{M-m}{M}=e^{-kt},$$

$$M-m=M\cdot e^{-kt},\quad M-M\cdot e^{-kt}=m,$$

$$m=M\cdot(1-e^{-kt}).$$

This equation corresponds to the experimental conditions at t = 0, m = 0, while at t = ∞, m = M.

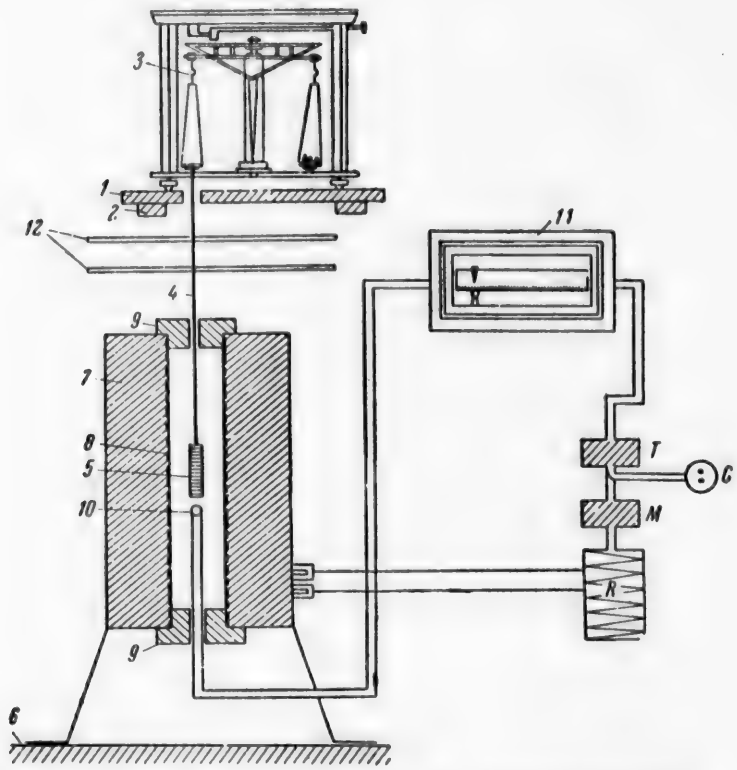

Fig. 1. Apparatus for investigation of the rate of high-temperature oxidation of EI-437B alloy by periodic weighing.
1) Shelf, 2) support, 3) analytical balance, 4) platinum wire, 5) test specimen, 6) iron plate, 7) furnace, 8) heating element, 9) asbestos, 10) thermocouple, 11) potentiometer, 12) asbestos screens, R) rheostat, M) magnetic starter, T) stepdown transformer, C) alternating-current source.

For calculation of M we assume that in Equation (1) kM = a, $M = \frac{a}{b}$, and hence k = b; Equation (1) then becomes

$$\frac{dm}{dt} = a - bm. \tag{3}$$

Since the oxidation of EI-437B alloy in our experiments was continued for 8 hours, for the first 4 hours of the experiment the following relationship is valid:

$$m_4 = 4a - b\int_0^4 m dt \tag{4}$$

and for 8 hours of oxidation

$$m_8 = 8a - b\int_0^8 m dt. \tag{4a}$$

The form of the oxidation curves (Fig. 2) makes it possible to solve the integral in Equations (4) and (4a) by the Simpson rule [3]:

$$S = \frac{h}{3}(y_0 + 4y_1 + y_2). \tag{5}$$

Since h = 1, the calculation is performed by means of the equation

$$S = \frac{1}{3}(y_0 + 4y_1 + y_2).$$

At 800°:

$$S_1 = \frac{1}{3}(0 + 4 \cdot 0.01618 + 0.02237) = 0.02903,$$

$$S_2 = \frac{1}{3}(0.02237 + 4 \cdot 0.02904 + 0.03381) = 0.05745,$$

$$\int_0^4 m dt = S_1 + S_2 = 0.08648;$$

$$S_3 = \frac{1}{3}(0.03381 + 4 \cdot 0.03716 + 0.04523) = 0.07589,$$

$$S_4 = \frac{1}{3}(0.04523 + 4 \cdot 0.05286 + 0.06428) = 0.10678,$$

$$\int_0^8 m dt = S_1 + S_2 + S_3 + S_4 = 0.26915;$$

$$0.03381 = 4a - b \cdot 0.08648,$$

$$0.06428 = 8a - b \cdot 0.26915,$$

and hence b = 0.0347 = k, a = 0.00938.

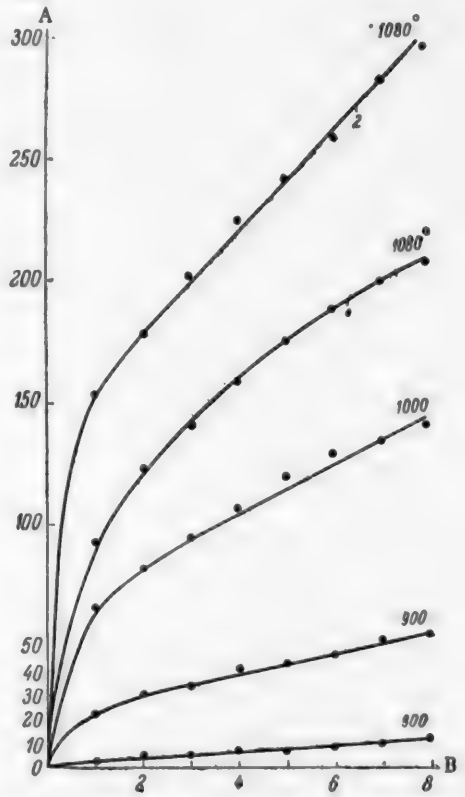

Fig. 2. Variations of m with the temperature and duration of the experiment.
A) Weight increase $m \cdot 2 \cdot 10^2$ (mg/cm²), B) time (hours). 1) 1st melting; 2) 2nd melting.

$M = \frac{a}{b} = 0.27$, and therefore for the experiments at 800° we have the equation

$$m_1 = 0.27 \cdot (1 - e^{-0.0347 \cdot t}). \quad (6)$$

Similar calculations were performed for 900, 1000, and 1080°; the following relationships, analogous to Equation (6), were obtained:

$$900° - m_2 = 0.31\ (1 - e^{-0.206t}), \quad (7)$$
$$1000° - m_3 = 0.763\ (1 - e^{-0.352t}), \quad (8)$$
$$1080° - m_4 = 1.09\ (1 - e^{-0.472t}), \quad (9)$$
$$1080° \text{ (2nd melting)} - m_5 = 1.55\ (1 - e^{-0.306t}). \quad (10)$$

The calculated values of the weight increase m are given in Table 1.

Values of $1 - e^{-kt}$ were calculated with the aid of five-figure tables [4].

Table 1 shows that the experimental values of the weight increase m are in good agreement with the values of m calculated from Equations (6-10). The rate constants in Table 1 can be used to derive an empirical equation for log k as a function of temperature

$$\lg k = \frac{A}{T} + B \quad (11)$$

and the equation

$$\lg \frac{k_2}{k_1} = \frac{\Delta E}{4.576} \left(\frac{1}{T_1} - \frac{1}{T_2} \right) \quad (12)$$

can be used to calculate the average activation energy for the oxidation of EI-437B alloy in air:

$$\Delta E = 35670 \text{ cal.}$$

The values of the constants A and B in Equation (11) are given below:

T (in °K)	A	B	log k experimental	log k calculated from Equation (11)
1073	27012	−26.63	−1.460	−1.460
1173	15872	−14.06	−0.533	−0.530
1273	12256	−10.08	−0.454	−0.453
1353	16680	−12.76	−0.428	−0.440

Gas-phase Corrosion of EI-437B Alloy in Nitrogen − Hydrogen Mixture

The second part of this work, namely the investigation of gas-phase corrosion of EI-437B alloy in nitrogen − hydrogen mixture, was deliberately carried out under pilot-plant conditions with the use of a works furnace for the heat treatment.

The corrosion tests were carried out in the following protective atmospheres: DND (dissociated nitrogen, dried, with 75% H_2), DNID-20 (dissociated nitrogen, incompletely burnt in chamber, dried with 20% H_2), and DNID-10 (dissociated nitrogen, incompletely burnt in chamber, dried with 10% H_2).

The nitrogen − hydrogen mixture was made by thermal decomposition of ammonia at 850-900° in a dissociation chamber. The gas was dried by means of silica gel and analyzed.

A large number of specimens of EI-437B alloy was tested in nitrogen − hydrogen mixtures with different proportions of nitrogen and hydrogen. The corrosion effect was determined gravimetrically.

The results were plotted in the form of a graph, shown in Fig. 3. This graph shows that oxygen and atmos-

TABLE 2

Mean Variations in the Weight of Specimens with the Heating Time at the Tempering Temperature at the Optimum Number of Gas Changes, 10 Heated in Muffle

Heat treatment		Average weight increase (mg/cm²) and composition of protective atmosphere		
t°C	Exposure (hours)	75% H_2 25% N_2	20% H_2 80% N_2	10% H_2 90% N_2
1040	1	0.10	0.17	0.27
1040	4	0.25	0.36	0.59
1040	8	0.30	0.38	0.24

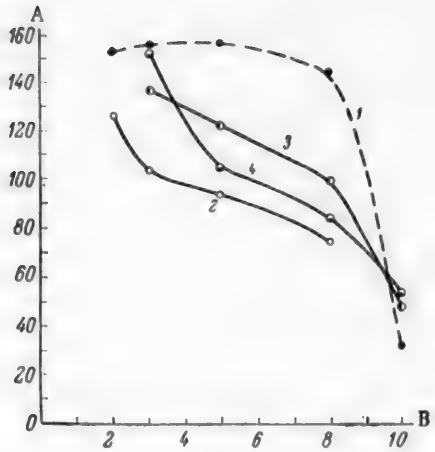

Fig. 3. Weight changes of specimens of EI-437B alloy in relation to the number of changes of the protective atmosphere (p. a.) in the muffle of the electric furnace, and the gas composition. Dew point from − 40 to − 50°.
A) Weight increase $m \cdot 2 \cdot 10^2$ (mg/cm²), B) number of changes of p. a. in the electric furnace chamber. Treatment in p. a. of the following compositions (%): 1) $75H_2 + 25N_2$ without muffle, 2) $75H_2 + 25N_2$ with muffle, 3) $20H_2 + 80N_2$ with muffle, 4) $10H_2 + 90N_2$ with muffle. Treatment conditions: heating in muffle at 1080°, exposure 2 hours, cooling in p. a.

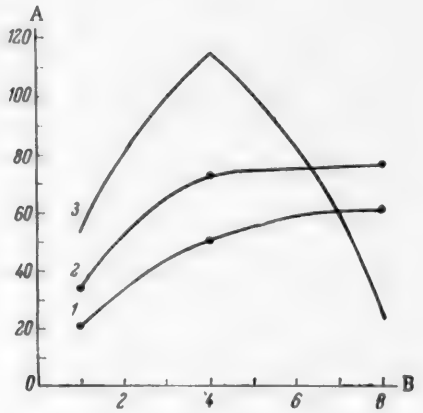

Fig. 4. Weight changes of specimens of EI-437B in relation to the heating time and composition of the protective atmosphere. 10 gas changes in furnace, dew point from − 50 to − 55°.
A) Weight increase $m \cdot 2 \cdot 10^2$ (mg/cm²), B) time (hours). Treatment in p. å. of the following compositions (%): 1) $75H_2 + 25N_2$, 2) $20\ H_2 + 80N_2$, 3) $10H_2 + 90N_2$.

pheric moisture adsorbed in the chamber of a furnace without a metallic muffle greatly increase gas-phase corrosion, while the presence of a metallic muffle diminishes corrosion. Moreover, the corrosion rate depends on the number of changes of the nitrogen − hydrogen mixture in the working chamber of the furnace − − with 10 changes, the corrosion rate is $^1/_4$ to $^1/_5$ the rate with 2, 3, or 5 changes.

This made it possible to conduct another series of experiments, in which the heating time as well as the gas composition was varied.

The results are plotted in Table 2.

The data in Table 2 were used to plot the weight increase of the specimens as a function of heating time and gas composition (Fig. 4).

TABLE 3

Mean Weight Changes of Specimens of EI-437B Alloy after Heat Treatment under the Optimum Conditions (Repeated Experiment)

Composition of protective atmosphere (%)	Number of changes of protective atmosphere in furnace	Heat-treatment conditions				Mean weight change (mg/cm²)	Dew point (°C)
		tempering		aging			
		t° C	time (hours)	t° C	time (hours)		
75 H_2 + 25 N_2	10	1080	8	750	16	0.33	−50
20 H_2 + 80 N_2	10	1080	8	750	16	0.49	−50
10 H_2 + 90 N_2	10	1080	8	750	16	0.56	−50
Air.	—	1080	8	750	16	1.85	−50

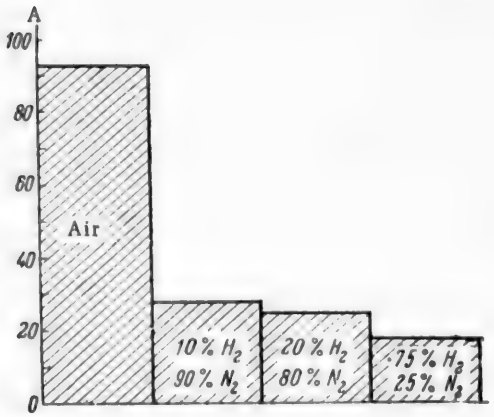

Fig. 5. Weight changes of specimens of EI-437B alloy in relation to the composition of the protective atmosphere.
A) Weight increase $m \cdot 0.5 \cdot 10^2$ (mg/cm²).

Fig. 4 shows that with the optimum number of changes (10) of the protective atmosphere in the furnace, the heating time has relatively less influence on the rate of gas-phase corrosion, although the latter is still considerable.

For a final determination of the conditions for the use of a protective atmosphere in the heat treatment of EI-437B alloy, a series of 24-hour experiments was carried out; each experiment consisted of 8 hours of heating at 1080° for tempering, and 16 hours of heating at 750° (aging).

The results are given in Table 3.

The data of this table were used to construct the block diagram in Fig. 5.

On the assumption that the process is parabolic, the data in Tables 2 and 3 can be used to find the average values of the rate constant for the process — — at 1040° $k_1 = 0.0002$ and at 1080° $k_2 = 0.000441$. Equation (12) gives $\Delta E = 69{,}800$ cal. This is nearly double the activation energy (35,670 cal) for the oxidation of EI-437B alloy in air. This indicates that the rate of gas-phase corrosion of the alloy is much lower in nitrogen — hydrogen mixture than in air, and emphasizes the protective properties of the gas.

Nitride formation. It is known that the metals in EI-437B alloy form nitrides with nitrogen [5].

The equation derived by Kubaschewski and Evans [6]

$$\Delta F_T = A + BT \lg T + cT,$$

was applied to nitride formation, and the free energies of certain reactions of nitride formation and the decomposition temperatures of nitrides were calculated.

For the reaction $Al_S + \frac{1}{2} N_{2G} = AlN_S$, one of us [7] derived the equation

$$\Delta F_T = -58160 - 0.45T \ln T + 0.045 \cdot 10^{-3}T^2 + 0.94 \cdot 10^5 T^{-1} + 28.35T,$$

solution of which for 1080 and 750° gives: $\Delta F_{1353°} = -24040$ cal and $\Delta F_{1023°} = -32210$ cal, and 2055° for the decomposition temperature of AlN.

The values of ΔF of formation, and decomposition temperatures (t) of some metal nitrides are given below:

Reaction	ΔF (cal) in heating of the alloy for tempering (1080°)	ΔF (cal) in aging of the alloy (750°)	Decomposition temperature of nitride (°C)
$Cr_G + \frac{1}{2}N_{2G} = CrN_G$	+1295	−6564	1020
$Ti_G + \frac{1}{2}N_{2G} = TiN_G$	−49384	−56924	3241
$3Si_G + 2N_{2G} = Si_3N_{4G}$	−70456	−96460	1985
$4Fe_G + \frac{1}{2}N_{2G} = Fe_4N_G$	+15408	+10157	—
$5Mn_G + N_{2G} = Mn_5N_{2G}$	−8520	−20533	1314
$3Mn_G + N_{2G} = Mn_3N_2$ amorph	+3446	+94	741
$3Mn_G + N_{2G} = Mn_3N_2$ mixed crystals	+3504	−5510	952

The above values of ΔF and t indicate that in the temperature range under consideration (750-1080°) the formation of the nitrides of chromium, titanium, silicon, manganese, and aluminum is themodynamically possible; some of the nitrides (TiN, Si_3N_4, AlN and Mn_5N_2) have very high decomposition temperatures, indicating that the thermal stability of these nitrides is high.

The formation rates of these nitrides are unknown, and require special investigation. Nevertheless, they are formed in the temperature range (750-1080°) used in the heat treatment of EI-437B alloy in nitrogen − hydrogen mixture, and the corrosion products probably contain a certain amount of nitrides.

On the other hand, experience shows that atmospheric oxygen cannot be displaced completely from the furnace by nitrogen − hydrogen mixture. Therefore the possibility of scale formation is not excluded when EI-437B alloy is heated in nitrogen − hydrogen mixture. This shows that the gas-phase corrosion of EI-437B alloy in nitrogen − hydrogen mixture is composed of two parallel processes − scale formation and nitride formation. The aggregate corrosive effect during 24 hours of heating of the alloy (8 hours at 1080° and 16 hours at 750°) is 0.33-0.56 mg/cm².

SUMMARY

1. Oxidation of EI-437B alloy in air in the 800-1100° temperature range conforms to the equation $m = M(1 - e^{-kt})$.

2. The oxidation proceeds at a fairly high rate − up to 1.5 mg/cm² of the alloy is burned out under laboratory conditions, and up to 1.85 mg/cm² in the large works furnace, during 8 hours of heating at the heat-treatment temperature (1080°). The probable explanation for the difference in the corrosion effects is that the large chamber of the works furnace contains adsorbed oxygen, which increases the oxidation rate at 1080°.

3. The differences of chemical composition and structure of the alloy, inevitable in different meltings, lead to differences in the oxidation rates, which become appreciable at 1080°, but are slight at 800, 900, and 1000°.

4. It is confirmed that the minimum condition for nonoxidative heating with avoidance of scale formation is drying of the protective atmosphere entering the furnace to a dew point of − 50 to − 55°; this corresponds to a moisture content of 0.004 − 0.002% in the protective atmosphere.

5. For nonoxidative heating of nickel-based alloys, a metallic muffle of EI-417 alloy should be placed in the working chamber of the electric furnace (iron-based alloys contain Cr, Ni, etc.).

6. In nonoxidative heating of EI-437B alloy, the protective atmosphere in the muffle should be changed at least 10 times.

7. Corrosion is much less rapid in nitrogen − hydrogen mixture than in air, and therefore this mixture can be recommended as a protective atmosphere in the heat treatment of alloys of the EI-437B type.

LITERATURE CITED

[1] E. A. Davidovskaia and Kestel', Metal Science and Treatment 10, 29 (1956).

[2] A. Preece and J. Lucas, J. Inst. Metals 1, 1, 219 (1952); O. Kubaschewski and B. Hopkins, Oxidation of Metals and Alloys (1955), 5 [Russian translation].

[3] Ia. Bezikovich, Approximate Calculations (1931), 188. [In Russian]

[4] B. I. Segal and K. A. Semendiaev, Five-Figure Mathematical Tables (1948). [In Russian]

[5] Gmelins Handbuch der anorg. Chemie, 8, Auflage, System – Nummer, 4, Stickstoff, 238, Fig. 10.

[6] O. Kubaschewski and E. Evans, Metallurgical Thermochemistry (1954), 352 [Russian translation].

[7] I. A. Makolkin, Coll. Papers VZPI, 13, 88 (1956).

Received March 16, 1957.

SYNTHESIS OF COPOLYMERS OF VINYL ACETATE WITH CROTONIC ACID AND ITS DERIVATIVES

S. N. Ushakov and E. M. Lavrent'eva

During recent years there has been so much progress in the theory of the copolymerization of vinyl compounds that quantitative predictions can be made concerning monomer reactivity in copolymerization. However, very little attention has been devoted to studies of unsaturated acids.

The copolymerization of acrylic, methacrylic, and crotonic acids has been studied [1]. The following systems were investigated: styrene – methacrylic acid, styrene – acrylic acid, vinylidene chloride – crotonic acid, and vinyl acetate – crotonic acid. The copolymerization constants r_1 and r_2 ($r_1 = 0.3 \pm 0.01$, $r_2 = 0.01 \pm 0.01$) for the last pair were calculated from analytical data for copolymers formed with less than 4% conversion. It was noted that there is an azeotropic effect in the system vinyl acetate – crotonic acid (but not in the system vinylidene chloride – crotonic acid).

Johanson [2] described the preparation and properties of five copolymers of vinyl acetate and crotonic acid, containing from 5.5 to 43% crotonic acid. He considered these copolymers to be ester acids of fairly high molecular weight, and represented their structure as follows:

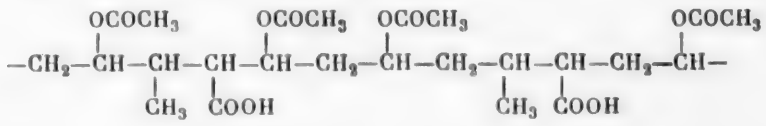

He showed that two molecules of crotonic acid cannot be joined together in the chain, but must have at least one vinyl acetate unit between them. It follows that the maximum content of crotonic acid in the polymer is 50%, with the crotonic acid and vinyl acetate units alternating.

We were interested in vinyl acetate – crotonic acid copolymers as starting materials for the production of a number of copolymeric derivatives of vinyl alcohol, including some containing nitrogen, by means of reactions in the copolymer chains.

Our starting materials for copolymerization were vinyl acetate, crotonic acid, and benzoyl peroxide as catalyst. The vinyl acetate had b. p. 72.5° at 760 mm, $d_{20}^{20} = 0.934$. The thermal characteristics of vinyl acetate polymerization were determined [3] before the copolymerization experiments. This method of characterization of the polymerization capacity of vinyl acetate makes it possible to identify individual batches and to collect fractions which correspond with adequate accuracy to the polymerization capacity of a selected prototype sample.

Crotonic acid was synthesized from malonic acid by the action of acetaldehyde, in pyridine with ethyl alcohol as solvent [4]. The crotonic acid had m. p. 72°, and acid number 650.9.

The vinyl acetate – crotonic acid copolymers were made from the components taken in various proportions, with benzoyl peroxide catalyst, at 68-70°. The acid number, acetate-group content (by saponification with water or alcoholic alkali [5]), viscosity, and solubility of the vinyl acetate – crotonic acid copolymers were determined.

The intrinsic viscosity was determined for dilute solutions of the copolymers in ethyl alcohol (0.1, 0.2, and 0.4 g of the copolymer in 100 ml of solution) by means of an Ostwald viscosimeter at 20°. The copolymer compo-

TABLE 1

Preparation of Vinyl Acetate – Crotonic Acid Copolymers with the Use of 2% Benzoyl Peroxide at 68-70°

Molar ratio of vinyl acetate to crotonic acid	Taken for reaction (g)		Yield, dry polymer (g)	Yield (% on amounts taken)	Acid no. of copolymer*	Crotonic acid content* (wt. %)	Vinyl acetate in copolymer* (wt.%)	Copolymer composition (molar)		Total (molar %)	Difference from 100 (molar %)	[η] at 20°	T_g (°C)
	vinyl acetate	crotonic acid						crotonic acid	vinyl acetate				
vinyl acetate	52.55	—	48.64	92.56	—	—	98.79	—	—	—	—	0.38	28
1 : 0.01	90.00	0.90	83.90	92.30	8.80	1.35	98.77	1.35	98.77	100.12	+0.12	—	—
1 : 0.02	80.85	1.61	69.08	83.77	14.42	2.20	97.41	2.20	97.41	99.61	−0.39	—	—
1 : 0.05	47.80	2.50	45.22	89.90	35.04	5.37	93.25	5.37	93.25	98.61	−1.38	0.26	28
1 : 0.1	45.15	5.01	41.59	82.86	69.32	10.62	88.16	10.62	88.16	98.78	−1.22	0.20	29
1 : 0.25	50.00	12.00	31.17	53.50	161.80	24.81	72.18	24.81	72.18	96.99	−3.01	—	—
1 : 0.3	81.15	24.25	62.83	59.61	171.95	26.36	70.73	26.36	70.73	97.09	−2.91	0.11	33
1 : 0.3	53.30	16.00	42.35	61.16	170.00	26.06	70.28	26.06	70.28	96.34	−3.66	0.10	36

*Mean of two determinations.

TABLE 2

Preparation of Vinyl Acetate – Crotonic Acid Copolymers with 0.2% (Experiment 20) and 0.5% (Experiment 19) of Benzoyl Peroxide at 68-70°. Molar ratio of vinyl acetate to crotonic acid taken = 1 : 0.003

Expt. No.	Taken for reaction (g)		Yield dry polymer (g)	Yield (% on amounts taken)	Acid number of copolymer*	Crotonic acid content (wt.%)	Vinyl acetate in copolymer (wt. %)	Molar comp. of copolymer		Total (molar %)	Difference from 100 (molar %)	[η] at 20°
	vinyl acetate	crotonic acid						crotonic acid	vinyl acetate			
19	129.2	3.90	62.35	46.85	21.34	3.27	95.88	3.27	95.88	99.15	−0.85	0.60
20	129.5	3.90	9.56	7.16	22.42	3.43	95.96	3.43	95.96	99.39	−0.61	0.79

*Mean of two determinations.

sition (in molar %) was calculated from the results of functional group determinations. The analytical data for the copolymers are given in Table 1.

Consideration of the data in Table 1 shows that:

1) the composition of the copolymer formed corresponds closely to the monomer content of the original mixture; 2) the intrinsic viscosity of the copolymers decreases with increasing crotonic acid content; 3) the copolymer yield, under otherwise equal conditions, decreases with increase of the amount of crotonic acid taken.

The relationship between the composition of the original mixture and that of the copolymer is in the main consistent with the values of the constants r_1 and r_2 ($r_1 = 0.3 \pm 0.01$, $r_2 = 0.01 \pm 0.01$) for this monomer pair [1].

In view of the fact that when vinyl acetate was copolymerized with crotonic acid in presence of 2% of benzoyl peroxide the intrinsic viscosity of the copolymers was low, experiments were performed with smaller amounts of benzoyl peroxide (0.5 and 0.2%). As was to be expected from the theory of radical copolymerization, the copolymer composition did not change on decrease of the amount of benzoyl peroxide (the constants r_1 and r_2 are independent of the amount of catalyst), but the intrinsic viscosity rose (Table 2).

In determinations of the solubility of vinyl acetate – crotonic acid copolymers it was found that the copolymer is completely soluble in weak alkalies (6% aqueous ammonia, aqueous-borax solution) even when the cro-

TABLE 3

Analysis of Vinyl Acetate – Ammonium Crotonate Copolymer

Copolymer treatment conditions	Crotonic acid in copolymer (molar %)	Theoret. content nitrogen in ammonium salt (wt.%)	Nitrogen found* (wt. %)	Nitrogen content (% of theoretical)	Vinyl acetate content* (wt. %)	Copolymer composition (molar %)			Total (molar %)	Difference from 100 (molar %)
						vinyl acetate	ammonium salt	crotonic acid		
With theoretical amount of ammonia.	26.06	4.18	3.23	77.27	67.73	71.54	20.65	8.42	100.61	+0.61
With double the theoretical amount of ammonia.	26.06	4.18	4.30	102.00	66.70	70.51	27.89	0	98.40	−1.67
	24.81	3.96	3.91	98.7	71.30	74.84	25.23	0	100.07	+0.0
	24.81	3.96	4.21	106.00	68.07	71.86	27.26	0	99.12	−0.88

*Mean of two determinations.

TABLE 4

Analysis of Vinyl Acetate – Crotonamide Copolymers Made by Dehydration in Current of Ammonia

Crotonic acid in copolymer (molar %)	Amt. ammonium crotonate copolymer taken (g)	Amt. crotonamide copolymer obtained (g)	Yield (% on amount taken)	Theoret. amt. water liberated (ml)	Water liberated (ml)	Theoret. nitrogen content (wt. %)	Nitrogen found* (wt. %)	Nitrogen content (% of theoret.)	$OCOCH_3$ content* (wt. %)	Vinyl acetate content* (wt. %)	Copolymer comp. (molar %)		Total (molar %)	Difference from 100 (molar %)
											vinyl acetate	crotonamide		
26.06	5.80	5.75	99.14	0.26	0.25	4.43	3.45	77.82	48.08	70.08	69.84	21.15	90.99	−9.01
26.06	3.90	3.78	97.05	0.17	0.15	4.43	3.98	89.77	48.44	70.59	70.37	24.38	94.75	−5.25
24.81	7.50	6.50	96.66	0.32	0.35	4.41	3.85	87.30	49.73	72.49	72.26	23.60	95.86	−4.14
26.44	16.25	15.21	93.60	0.75	0.80	4.60	3.43	74.57	45.53	66.35	66.11	21.07	87.18	−12.82
26.44	16.15	15.12	93.05	0.93	0.90	4.60	3.68	80.00	45.62	66.50	66.24	22.56	88.80	−11.20

*Mean of two determinations.

tonic acid content of the copolymer is very low (0.01 mole of crotonic acid per mole of vinyl acetate). All the copolymers formed, containing from 1 to 30 molar % of crotonic acid, are soluble in ethyl and methyl alcohols, acetone, and benzene. The copolymer of vinyl acetate and ammonium crotonate [6] was prepared by treatment of solid vinyl acetate – crotonic acid copolymer with aqueous 11% ammonia solution.

For complete characterization of the composition of copolymers neutralized by ammonia, the copolymers of vinyl acetate and ammonium crotonate were analyzed. The acetate group contents, nitrogen (by the Dumas semimicro method), and crotonic acid (by the acid number) were determined. The analytical results are given in Table 3.

It is clear from Table 3 that when the theoretical amount of ammonia was taken, the amount of nitrogen in the copolymer of vinyl acetate and ammonium crotonate is only 77.27% of the theoretical. If excess ammonia is used, the nitrogen content of the copolymer is close to the theoretical.

We prepared, for first time, copolymers of vinyl acetate and crotonamide by thermal dehydration of

TABLE 5

T_g of Copolymers of Vinyl Acetate with Crotonic Acid and its Derivatives

Experiment No	Crotonic acid content of vinyl acetate – crotonic acid copolymer (molar %)	Glass-transition temperature (T_g) of copolymer (°C)		
		with crotonic acid	with ammonium crotonate	with crotonamide
1	5.37	28	—	—
2	10.62	29	—	—
3	23.25	33	46	50
10	26.06	36	49	53
4	33.20	47	68	78

ammonium derivatives of the copolymer. The reaction was carried out by distillation of the liberated water with vapor of a solvent immiscible with water (benzene) in a Dean and Stark apparatus, without addition of catalyst. It was found that under these conditions dehydration of the ammonium-salt units in the copolymer proceeds easily and smoothly with quantitative separation of water. The first drop of water falls to the bottom of the trap 10 minutes after the benzene has started to boil, and after about 30 minutes the separation of water is complete. The amount of liberated water does not increase during further heating for 2 hours.

After the dehydration, the vinyl acetate – crotonamide copolymer was filtered off to remove benzene, washed on the filter, and dried under vacuum at 60-65° to constant weight. The composition of this vinyl acetate – crotonamide copolymer was determined by analysis for acetate groups, amide groups (from the nitrogen content determined by the Dumas semimicro method), and acid groups (by titration with 0.1 N alcoholic KOH solution).

However, we found that free ammonia is also partially split off during dehydration. Therefore the vinyl acetate – crotonamide copolymer contains, in addition to amide groups, crotonic acid residues (partial liberation of ammonia was also observed in special experiments on the dehydration of pure ammonium crotonate).

In order to decrease the liberation of ammonia, thermal dehydration of the copolymer in benzene in a current of ammonia was carried out. When the dehydration was performed in a current of ammonia, the amount of ammonia split off from the copolymer decreased sharply, and the nitrogen content rose accordingly. Analytical data for the vinyl acetate – crotonamide copolymer prepared by dehydration in a current of ammonia are presented in Table 4.

Consideration of the data in Table 4 shows that: 1) the total content of vinyl acetate and crotonamide, calculated as a molar percentage, is generally short of 100%, and 2) when the theoretical quantity of water, calculated for the formation of amide from the ammonim salt, is liberated, the nitrogen content of the dehydrated polymer is also often below the theoretical value.

The possible explanation of this result, obtained for all the polymers studied, is the occurrence of a reaction between the functional groups in the copolymer with formation of imide and γ-lactone groups [7].

The formation of an imide group in the liberation of ammonia is unlikely, as this requires the presence of two adjacent crotonamide units, which is not characteristic for this monomer pair:

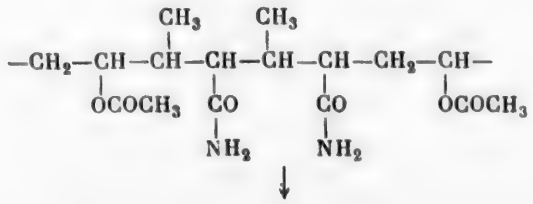

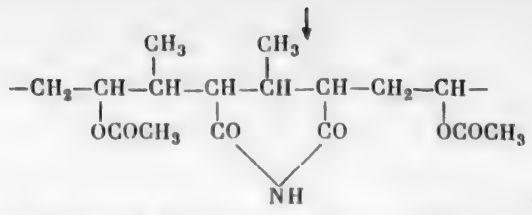

The possibility of imide-bridge formation between chains is not excluded in some cases.

Some evidence in favor of the foregoing is provided by the observed increase of the difference between the sum of the functional groups determined (imide groups were not determined) and the sum of the molar percentages, which should be 100.

For characterization of certain physical properties of the vinyl acetate – crotonic acid, vinyl acetate – ammonium crotonate, and vinyl acetate – crotonamide copolymers, their glass-transition temperatures (T_g) were determined.

A mercury dilatometer [8] was used for the determinations. The results of the T_g determinations are given in Table 5.

The glass-transition temperature of polyvinyl acetate (prepared under similar polymerization conditions) was found to be 28°, and that of the polyvinyl alcohol obtained from it was 84-85°; these values are in agreement with literature data.

The data in Table 5 show that: 1) the glass-transition temperature increases from 28 to 47° with increase of the crotonic acid content of the copolymer over the stated range; 2) as we pass from the copolymer of vinyl acetate and crotonic acid (~33%) to the copolymers with the ammonium salt and crotonamide (with equal molar % of the corresponding units), T_g increases from 47 to 68° respectively. This change of T_g is a natural consequence of changes in the polarity of the substituent groups and in the forces between the macromolecular chains.

Thus, by the introduction of crotonamide (~25 molar %) into the polyvinyl acetate chain, the glass-transition temperature can be raised by about 50°, with an improvement of the technical properties of polyvinyl acetate (as a plastic).

SUMMARY

1. Copolymers of vinyl acetate and crotonic acid were synthesized by radical copolymerization in presence of benzoyl peroxide, and copolymers of vinyl acetate with ammonium crotonate and crotonamide were prepared by means of reactions in the copolymer chains.

2. The glass-transition temperature of the copolymers depends on the nature of the substituent, and increases in the series: crotonic acid – ammonium crotonate – crotonamide. Increase of the concentrations of the corresponding units also raises the glass-transition temperature.

LITERATURE CITED

[1] E. Chapin, G. Ham, and C. Mills, J. Polymer Sci. 4, 597 (1949).

[2] S. Johanson, Svensk Kemisk Tidskrift 60, 6, 122 (1948).

[3] A. Nikolaev, Candidate's Dissertation, Lensoviet Tech. Inst. Leningrad (1953).*

[4] F. Kaufler, Monatsh 53, 121 (1929); H. Schieber, and J. Magasanik, Ber. 48, 1810 (1915).

[5] K. Gibello, Les Viniliques d' Aujourdhui, Dunod, Paris, 456 (1953).

[6] German Patent 571,665.

[7] T. Alfrey, J. Bohrer, and H. Mark, Copolymerization (IL, 1953), 146 [Russian translation]; T. Alfrey, C. Lewis, and B. Magel, J. Am. Ch. Soc. 71, 3793 (1949); H. Fikentscher, U. S. Patent 2067706, 12 Jan. 1937.

[8] T. Kononova, Candidate's Dissertation, Lensoviet Tech. Inst. Leningrad (1952).*

Received August 5, 1957.

* In Russian.

SULFONIC ION-EXCHANGE RESINS BASED ON POLYSTYRENE AND FORMALDEHYDE

A. A. Vasil'ev and A. A. Vansheidt

(Institute of High-Molecular Compounds, Academy of Sciences USSR)

Among the monofunctional sulfonic ion-exchange resins, which have a number of advantages over sulfonated-phenol cation exchangers, the most widely used are the polystyrene sulfonic resins. Sulfonated polystyrene resins are made by sulfonation of copolymers of styrene with various cross-linking components, usually divinylbenzene. Methods of synthesis based on sulfonation of the original monomers are unsuitable for the production of sulfonated styrene resins. Sulfonation of styrene by strong sulfuric acid results in resinification. Sulfonation of styrene by means of sulfuric anhydride in complex form [1, 2] results in the formation of ω-styrenesulfonic acid, $C_6H_5 - CH = CH - SO_3H$, which does not polymerize.

The exchange capacity of sulfonated cation exchangers based on styrene and divinylbenzene is 4.5-5 meq/g. They have considerable chemical resistance (in particular, to oxidizing agents) even at elevated temperatures (up to 80-90°), and good mechanical strength. Among the disadvantages of these methods for the production of cation exchangers are the scarcity and high cost of divinylbenzene.

Technical polystyrene, which is one of the main products of the plastics industry, has not been used in the production of sulfonated ion exchangers. Polystyrene is a thermoplastic product, soluble in aromatic hydrocarbons, aliphatic ethers, and ketones. When polystyrene is sulfonated without dissolution, products of very low mechanical strength and very high swelling are formed.

Polystyrene can be dissolved by the vigorous action of sulfonating agents [3]. It was of considerable interest to search for a cross-linking agent which would yield insoluble products by interaction with soluble polystyrene-sulfonic acids.

Investigations carried out in the Institute of High-Molecular Compounds, Academy of Sciences USSR, showed that formaldehyde can act as a cross-linking agent of this type. It is known that aliphatic aldehydes can condense with unsaturated cyclic hydrocarbons, including aromatic hydrocarbons, in presence of concentrated or fuming sulfuric acid to yield insoluble solid amorphous products [4-6].

Nastiukov [4] has shown that the action of concentrated sulfuric acid on a mixture of benzene and formaldehyde yields diphenylmethane and more complex resinous products; i. e., the aromatic nuclei are bridged by methylene groups. It was therefore likely that sulfonated polystyrenes might also react with formaldehyde, and that this reaction, as the result of cross linking of the macromolecules by CH_2 groups, should yield insoluble space polymers containing sulfo groups and having the properties of cation-exchange resins. Experiments showed that condensation of this type does occur when soluble polystyrenesulfonic acids are heated with formaldehyde solution or with solid formaldehyde polymer. Heat treatment of the resultant gel reduces its swelling and increases its mechanical strength. The product is crushed, washed to remove free sulfuric acid and degradation products, sifted, and dried at room temperature; it is then suitable for use as an ion exchanger (SSF).

In our experiments, polymer made by emulsion, or block-polymerized and crushed polymer, was sulfonated by the action of excess of oleum, not less than 6 parts per 1 part of polymer, at 200-205° until it was completely dissolved. Solution of the polystyrene in oleum was accompanied by partial degradation of the macromolecules and by oxidation processes, as shown by evolution of sulfur dioxide and darkening of the mixture. Formaldehyde was added to the sulfonated mass at room temperature in the form of paraform or formalin, not less than one molecule per monomer unit in the polystyrene molecule being added, and the mixture was then heated cautiously.

TABLE 1

Effect of the Proportions of Sulfonating Agent and Polystyrene on the Properties of SSF Resins*

Weight ratio of oleum to polystyrene	Gel heating time (hours)	Swelling Coefficient	Sulfur content (%)		Exchange capacity (meq/g)
			total	active	
6:1	0	6.5	16.00	14.23	4.45
9:1	0	17.5	16.57	14.42	4.51
6:1	2	3.9	15.29	14.17	4.42
9:1	2	10.4	16.38	14.67	4.59
6:1	4	3.6	15.09	14.03	4.39
9:1	4	7.6	16.38	14.98	4.68
6:1	8	3.4	15.06	13.73	4.29
9:1	8	6.2	16.05	15.20	4.75

* Oleum with 13.2% SO_3, and 1.1 molecule of formaldehyde (in the form of 91.3% paraform) per styrene monomer unit, were used in these experiments. The gel was heated at 130°.

TABLE 2

Effects of Temperature and Time of Heat Treatment on the Properties of SSF Resins*

Conditions of heat treatment		Swelling coefficient	Sulfur content (%)		Exchange capacity (meq/g)
temperature (in°)	time (hours)		total	active	
—	0	6.5	16.00	14.23	4.45
130	2	3.9	15.29	14.17	4.42
155	2	3.5	15.80	14.05	4.40
130	4	3.6	15.09	14.03	4.39
155	4	3.2	15.29	14.23	4.45
180	4	3.1	14.72	13.91	4.35
130	8	3.4	15.06	13.73	4.29
155	8	2.8	14.50	13.40	4.19
180	8	2.7	12.89	12.50	3.91

* The sulfonation agent was oleum (13.2% SO_3), 6 parts by weight to 1 part of polystyrene, CH_2/Ar = =1.1 (91.3% paraform was used).

Gel formation took place at 130-150°. The gel was heated further at 130-180° in order to increase its mechanical strength. The resin was crushed, washed with water and 1 N caustic potash solution (to remove excess sulfuric acid and degradation products), regenerated by 2 N hydrochloric acid, and finally washed with water to a neutral reaction to methyl orange. The resin was then sifted, dried at room temperature, and investigated; the total sulfur content of the resin and sulfur present in the form of sulfo groups (i. e., active sulfur) were determined; the total exchange capacity was calculated from the results. In addition, the swelling coefficient of the resin, the mechanical strength, and resistance to alkalies, nitric acid, and oxidizing agents were determined.

It was found that this procedure yields cation exchangers of a high exchange capacity, reaching 4.2-4.6 meq/g, with swelling coefficients of 2.4-3.2.

It follows from the data in Table 1 that variations of the reagent ratio from 6:1 to 9:1, and of the heating time, have little effect on the exchange capacity of the resins; with the smaller amount of oleum the capacity decreases with heating time (from 4.45 to 4.29 meq/g), and with the larger amount of oleum it increases (from 4.5 to 4.75 meq/g).

The swelling coefficient of the resins decreases in both cases with increase of the heating time, owing to

TABLE 3

Effect of the Amount of Formaldehyde Added on the Properties of SSF Resisns•

Experiment No.	$\frac{CH_2}{Ar}$	Formaldehyde added as							
		90% paraform				33% formalin			
		swelling coefficient	sulfur content (%)		exchange capacity (meq/g)	swelling coefficient	sulfur content (%)		exchange capacity (meq/g)
			total	active			total	active	
1	1.1	2.45	14.31	12.81	4.00	2.4	14.91	12.90	4.02
2	2.2	2.2	13.71	12.60	3.92	2.8	15.39	13.50	4.20
3	4.4	2.1	12.90	11.41	3.56	3.2	15.50	13.92	4.35

• The sulfonation agent was oleum (10% SO_3), 6 parts by weight to 1 part of polystyrene; gel heated for 12 hours at 155-160°.

increased cross linking of the chains. However, the presence of a large excess of oleum seems to have little favorable effect on cross linking by condensation with formaldehyde, as the swelling coefficient of the resins formed under these conditions is 2 to 3 times the swelling coefficient of resins obtained with the use of 6 parts of oleum, and its value is 6.2 even after prolonged heat treatment of the gel, whereas the resins formed from gels made with the use of 6 parts of oleum, heated for eight hours at 130°, have a swelling coefficient of 3.4.

If the gel is heated at higher temperatues, for example at 155 or 180°, then, as is seen in Table 2, the swelling coefficient of the resins is reduced to 2.7-2.8, with a simultaneous decrease of exchange capacity to 4.2-3.9 meq/g.

The effect of the amount of formaldehyde on the properties of SSF resins depended on whether the formaldehyde was introduced as paraform or as formalin. It follows from the data in Table 3 that in the former case increase of the amount of CH_2O from 1.1 to 4.4 molecules per monomer unit resulted in decreases of the swelling coefficient and exchange capacity, and in less decrease in the particle size of the resin when shaken with water, i. e., an increase of mechanical strength. The reverse was the case when formalin was used; i. e., the swelling coefficient and exchange capacity increased and the strength decreased, although with small amounts of the aldehyde the resins differed little in properties from those formed in presence of paraform. The explanation is that when formalin was used, water was introduced into sulfonated mass together with formaldehyde; in Experiments 2 and 3 (Table 3) this water not only absorbed completely all the sulfuric anhydride present in the mixture, but also greatly diluted the sulfuric acid, and thereby created less favorable conditions for condensation of the aldehyde with the polymer, i. e., for formation of cross links between the chains.

The exchange capacity of SSF cation exchangers was not changed after 20 minutes of heating on a boiling water bath with 1 N caustic potash, 0.1 N nitric acid, or 0.1 N potassium permanganate, or after the air-dry resins had been heated at 110° for 20 hours [7]. Thus, SSF resins have adequate chemical and thermal stability, but in mechanical strength and exchange capacity they are somewaht inferior to sulfonated styrene resins made by sulfonation of styrene – divinylbenzene copolymers. The probable explanation is that the high sulfonation temperature favors degradation of the original polystyrene molecules as the result of oxidation by sulfuric anhydride, which under these conditions is partially reduced to sulfur dioxide. On the other hand, as the tables show, the total sulfur content present in the form of sulfo groups and easily determined by titration; this is probably due to partial conversion of the sulfo groups into sulfone or other nonacid groups.

Finally, comparison of the exchange capacities of resins obtained under different conditions with their swelling coefficients shows that decrease of the latter generally leads to some decrease of exchange capacity. This may be ascribed to displacement of sulfo groups in the sulfonated polystyrene by CH_2 groups in the course of cross linking.

Nevertheless, SSF resins are little inferior in their exchange capacity (4.2-4.6 meq/g) to the usual sulfonated polystyrene resins (KU-2, SDV, Dowex-50, Amberlite IR-120), the exchange capacity of which does not exceed 5 meq/g, but which are made from less available materials.

Among the merits of SSF cation exchangers is their higher selectivity for certain antibiotics (terramycin, aureomycin) [8].

EXPERIMENTAL *

In most of the sulfonation experiments emulsion-polymerized polystyrene of molecular weight about 100,000 was used. In some experiments crushed block-polymerized polystyrene, of molecular weight about 50,000, was sulfonated.

The exchange capacities and swelling coefficients of the resins from the two polystyrenes were approximately equal, but the mechanical strength was lower for resins made from polystyrene of molecular weight 50,000 than for resins made from emulsion-polymerized polystyrene.

Different sulfonation agents were used, from 92% sulfuric acid to oleum containing 65% SO_3. The use of oleum of high concentrations did not give any better results than oleum of low SO_3 content (about 3-5%).

The exchange capacities of the resins were of the same order in all cases; to dissolve the polystyrene, not less than 6 parts of oleum of any concentration per 1 part of polystyrene was needed.

If 92% sulfuric acid was used, weight parts of sulfuric acid per 1 part of polystyrene was required to dissolve the polystyrene. Formaldehyde was used either in the form of 33-35% solution, or (in most of the experiments) as paraform, containing 91-95% CH_2O.

It was found that polystyrene can be sulfonated with much smaller amounts of oleum than those indicated above; with oleum and polystyrene in 2:1 ratio the resins formed have the same exchange capacity as with a 6:1 ratio. However, at ratios less than 6:1 the polystyrene does not dissolve in oleum, and the resins formed have very high swelling coefficients, greater than 10, and very low mechanical strength. The disadvantages of the use of oleum – polystyrene ratios greater than 6:1 were noted earlier.

The optimum oleum – polystyrene ratio is therefore 6:1.

Polystyrene was usually sulfonated in round-bottomed wide-necked flasks, on air baths or high-boiling oil baths, with stirring. All the oleum (containing 5-10% SO_3) was introduced at the start of heating. When 50-60° was reached, the contents of the flask consisted of a powder like mass; the stirring was then temporarily stopped. At 200-205° the polystyrene began to dissolve; to accelerate the process, the temperature was usually raised to 210-215°. The stirrer was switched on as soon as the decrease in the viscosity of the mass made this possible. After most of the flask contents had become liquid, the heating was performed very cautiously at temperatures not higher than 205°, in order to avoid ejection of the mass from the flask. The heating was stopped when a sample of the mass was completely soluble in water and no lumps of undissolved polystyrene were present in the mass. The mass was cooled to room temperature, and paraform in a ratio of 1-2 molecules, or formalin in a ratio of 1.0-1.1 molecules of CH_2O per monomer unit, was added with thorough stirring. The gel formation and subsequent heat treatment were either performed in the same reaction flask, or the sulfonated mass with the added formaldehyde was poured onto metal trays which were placed in a thermostat. The temperature in the thermostat was gradually raised, and at 130-150° the gel was formed, which was then usually heated at 155-160°. Heat treatment at 180° led to an appreciable decrease in the exchange capacity of the resins without any significant decrease of swelling. Heat treatment at 130° yielded resins of lower mechanical strength.

In several experiments polystyrene of molecular weight about 15,000-20,000 was sulfonated. This polystyrene, which was a very brittle product resembling colophony, could be dissolved in oleum or sulfuric acid at about 150-160°. The resins formed were not inferior in exchange capacity to resins obtained from polystyrene of higher molecular weight, but their mechanical strength was very low.

After the heat treatment the products were crushed and washed thoroughly with water, treated for 2-3 days with 1 N caustic soda solution to remove excess sulfuric acid and degradation products**, regenerated by 2 N hydrochloric acid, and washed with water to a neutral reaction to Methyl Orange. A grain fraction 0.3-1.5 mm in size was separated during the first washing. The resins were dried at room temperature.

---

*V. S. Matrosova and T. V. Gerasimiuk took part in the experimental work.

**The caustic soda solution was changed every 12 hours.

The methods used for testing the resins are described in our previous paper [9].

SUMMARY

1. A method for the synthesis of SSF ion-exchange resins is described; it consists of sulfonation of polystyrene followed by the action of formaldehyde on the soluble sulfonation products.

2. SSF cation exchangers have a high exchange capacity (4.2-4.6 meq/g, with a swelling coefficient of 2.4-3.2), good chemical and thermal resistance, and are made from more readily available materials than resin based on styrene – divinylbenzene copolymers.

LITERATURE CITED

[1] F. Bordwell, C. Suter, J. Hoblert, and C. Kondestvedt, J. Am. Ch. Soc. 68, 139 (1940).

[2] A. P. Terent'ev and A. V. Dombrovskii, J. Gen. Chem. 20, 1875 (1950).*

[3] G. B. Bachman, H. Hellman, K. R. Robinson, R. W. Finholt, E. J. Kahler, L. J. Filar, L. V. Heisley, L. L. Lewis, and D. D. Micucci, J. Org. Chem. 12, 119 (1947).

[4] A. M. Natiukov, Introductory Course of Technical Chemistry of Plastics (ONTI, Goskhimizdat, 1934), 106. [In Russian]

[5] E. I. Orlov, Formaldehyde (ONTI, Chem. Theoret. Press), 88. [In Russian]

[6] C. Ellis, Chemistry of Synthetic Resins (ONTI, People's Commissariat of Trade and Industry, 1938), 394 [Russian translation].

[7] A. A. Vasil'ev, J. Appl. Chem. 30, 1022 (1957).*

[8] G. V. Samsonov, Chromatography, its Applications in Biology (State Medical Press, 1955), 162, 167. [In Russian]

[9] A. A. Vasil'ev and A. A. Vansheidt, J. Appl. Chem. 31, 9, 1075 (1958).*

Received November 26, 1957.

*Original Russian pagination. See C. B. Translation.

STUDY OF THE CHEMICAL STRUCTURE OF SKB SODIUM DIVINYL RUBBER (MADE BY THE ROD PROCESS)

A. I. Iakubchik, S. K. Zykova, and S. P. Goncharuk

(Chair of High Polymers, the A. A. Zhdanov (Order of Lenin) State University, Leningrad)

The object of the present investigation was a study of the chemical structure of SKB sodium divinyl rubber (made by the rod process). The available information on the chemical structure of this rubber includes data on the relative contents of 1, 2 and 1, 4 units, and on unsaturation [1]. The main method used for investigation of chemical structure was ozonolysis, whereby it is possible to determine the relative contents of 1, 2 and 1, 4 units, the sequence of the units, and size of the macromolecular segments of the rubber.

The rubber ozonides were decomposed by acetyl hydroperoxide in acetic acid [2]. With this method of decomposition, the ozonolysis products consist of a mixture of carboxylic acids.

The mixtures of carboxylic acids were separated by means of partition chromatography [3]. This method has already been used for separation of the ozonolysis products of emulsion-polymerized divinyl and sodium divinyl rubbers made in America [4]. The present investigation consisted of a study of the decomposition products of the ozonides of SKB rubber.

Satisfactory conditions have been found [3] for the separation of standard acids, i. e., acids expected to be present in the ozonolysis products of divinyl rubber.

The same conditions (these include the type of silica gel, the elution rate, type of column, developer, etc.) were used to separate the mixture of carboxylic acids formed by ozonolysis of SKB. Chromatograms of the acid products formed by ozonolysis of SKB rubber are shown in Figs. 1-3.

The course of separation of the mixture was followed by means of titration of the eluate (3 or 4 ml portions) by 0.017 N and 0.029 N aqueous sodium hydroxide in presence of phenolphthalein. The titration results were represented graphically, the volume of alkali solution (in ml) used for titration being plotted against the amount (in ml) of the eluate.

It follows from the chromatograms (Figs. 1, 2) that the products formed by oxidative decomposition of SKB ozonides comprise a fairly complex acid mixture containing 11 components. Of these 11 acids, 7 were identified; These corresponded to the most prominent peaks in the chromatogram. Most of the acids in the mixture were identified chromatographically from the volume peaks [5] and elution thresholds [6]. The unknown acid mixture in 60% solution of tertiary amyl alcohol in chloroform was passed through the column (Fig. 1). The following standard acids [3] were passed separately through the same column under precisely the same conditions; acetic, formic, succinic, 1, 2, 4, 6-hexanetetracarboxylic.

The chromatograms of the standard acids (dash lines) were plotted together with the chromatogram of the unknown mixture (Fig. 1). Comparison of the chromatograms showed that the volume peaks and elution limits of the acids in the unknown mixture coincide or almost coincide with those of the corresponding standard acids. The chromatographic identification of the acids was confirmed by chemical analysis of individual fractions of the eluate, corresponding to definite peaks on the chromatogram. The succinic, 1, 2, 4-butanetricarboxylic, and formic acids could have been formed from the 1, 4-1, 4; 1, 4-1, 2-1, 4 regions; 1, 2, 4, 6-hexanetetracarboxylic acid, from a region consisting of $1, 4 - (1, 2)_2 - 1, 4$ units. This region might be expected to give rise to three isomers: 1, 4-1, 2-1, 2-1, 4; 1, 4-1, 2-2, 1-1, 4; 1, 4-2, 1-1, 2-1, 4 correspondingly, oxidation of the ozonolysis products of these regions should yield three isomers: 1, 2, 4, 6-; 1, 3, 4, 6-; 1, 2, 5, 6-hexanetetracarboxylic acid.

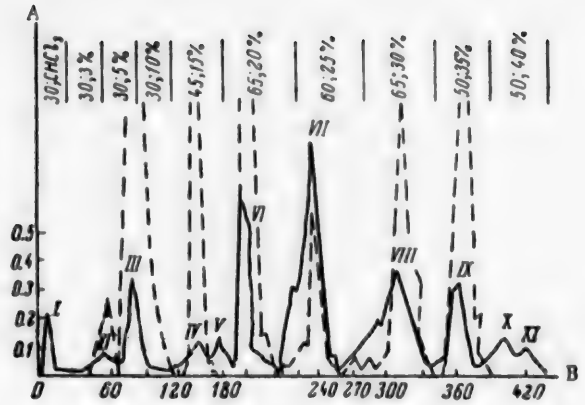

Fig. 1. Chromatogram of a mixture of acid products formed by ozonolysis of SKB rubber ("viscous acids"), and chromatograms of standard acids separated in the small column.

A) Volume of 0.017 N alkali solution (ml), B) volume of eluate (ml). Chromatograms of the standard acids are represented by dash lines. Peaks of acids: II) Levulinic; III) acetic; IV) formic; VI) succinic; VII) 1, 2, 4-butanetricarboxylic; VIII) 1, 2, 3-propanetricarboxylic; IX) 1, 2, 4, 6-hexanetetracarboxylic. The same notation is used in the other figures. Peaks I, V, X, and XI were not identified. The numbers on top indicate the development system, the percentage content of butyl alcohol in chloroform, and the amount of this developer in ml.

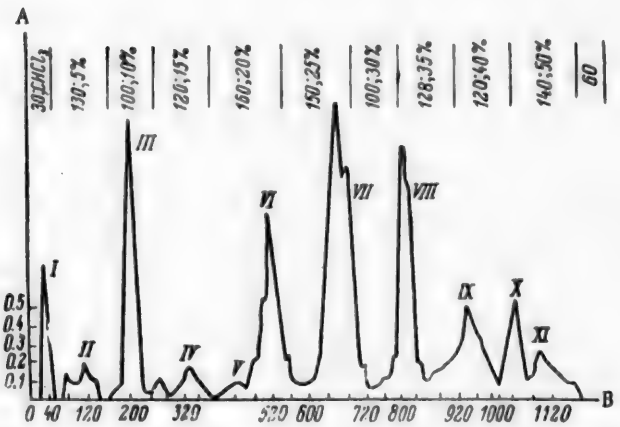

Fig. 2. Chromatogram of a mixture of acid products of ozonolysis of SKB rubber ("viscous acids"), separated in the medium column.

A) Volume of 0.029 N alkali solution (ml), B) volume of eluate (ml). (See legend to Fig. 1).

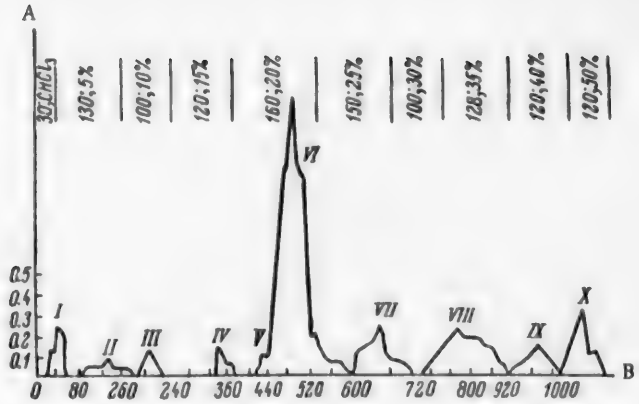

Fig. 3. Chromatogram of a mixture of the products of oxidative decomposition of ozonides from SKB rubber ("crystalline acids"), separated in the medium column.
A) Volume of 0.029 N alkali solution (ml), B) volume of eluate (ml). (See legend to Fig. 1).

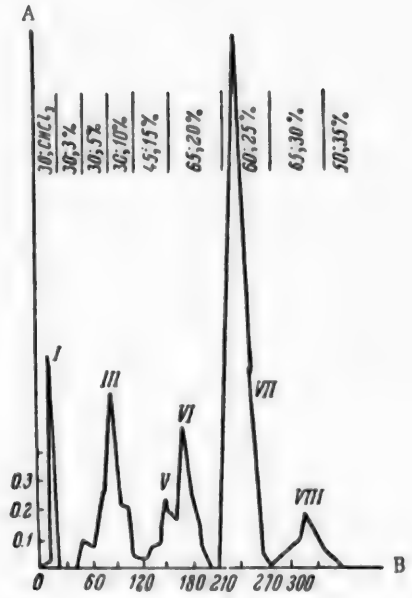

Fig. 4. Chromatogram of a mixture of the products of oxidative decomposition of vinyl-1-cyclohexene-3 ozonide.
A) Volume of 0.017 N alkali solution (ml), B) volume of eluate (ml). (See legend to Fig. 1).

For identification of Peak IX (Fig. 1), 1, 2, 4, 6-hexanetetracarboxylic acid, prepared by the method used by Alekseeva [7, 8], was passed through the column under the conditions used for the unknown acid mixture. The volume peak and the elution limits of the synthetic acid coincided with those of Peak IX in Fig. 1. Hence it may be concluded that the products of oxidative decomposition of the ozonides of sodium divinyl rubber contained 1, 2, 4, 6-hexanetetracarboxylic acid, as it is known that in the presence of several polar groups the mobility of a compound in the chromatographic column depends not only on the length of the hydrocarbon chain and the number of polar groups, but also on the relative positions of these groups. For example, the mobility of a compound is lower if the carboxyl groups are closer together [9].

It follows from all the foregoing that the macromolecules of SKB sodium divinyl rubber contain 1, 4-(1, 2)$_2$-1, 4 regions.

A few milligrams of the acid corresponding to Peak X was isolated, and its silver salt prepared.

The elementary analysis of the salt (in %) was: 21.4 C, 2.20 H, 57.25 Ag, 19.14 O.

The equivalent, from the silver salt, was 81.5.

Acetic acid was introduced during oxidative decomposition of the rubber ozonides. The acid had not been completely distilled from the ozonolysis products, and this accounts for the presence of Peak III, corresponding to acetic acid, in the chromatogram (Fig. 1). Of course, the possibility is not excluded that acetic acid may be formed as a secondary product in the oxidative decomposition of ozonides (10, 11).

Levulinic acid may have been formed: 1) in the ozonolysis of the isomerized 1, 4-1, 2-1, 4 region (by

Composition of the Mixture of Ozonolysis Products of SKB Rubber (Made by the Liquid-Phase Process), and Contents of the Carbon Skeleton of the Rubber in Different Regions of the Rubber Macromolecule (in %)

Peak No.	Acid	Amt. acid in the rubber ozonide decomp. prod. (g)	Wt. of carbon in acid (g)	Cont. of carbon skeleton of rubber in acid %	Region from which the acid was formed	Cont. of the carbon skeleton in the region (%)	Contents of carbon skeleton in units (%)	
							1,2	1,4
II	Levulinic	0.809	0.418	3.73	1.4-1.2-1.4 with migration of double bond in 1,2 unit	5.97	2.98	2.98
III	Acetic	1.434	—	—	—	—	—	—
IV	Formic	0.245	0.098	0.87	—	—	—	—
VI	Succinic	3.320	1.350	12.05	1,4—1,4	12.05	—	12.05
VII	1,2,4-Butanetricarboxylic	4.148	1.835	16.40	1,4—1,2—1,4	18.74	9.37	9.37
VIII	1,2,3-Propanetricarboxylic	2.9140	1.190	10.63	1,4-1,4 with branching at the α-methylene group	10.63	—	10.63
IX	1,2,4,6-Hexanetetracarboxylic	1.842	0.845	7.95	$1,4(1,2)_2$—1,4	8.95	5.96	2.98
X		1.529	—	—	—	—	—	—
	Total:	16.241	5.736	51.22	—	56.34	18.31	38.01

migration of the double bond in the 1, 2(4) unit); 2) in the course of ozonolysis, as the result of a peroxide – formate regrouping [12].

In both cases ultimately the 1, 4-1, 2-1, 4 region yields ketoadipic acid by oxidative decomposition; partial decarboxylation of this acid gives levulinic acid [4, 13).

1, 2, 3-Propanetricarboxylic acid (Peak VIII) had already been detected by Marvel in the products of oxidative decomposition of the ozonides of America B 318 sodium divinyl rubber and of several emulsion polymers of divinyl and its copolymers with styrene [4]. 1, 2, 3-Propanetricarboxylic acid could have been formed, in polymerization in presence of alkalies, from the 1, 4-1, 4 region, branched at the α-methylene group, which might have resulted from the metalation reaction [4, 13].

However, Marvel points out [4] that 1, 2, 3-propanetricarboxylic acid may be formed partially as a secondary product, in the oxidative decomposition of divinyl-rubber ozonides by hydrogen peroxide, from the 1, 4-1, 2-1, 4 region.

Secondary reactions are also possible in the decomposition of rubber ozonides by acetyl hydroperoxide, which was our method. To confirm this, we ozonized vinyl-1-cyclohexene-3, which has the combination of 1, 4-1, 2 units characteristic of divinyl polymers, and decomposed the product by means of acetyl hydroperoxide.

The acids formed by ozonolysis of vinyl-1-cyclohexene-3 were separated in the chromatographic column under the conditions used for the ozonolysis products of SKB rubber. The chromatogram (Fig. 4) shows that in addition to the normal products of ozonolysis – 1, 2, 3-butanetricarboxylic and formic acids – and acetic acid (used in the oxidative decomposition of the ozonides), the mixture contained 1, 2, 3-propanetricarboxylic acid, which in this instance is an anomalous decomposition product of vinyl-1-cyclohexene-3 ozonide [12].

The hypothesis that in the case of sodium divinyl rubber 1, 2, 3-propanetricarboxylic acid may be formed as the result of metalation is plausible, because organic sodium compounds can undergo metalation. However, the possibility of its formation during oxidative decomposition of the ozonides cannot be excluded. Our calculations of the amount of 1, 2, 3-propanetricarboxylic acid were based on the former hypothesis.

Chromatographic data for the crystalline and viscous portions of the oxidative-decomposition products of the rubber ozonides (Figs. 2, 3) were used to calculate the composition of the mixture and the % content of the carbon skeleton of the rubber in each acid. These results were used to determine the contents of the carbon skeleton of the rubber in the regions from which these acids were formed. The results are given in the Table.

The acids identified chromatographically contained 51.22% of the carbon skeleton of the rubber, and the distilled formic acid and formaldehyde contained 12.33%; i. e., the acids contained a total of 63.33% of the carbon skeleton of the rubber.

The ozonolysis process is undoubtedly accompanied by secondary reactions [4, 12, 13]. For example, succinic acid could be formed not only from the 1, 4-1, 4 region, but also by oxidation of levulinic acid, which in its turn could have originated from the 1, 4-1, 2-1, 4 region. Acetic acid, which was disregarded in the calculations relating to the carbon skeleton of the rubber, could also have been formed by oxidation of levulinic acid [10]. The foregoing partially accounts for the incomplete balance of the carbon in the rubber; however, it in no way diminishes the significance of the ozonolysis method for investigation of the chemical structure of synthetic divinyl rubbers, but merely draws attention to the need for a more thorough study of ozonation and ozonide decomposition processes.

EXPERIMENTAL

The SKB sodium divinyl rubber (made by the rod process) was purified by twofold precipitation by ethyl alcohol from 3% solution in benzene.

The purified rubber was dried under vacuum at room temperature, and then sealed in tubes filled with nitrogen. The solution and precipitation stages were performed in oxygen-free nitrogen. The elementary composition of the rubber was determined:

Found %: I 88.41 C, 11.18 H;
C_4H_6. Calculated %: II 88.39 C, 11.26 H;
88.88 C, 11.11 H.

The unsaturation of the rubber, determined by Vasil'ev's method [14], was 87.73%. The relative content of units with an external double bond (1, 2 units) was found to be 52.76 from the amounts of formic acid and formaldehyde. The ozonation of the rubber was performed in previously-purified ethyl acetate [15] by the method described previously [16].

At the end of the ozonation most of the ethyl acetate was distilled from the ozonide solution at 8-10 mm Hg, and to each portion of ozonide formed from 3 g of rubber equal volumes of acetyl hydroperoxide and acetic acid were added, as described by Wilms [2], followed by excess of acetyl hydroperoxide after some time. After the products had been allowed to stand for 15-20 hours at 40-50°, the oxidative decomposition of the ozonides could be assumed to be virtually complete. Excess acetyl hydroperoxide and other peroxides which might have been formed during the decomposition of the ozonides was decomposed by addition of platinum black to the solution of the products of oxidative decomposition. The absence of carbonyl compounds was confirmed by the Schiff and silver mirror tests. Acetic acid was removed from the decomposition products of the ozonides by distillation at 8-10 mm from a water bath at 30-40°.

After removal of the acetic acid, the ozonolysis products were separated into two parts by means of purified ethyl ether: "crystalline acids," which were insoluble in ether, and consisted mainly of succinic acid; and "viscous acids," which were soluble in ether. Both parts were analyzed by the chromatographic method.

The total weight of rubber ozonized was 12.70 g, containing 11.19 g of carbon. The carbon found in the identified acids was 5.74 g, or 51.22% (see Table). To this we must add the carbon from the rubber skeleton, contained in the formic acid and aldehyde distilled together with the solvent from the ozonolysis products, i. e., 12.33%. In all, 63.55% of the carbon skeleton of the rubber was accounted for in the identified acids.

Chromatographic analysis. The silica gel, solvents, elution rate, amount of acid solution, and acid concentrations were selected with the aid of standard-acid mixtures [3]. Development systems for use with the small (inner diameter 16 mm, 7 g of silica gel), medium (inner diameter 18 mm, 22 g of silica gel), and large (inner

diameter 24 mm, 45-50 g of silica gel) columns were worked out, for use in separation of acid mixtures formed by the oxidative decomposition of the rubber ozonides.

The small column was used for identification of the acids in the mixture, in order to save time and reduce the amounts of standard acids used. The medium and large columns were used for separation and accumulation of the individual components of the mixtures.

The chromatogram in Fig. 1 was obtained as follows. 0.2 ml of a solution containing 0.037 g of "viscous acids" in 60% tertiary amyl alcohol in chloroform was passed through the small column. The flow rate of the solvent was 0.8 ml/minute.

After the chromatogram of the unknown mixture had been obtained, the individual acids were identified by comparison of the chromatogram of the mixture (Fig. 1) with chromatograms of individual standard acids. The standard acids were passed through the same column under the identical conditions.

A definite weight of each acid was dissolved in 60% tertiary amyl alcohol. 0.2 ml of the acid solution, containing from 0.0027 to 0.008 g of acid, was taken for the separation. The following standard acids were used: levulinic; acetic; formic; 1,2,4-butanetricarboxylic; 1,2,3-propanetricarboxylic; and 1,2,4,6-hexanetetracarboxylic.

Fig. 1 shows that the peaks for the standard acids coincided or almost coincided with the peaks and the elution thresholds for the unknown mixture. The chromatographic identification was confirmed by chemical analysis. This required separation and accumulation of the acids. The medium and large columns were used for isolation and accumulation of the acids. For separation, 1 ml of solution containing 0.1585 g of "viscous acids" was introduced into the medium column. The column was then developed (eluted) by means of eluents of different polarity, which depends on the butanol content of the chloroform. Both the butanol and the chloroform were saturated with water before being mixed. The elution rate was 1 ml/minute. Each 4 ml of the eluate was titrated by aqueous 0.0291 N caustic soda.

The chromatogram of the "viscous acids" is given in Fig. 2.

A solution of the crystalline part of the mixed ozonolysis products (0.0659 g of mixed acids in 2 ml of solution) was passed through the same column under exactly the same conditions. The chromatogram is given in Fig. 3.

The results in the chromatogram (Fig. 2) were used for isolation of the fractions corresponding to the individual peaks from the viscous part of the mixture of ozonolysis products.

3 ml of the acid solution, containing 0.55 g of mixed acids, was taken for the separation.

After sufficient material had been accumulated, chemical analysis of the individual fractions was carried out.

Peaks II, III, and IV were identified chromatographically. Peak VI, according to chromatographic data, corresponded to succinic acid. Repeated separation of the mixture in the medium and large columns yielded a quantity of Fraction VI, corresponding to Peak VI. Most of the solvent (30% butanol, 70% chloroform) was distilled from this fraction at 8 mm and 30-35° on the water bath. The distillation of the solvent was then continued at 2-3 mm. The crystalline mass which remained after distillation of the solvent was repeatedly washed with ethyl ether. All the other fractions were similarly treated.

The dried acid was identified by its m. p., 183-184°; a mixed sample with succinic acid (m. p. 183°) melted at 184°. The neutralization equivalent was 59.8. Calculated for $C_4H_6O_4$ – 59. Peak VII corresponded to 1, 2, 4-butanetricarboxylic acid. The fractions corresponding to Peak VII were combined and treated as described above.

The acid had m. p. 116-117°, and a mixed sample with 1, 2, 4-butanetricarboxylic acid (m. p. 117°) prepared from vinylcyclohexene melted at 117°. The neutralization equivalent was 64.52. The Ag content of the silver salt was 63.42%; calculated for $C_7H_7O_6Ag_3$ – 63.3%. The equivalent, from the silver salt, was 63.15, molecular weight 189.45. Calculated for $C_7H_{10}O_6$: equivalent 63.36; molecular weight 190.98.

According to the chromatogram, Peak VIII corresponds to 1, 2, 3-propanetricarboxylic acid, but the results of elementary microanalysis did not agree with calculated values for propanetricarboxylic acid.

Found %: 52.60 C, 7.92 H, 39.47 O;
$C_6H_8O_6$. Calculated %: 50.91 C, 4.58 H, 54.51 O.

The suggestion that the acid became esterified during collection of the fractions, when the acid was in 30-35% butanol solution, and during distillation of the solvent, was confirmed.

Analysis of the silver salt of the substance (formed by way of the sodium salt of the acid) showed 48.50% of Ag. The calculated content for the silver salt of the monobutyl ester is 48.38%.

Peak IX corresponds to 1, 2, 4, 6-hexanetetracarboxylic acid. The acid was identified by analysis of the silver salt. The silver salt was prepared by way of the ammonium salt.

The Ag content of the silver salt, by analysis, was 55.80%. The acid salt of hexanetetracarboxylic acid, $C_{10}H_{11}O_8Ag_8$, was evidently formed, with a calculated Ag content of 55.52%, as the calculated value for the neutral salt $C_{10}H_{11}O_8Ag_4$ is 62.5% Ag.

Elementary microanalysis of the acid salt gave the following results:

Found %: 20.48 C, 2.20. H, 55.37 Ag.
$C_{10}H_{11}O_8Ag_3$. Calculated %: 20.60 C, 1.88 H, 55.52 Ag.

Peak X. None of the available seven model acids gave volume peaks and elution thresholds corresponding to Peak X, so that the latter was not identified chromatographically. A very small amount of the substance of Peak X was collected. Its silver salt was obtained. Elementary microanalysis of the salt gave the following results (%): 21.40 C, 2.20 H, 57.25 Ag, 19.14 O. The equivalent, by the silver salt, is 81.5. The simplest empirical formula for the acid of Peak X is $C_3H_4O_2Ag$. The position of the acid on the chromatogram and analysis of the silver salt suggests only that the acid of Peak X may have the formula $C_{10}H_{14}O_7$.

Peaks II, III, and IV were identified chromatographically.

SUMMARY

1. 63.55% of the carbon skeleton of the rubber could be accounted for in the identified products of the oxidative decomposition of ozonides of SKB sodium divinyl rubber. The chromatographic results were confirmed by chemical analysis.

2. From the nature of the acids found in the oxidative-decomposition products of the rubber ozonides it may be concluded that the macromolecules of SKB rubber contain regions of the following structure: 1, 4-1, 4 with 1, 4 units repeated at least twice consecutively; 1, 4-1, 2-1, 4 with migration of the double bond in the 1, 2 unit; 1, 4-1, 2-1, 4 – alternate 1, 2 and 1, 4 units; 1, 4-1, 4 – with possible subsequent branching at the α-methylene group; 1, 4-1, 2-1, 2-1, 4 alternation of 1, 4 units with pairs of 1, 2 units.

LITERATURE CITED

[1] A. I. Iakubchik, A. A. Vasil'ev, and V. M. Zhabina, J. Appl. Chem. 17, 107 (1944).

[2] H. Wilms, Lieb. Ann. 567, 1-3, 96 (1950).

[3] A. I. Iakubchik and S. K. Zykova, J. Appl. Chem. 29, 10, 1591 (1956).*

[4] C. S. Marvel, and W. M. Schilling, et al. J. Org. Ch. 16, 6, 838, 854 (1951).

[5] C. S. Marvel and Rands, J. Am. Chem. Soc. 72, 6, 2642 (1950).

[6] L. Ramsey, and W. P. Patterson. J. Ass. Off. Agr. Chem. 31, 139 (1948).

[7] E. N. Alekseeva, J. Gen. Chem. 9, 15, 1426 (1939).

[8] E. N. Alekseeva and V. D. Mezhov, J. Gen. Chem. 22, 10, 1813 (1952).

[9] N. A. Fuks, Proc. All-Union Conf. on Chromatrography (1950) [In Russian] (Acad. Sci. USSR, 1952), 56.

[10] G. Ebermeyer, Uber den Ozonabbau des Kautschuks. Inaugural/Dissertation, Erbangen (1931).

* Original Russian pagination. See C. B. Translation.

[11] A. I. Iakubchik, N. G. Kasatkina, et al. J. Gen. Chem. 27, 1195 (1957).

[12] K. Ziegler, Lieb. Ann. 567, 43, 99 (1950).

[13] A. I. Iakubchik, in the book: Academician Lebedev [in Russian], (Moscow, Izd. AN SSSR, 1954), 197.

[14] M. S. Rozhdestvenskii, Trans. Inst. Pure Reagents 8, 122 (1929).

[15] A. I. Iakubchik, N. G. Kasatkina, and T. E. Pavolvskaia, J. Gen. Chem. 25, 1473 (1955).•

Received April 2, 1957.

• Original Russian pagination. See C. B. Translation.

COMPONENT RATIO IN THE SYNTHESIS OF VINYL ACETATE BY HETEROGENEOUS CATALYSIS

I. A. Arbuzova, S. N. Ushakov, and E. N. Rostovskii

The principal method for the synthesis of vinyl acetate is by the reaction of acetylene with acetic acid, effected in the liquid or vapor phase. Despite the fact that the vapor-phase process is widely used in industry, relatively little information on it is available in the literature. Apart from a few patent references [1, 2], the paper by Ushakov and Fainshtein [3], and our earlier work [4], deal with studies of the vapor-phase synthesis of vinyl acetate. At that time we determined the conditions for almost complete conversion of acetic acid to vinyl acetate when the process is carried out with a large excess of acetylene. A study was also made of the conditions in which catalyst life is increased, and of the factors which lower catalyst activity during prolonged operation. Brief information on the industrial production of vinyl acetate in Germany appeared in the postwar years. Copenhaver and Bigelow [5] and Green [6] have presented data on the process at the Hoechst works. The synthesis was carried out at 170-210°, with acetylene and acetic acid in approximately 8:1 ratio; the conversion of acetic acid is about 60% [6]. It has also been reported [7] that in another German plant (Burghausen) the conversion of acetic acid is 30%, because of the high acetylene feed rate.

The question of the influence of the component ratio on the synthesis, and on catalyst activity has not been adequately considered in the literature.

The present communication deals with a study of the effect of variations of the component ratio (acetylene to acetic acid) on the principal process characteristics – conversion of acetic acid into vinyl acetate, and catalyst activity.

EXPERIMENTAL

Experiments with mixtures of higher acetylene contents, containing approximately from 20 to 11 moles of acetylene per mole of acetic acid, were performed by the method described in our earlier paper [4]. A mixture of acetic acid vapor and acetylene, made in a separate evaporator, was passed over the heated catalyst. The reaction tube contained 14 g of catalyst (15.5% of zinc acetate on AG carbon in 3-4 mm granules). Acetylene was passed at 10 liters per hour through the catalyst heated to 200°. The space velocity was 380 liters per liter of catalyst per hour. The amount of acetic acid fed in varied from 1 mole per 22 moles of acetylene to 1 mole per 11.5 moles of acetylene; this was achieved by variations of the evaporator temperature between 35 and 45° (the time of contact between the reactants and the catalyst varied from 3.7 to 3 seconds). The conversion of acetic acid was estimated by analysis of samples taken from the vapor phase. The experimental results are plotted in Figs. 1 and 2. The same diagrams include curves for the specific activity of the catalyst, calculated by means of the formula

$A = \frac{R \cdot 1.433 \cdot B}{C}$ g of vinylacetylene per g of catalyst per hour, where R is the acetic acid rate (in G/hour), B is the % conversion of acetic acid, and C is the amount of catalyst (g).

Fig. 1 shows that when the amount of acetylene is increased from 11.5 to 22 moles per mole of acetic acid the degree of conversion rises from 68 to 97%, while the specific activity of the catalyst falls from 0.170 g to 0.113 g of vinyl acetate per g of catalyst per hour.

Fig. 2 represents data on the influence of temperature on the conversion of acetic acid and specific activity

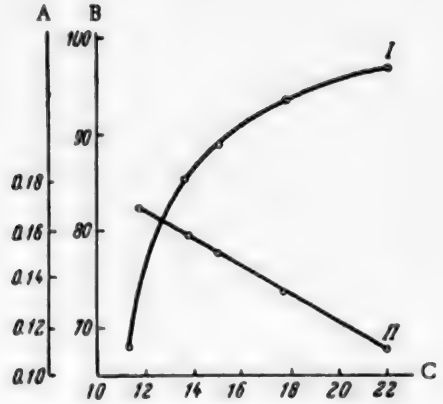

Fig. 1. Effect of component ratio on conversion (I) and specific activity of the catalyst (II). Temperature 200°, catalyst 15.5% zinc acetate on AG carbon.
A) Catalyst activity (in g/g. hour), B) conversion (%), C) molecular ratio of acetylene to acetic acid.

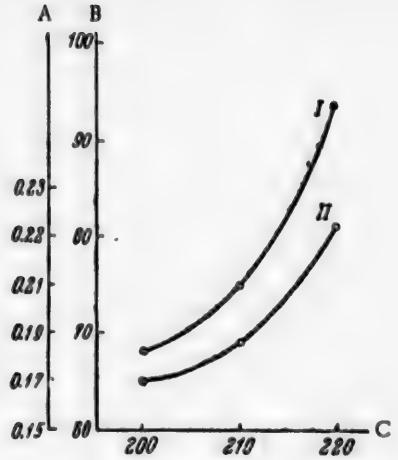

Fig. 2. Effect of temperature on conversion (I) and specific activity of the catalyst (II). Catalyst 15.7% zinc acetate on AG carbon, component ratio 11.5:1, contact time 3 seconds.
A) catalyst activity (in g/g·hour), B) conversion (%), C) temperature (°C).

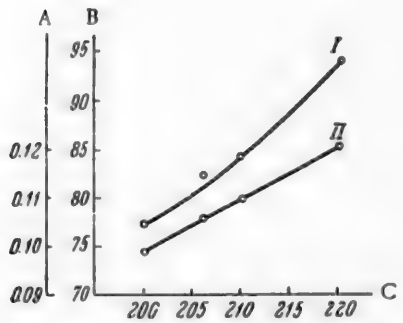

Fig. 3. Effect of temperature on conversion (I) and specific activity of the catalyst (II). Catalyst 17.7% zinc acetate on AG carbon, component ratio 5:1, contact time 13 seconds.
A) Catalyst activity (in g/g·hour), B) conversion (%), C) temperature (°C).

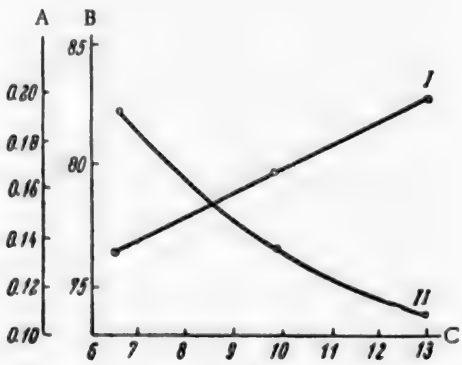

Fig. 4. Effect of contact time on conversion (I) and specific activity of the catalyst (II). Catalyst 15.7% zinc acetate on AG carbon, component ratio 5:1, temperature 200°.
A) Catalyst activity (in g/g·hour), B) conversion (%), C) contact time (seconds).

in synthesis performed at a molar ratio of 11.5:1 of acetylene to acetic acid. The curves in Fig. 2 show that the conversion of acetic acid and the specific activity of the catalyst increase with the reaction temperature.

A somewhat modified method was used for studies of the process at molecular ratios of acetylene to acetic acid between 5:1 and 3:1. Acetic acid was fed into the catalyst tube at a constant rate; this was effected by the use of a buret adapted on the principle of a Mariotte vessel. The components were mixed and preheated in the front part of the tube, not filled with catalyst. The reaction tube was charged with 56 g of catalyst (16.5%°of zinc acetate on AG carbon). Acetylene was passed through the heated catalyst at 10 liters per hour (the space

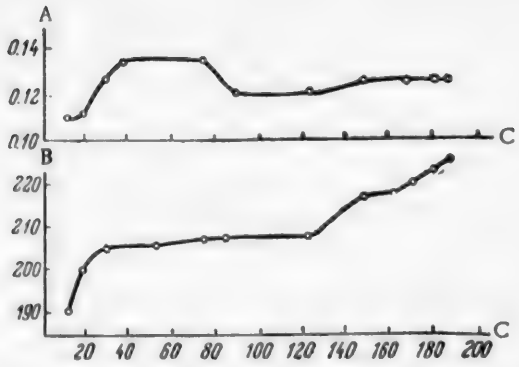

Fig. 5. Results for 190 hours of catalyst operation. Catalyst 17.5% zinc acetate on AG carbon, component ratio 5:1, contact time 9.75 seconds. A) Catalyst activity (in g/g· hour), B) temperature (°C), C) time (hours).

velocity of acetylene was about 95 liters per liter of catalyst per hour), and acetic acid was fed in at 5 g/hour (the molar ratio of acetylene to acetic acid was approximately 5:1). The gaseous mixture after catalysis was condensed in receivers, the first of which was cooled to − 15°, and the second to − 45°. Completeness of condensation was checked with the aid of a U-shaped tube filled with activated carbon previously saturated with acetylene. When the receiver was cooled to − 45°, the condensation was virtually complete. The condensate was analyzed for its vinyl acetate and acetic acid contents. The conversion of acetic acid and the specific activity of the catalyst were calculated from the analytical results. In some of the experiments vinyl acetate and acetic acid were isolated by distillation. The results of these experiments, with higher concentrations of acetic acid, are plotted in Figs. 3 and 4.

Synthesis of Vinyl Acetate at 3:1 Ratio

Ratio of acetylene to acetic acid (molar)	Contact time (seconds)	Reaction temperature (°C)	Composition of condensate (%)			Conversion of acetic acid (%)	Catalyst activity g/g·hour)
			vinyl acetate	acetic acid	total		
1:2.7	21	190-195	92.0	4.7	96.7	82.8	0.106
1:2.9	23	190-195	93.4	2.8	96.2	84.0	0.135
1:3	22	240	60.4	26.6	87.0	53.6	0.263

Comparison of the data in Fig. 3 with the data in Fig. 2, obtained when the process was carried out at a molar ratio of 11.5:1 of acetylene to acetic acid, shows that for an approximately equal degree of conversion the synthesis with 5:1 component ratio must be carried out with an approximately 4-fold increase of the contact time, which leads to a decrease of the specific activity of the catalyst. Fig. 4 shows the results obtained in the synthesis of vinyl acetate at a 5:1 molar ratio of acetylene to acetic acid, with variations of the contact time from 6.5 to 13 seconds; it is seen that the specific catalyst activity increases and the conversion of acetic acid decreases with decrease of the contact time.

The foregoing graphs represent the results of experiments carried out with fresh catalyst with 5-6 hours of operation.

Fig. 5 shows results for 190 hours of catalyst operation in synthesis carried out at a molar ratio of 5:1 of acetylene to acetic acid.

The curves in Fig. 5 indicate that after the catalyst activity has decreased it may be restored to a considerable extent by increase of temperature.

The table contains certain data on the synthesis of vinyl acetate with acetylene and acetic acid in a molar ratio of 3:1.

These data show that increase of the reaction temperature to 240° raises the catalyst activity, but the amounts of by-products (mainly ethylidene esters and their decomposition products) increase; these by-products are not formed to any practical extent if a large excess of acetylene is used.

Comparison of different conditions of vinyl acetate synthesis, with variations of the component ratio and temperature, shows that, dependent on the temperature and the contact time, a high degree of conversion of

acetic acid into vinyl acetate, or high catalyst activity, may be achieved over the entire range of acetylene – acetic acid ratios studied (from 22 to 3 moles of acetylene per mole of acetic acid).

SUMMARY

The effects of variations of the acetylene – acetic acid ratio on the conversion of acetic acid into vinyl acetate and on catalyst activity have been determined.

LITERATURE CITED

[1] W. O. Herrmann, H. Deutsch, E. Baum, and M. Mugdan, German Patent 403,784 (1924).

[2] W. O. Herrmann, H. Deutsch, and E. Baum, German Patent 485,271 (1927).

[3] S. N. Ushakov and Iu. M. Fainshtein, Plastics 1 (1933); Ind. Eng. Chem. 26, 561 (1934).

[4] S. N. Ushakov, E. N. Rostovskii, and I. A. Arbuzova, J. Appl. Chem. 13, 1629 (1940).

[5] I. Copenhaver and M. Bigelow, Acetylene and Carbon Monoxide (N. Y., 1949) 25.

[6] L. W. Green, Chem. Eng. 54, 7, 98 (1947).

[7] N. Platzer, Modern Plastics 28, 1, 113 (1950).

Received May 14, 1957.

HERBICIDES FROM PHENOLS IN TAR OBTAINED BY PYROLYSIS OF WOOD

V. Kovalev and D. Tishchenko

(The S. M. Kirov Academy of Wood Technology)

Selective herbicidesare substances which, in definite dosages, kill plants of particular families but do not harm plants of other families, so that they can be used for "chemical weeding." In most cases herbicides in small doses act as growth stimulators for all plants [1], and sometimes they increase the yields obtained from weed-free crops. The most universal selective herbicides are 2, 4-dichlorophenoxyacetic acid (2, 4-D) and 2-methyl-4-chlorophenoxyacetic acid (MCP), which were first proposed and tested in England [2], and almost simultaneously in the U. S. A. [3]. Since 1946 these and certain other substituted phenoxyacetic and phenoxycarboxylic acids were tested in other countries and in the USSR [4]. When cereal crops (rye, wheat, millet, etc.) are sprayed (usually from aircraft) with dilute solutions of 2, 4-D or MCP, about 1 kilogram per hectare, dicotyledonous weeds (goosefoot, mustard, thistle, amaranth, etc.) are destroyed or suppressed, while cereals are unharmed and the average yield is increased by 3-6 centners. The same chemicals, when applied at a rate of 2-4 kg per hectare, destroy birch, alder, and certain other deciduous trees but do not harm conifers; this eliminates the need for costly hand weeding of forest plantations and accelerates the growth of valuable trees in forests of the taiga zone.

There has been a great demand for 2, 4-D and MCP in agriculture and forestry, but as their manufacture requires phenol and o-cresol, which are used for the production of other equally important materials, the demand cannot be met fully by the chemical industry in the immediate future. This justifies any attempt at the production of herbicides of this type from any other phenols or mixtures, more readily available than phenol or o-cresol.

The phenol fraction, boiling at 180-210°, from the settled tar produced in wood pyrolysis (dry distillation, gasification) has a fairly constant composition, irrespective of the pyrolysis method or of the kind of wood, and contains about 25% phenol, about 10% o-cresol, 30-40% guaiacol, and smaller amounts of p-cresol, o-ethylphenol, and xylenols.

It is known that chlorinated p-cresoxyacetic acids have no herbicidal properties; the properties of chlorinated guaiacoxyacetic acids were not known to us. If the latter proved to be herbicidal, then in a mixture of substituted phenoxyacetic acids, made by condensation of phenolates of the above-named fraction with sodium chloroacetate followed by chlorination, the content of physiologically active chlorophenoxyacetic acids (2, 4-D, MCP, chloroguaiacoxyacetic acids) might exceed 75-80½, and the mixture might be an acceptable selective herbicide.

To test this hypothesis, monochloroguaiacoxyacetic acid, 4, 6-dichloroguaiacoxyacetic acid, and a mixture of chlorinated phenoxyacetic acids from the above-named phenols were prepared. Two known methods were used for synthesis of the acids: 1) condensation of phenolates with sodium chloroacetate followed by chlorination of the phenoxyacetic acids to a definite chlorine content, and 2) chlorination of phenols to a definite chlorine content followed by condensation of the chlorophenolates with sodium chloroacetate. Subsequent trials showed that mixtures containing about 30% chlorine, with an equivalent of about 250, which corresponds to dichlorophenoxyacetic acids (the average molecular weight of the phenol mixture being about 114), are physiologically active. These preliminary trials were conducted in 1954 and 1955 by I. V. Shutov in the Laboratory of the Institute of Forestry (delayed germination of peas), by N. A. Shipinov (in the Laboratory of the Institute of Plant Protection, spraying of pea shoots), by A. V. Voevodin under field conditions in the Kuban' province, and by ourselves in the Novgorod province. The results of these preliminary trials showed that our herbicides approach 2, 4-D in physiological activity, although our mixture contains not more than 35% of 2, 4-D and MCP.

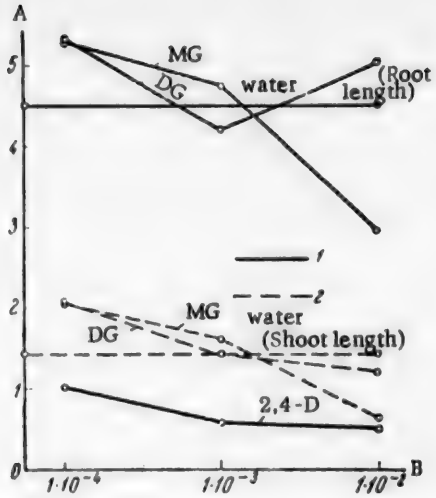

Fig. 1. Effects of MG and DG solutions on seed germination.
A) Length of pea roots and shoots (cm), B) concentrations of phenoxyacetic acid solutions (%).
1) Root length, 2) shoot length.

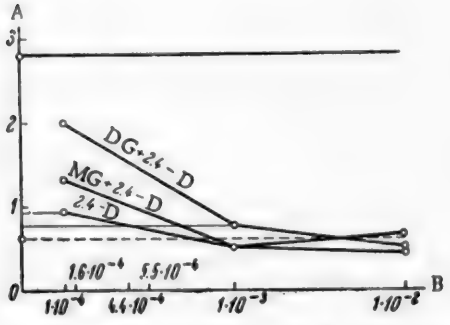

Fig. 2. Effects of solutions of 2, 4-D and its mixtures with MG and DG on germination of peas.
A) Length of pea roots, B) solution concentration (%). Continuous lines represent the root lengths.

Therefore chloroguaiacoxyacetic acids must be either selective herbicides or synergists of 2, 4-D and MCP (synergism is increase of the physiological activity of an active substance by addition of an inactive one). We therefore carried out a laboratory investigation of 2, 4-D, 4-chloroguaiacoxyacetic acid (MG), and 4, 6-dichloroguaiacoxyacetic acid (DG), and studied the effects of their dilute aqueous solutions, as compared with water, in the germination of seeds. Boiarkin's method [5] did not give reproducible results; our data were obtained in the germination of peas under isothermal conditions, with air of 100% relative humidity drawn through the experimental chamber. The germination time was 106 hours. The seeds were previously soaked for 24 hours in distilled water. The results of the first series of experiments are plotted in Fig. 1.

In the evaluation of these results it should be remembered that nearly all selective herbicides stimulate growth when used in low concentrations, retard growth at higher concentrations, and kill plants at yet higher concentrations. The length of the pea roots mean of 75 seeds, water as control, 4.5 cm is indicated by continuous lines, and of the shoots (the same, 1.5 cm), by dash lines.

The graph shows that at these concentrations 2, 4-D suppresses growth (0.0001 and 0.001%) or kills pea seeds (0.01%); MG either stimulates growth (0.0001 and 0.001%) or slightly suppresses it (0.01%); DG only stimulates root growth (the inflection on the curve at 0.001% requires further investigation) and stimulates shoot growth at 0.0001%, without suppressing it at higher concentrations.

It was stated earlier that our mixture was physiologically active with a chlorine content over 28%; therefore it does not contain MG. The graph shows that in the given concentrations DG does not act as a herbicide, but stimulates the growth of peas.

Fig. 2 shows the effects of solutions of 2, 4-D and its mixtures with MG and DG of concentrations higher than the total concentration mentioned above (0.01, 0.001 and 0.0001%) and peas (germination time about 70 hours). The weight ratio of 2,4-D to MG or DG in the mixtures was 1:5, i. e., the 2, 4-D content of each of these three solutions was 1/6 of the content in the 2, 4-D solution of the same concentration.

The ordinates in Fig. 2 represent the root lengths for these three points. A mixture of MG with 2, 4-D suppresses root growth to a greater extent than 2, 4-D in equivalent concentration, over almost the whole curve; for example, the effect with a total concentration of 0.001% is the same as with 0.001% of 2, 4-D. DG is a synergist for 2, 4-D at total concentrations of 0.0036% and less; for example, at a total concentration of 0.001% (0.00016% 2, 4-D) the suppression of root growth is the same as in a 0.00044% solution of pure 2, 4-D. Therefore MG and DG are synergists for 2, 4-D.

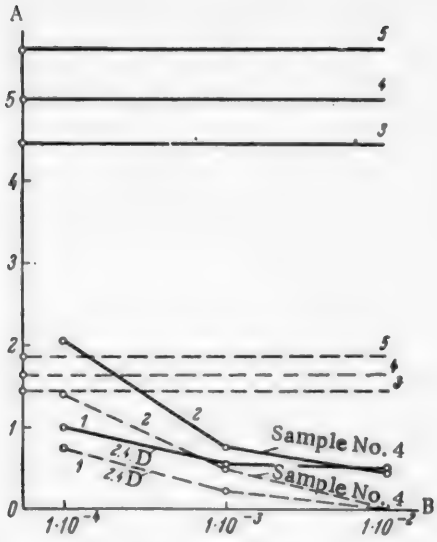

Fig. 3. Effects of solutions of Sample No.4 and 2, 4-D on the germination of peas. A) Length of pea roots and shoots, B) solution concentration (%). Continuous lines represent root length; dash lines, shoot length.
1) Solution of 2, 4-D, 2) Sample No.4, 3) water, 4) 2, 4-D (10^{-7}% solution), 5) Sample No 4 (10^{-7}% solution).

Finally, peas were allowed to germinate under the same conditions in solutions of 2, 4-D and of chlorophenoxyacetic acids made from the 180-210° phenol fraction from wood pyrolysis (Sample No.4). It has already been stated that selective herbicides act as stimulators of plant growth at low concentrations. To test the stimulating action of Sample No.4, we germinated peas in its solutions and solutions of 2, 4-D of $1 \cdot 10^{-7}$% concentration. The results, plotted in Fig. 3, show that Sample 4 is a better stimulator than 2, 4-D. It contains about 40% of chloroguaiacoxyacetic acids. It is known that ferulic acid (β-guaiacylacrylic acid) is a synergist of plant-growth stimulators [6]; it contains the same guaiacol residue as guaiacoxyacetic acids. Fig. 3 also shows the results for germination of peas in 0.01% solutions of 2, 4-D and Sample No 4; Sample No 4 has a greater suppressing effect on root growth than 2, 4-D, but in 0.001% and 0.0001% concentrations its effect is somewhat weaker than that of 2, 4-D.

Of course, the significance of the experimental results in these three diagrams should not be overestimated, but they showed that results acceptable for practical purposes could be obtained in the future.

In 1955 four samples were prepared, differing somewhat in their chlorine contents and therefore in equivalents. They were sent to the All-Union Institute of Plant Protection (A. V. Voevodin) for field trials.

TABLE 1
Trials of Samples Nos.1 and 3 on Wheat Sowings in the Krasnodar Region

Weeds	% of weeds destroyed		
	2,4-D	No.1	No.3
Bindweed	100	91	90
Mustard	100	100	100
Pigweed	47	51	36
Thistle	90	74	67
Amaranth	32	64	43
Application of chlorophenoxyacetic acids (in kg/hectare)	1000	1,175	1,325

The trials were conducted on wheat sowings in the Krasnodar region. Only the percentage destruction of weeds was recorded. The best results were obtained with Sample No.1 (equiv 233) and No.3 (equiv 248). The plots, 0.1-0.25 hectare in area, were sprayed from a land machine in dry weather. The results of the experiments are given in Table 1.

These results show that in their effects on weeds Samples No.1 and No.3 are fully comparable to 2, 4-D only if somewhat larger amounts are used. At the application rates of No.1 and No.3 given in the table, not more than 0.45 kg of 2, 4-D and MCP was introduced per hectare, and the observed destruction of weeds can be attributed only to the synergetic action of DG.

TABLE 2

Comparative Effects of 2, 4-D and Sample No.2 on Young Alder and Birch Plants

Herbicide	Plants (% of total on plot)				
	completely withered	crown withered, runners from root	more than half the crown withered	less than half the crown withered	undamaged
			Birch		
No 2	32	16	32	20	0
2, 4-D	39	30	11	19	1
			Alder		
No 2	28	32	12	28	0
2, 4-D	78	16	2	4	0

Sample No.2, which gave somewhat worse results with wheat weeds (not given in the table), was tested in the summer of 1955 by I. V. Shutov of the Central Scientific Research Institute of Forestry, at the Siverskaia Forestry Station, on forest flora; the dosage of chlorophenoxyacetic acids was 2 kg/hectare, and 2, 4-D was applied at the same rate for the controls. In the summer of the same year the leaves of birch and alder completely withered and fell under the influence of both herbicides, aspen was slightly damaged (the tips of young shoots became withered and curved) in both cases, spruce was unharmed, and young pine shoots were appreciably damaged by 2, 4-D. The final evaluation was carried out in the summer of 1956.

Sample No.2 did not harm pine, while 2, 4-D damaged 51% of the pine plants (twisted and withered shoots).

All the 1955 trials were performed with sodium salts of the herbicides; these salts were found to be difficult to dissolve and inconvenient to use, so that difficulties arose in the field trials and the results were not fully reproducible.

For the 1956 field and laboratory trials we prepared the readily soluble triethanolamine salts of five samples (Nos.1-5) of chlorophenoxyacetic acids, made by two methods: 1) condensation of phenolates with sodium chloroacetate followed by chlorination of the phenoxyacetic acids, and 2) chlorination of phenols and condensation of chlorophenolates with sodium chloroacetate (Samples Nos.2-4). Samples Nos.2-4 were rejected, mainly because of their high chlorophenol contents. Sample No.1 was prepared from phenols boiling in the 180-210° range, containing 8.0% methoxyl; the sample therefore contained about 33% of chloroguaiacoxyacetic acids. Sample No.5 was prepared from the same phenol fraction, but part of the guaiacol was removed until the residual methoxyl content was 2.5% (the content of chloroguaiacoxyacetic acids was about 10%).

These samples were tested at the Zernograd State Selection Station (Rostov province), with the assistance of V. A. Makarova of the Station staff, on sowings of summer wheat and millet. The spring of 1956 was cold and rainy; three hours after the wheat had been sprayed there was a downpour of rain, which could not fail to affect the results of the trials. All the trials were performed in triplicate. The results are presented in Table 3.

In evaluation of the data in Table 3 it should be remembered that 1-1.2 kg of 2,4-D per hectare is generally the maximum permissible dose; higher rates suppress cereal plants. 1 kg of Sample No.1 contained not more than 0.4 kg of 2, 4-D and MCP and 0.3 kg of DG, and 1 kg of No. 5, not more than 0.6 kg and 0.1 kg respectively. Therefore the maximum permissible dosage of No.1, on these grounds, is 3 kg/hectare, and of No.5, only 2 kg/hectare. With 3 kg of No.1 per hectare there was introduced 0.9 kg of DG which, as was shown earlier, is not only a synergist of 2, 4-D but also a stimulator of plant growth; while with 2 kg of No.5 only 0.2 kg of DG was introduced. This accounts for the increased yield of wheat with a dosage of 3 kg of No.1 per hectare, despite the weed content of the sowing and the comparable destruction of weeds as the result of treatment with 2, 4-D.

TABLE 3

Trials of Samples Nos.1 and 5 on Wheat at the Zernograd State Selection Station

Herbicide, and application rate (kg/hectare)		Weeds killed (%)	Wheat yield (centners/hectare)
Controls		–	12.6
2,4-D,	1.0	67.3	15.7
No 1	1.0	24.9	12.7
No 1	2.0	50.7	15.4
No 1	3.0	78.8	19.4
No 5	1.0	21.1	10.8
No 5	2.0	62.3	15.1
No 5	3.0	71.1	15.0

TABLE 4

Trials of Samples on Millet

Herbicide, and application rate (kg/hectare)	Weediness of sowing			Contaminated of millet grain							Yield (centners/hectare)
	weeds killed (%)	damage to surviving weeds	average weed weight (g/m^2)	% of total grain	total	goosefoot	amaranth	rapeseed	cabbage	others	
Control	—	—	2253	6.2	91110	47710	38550	4250	510	90	13.8
2,4-D 0.5	36.6	Weak	890	3.3	56760	30700	25950	60	–	50	17.3
2,4-D 1.0	59.6	Moderate	666	Few	Few	Few	Few	Few	Few	Few	29.5
№ 1 1.0	40.3	Strong	404	None	None	None	None	None	None	None	32.5
№ 1 2.0	56.5	Very strong	249	"	"	"	"	"	"	"	42.4
№ 1 3.0	38.9	The same	172	"	"	"	"	"	"	"	42.9
№ 5 1.0	41.1	Strong	230	"	"	"	"	"	"	"	37.5
№ 5 2.0	51.1	Very strong	186	"	"	"	"	"	"	"	34.2

The millet trials were conducted in warm and dry weather, and gave more conclusive results. The millet sowings were strongly contaminated with weeds. The results of the trials are summarized in Table 4.

In evaluation of the data it should be remembered that the growth conditions of the millet and weeds were very favorable (the soil was abundantly moist). First, it should be noted that, at 1 kg/hectare, 2, 4-D and Nos.1 and 5 all caused the same degree of weed destruction (39-41%), but the surviving weeds were retarded much more by Samples Nos.1 and 5, did not form the top whorl, and yielded no seeds, which was equivalent to their complete destruction, whereas with 2, 4-D applied at a rate of 1 kg per hectare there was some seeding of the weeds. The yield data are even more remarkable. The largest increase with the use of 2, 4-D was 15.7 centners/hectare over the control. This large increase can only be explained by a high contamination of the control sowings. The greatest increase with Sample No.5 was 23.7 centners per hectare, and with No.1, 29.1 centners per hectare; this cannot be due only to the destruction or suppression of dicotyledonous weeds. The explanation should be sought only in the stimulating effect of DG on millet. No.5, which contained only 10% DG and about 60% 2, 4-D and MCP, gave the highest yield when applied at a rate of 1.0 kg/hectare, and the yield decreased with 2.0 kg/hectare: 2 kg of No.5 contains about 1.2 kg of 2, 4-D, and MCP, while millet is more sensitive than other cereals to 2, 4-D, and this accounts for the decreased yield – the suppressing effect of 2, 4-D is not counterbalanced by the stimulating effect of the small amount (0.2 kg) of DG. In the case of No.1, an application of 2.0 kg/hectare includes about 0.8 kg of 2, 4-D and MCP and about 0.66 kg of DG, and an application of 3 kg/hectare, 1.2 kg and 0.99 kg

respectively. At a rate of 2.0 kg/hectare, when the dose of 2, 4-D is moderate, the large amount of the synergist and growth stimulator (DG) assists the complete suppression of dicotyledonous weeds and stimulates the growth of millet. When the application rate of No.1 is 3.0 kg/hectare, the unfavorable effect of the limiting dose of 2, 4-D (1.2 kg/hectare) on millet seems to be balanced by the stimulating effect of the increased amount of DG (0.99 kg/hectare), and therefore the yield did not increase to any appreciable extent over that given by an application of 2.0 kg of No.1 per hectare (42.4-42.9 centners/hectare). It should also be noted that Nos.1 and 5, applied at rates of 1.0 kg/hectare, resulted in much higher yields than 1.0 kg of 2, 4-D; this is accounted for by the synergetic and stimulating effects of the DG present in them.

Thus, it may be concluded from the results of these laboratory and field trials that DG is both a synergist and a plant-growth stimulator. Therefore chlorinated phenoxyacetic acids obtained from the 180-210° fraction of wood-tar phenols, containing guaiacol, are not only effective selective herbicides, but also stimulate the growth of plants resistant to their herbicidal action. These properties of our herbicides open up extensive possibilities for increasing the yields of cereal crops; these require further investigation.

EXPERIMENTAL

Preparation of MG and DG. Through weighed quantities of melted guaiacol, 1 and 2 moles of chlorine respectively were passed. In the distillation of the reaction products, the principal fraction distilled at 125-127° and 20 mm in the first case, and at 145-150° and 20 mm in the second. In the first case the substance contained 23.0% chlorine (Carius); chloroguaiacol contains 22.5% chlorine. The fraction solidified in the receiver, and melted at about 20°. It was probably composed mainly of 4-chloro-2-methoxyphenol (4-chloroguaiacol), as the boiling point of 6-chloroguaiacol is only a little higher than that of guaiacol.

In the second case the principal fraction contained 37.2% chlorine, solidified in the receiver, and melted at about 110°. It consisted mainly of 4, 6-dichloroguaiacol (36.7% Cl).

Monochloroguaiacol and dichloroguaiacol were converted into the corresponding phenoxyacetic acids by the usual method of condensation of the phenolates with sodium chloroacetate. 4-Chloroguaiacoxyacetic acid (MG), recrystallized from benzene or water, melted at 135°, and had an equivalent of 216 (calculated for $C_9H_9ClO_4$ – 216.5).

4, 6-Dichloroguaiacoxyacetic acid (DG), recrystallized from ligroine, melted at 151° and had an equivalent of 249 (calculated for $C_9H_8Cl_2O_4$ – 251).

We have shown that phenols boiling in the 180-210° range obtained from wood tar are of relatively constant composition, irrespective of the pyrolysis method (dry distillation or gasification) and the nature of the wood. Their guaiacol content varies from 33% (8.0% OCH_3) to 42-43% (11.0-11.5% OCH_3). Two methods were tried for conversion of these phenols into mixtures of chlorinated phenoxyacetic acids: 1) chlorination of phenols to 38-40% chlorine content (corresponding on the average to dichlorophenols), and condensation of chlorophenolates with sodium chloroacetate; 2) condensation of phenolates with sodium chloroacetate and chlorination of the mixtuture of phenoxyacetic acids to an equivalent of 238-256 (on the average, the dichloro acids). The first method was less effective, as up to 20-25% of pitch is formed in the distillation of chlorophenols, and work with chlorophenols is inconvenient because of their unpleasant odor. Chlorination of phenoxyacetic acids (the second method) can be successfully effected either in solution (in acetic acid) or in the melted state. In both cases the chlorination is rapid, without breakthrough of chlorine. Care should be taken to remove hydrogen chloride, for example in a current of air or nitrogen, as otherwise the final product contains considerable amounts of chlorophenols (up to 15-18%) formed by the action of hydrogen chloride on chlorophenoxyacetic acids; for example:

$$C_6H_3Cl_2 - O - CH_2 - COOH + HCl \rightleftharpoons C_6H_3Cl_2OH + ClCH_2COOH.$$

Sample No.5 was made from the same phenols, but part of the guaiacol was first removed from them by saponification with a solution of caustic soda at 270° for 80 minutes [7], followed by distillation of the phenols and collection of the 180-210° fraction. The fraction contained 10% guaiacol; it was converted into a mixture of chlorophenoxyacetic acid by the second method. It contained 16.7% chlorophenols, and 83.3% chlorophenoxyacetic acids of equivalent 238. Both samples were converted into the triethanolamine salts by the mixing of 50% aqueous solutions of triethanolamine with 50% acetone solutions of the acids, followed by distillation of the acetone and part of the water. In the field trials of all the samples, the dosage per hectare was calculated in terms of the active principle (chlorophenoxyacetic acids), and all the samples were accordingly analyzed.

The 1954 and 1955 field trials of our herbicides, reported above, all consisted of unduplicated experiments, so that the results could not be accepted as completely reliable. The 1956 trials were performed in triplicate; three plots under similar conditions (soil, relief, distance from the protecting strip, degree of weed contamination, etc.) were selected for the trials; in equal sections of each plot sowings were sprayed from a land machine by solutions of each of the three herbicides tested.

SUMMARY

1. A mixture of chlorophenoxyacetic acids, containing about 28-30% chlorine, and having an equivalent of about 235-250, made from the 180-210° phenol fraction from wood tar, is a good selective herbicide which destroys dicotyledonous plants and certain deciduous trees. The mixture contains not more than 25% of 2, 4-D and MCP. The high physiological activity of the mixture is due to the presence of considerable amounts (up to 40%) of chloroguaiacoxyacetic acids, which we have shown to be synergists for 2, 4-D and stimulators of plant growth.

2. In 1956 trials a 3-fold increase of millet yield, relative to the control, was achieved as the result of spraying of weed-infested sowings with our herbicide; this is accounted for not only by the virtually complete destruction of dicotyledonous weeds, but also by stimulation of the growth of millet.

LITERATURE CITED

[1] P. Riepma, Proc. Brit. Weed Control. Conf. 425 (1954); 445 (1955).

[2] G. E. Blackman, Nature 155, 500 (1945); R. E. Slade, W. I. Templeman, and W. A. Sexton, Nature 155, 497; W. I. Templeman, Agriculture 53, 105 (1946); W. A. Sexton, R. E. Slade, and W. I. Templeman, British Patent 573,929 (1941).

[3] C. L. Hamner, and H. B. Teckey, Science 100, 154 (1944); P. C. Marth, I. W. Mitchell, Bot. Gaz. 106, 224 (1944).

[4] I. I. Gunar and M. Ia. Berezovskii, Chemical Methods of Weed Control (in Russian] (State Agricultural Press, 1952); N. N. Mel'nikov, Iu. A. Baskakov, and K. S. Bokarev, Chemistry of Herbicides and Plant-Growth Stimulators [in Russian] (State Sci. Tech. Press Chem. Lit. Moscow, 1954).

[5] A. N. Boiarkin, Proc. Acad. Sci. USSR 7, 2 (1947).

[6] Hemberg, Physio. Plantarum 4, 437 (1951).

[7] D. V. Tishchenko, B. V. Foliadov, and N. I. Nosova, J. Appl. Chem. 29, 1447 (1956).*

Received March 12, 1957.

* Original Russian pagination. See C. B. Translation.

HYDROFLUORINATION OF VINYLACETYLENE WITH A SUSPENDED CATALYST*

I. I. Dolgopol'skii, I. M. Dobromil'skaia, and B. A. Byzov

The synthesis of fluoroprene by the hydrofluorination of vinylacetylene over a solid catalyst [1] has a number of disadvantages, especially if carried out on the large scale:

1) difficulties in removing the heat of reaction, as the hydrofluorination process is highly exothermic; 2) rapid decrease of catalyst activity owing to deposition of of resins formed by polymarization of unsaturated compounds under the influence of excess hydrogen fluoride; 3) the relatively low output per unit volume of catalyst.

A much simpler and more efficient method is hydrofluorination of vinylacetylene with the aid of a suspension of the catalyst in an organic solvent. A study was therefore made of the hydrofluorination of vinylacetylene with a suspended catalyst. The reaction was effected by the passage of vinylacetylene and hydrogen fluoride through a suspension of mercuric oxide in vaseline oil, which is free from unsaturated hydrocarbons and inert to hydrogen fluoride. In the hydrofluorination of vinylacetylene with a suspended catalyst we have a three-phase heterogeneous system: gas – liquid – solid (catalyst). To ensure contact of vinylacetylene and hydrogen fluoride with the catalyst, they must pass from the gas phase into solution, and then diffuse to the catalyst surface. It is known that the reaction rate in heterogeneous catalysis with a suspended catalyst depends on a number of factors, which include the rate of stirring [2]. The effect of stirring on the rate of hydrofluorination of vinylacetylene was studied with 10 and 15% of mercuric oxide in the vaseline oil. The rate of stirring was varied in the range of 450-1200 revolutions/minute (Fig. 1).

The productivity of the catalyst mixture with different contents of catalyst in the vaseline oil was studied, in order to determine the conditions under which the process is governed by the reaction kinetics. It was found that the kinetic region is easily attained with contents of 5-10 and 15% of mercuric oxide.

The rate of vinylacetylene hydrofluorination is a linear function of the mercuric oxide content; this confirmation that the reaction proceeds in the kinetic region (Fig. 2).

Because of the considerable dilution of the gaseous reaction mixture with nitrogen, used with the solid catalyst (the molar ratio of vinylacetylene to nitrogen was 1:2 or 1:3), the reaction products had to be separated from the gaseous mixture either by means of low-temperature condensation, or by selective absorption in solvents.

It was shown that if a suspended catalyst is used, the dilution of vinylacetylene by nitrogen can be reduced to a molar ratio of 1:0.3 without appreciable changes in the amount of resins formed (Fig. 3). It was not possible to decrease the degree of dilution with inert gas any further, or to eliminate its use completely in the hydrofluorination of vinylacetylene, as this minimum ratio (0.2-0.3 mole of nitrogen per mole of vinylacetylene) is necessary for the supply of hydrogen fluoride and for determination of the amount used. If the hydrogen fluoride could be measured by means of special instruments, it would be possible to eliminate the use of inert gas entirely. It would then be possible to condense the reaction products at 0-10°.

In the hydrofluorination of vinylacetylene with a suspended catalyst, the concentrations of the reaction components (vinylacetylene and hydrogen fluoride) are determined by their solubilities in the catalytic mixture. It was found that, at a reaction temperature of 60°, the solubility of vinylacetylene is about 18-19 times the solubility of hydrogen fluoride (Fig. 4). This leads to the conclusion that the limiting factor under these conditions is the solubility of hydrogen fluoride in the catalytic mixture, which determines the rate of vinylacetylene hydrofluorination.

*Communication II in the series on the synthesis of fluoroprene.

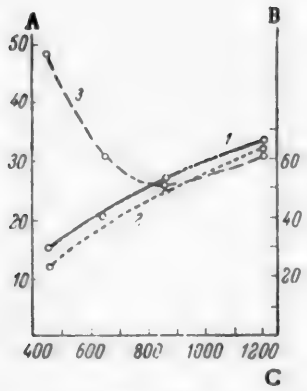

Fig. 1. Effect of the rate of stirring on the rate of hydrofluorination of C_4H_4 (10% HgO).
A) Conversion of C_4H_4 and yield of resins (%), B) output per 1 kg of catalyst (g/hour), C) stirrer speed (revolutions/minute). Curves: 1) Conversion of C_4H_4, 2) catalyst output, 3) resin yield.

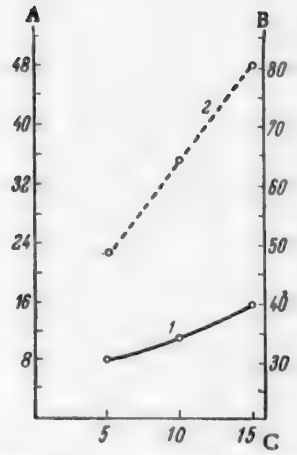

Fig. 2. Effect of HgO concentration in the suspension on the rate of hydrofluorination of C_4H_4.
A) Conversion of C_4H_4 (%), B) output per 1 kg of catalyst (g/hour), C) HgO concentration (%).
Curves: 1) Conversion of C_4H_4, 2) catalyst output.

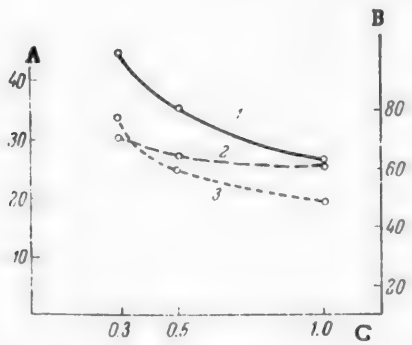

Fig. 3. Effect of dilution of the gaseous mixture with nitrogen on the rate of hydrofluorination of C_4H_4.
A) Conversion of C_4H_4 and yield of resins (%), B) output per 1 kg of catalyst (g/hour), C) N_2: C_4H_4 ratio.
Curves: 1) Conversion of C_4H_4, 2) resin yield, 3) catalyst output.

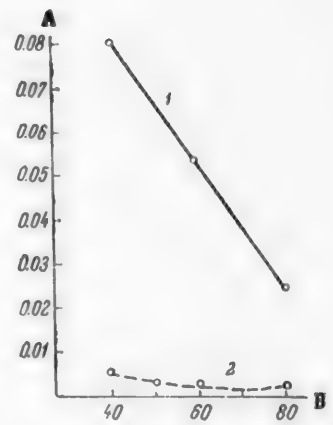

Fig. 4. Solubilities of vinylacetylene and hydrogen fluoride in vaseline oil at various temperature (°C).
Curves: 1) Solubility of C_4H_4, 2) solubility of HF.

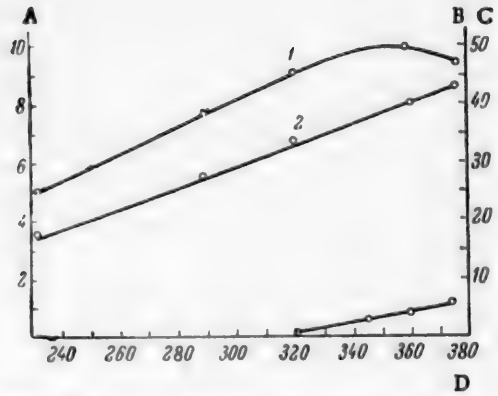

Fig. 5. Effect of partial pressure of HF vapor on the rate of hydrofluorination of C_4H_4. A) Amount of HF reacted (g/hour), B) conversion of C_4H_4 to C_4H_5F (%), C) yield of difluorobutene (%), D) partial pressure of HF vapor (mm Hg).

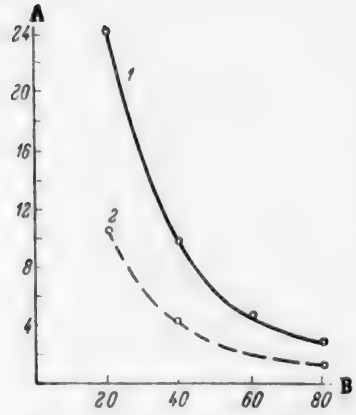

Fig. 6. Solubilities of C_4H_4 and C_4H_5F in vaseline oil. A) Solubility (%), B) temperature (°C). Solubility of: 1) fluoroprene, 2) vinylacetylene.

Investigation of the effect of the molar ratio of hydrogen fluoride to vinylacetylene on the reaction rate and the conversion of both components showed that the optimum molar ratio is 1:1. Decrease of the molar ratio to 0.75:1 and 0.5:1 results in lower conversion of vinylacetylene, while the conversion of hydrogen fluoride remains unchanged. This last result is probably explained by a decrease of the solubility of hydrogen fluoride, which is a linear function of the partial pressure of HF vapor over the catalyst (Fig. 5). Increase of the molar ratio of HF to vinylacetylene to 1.15:1 or 1.25:1 results in an appreciable increase in the rate of the secondary reaction, formation of difluorobutene, while the yield of fluoroprene remains in the same range as before.

The effect of temperature in the 40-80° range was also studied. The selection of the reaction temperature was determined by the amount of resins formed with an optimum yield of fluoroprene. The experimental results showed that the maximum yields of fluoroprene are obtained at 60°. Decrease of the reaction temperature to 40° raised the resin yield. This may be due to the considerable increase of the solubilities of vinylacetylene and of the fluoroprene formed in the reaction mixture (Fig. 6). Analysis of the resins formed in the catalytic mixture shows that they are formed mainly by polymerization of fluoroprene and vinylacetylene under the influence of hydrogen fluoride.

Increase of the reaction temperature to 80° leads to a more rapid decrease of catalyst activity.

One of the main problems in the application of this process for the synthesis of fluoroprene is the choice of a method for separation of the reaction products, yielding fluoroprene of adequate purity.

A study of the effect of the vinylacetylene content of fluoroprene on the quality of fluoroprene rubber [3] showed that the maximum permissible amount of vinylacetylene in fluoroprene is 0.2%. After removal of hydrogen fluoride, the hydrofluorination products of vinylacetylene form a mixture which consists mainly of unchanged vinylacetylene (b. p. 5°), fluoroprene (b. p. 11.9°), and difluorobutene (b. p. 24.5°).

Thus, the difference between the boiling points of the components to be separated is about 7°, so that a fractionating column of high efficiency must be used. It has been shown experimentally that pure fluoroprene can be obtained with the aid of a batch-action packed column with an efficiency of 24 theoretical plates.

EXPERIMENTAL

The hydrofluorination of vinylacetylene was performed in a cylindrical iron apparatus with two inlet tubes, for vinylacetylene and hydrogen fluoride. The apparatus was fitted with a propeller stirrer, a thermocouple socket, and an outlet tube for the reaction products. The reactor was immersed in a water thermostat. The reactor was

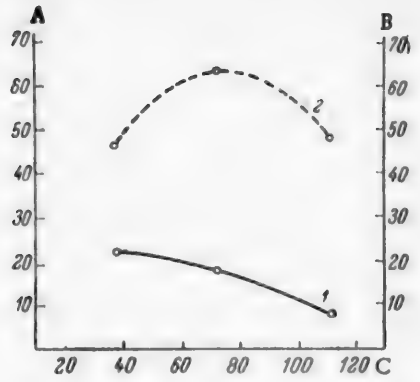

Fig. 7. Effect of the C_4H_4 feed rate on the rate of hydrofluorination of C_4H_4 (5% HgO).
A) Conversion of C_4H_4 (%), B) output per 1 kg of catalyst (g/hour), C) C_4H_4 feed rate (g/hour).
Curves: 1) conversion of C_4H_4, 2) catalyst output.

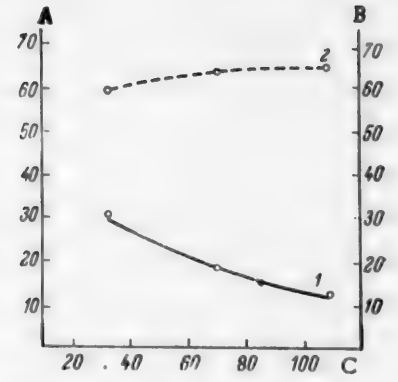

Fig. 8. Effect of the C_4H_4 feed rate on the rate of hydrofluorination of C_4H_4 (10% HgO).
Coordinates and curves as in Fig. 7.

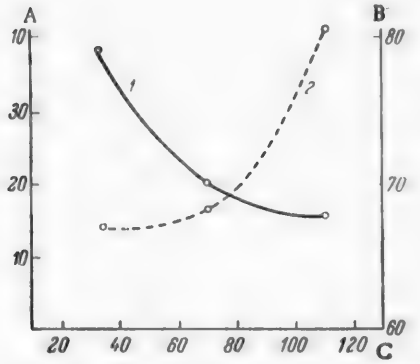

Fig. 9. Effect of the C_4H_4 feed rate on the rate of hydrofluorination of C_4H_4 (15% HgO).
Coordinates and curves as in Fig. 7.

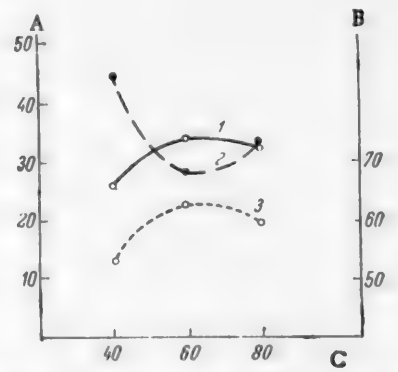

Fig. 10. Effect of temperature on the rate of hydrofluorination of C_4H_4.
A) Conversion of C_4H_4 and resin yield (%), B) output per 1 kg of catalyst (g/hour), C) temperature (°C).
Curves: 1) conversion of C_4H_4, 2) resin yield, 3) catalyst output.

charged with a previously-prepared suspension of mercuric oxide in vaseline oil, not more than 50% of the total reactor space being filled. The gaseous mixture leaving the reactor (unchanged vinylacetylene, hydrogen fluoride, fluoroprene, difluorobutene, and nitrogen) was passed through neutralization vessels (with 15% KOH) to absorb the hydrogen fluoride. The moist gas free from hydrogen fluoride (mixture of nitrogen, vinylacetylene, fluoroprene) was passed through a drying column filled with fused $CaCl_2$ and then collected in condensers cooled by means of a mixture of solid carbon dioxide and acetone. The course of the hydrofluorination was studied by determinations of the condensate composition (contents of vinylacetylene, fluoroprene, and difluorobutene).

Effect of stirring on the reaction rate. The experiments were conducted under comparable conditions, with 15 and 10% of mercuric oxide in the oil. The stirring rate was varied in the range of 450-1200 rpm. The results are given below.

Effect of Stirring on the Rate of Hydrofluorination of Vinylacetylene (average data)

Content of mercuric oxide in the catalytic mixture (%)	15				10				10	
Ratio of vinylacetylene to nitrogen	1 : 1				1 : 1				1 : 0.5	
Stirring rate (rpm)	460	680	860	1200	450	650	860	1200	650	860
Conversion of vinylacetylene (%)	13.3	18.3	35.6	35.3	13.3	18.1	26.8	33.1	23.8	36.6
Output of fluoroprene (in g/hour) per 1 kg of catalyst suspension	26.2	31.6	61.5	61.2	24.0	32.3	48.6	61.2	46.9	61.4
Resin yield, calculated on fluoroprene (%)	47.5	43.5	29.0	31.0	47.0	35.1	26.8	30.6	44.5	26.2

These results show that when the concentration of mercuric oxide is 15%, the conversion of vinylacetylene and catalyst output increase gradually with increase of the stirring rate from 450 to 1200 rpm, reaching a maximum at 860 rpm. Further increase of the stirring rate to 1200 rpm has virtually no effect on the fluoroprene yield. When the concentration of mercuric oxide is 10%, the same degree of conversion is achieved at 1200 rpm. At the same time it was found that if the ratio of vinylacetylene to nitrogen is decreased to 1 : 0.5, similar yields of fluoroprene, with 10% mercuric oxide, are obtained at 860 rpm. On the basis of these results a stirring rate of up to 900 rpm was adopted in the process.

Experimental conditions. Amount of vaseline oil taken was 250 g, 25 g of mercuric oxide, molar ratio of vinylacetylene to hydrogen fluoride 1 : 1, stirring rate 860 rpm, temperature 60°. The dilution of vinylacetylene with nitrogen was in ratios of 1 : 1, 1 : 0.5, 1 : 0.3.

It follows from the results in Fig. 3 that with decrease of the molar ratio of vinylacetylene to nitrogen from 1 : 1 to 1 : 0.5 the conversion of vinylacetylene increases from 26.4 to 36.7%, and the output per 1 kg of catalyst suspension rises on the average from 48.4 to 60.2 g/hour. The resin yield lies in the range of 25.8-27.2%, i. e., it remains almost constant. If the amount of nitrogen is decreased from 0.5 to 0.3 mole, the conversion of vinylacetylene rises from 35.2 to 43.6%, and the catalyst output increases on the average from 60.2 to 77 g/hour. The amount of resins increases slightly (from 27.2 to 30.6%).

Effect of the vinylacetylene feed rate. In this series of hydrofluorination experiments, carried out with vinylacetylene and nitrogen in a molar ratio of 1 : 0.5, and with mercuric oxide concentrations of 5, 10, and 15%, the feed rate of vinylacetylene was varied in the range of 38-110 g/hour.

It follows from the data in Fig. 7 that with 5% of mercuric oxide the reaction proceeds in the kinetic region at feed rates of vinylacetylene in the range of 38-70 g/hour.

When the mercuric oxide concentration is 10% (Fig. 8), the kinetic region is reached when the feed rate of vinylacetylene is 70 g/hour, but there is no bend in the curve even at 110 g/hour.

When the mercuric oxide concentration is 15% (Fig. 9), the kinetic reaction region is possibly reached when the feed rate of vinylacetylene is 110 g/hour, but these results require confirmation, as the effect of further increases of the feed rate of vinylacetylene was not studied.

Effect of mercuric oxide content on the reaction rate. The reaction rate was found to depend on the mercuric oxide content of the vaseline oil if the other conditons in the hydrofluorination of vinylacetylene were constant.

Comparative data on the solubilities of hydrogen fluoride and vinylacetylene in vaseline oil. The solubility of hydrogen fluoride was determined at 20, 40, 60, and 80°, in the laboratory reactor used in the hydrofluorination of vinylacetylene. The solubility of vinylacetylene at 20, 40, 60 and 80° was determined under the same conditions. The results are plotted in Fig. 5.

Effect of molar ratio of hydrogen fluoride to vinylacetylene. In order to determine the influence of the molar ratio of the components on the hydrofluorination of vinylacetylene, variations of the molar ratio of hydrogen fluoride to vinylacetylene between 0.5 : 1 and 1.25 : 1 were studied.

Correlation of the variations of partial pressure of hydrogen fluoride over the catalytic mixture with the degree of conversion of vinylacetylene shows that the rate of addition of hydrogen fluoride to vinylacetylene is a linear function of the partial pressure of hydrogen fluoride vapor over the catalyst suspension.

Effect of temperature. The experiments were conducted under comparable conditions, with vinylacetylene and nitrogen in 1 : 0.5 molar ratio, 10% of mercuric oxide, and at a stirring rate of 860 rpm (Fig. 10).

Decrease of the reaction temperature to 40° lowers the conversion of vinylacetylene and the catalyst output, and increases resin formation.

If the reaction temperature is raised to 80°, the conversion of vinylacetylene, catalyst output, and resin formation remain on much the same level as at 60°. However, the catalyst activity decreases much more rapidly, probably because of reduction of mercuric salts.

Determinations of the solubilities of vinylacetylene and fluoroprene in vaseline oil at 20, 40, 60, and 80° (Fig. 7) showed that a decrease of temperature from 60 to 40° approximately doubles the solubilities and this favors increased resin formation.

SUMMARY

1. A method has been developed for the synthesis of fluoroprene by hydrofluorination of vinylacetylene with a suspended catalyst (a suspension of mercuric oxide in vaseline oil).

2. A number of factors in the hydrofluorination of vinylacetylene, and conditions under which the reaction occurs in the kinetic region, were studied; it was found that, with 10 and 15% of mercuric oxide in the vaseline oil, and with vinylacetylene, hydrogen fluoride, and nitrogen in the molar proportions of 1 : 1 : 0.5 the optimum rate of stirring is in the range of 900-1200 revolutions/minute.

3. The reaction rate is shown to be a linear function of the mercuric oxide content; the optimum reaction temperature was found to be about 60°.

LITERATURE CITED

[1] I. I. Dolgopol'skii, I. M. Dobromil'skaia, and B. A. Byzov, J. Appl. Chem. 31, 10, 1534 (1958).•

[2] S. Iu. Elovich and G. M. Zhabrova, Theoretical Principles of Fat Hydrogenation [in Russian] (Izd. AN SSSR, 1958).

[3] I. V. Rokitianskii and R. L. Rabinovich, Coll. Trans. All-Union Sci. Res. Inst. Synthetic Rubber 4, 170.

Received October 4, 1957.

• Original Russian pagination. See C. B. Translation.

INFLUENCE OF USED CATALYST ON THE ACIDITY INCREASE OF HYDROGENATED FAT

V. P. Golendeev, K. G. Bogareva, E. I. Bobkova, and O. N. Dobrynina

The Gor'kii Polytechnic Institute

When used copper – nickel catalyst is utilized for high-temperature hydrogenation of fats, in a number of cases the acidity of the hydrogenated fat rises above the permissible level.

The acidity increase depends on the amount and quality of the used catalyst, and is caused by the influence of its individual components which accumulate on the catalyst surface in the course of hydrogenation.

The available literature [1, 2] does not contain adequate information on the composition of used catalyst and on the influence of impurities accumulating in it on the hydrogenation process.

The purpose of the present investigation was to study the composition of used copper – nickel catalyst and its influence on the acidity increase of the hydrogenated fat.

EXPERIMENTAL

Study of the composition of used copper – nickel catalyst. Used copper – nickel catalysts are usually characterized in terms of certain data obtained by laboratory analysis [3]: percentage fat content, metal contents (nickel and copper), and catalytic activity determined by hydrogenation of a sample under standard conditions.

For investigations of the used catalyst, the most important aspects in our view were studies of the fat component of the catalyst, and of the causes of the stable bonding between the catalyst and a part of the fat, not separated by filtration. Instead of the usual combustion method for determination of fat in used catalyst, we extracted the fat by means of ethyl ether or chloroform on a glass filter. It was found that part of the fat (up to 8% in some samples) is firmly held on the catalyst surface and is not removed by extraction in ether or chloroform; i. e., it is present as bound fat, which can be separated from the catalyst only after treatment with 10% sulfuric acid and subsequent solvent extraction.

Seven samples of used catalysts, including one from the Moscow Hydrogenation Plant for comparison, were taken for the investigation.

The results of determinations of free and bound fat by ether extraction, and total fat by combustion, are summarized in Table 1.

It follows from Table 1 that the fat content of used catalyst as determined by the combustion method is almost always higher than the value given by the extraction method; this is probably because of the combustion of all the organic content of the sample which includes, in addition to fat, proteins and mucins adsorbed on the catalyst surface.

The analytical results show that the extraction of fat from the used catalyst by solvents – ethyl ether or chloroform – does not go to completion. A part of the fat, from 1.4 to 8% in our experiments, is retained on the catalyst surface as so-called bound fat, which is extracted completely by the solvent only after treatment of the sample with 10% sulfuric acid.

TABLE 1

Analytical Data for Used Catalyst

Origin of catalyst sample	Fat content, determined by combustion (%)	Fat content, determined by extraction (%)	Bound-Fat content (%)	Total fat content (%)	Difference (%)	Contents of (%)	
						nickel	copper
From filter presses	56.5	48.52	8.1	56.62	−0.12	9.03	2.1
From yard of "Salolin" section	52.4	46.75	3.84	50.6	+1.8	12.3	1.06
From Moscow Hydrogenation Plant	56.66	51.35	3.93	55.28	+1.38	11.9	1.25
From filter presses	56.7	53.3	2.47	55.77	+0.93	11.9	1.58
Average sample from filter presses	58.0	52.56	4.23	56.79	+1.21	11.75	4.6
	57.0	52.6	1.46	54.06	+2.94	—	—
	56.9	52.9	2.74	55.64	+1.26	—	—

TABLE 2

Percentage Contents of Calcium Oxide and Magnesium Oxide in Samples of Used Catalyst

Origin of catalyst sample	CaO content (%)	Magnesium oxide content (%)	Bound fat (%)	Presence of nickel soap
From yard of "Salolin" section	1.4	0.12	3.84	Present
Average sample taken from filter presses during: December 30 and 31, 1954; first half of May 1955.	1.32	0.16	4.23	The same
	0.64	0.02	2.74	Traces
From Moscow Hydrogenation Plant	0.6	Traces	3.93	The same

TABLE 3

Analyses of Catalyst Powders

No. of catalyst powder	Contents (%)			
	CaO	nickel	copper	water
771	2.0	34.33	9.3	5.4
683 + 625	2.5	28.49	8.4	6.1
37	2.0	36.52	9.3	6.4
44	1.88	30.2	7.6	6.5
66	2.3	29.4	6.5	6.9
139	1.73	29.08	6.75	6.34
Mixed powders	2.76	31.4	7.05	—

TABLE 4

Accumulation of Calcium in Catalyst Powders with Hard Water Used for the Washing

Copper – nickel solution before precipitation			Catalyst powder after washing and drying			Increase of CaO content	No. of catalyst powder
volume of solution (liters)	CaO content (g/liter)	total CaO (kg)	weight of catalyst powder (kg)	CaO content (%)	total CaO (kg)		
1072.4	0.24	0.2573	70	2.0	1.4	5-fold	37
1532.0	0.22	0.337	72	1.88	1.35	4-fold	44

*Distilled water used for the washing.

TABLE 5

Analysis of Catalyst Powders Washed with Demineralized Water

No. of catalyst powder	% contents of			
	CaO	nickel	copper	water
159	0.65	28.6	8.8	7.1
162	0.3	28.47	9.4	6.0
172	1.0	26.5	6.0	6.0
Laboratory powder* . .	0.3	21.41	5.7	—

TABLE 6

Calcium Oxide Balance in Hydrogenation of Oil in Presence of Copper – Nickel Catalyst

Oil taken			Catalyst powder taken			Total CaO (kg)	Used catalyst collected			Hardened fat obtained			Total CaO (kg)
weight of oil (tons)	CaO content (%)	total CaO (kg)	amount (kg)	CaO content (%)	total CaO (kg)		amount (kg)	CaO content (%)	total CaO (kg)	weight (tons)	CaO content (%)	total CaO (kg)	
175	0.005	8.75	478	2.78	13.29	22.0	1323	1.32	17.46	175	0.004	7.0	24.46

Subsequently it was shown in numerous experiments that most of this fat is bound in the form of soaps (calcium, magnesium, nickel, and sodium salts). The quantitative contents of these soaps may be estimated from the acidity of the bound fats after decomposition of the constituent soaps by mineral acid.

In the samples studied, the acidity of the bound fat varied from 46 to 77%, i. e., roughly ½ to ¾ of the bound fat was present in the form of soaps.

It was first shown qualitatively that soaps extracted from used catalyst by warm alcohol contained the alkaline-earth metals calcium and magnenesium in addition to sodium, while extracts of most of the samples in hot butanol also contained nickel soaps (shown by the reaction with dimethylglyoxime) [4].

The quantitative contents of calcium and magnesium salts are given by the analytical data for samples of used catalyst, presented as percentage contents of calcium oxide and magnesium oxide, and summarized in Table 2.

If follows from the data in Table 2 that the contents of calcium oxide in the catalyst samples studied varies from 0.6 to 1.4%, and of magnesium oxide, from 0.02 to 0.16%, which is considerable. Evidently only a part of this calcium oxide and magnesium oxide is present in soap form, while the rest is in the form of carbonates and sulfates of these metals.

However, in the conditions of high-temperature hydrogenation in presence of free fatty acids, these salts of alkaline-earth metals may act as reserve materials for the formation and accumulation of calcium and magnesium soaps. It is known [5-7] that under favorable conditions calcium and magnesium soaps catalyze the hydrolysis of fats, which goes as far as the formation of glycerol and free fatty acids. Therefore, as we shall show later, the presence of calcium and magnesium soaps in fats undergoing hydrogenation is undesirable, as under conditions of high-temperature hydrogenation this leads to an acidity increase of the product above the permissible level.

Causes of the accumulation of calcium and magnesium salts in used catalyst. For determination of the causes of formation of calcium and magnesium soaps, and of other salts of these metals, and of their accumulation in used catalyst, experiments were carried out both in the laboratory and under production conditions. These experiments showed that calcium and magnesium enter the used catalyst with the copper – nickel powder, as the carbonates and sulfates. Calcium and magnesium soaps are formed from these salts in the course of hydrogenation, and are partially introduced with the oil after its alkaline refining. The contents of calcium and magnesium salts in the copper – nickel powders under production conditions are indicated by analytical data for these powders, summarized in Table 3, where the calcium contents are calculated as calcium oxide.

It is clear from the data in Table 3 that copper – nickel powders contain considerable amounts of calcium salts (from 2.0 to 2.76%, calculated as calcium oxide).

Experiments showed that, in the existing methods for the production of catalyst powders, considerable amounts of calcium and magnesium salts accumulate in them in two ways.

First, they come from the copper and nickel sulfate solutions formed when the used catalyst is boiled with sulfuric acid, and partially from the bleaching powder used for oxidation of ferrous iron to ferric in the purification of these solutions. In this case, when the nickel and copper cations are precipitated as carbonates by the action of sodium carbonate, calcium and magnesium are also precipitated and enter to copper and nickel carbonate precipitates as the carbonates of calcium and magnesium.

Second, they come from the hard water used for the washing of the copper and nickel carbonate precipitates on filter presses. The calcium and magnesium salts are adsorbed on the carbonate precipitates, firmly retained on them, and enter the catalyst powder.

Analysis of a sample of town water used for washing of the carbonate precipitates gave a hardness of 12 to 14 degrees on the German scale (0.112 g of CaO and 0.016 g of magnesium oxide per liter).

To determine the extent of accumulation of calcium and magnesium salts when the copper and nickel carbonate precipitates are washed with hard water, an experiment was performed under production conditions, in which the volume of the copper – nickel solutions and their calcium contents before precipitation with sodium carbonate, and the calcium contents of the catalyst powders formed from these solutions, were determined.

The results are summarized in Table 4.

It follows from the data in Table 4 that when copper and nickel carbonate precipitates were washed with hard water, the calcium contents of the dried catalyst powders formed from these precipitates were 4 to 5 times the calcium contents of the copper – nickel solutions before precipitation.

Experiments were carried out to determine the extent to which the content of calcium salts in catalyst powders can be reduced if the carbonate precipitates are washed with demineralized water (purified by ion-exchange resins). The results of analyses of the catalyst powders obtained in these experiments are given in Table 5.

Comparison of the analytical data in Tables 5 and 3 shows that if the catalyst powders are washed with demineralized water their calcium content is reduced considerably.

Another source of calcium salts in the used catalyst is the refined oil used for hydrogenation. Analyses of

TABLE 7

Reproducibility of Hydrogenation Experiments without Additions of Soaps or Used Catalyst

Hydrogenated fat		
acidity	melting point (°C)	nickel content (%)
0.17	51	—
	50	0.0017
	50	0.0017
	50.5	0.0018
0.19	53	0.0020
0.18	53	—

these oils showed that they contained from 0.0017 to 0.005%, while the hydrogenated oil contained 0.004%.

The distribution of calcium salts in the starting materials and the final products is shown by the results of a hydrogenation experiment under production conditions, in which the calcium oxide balance was calculated. The results of this experiment are presented in Table 6.

It is clear from Table 6 that most of the calcium oxide which enters with the starting materials remains in the used catalyst (78%), and an additional amount (about 22%) accumulates from the oil after refining, in the form of calcium soaps. The discrepancy of the calcium oxide balance is about 2.5 kg (22.0 kg taken in, 24.46 kg found); the explanation is the difficulty in obtaining an average sample for analysis.

Laboratory experiments on the alkaline refining of oil showed that most calcium enters the oil if the latter is washed with hard water at 90°.

TABLE 8

Comparative Experiments on the Hydrogenation of Cottonseed Oil with Used Catalyst and with Catalyst Powder

Amount of used catalyst (g)	Nickel content (% on oil)	Amount of catalyst powder taken (g)	Hydrogenation time hours)	Hydrogenated oil			Hydrogen rate (liters/hour)
				acidity (%)	melting point (°C)	nickel content (%)	
—	0.15	0.35	6.0	0.29	64	0.002	10—12
—	0.15	0.35	5.0	0.28	67.5	—	
2.5	0.3	—	6.0	1.11	37.0	0.008	
1.83	0.3	—	6.0	0.87	38.3	0.007	
2.5	0.3	0.35	5.0	1.32	42.5	0.014	
1.83	0.3	0.35	5.0	1.09	48.0	0.010	
—	0.14	0.23	1.2	0.15	58.5	—	25
0.85	0.15	0.23	1.2	0.23	58.5	—	

Formation mechanism of calcium and magnesium soaps, and their influence on the hydrolysis of fats. Calcium and magnesium soaps are formed, first, by the double-decomposition reaction of sodium soaps, present in oils as the result of alkaline refining, with calcium and magnesium salts present in hard water.

$$2R-COONa+CaSO_4\rightarrow(R-COO)_2Ca+Na_2SO_4,$$

and second, by the decomposition of calcium and magnesium carbonates by free fatty acids

$$CaCO_3+2R-COOH\rightarrow(R-COO)_2Ca+H_2O+CO_2.$$

Calcium and magnesium soaps, which are insoluble in water, are readily soluble in fats and oils, especially at elevated temperatures.

A very interesting question is the mechanism of the catalytic action of calcium and magnesium soaps on the hydrolysis of fats. It seems likely that these soaps would have the highest catalytic activity on the surface of the copper – nickel catalyst, since they are present in the colloidal state, are readily adsorbed, and are concentrated on the surface.

TABLE 9

Effect of Calcium and Magnesium Soaps on Hydrolysis of the Hydrogenated Product

Amount of catalyst powder taken (g)	Nickel content (% on oil)	Soap added (g)		Hydrogen	Hydrogenated oil	
		calcium	magnesium		acidity (%)	melting poing (°C)
0.3	0.15	—	—	Dry	0.17	53
		—	—	Humidified	0.29	53
		0.1	—	Dry	0.42	53
		0.1	—	Humidified	0.47	54
		0.08	0.02	The same	0.50	51
0.46	0.16	—	—	Dry	0.16	47
		—	—	Humidified	0.28	49
		0.123	0.03	The same	0.55	47

TABLE 10

Hydrogenation of Oil, with Determination of the Fatty Acids Carried over by Hydrogen

Amount of catalyst powder taken (g)	Nickel content (% on oil)	Soap added (g)		Hydrogen	Volatile-acid content (%)	Hydrogenated oil	
		calcium	magnesium			acidity	melting point (in °)
0.46	0.16	—	—	Dry	1.02	0.28	49
		—	—	Humidified	1.02	0.29	53
		0.123	0.03	The same	1.6	0.69	46.5
		0.123	0.03	" "	1.48	0.55	47
		0.123	0.03	" "	1.54	0.48	47

A possible mechanism of the catalytic action of calcium and magnesium soap may be the following: at the elevated temperature of hydrogenation, in presence of water vapor in the hydrogen gas, these soaps are first partially hydrolyzed to form basic soaps, which subsequently decompose the fat with formation of the original neutral soap and incomplete glycerides according to the scheme

$$(R-COO)_2Ca + HOH \rightarrow HO-Ca-OOC-R + R-COOH,$$

$$\begin{array}{l} CH_2-OOC-R \\ | \\ CH-OOC-R \\ | \\ CH_2-OOC-R \end{array} + HO-Ca-OOC-R \rightarrow (R-COO)_2Ca + \begin{array}{l} CH_2-OOC-R \\ / \\ CH-OH \\ \backslash \\ CH_2-OOC-R \end{array}$$

The free fatty acids formed by hydrolysis diffuse into the oil and raise the acidity of the hydrogenated product.

The hypothesis that hydrolysis of the fat takes place on the catalyst surface is confirmed by the fact that the fat isolated from the used catalyst by ether extraction had a higher acetyl number than the hydrogenated products, namely: the fat isolated from the used catalyst had acetyl number 10, while the acetyl number of the hydrogenated fat was 5, or a half of the former.

Experiments on oil hydrogenation in presence of calcium and magnesium soaps. After it had been determined how calcium and magnesium soaps enter and accumulate in the used catalyst, it was necessary to carry out experiments on the effect of the used catalyst on the increase of acidity of the hydrogenated fat in the course of hydrogenation.

The hydrogenation experiments were performed under laboratory conditions in glass test tubes 240 mm long and 40 mm in diameter. Each experiment was performed simultaneously in three tubes, heated in a crucible furnace, with the temperature kept constant with the aid of a rheostat. Refined oil was put into the tubes (50-70 ml in each), and heated to 240-250° with gentle agitation by means of hydrogen fed in from the hydrogen supply

line. When the temperature reached 250°, the catalyst (0.15%, calculated as metallic nickel on the oil) was added.

The temperature was raised to 258-260°; the hydrogen rate was increased to 25 liters/hour, and was regulated by means of a rheometer.

To determine the reproducibility of duplicate experiments, the oil was first hydrogenated with catalyst powder only (laboratory sample), without any additions of soaps. The results of these experiments are summarized in Table 7.

It is clear from Table 7 that adequate reproducibility was obtained; the percentage contents of free fatty acids (acidity), and the nickel contents of all the samples were in agreement.

To determine the extent to which used catalyst influences the acidity increase of the hydrogenated fat, hydrogenation experiments were performed under the same conditions as before, but one of the tubes contained used catalyst with the maximum content of bound fat (8.1%), the second contained catalyst with the minimum content of bound fat (.384%), while the third contained only fresh (laboratory) catalyst powder or a mixture of catalyst powder and used catalyst. The mixtures of used catalyst with catalyst powder were in 2:1 or 1:1 ratio; the hydrogen rate was 10-12 or 25 liters/hour. At the lower hydrogen rate the duration of the experiment was 5-6 hours, and at the higher rate, 1.2 hours.

The results of experiments on the influence of used catalyst on hydrolysis of the treated oil are given in Table 8.

It follows from the analytical data in Table 8 that when used catalyst was added the acidity of the hydrogenated oil increased in proportion to the content of bound fat (soap) in the used catalyst. The nickel content of the filtered hydrogenated product increased in the same relationship. The comparative results are especially prominent at the lower hydrogen rate (10-12 liters/hour), i. e., when the losses of volatile fatty acids in the escaping hydrogen are less.

A series of experiments in which calcium and magnesium soaps prepared in the laboratory were added to the hydrogenation samples, in order to confirm that the soaps present in the used catalyst result in increased acidity of the hydrogenated product. The experiments with the use of calcium soap, and mixtures of calcium and magnesium soap, were performed under the same conditions as the experiments with the used catalyst. The amount of calcium soap added was approximately equal to the amount which accumulates in the used catalyst. In the mixtures of calcium and magnesium soaps, the calcium – magnesium ratio was roughly the same as in hard water (1:0.1).

Both dry and humidified hydrogen was used in these experiments. For humidification, the hydrogen was passed through a flask $^1/_5$ full of water. The experimental data and analytical results for this series of experiments are summarized in Table 9.

The experimental results in Table 9 show that in all cases when calcium or calcium + magnesium soaps were added to the oil for hydrogenation the acidity of the product was higher than that found when pure catalyst powder (without soap) was used. The average acidity increase was 0.5%, whereas without added soaps the average acidity was about one half, or 0.25%.

The small acidity increases, as compared with those found under production conditions, are noteworthy. This result may be attributed to considerable losses of volatile fatty acids in the stream of hydrogen under laboratory conditions.

For confirmation of this hypothesis, several additional laboratory experiments were carried out, in which the fatty acids lost with the hydrogen stream were taken into account. A long glass tube was inserted into the hydrogenation tube; the long tube retained oil spray, while the volatile fatty acids were carried over with the hydrogen stream. The whole apparatus was weighed before and after the experiment. The weight difference was taken to be equal to the loss of volatile fatty acids.

The results of this series of experiments are summarized in Table 10.

It follows from the data in Table 10 that in laboratory experiments on oil hydrogenation with addition of calcium + magnesium soaps the average amount of fatty acids lost with the hydrogen (calculated as oleic acid) is 1.5%, and the average residual acidity of the hydrogenated oil is 0.57%.

Therefore, in absence of losses of fatty acids, the acidity of the hydrogenated product should be about 2-2.1%. Values of that order are obtained under production conditions. When oil is hydrogenated without calcium + magnesium soaps, up to 1% of fatty acids hydrogenated without calcium + magnesium soaps, up to 1% of fatty acids is lost with the hydrogen stream, and the residual acidity of the product is 0.25%. In this case the total acidity in absence of losses should be 1.25%.

The results of these supplementary experiments also demonstrate the influence of calcium and magnesium soaps on the increase in the acidity of hydrogenated oil (approximately 2-fold) during hydrogenation.

Method for determination of free and bound fat in used catalyst. A weighed sample of 2-2.5 g of finely divided used catalyst was extracted several times with ether. The ether extracts were decanted onto a No.4 Schott funnel, and the residue was rinsed onto the filter by means of ether. The ether extracts were filtered off by means of a water-jet or vacuum pump. The residue on the funnel was washed with ether until 2-3 drops of the ether extract, when placed on a piece of filter paper, left no grease spot after evaporation of the ether.

All the ether extracts were collected in a wide test tube, inserted in a suction flask under the Schott funnel. The ether extracts were transferred from the test tube into a weighed flask, and the tube was rinsed out with ether which was added to the flask. The ether was distilled off on a water bath with the aid of a water-cooled condenser, and the residual fat was dried at 70-80° to constant weight.

The content of free fat (%) is $\frac{(A - b) \cdot 100}{W}$,

where A is the weight of the flask with the residual fat, b is the weight of the empty flask, and W is the weight of used catalyst taken.

The defatted residue from the Schott funnel was transferred to a beaker, the funnel was washed with hot 10% sulfuric acid solution, and the acid layer was drawn through and poured off into the beaker, which was then warmed until the soaps were completely decomposed. The beaker was then cooled and its contents transferred into a separating funnel, and the fatty substances were extracted with ether. The acid ethereal extract was washed with distilled water to a neutral reaction. The ethereal extracts were combined in a weighed flask, the ether was evaporated off, and the residue dried at 70-80° to constant weight*.

The bound-fat content (%) is: $\frac{(a - c) \cdot 100}{W}$,

where a is the weight of the flask with the bound fat; c is the weight of the empty flask; W is the weight of used catalyst taken**.

SUMMARY

1. In the development of a method for investigating the composition of used catalyst it was found that when the used catalyst is treated with solvents (ether or chloroform), part of the fatty substances (up to 8%) is not extracted but remains bound with the catalyst, mainly in the form of calcium, magnesium, nickel, and sodium soaps.

2. Calcium and magnesium soaps catalyze hydrolysis of the fat and raise the acidity of the product in high-temperature hydrogenation.

3. Calcium and magnesium soaps enter the used catalyst from oil after alkaline refining, and with catalyst powders.

4. For repeated use of copper – nickel catalyst, it is important not to allow calcium and magnesium soaps to accumulate in it; with this object in view the copper and nickel carbonate precipitates must be washed with demineralized water, hydrogen peroxide and air must be used as oxidizing agents in regeneration of the nickel solutions, calcium and magnesium salts must be prevented from entering the copper – nickel solutions, and calcium and magnesium soaps must be kept out of the oil during refining.

*When bound fat is decomposed by sulfuric acid, free fatty acids, neutral fat, and other fatty substances are formed. All these substances are conventionally described as bound fat.

**A. G. Frolova took part in the experiments and in the analytical determinations.

LITERATURE CITED

[1] E. Etinburg, N. Vengerova, and G. Gol'shtein, Oil and Fat Ind. 12, 574 (1935).

[2] P. Artamonov, Oil and Fat Ind. 11, 535 (1936).

[3] Technical Control and Accounting in Fat-Processing Plants, Part I, The Hydrogenation Industry [in Russian] (Food Industry Press, 1940); Technical Control and Accounting in the Oil-Producing and Fat-Processing Industry [in Russian] 1 (1952), 112.

[4] V. P. Golendeev, Oil and Fat Ind. 4 (1958).

[5] G. S. Petrov and A. Iu. Rabinovich, splitting of Fats and Production of Glycerin [in Russian] (1934), 18.

[6] Ubbelohde, Splitting of Fats and Production of Glycerin (1934), 8 [Russian translation].

[7] A. E. Chichibabin, Fundamental Principles of Organic Chemistry, 1 [in Russian] (1953), 425, 431.

Received November 5, 1956.

UPGRADING OF STRAIGHT-RUN GASOLINES BY LOW-TEMPERATURE DEHYDROGENATION OVER PLATINIZED CARBON*

N. I. Shuikin, Kh. M. Minachev, S. S. Novikov, N. F. Kononov, and I. L. Garanin

During the past five years the leading position in the production of high-grade gasolines and aromatic-hydrocarbon concentrates have been occupied by catalytic reforming, at high temperatures (up to 500°) and pressures (up to 70 atmos), of various petroleum distillates. Among such processes are: 1) platinum hydroforming (platforming) over a fixed regenerated [1-3] or nonregenerated [4-5] catalyst (platinum on alumina or aluminosilicate), and 2) hydroforming [6] in a fluidized bed of catalyst (usually alumina – molybdena).

Despite the extensive use of these processes, which have attained considerable importance in a number of countries, especially U.S.A., another catalytic method may be used for purifying gasolines and producing aromatic hydrocarbons. This method, developed in our country by Zelinskii and Shuikin [7], and named the low-temperature dehydrogenation process, has a number of advantages over the above-named methods for upgrading of gasolines from low-sulfur naphthenic petroleums. It is characterized by exceptionally low gas and coke formation; dehydrogenation may be performed at 300° and atmospheric pressure, so that ordinary carbon steel, instead of costly alloy steels, may be used.

In the development of this method it became necessary to carry out extensive experimental work in a search for a catalyst of high activity, stability, and reproducibility, with the minimum content of active metal. Thorough investigations of the formation conditions of Pd, Rh, Ru, Ni, and Co catalysts showed that it is possible to produce such catalysts with very low metal contents [8-15], but retaining high activity and stability. The most suitable of the catalysts studied under laboratory conditions was platinized carbon, which conformed fully to the specifications for industrial catalysts in its catalytic properties, simplicity of preparation, and ease of regeneration of the platinum.

Table 1 contains data on the activity and stability of a number of platinum catalysts used for aromatization of Surakhany gasoline. The data in Table 1 show that catalysts containing 0.5% of platinum and over retain relatively high activity for 600 hours of service.

The present investigation consisted of a study of the activity and stability of platinum catalysts in the aromatization of gasolines in a model and a pilot unit.

Aromatization of Surakhany and Il'skii-Khadyzhensk Gasolines in Contact with 4% and 2% Platinized Carbon in a Model Unit

Catalyst preparation. The dissolution of Pt for formation of H_2PtCl_6, and preparation of the catalyst, are described below. Activated birchwood charcoal was used.

The prepared catalyst, 4800 ml in volume, was put into the reactor.

Original gasolines. Il'skii-Khadyzhensk and Surakhany gasolines were used for the experiments. Sulfur compounds were removed by treatment with 3% oleum, which reduced the sulfur content from 0.019% to traces.

Experimental procedure. Experiments on the aromatization of Surakhany and Krasnodar gasolines were performed in the model unit shown schematically in Fig. 1. The gasoline feed rate was 0.30-0.32 hour^{-1}.

* The investigation was performed with the assistance of L. M. Klochko and Z. M. Ivanova.

TABLE 1

Aromatization of Surakhany Gasoline over Pt – Carbon Catalysts of Different Metal Contents T = 300°, v** = 0.32 hour^{-1}

Catalyst No.	Pt content of catalyst wt. %)	Aromatics in catalyzate (vol. %) after catalyst service time (hours)						
		initial period	72	136	192	300	516	600
1	1	50.0	50.0	47.5	47.5	47.6	39.0	39.0
2	4	48.0	45.0	45.0	43.0	42.0	42.0	42.0
3	0.5	47.0	35.0	35.0	35.0	33.0	32.0	32.0
4	0.25	44.0	19.0	—	—	—	—	—
5	0.1	31.0	14.5	—	—	—	—	—

** The space velocity of the gasoline is given in liters/liter of catalyst per hour.

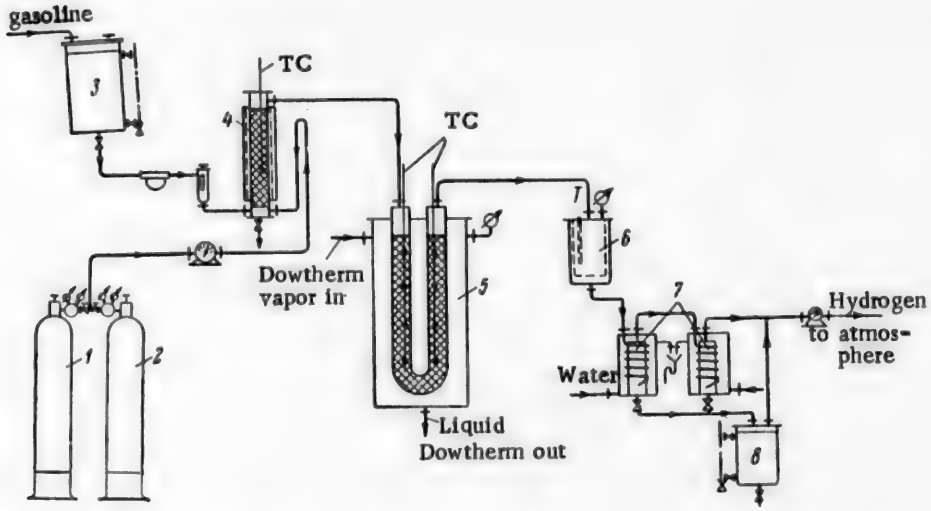

Fig. 1. The model unit. 1) Hydrogen cylinder, 2) nitrogen cylinder, 3) measuring vessel, 4) evaporator, 5) reactor, 6) trap, 7) separating condensers, 8) receiver.

Catalyzate samples were taken at 8-hour intervals. The reduced catalyst was highly effective in dehydrogenation. Table 2 contains selected data illustrating variations of the catalyst activity with the duration of the process and the amount of gasoline passed. After 1178 liters of Surakhany gasoline had been passed over the catalyst, the content of aromatic hydrocarbons in the catalyzate was still considerable, 36%, or only 9% below the initial value. After the catalyst had been used for 874 hours with Surakhany gasoline, the latter was replaced by the Il'skii-Khadyzhensk product. The process was continued with this gasoline for about 100 hours, when the activity of the catalyst fell appreciably. The explanation for the fall of catalyst activity during aromatization of Il'skii-Khadyzhensk gasoline is that the purified gasoline still contained some sulfur compounds, which gradually poisoned the catalyst.

The catalyst was used for aromatization during a total time of 962 hours. During this time 1405.6 liters of gasoline was passed; this corresponds to 35.15 liter of aromatized gasoline per g of platinum.

For further verification of the laboratory data, it was decided to carry out aromatization of Surakhany gasoline in the model unit over Pt – carbon catalyst containing only 2% of the metal.

TABLE 2

Variation of Activity of 4% Pt – Carbon Catalyst During Aromatization of Gasolines

Time (hours)	n_D^{20}	d_4^{20}	Content of aromatics in catalyzate (%)	v (hour^{-1})	Temperature (°C)
42	1.4420	0 786	49.5	0.32	298
170	1.4420	0.785	46.0	0.32	298
272	1.4400	0.781	42.0	0.31	301
356	1.4385	0.777	39.5	0.32	301
800	1.4362	0.777	36.0	0.28	315
874*	1.4328	0.771	32.0	0.29	319
882	1.4265	0.758	30.0	0.29	318
962	1.4165	0.742	23.0	0.29	318

*After 874 hours, Surakhany gasoline was replaced by the Il'skii-Khadyzhensk product.

TABLE 3

Variation of Activity of 2% Pt – Carbon Catalyst During Aromatization of Surakhany Gasoline

Time (hours)	n_D^{20}	d_4^{20}	Content of aromatics (%)	v (hour^{-1})	Temperature (°C)
43	1.4425	0.785	46.0	0.29	297
172	1.4390	0.778	43.5	0.29	295
478	1.4350	0.773	41.0	0.28	310
679	1.4308	0.769	30.5	0.29	313
931	1.4290	0.767	25.0	0.28	322

Data on the variation of the activity of this catalyst with time are presented in Table 3; it is seen that 2% platinized carbon also has high stability and retains its activity for 930 hours.

Comparison of the activities of 2% and 4% catalysts shows that they both have quite high activity and stability.

The experimental data obtained in the study of the catalytic properties of two samples of platinum catalyst in the aromatization of Surakhany gasoline justified trials of these catalyst on the pilot scale.

Aromatization of Surakhany Gasoline in Contact with 4% Platinized Carbon in the Pilot Unit

Characteristics of the raw material. The material used for the aromatization was straight-run Surakhany gasoline of the following characteristics: $d_4^{20} = 0.7465$, $n_D^{20} = 1.4130$, aromatics 1.2%, sulfur content 0.004%. The octane number of the gasoline with 4 ml of tetraethyllead, determined by the engine method, was 82.

Engler Distillation at 747 mm

Start of boiling 66° 50% 103°
10% 86° 95% 135°
End of boiling 152°

The gasoline was treated with 3% oleum in order to remove sulfur compounds. The purified and distilled gasoline had the following properties: $d_4^{20} = 0.7465$, $n_D^{20} = 1.4125$, aromatics 0.6%. The boiling range in the Engler distillation was almost unchanged.

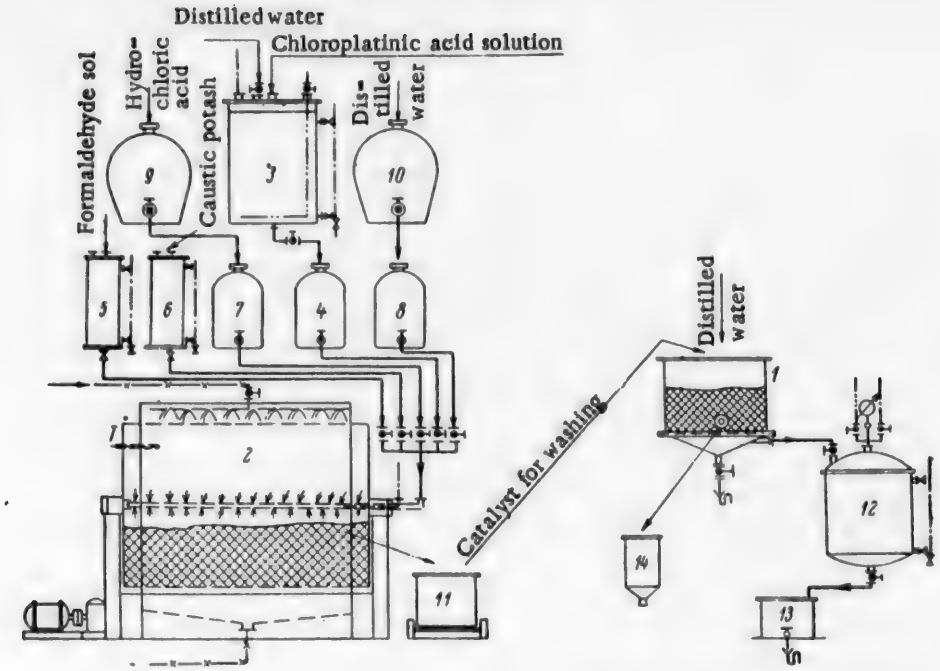

Fig. 2. Unit for deposition of platinum on carbon. 1) Suction filter, 2) drum, 3) vessel for chloroplatinic acid, 4) meter for chloroplatinic acid, 5) meter for formaldehyde, 6) meter for caustic potash solution, 7) meter for hydrochloric acid, 8) meter for distilled water, 9) vessel for hydrochloric acid, 10) vessel for distilled water, 11) trolley, 12) vessel for wash waters, 13) trap, 14) catalyst hopper.

TABLE 4

Variation of the Activity of 4% Pt – Carbon Catalyst in Aromatization of Surakhany Gasoline

Time (hours)	Amount of gasoline passed (ml)	n_D^{20} of catalyzate	Aromatic hydrocarbons in catalyzate (vol. %)
Catalyst made in the pilot plant			
126	3780	1.4420	42.5
342	10260	1.4410	41.5
800	24000	1.4385	38.0
1046	31380	1.4385	38.0
1300	39000	1.4370	36.4
1356	40680	1.4350	34.0
Catalyst made in the laboratory			
117	3510	1.4420	42.5
355	10650	1.4415	42.0
829	24870	1.4385	38.0
1125	33750	1.4350	34.0
1205	36150	1.4340	33.0

TABLE 5

Results of Tests of 4% Pt – Carbon Catalyst in the Pilot Plant at 300-305°

Time (hours)	Catalyzate		Aromatic hydrocarbons in catalyzate (vol. %)	Gasoline feed rate (liters/hour)
	d_4^{20}	n_D^{20}		
30	0.7768	1.4365	35.2	200
234	0.7761	1.4350	34.0	150
286	0.7718	1.4330	32.0	200
490	0.7711	1.4330	31.7	165
690	0.7728	1.4335	32.1	165

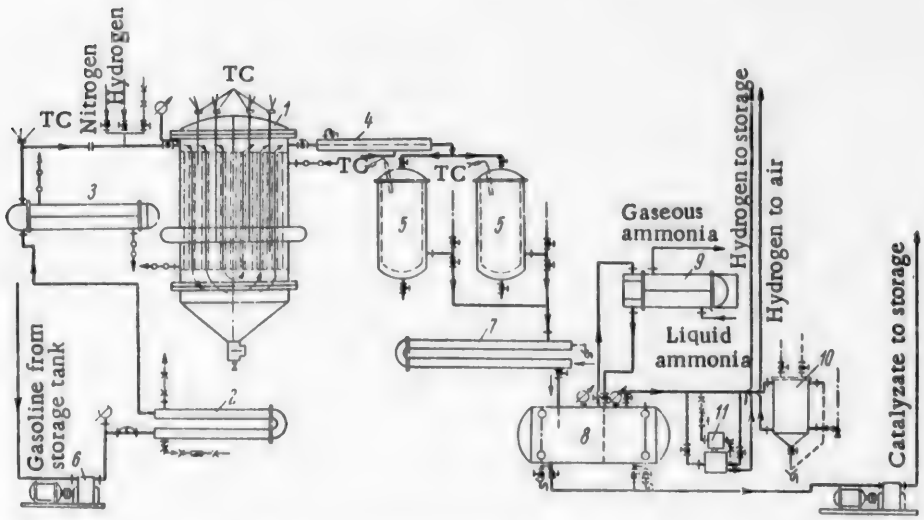

Fig. 3. Unit for aromatization of gasoline.

Preparation of 4% platinized carbon. The catalyst was prepared from activated birchwood charcoal, of factory origin, of 5-9 mm grain size and 1.5-1.6% ash content. The 1-hour activity for ether was 28.5%.

For the preparation of 150 kg of platinized carbon, 6 kg of spongy platinum was dissolved in aqua regia in two porcelain vessels on a water bath. Pure concentrated hydrochloric (sp. gr. 1.18) and nitric (sp. gr. 1.37) acids were added alternately in small portions with continuous stirring. When the platinum was dissolved, excess nitric acid was removed by treatment of the solution with concentrated hydrochloric acid, and excess of the latter was removed by evaporation of the solution with addition of distilled water at intervals.

Deposition of platinum on the carbon. The carbon was first washed with distilled water to remove OH ions, in one of the suction filters shown in Fig. 2. The washed carbon was dried in a vacuum drying oven to constant weight at 75-80° and 200-260 mm. The Pt was deposited on the carbon in an installation consisting of two similar units, one of which is shown in Fig. 2. 72 kg (about 350 liters) of the carbon was fed through a hatch into the steel drum 2, 1200 liters in volume. The drum was lined inside with polyvinyl chloride sheet. All the ducts and valves for supply of the reactants into the drum were also made of polyvinyl chloride. The drum was contained in an insulated casing, into the top part of which mineral oil was fed, to cool or heat the drum. A perforated tube, which remained stationary during rotation of the drum, was placed axially inside it. The liquid components were introduced into the drum through this tube. The H_2PtCl_6 solution was fed into the drum from the vessel 3 through the meter 4. The carbon was impregnated with the H_2PtCl_6 solution for 1 hour 30 minutes, with continuous rotation of the drum. The total amount of H_2PtCl_6 solution (for the two drums) was 278 liters. After half an hour, 35% formaldehyde solution was fed into the drum for 30 minutes from the metering vessel 5. The amount of

formaldehyde solution was 15 liters (2.5 liters per kg of platinum). After the formaldehyde had been added, the drum contents were cooled to 14°. Freshly prepared 50% KOH solution was gradually fed into the rotating drum at that temperature from the metering vessel 6. The solution was fed in at such a rate that after the calculated amount of KOH solution had been added the temperature inside the drum did not exceed 30-35%. A total of 27 liters of 50% solution (4.5 liters per kg of platinum) was added. After the KOH solution had been added, the temperature of the drum contents was raised to 45-50° for 2 hours. For neutralization of excess acid, 1:1 hydrochloric acid was then introduced into the drum until an acid reaction was obtained on Congo red paper. After 12 hours the catalyst was transferred to the suction filter 1 and washed with hot distilled water to a negative reaction for Cl' ions. The amount of catalyst obtained was 650 liters.

Tests of the catalysts under laboratory conditions. For comparison, a similar catalyst was prepared in the laboratory simultaneously with the pilot-plant preparation. Both catalysts were subjected to prolonged tests, under conditions of 24-hour operation, for aromatization of purified Surakhany gasoline. The catalysts were charged into tubes of ordinary steel, 100 ml (22 g) in each. The catalysts were reduced by means of hydrogen (from a cylinder), the temperature being gradually raised to 305°. Gasoline was passed at 0.3 $hour^{-1}$.

The results of prolonged tests of both catalyst samples are given in Table 4. It is seen that both catalysts had high activity and stability. After 1200-1350 hours the degree of aromatization of Surakhany gasoline fell by 10.5-11% below the initial level.

Pilot-plant aromatization of gasoline. The catalyst was put into a Dowtherm-heated reactor consisting of 72 tubes 82 mm in diameter and 2400 mm long, made of chrome steel. 650 liters of catalyst was put uniformly into these tubes.

A diagram of the unit used for the aromatization is shown in Fig. 3.

Air was removed by a stream of nitrogen from the reactor 1, evaporator 2, superheater 3, condenser 4, and traps 5. The catalyst was then reduced by hydrogen passed through at 3-4 m^3/hour for 12 hours: 3 hours at 150°, 3 hours at 250°, and 6 hours at 300°. At the end of the reduction, the hydrogen rate was lowered to 0.1-0.2 m^3/hour and gasoline vapor was fed in at a rate of 0.3 $hour^{-1}$. The gasoline was fed from the storage tank by means of the pump 6, and passed through a meter into the evaporator 2. The gasoline vapor was then superheated to 260° in the tubular superheater 3 by means of Dowtherm vapor, and passed into the reactor 1 for aromatization. On leaving the reactor, the vapor of aromatized gasoline together with the liberated hydrogen entered one of the traps 5, equipped with filter material. The vapor – gas mixture then passed into the cooling condenser 7, and then into the first section of the gas separator 8, where hydrogen was separated from the condensate. The hydrogen, containing gasoline vapor then passed to the condenser 9, cooled by ammonia to – 5°, and then escaped into the air through the hydraulic seal 10 or, as necessary, was fed by means of the compressor 11 into a storage vessel to make up hydrogen losses. The temperature in the reactor was maintained at 300-305°. Selected data are presented in Table 5.

These results show that the aromatization of gasoline continued at almost the same level for 700 hours. The catalyst remained active at the end of the process.

After the tests the catalyst was removed from the reactor, and the Pt – carbon was burned in a special apparatus for regeneration. The Pt obtained after combustion of the carbon was treated first with distilled water and then with dilute hydrochloric acid to remove any ferric oxide and other ash impurities which might have been present. The recovered Pt was used for preparation of the next batch of catalyst.

The losses were 6.34 tons or 6.3%. Such losses are not typical. With proper adjustment of the cooling system they can be reduced by at least one half. The octane number of the gasoline with 4 ml of tetraethyllead, determined by the engine method, was 95.5, and the quality, determined by the Z-S method, was 160 units.

SUMMARY

1. Low-temperature catalytic aromatization of straight-run gasoline was effected on the pilot-plant scale; it is shown that high-grade gasolines can be obtained by this method.

2. The catalyst (platinized carbon), containing not more than 2-4% of platinum, has high activity and stability.

LITERATURE CITED

[1] V. Haensel and L. Schmerling, U. S. Patent 2658628 (1953); C. A. 48, 2292 (1954).

[2] J. G. Eckhouse, Petrol. Eng. 26, 4, 26 (1955).

[3] J. C. Dart, A. G. Oblad, and H. Heineman, Erdol and Kohle 1, 9 (1955).

[4] J. H. Forester, A. L. Conn, and I. B. Malloy, Oil and Gas. J. 53, 49, 139 (1954).

[5] J. K. Roberts and E. W. Shankl, Fourth World Petrol. Congress, Rome, Proceedings, Sect. III D (1955).

[6] C. W. Tyson, E. W. Nicolson, and E. J. Cornowski, Oil and Gas. J. 53, 3, 124 (1954).

[7] N. D. Zelinskii and N. I. Shikin, J. Gen. Chem. 4, 901 (1934); Bull. Acad. Sci. USSR, Div. Math, Nat. Sci. 229 (1935); J. Appl. Chem. 9, 260 (1936); N. I. Shuikin, Progr. Chem. 15, 343 (1946).

[8] A. M. Rubinshtein, Kh. M. Minachev, and N. I. Shuikin, Proc. Acad. Sci. USSR 62, 497 (1948).

[9] A. M. Rubinshtein, Kh. M. Minachev, and N. I. Shuikin, Proc. Acad. Sci. USSR 67, 287 (1949).

[10] Kh. M. Minachev and N. I. Shuikin, Proc. Acad. Sci. USSR 72, 61 (1950).

[11] A. M. Rubinshtein, Kh. M. Minachev, and N. I. Shuikin, Proc. Acad. Sci. USSR 71, 1073 (1950).

[12] N. I. Shuikin, Kh. M. Minachev, and A. M. Rubinshtein, Proc. Acad. Sci. USSR 79, 89 (1951).

[13] N. I. Shuikin, Kh. M. Minachev, and I. D. Rozhdestvenskaia, Proc. Acad. Sci. USSR 72, 911 (1950).

[14] Kh. M. Minachev, N. I. Shuikin, and I. D. Rozhdestvenskaia, Proc. Acad. Sci. USSR 76, 543 (1950).

[15] Kh. M. Minachev, N. I. Shuikin, and I. D. Rozhdestvenskaia, Bull. Acad. Sci. USSR, Div. Chem. Sci. 2, 338 (1954).

Received July 23, 1957.

BRIEF COMMUNICATIONS

A NEW COOLING BRINE FOR CONDENSATION OF NITROGEN OXIDES FROM NITROUS GASES

M. A. Miniovich, A. L. Shneerson, and V. A. Klevke

The cooling brine used for separation of nitrogen oxides in the liquid state from nitrous gases is a solution of calcium nitrate containing 42-44% $Ca(NO_3)_2$. It has been found in practice that with the use of this brine a working temperature below − 25° cannot be maintained in the condensation of nitrogen oxides. In order to increase the degree of condensation of nitrogen oxides from nitrous gases under excess pressure, and therefore to increase the output per unit equipment surface, it was necessary to find another cooling brine for operation at the boiling point of ammonia, about − 30°.

The cooling brine used in condensation of nitrogen oxides from nitrous gases should have the following main properties: 1) it should not freeze at the operating temperature, between − 30 and − 32°; 2) it should not react chemically with liquid nitrogen oxides (in the event of leaks in the equipment, etc.); 3) it must not attack the metals from which the equipment for condensation of the nitrogen oxides is constructed; 4) its viscosity should be about the same as that of calcium nitrate brine, i. e., about 20 centipoises at − 20°.

The material of the greatest interest for use as a cooling brine was a solution of magnesium nitrate, the eutectic point of which in a solution containing 32.3% $Mg(NO_3)_2$ is − 31.87°. However, the eutectic point of this solution is so close to the required working temperature that it would not be suitable for use under production conditions.

Even slight decreases of the solution concentration (by 0.8-1% $Mg(NO_3)_2$) would lead to deposition of the solid phase, with all its consequences. It was therefore necessary to find conditions in which the cooling brine froze at several degrees below the working temperature, but conformed to all the above-mentioned requirements.

EXPERIMENTAL

The systems $Mg(NO_3)_2 - NaNO_3 - H_2O$ and $Ca(NO_3)_2 - NaNO_3 - H_2O$ were studied over narrow concentration ranges. The temperatures at which a solid phase appeared in the solutions, and the solution viscosities were determined. The temperature at which the solid phase appeared was determined by the cryoscopic method in the Beckmann apparatus. The thermometer used for the temperature measurement, on which the setting of the Beckmann thermometer was based, was previously tested at three points: ice, calcium nitrate solution, and magnesium nitrate solution. The accuracy was ±0.5°. The solution viscosities were measured by the ball fall method.

The solutions used in the investigation were prepared from chemically pure reagents and from technical materials (calcined magnesia and nitric acid). The calcined magnesia used for preparation of magnesium nitrate solutions conformed to GOST 13-844-43, and contained the oxides of calcium and iron, sulfates, and other impurities.

Table 1 contains data (average values) on the temperatures of solid-phase formation in relation to the composition and concentrations of the solutions made from chemically pure reagents.

It follows from the data in Table 1 that in a solution containing 30.8% $Mg(NO_3)_2$ and 5.2% $NaNO_3$ a solid phase appears only at − 36.2°. Decreases of ~ 2% in the concentration of the solution raise the temperature at which the solid phase forms by 5°. In the case of calcium nitrate solution, addition of sodium nitrate lowers the temperature only to − 33°, and the viscosity is increased severalfold.

TABLE 1

Exp. No.	Comp. of solution (%) $Ca(NO_3)_2$	$Mg(NO_3)_2$	$NaNO_3$	Temp. of solid-phase formation (°C)
1	44.0	—	—	—28.0
2	39.4	—	10.5	—33.0
3	38.8	—	9.9	—33.4
4	37.6	—	9.5	—30.4
5	37.8	—	9.8	—30.8
6	37.0	—	9.4	—29.2
7	—	32.3	—	—31.8
8	—	30.8	5.2	—36.2
9	—	29.0	5.2	—31.3

TABLE 2

Comp. of solution	Contents of components (%)	Temp. of determination (°C)	Viscosity (centipoises)
$Ca(NO_3)_2$	42.0	—20.0	18.2
$Ca(NO_3)_2$	38.8		
$+NaNO_3$	10.0	—28.0	56.0
$Mg(NO_3)_2$	32.2	—28.0	15.6
$Mg(NO_3)_2$	30.8		
$+NaNO_3$	5.2	—28.0	19.0

TABLE 3

Exp. No.	Comp. of solution (%) $Mg(NO_3)_2$	$NaNO_3$	$Ca(NO_3)_2$	$Fe(NO_3)_3$	$MgSO_4$	$Mg(NO_3)_2$ content per 100 g H_2O	Temp. of solid-phase formation (°C)	Viscosity at −28°C (centipoises)	Density at −28°C
1	30.8	5.20	0.375	0.046	0.128	48.5	—37.5	25.0	1.347
2	30.0	5.06	0.365	0.045	0.124	46.5	—34.7	—	—
3	29.3	4.95	0.357	0.044	0.122	44.9	—32.5	—	—

Therefore, if the cooling brine made from magnesium nitrate with added sodium nitrate should become accidentally diluted under production conditions, the working temperature of the brine would still remain low enough.

Table 2 contains viscosity data on pure solutions of calcium and magnesium nitrates, and solutions with sodium nitrate added.

The data in Table 2 show that the viscosity of calcium nitrate solution is raised sharply by addition of sodium nitrate. However, addition of sodium nitrate to magnesium nitrate solution has very little influence on the viscosity of the latter.

These results led to the conclusion that a solution of magnesium nitrate containing about 31% $Mg(NO_3)_2$ with addition of 5.0 − 5.2% $NaNO_3$ is the most suitable cooling brine for use in condensation of liquid nitrogen oxides from nitrous gases. It was accordingly important to determine the temperature of solid-phase formation and the viscosity of the brine if it is made from technical raw materials containing the above-named impurities.

The experimental results* (average values) are given in Table 3 and plotted in the diagram.

It follows from these results that the impurities present in the cooling brines made from technical raw materials have no significant influence on the temperature of solid-phase formation or the brine viscosity. Data for the brine made from technical raw materials and for the brine made from pure reagents all lie on the same straight line.

With 44.9 g of magnesium nitrite per 100 g of water (Table 3, Experiment No. 3), the solid phase appeared −32.5°, and with 43.9 g per 100 g of water, at −31.3° (Table 1, Experiment No. 9). The observed raising of

*Experiments conducted by A. S. Kantor.

Variation of the temperature of solid-phase formation with the $Mg(NO_3)_2$ content of the brine.
A) Temperature of solid-phase formation (°C), B) $Mg(NO_3)$ content per 100 g H_2O.

the temperature must be attributed to the decreased concentration of magnesium nitrate in the solution, and not to the effect of impurities entering the brine from the technical raw materials.

On the basis of the laboratory results, a brine was prepared at one of the factories from calcined magnesia, 56% nitric acid, and sodium nitrate; the composition corresponded to the solution in Experiment No. 1 (Table 3). Tests of this brine showed that a working temperature of − 32° is soon reached by evaporation of ammonia, and the brine was used for condensation of liquid nitrogen oxides from nitrous gases.

SUMMARY

1. A cooling brine, containing about 31% $Mg(NO_3)_2$ and 5.2% $NaNO_3$, has been made from technical raw materials; it can be used for condensation of nitrogen oxides at temperatures from − 30 to − 32°.

2. Addition of 5.0-5.2% $NaNO_3$ to a solution containing 31% $Mg(NO_3)_2$ lowers the temperature of solid-phase formation by several degrees, and the brine formed is almost of the same viscosity as the calcium nitrate brine used in the plant.

Received November 25, 1957

ALUMINATE – BORATE ANOMALY OF THE OPTICAL PROPERTIES OF SILICATE GLASSES

E. I. Galant and A. A. Appen

The refractive indices of silicate glasses without boric anhydride generally increase appreciably as SiO_2 is replaced by Al_2O_3 [1]. However, if such replacement takes place in borosilicate glasses, this relationship does not hold. The reverse effect may be observed in this case [2]. This fact is worthy of detailed investigation, as silicate glasses containing B_2O_3 and Al_2O_3 simultaneously are widely used in the optical industry. It is necessary to determine the specific characteristics in the variations of the optical properties of complex aluminoborosilicate glasses. The first results of such an investigation are presented below.

5 series of glasses were prepared. In Series I and II the effects of B_2O_3 and Al_2O_3, introduced separately into the glasses, on the optical properties were studied. In Series III, IV, and V, SiO_2 was replaced, mole for mole, by Al_2O_3 in presence of different amounts of B_2O_3. The refractive index n_D and the mean dispersion $n_F - n_C$ were determined experimentally by means of a Pulfrich refractometer, and were also calculated, for comparison, by Appen's method [3].

The results are presented in the table.

The relative variations of the refractive index, $\Delta n_D 10^4$, are plotted in the diagram.

For the system $Na_2O - B_2O_3 - SiO_2$ (Series I) the refractive-index curve has a distinct maximum. This conforms the findings of English and Turner [4], and of Turner and Winks [5].

With regard to the effect of Al_2O_3, our results are new and especially significant.

The introduction of increasing amounts of Al_2O_3 instead of SiO_2 in the system $Na_2O - Al_2O_3 - SiO_2$ results in a continuous increase of the refractive index of the glasses (Series II). Quite different effects are observed on similar modification of the composition of glasses of Series III, IV, and V, containing boric anhydride.

In presence of a small amount (5%) of B_2O_3, replacement of SiO_2 by Al_2O_3 also leads to an increase of n_D, but the n_D curve in this case has a maximum (Series III).

With 11% B_2O_3 in the glass, the introduction of only the first one per cent of Al_2O_3 results in a slight increase of n_D; further replacement of SiO_2 by Al_2O_3 produces a distinct decrease of n_D (Series IV).

The decrease of n_D on replacement of SiO_2 by Al_2O_3 is especially pronounced in Series V, with 17% B_2O_3.

The good agreement between the calculated and measured values of n_D should be noted. The curves plotted from the calculated data lie very close to the curves representing the experimental results. This confirms the validity of the theoretical premises on which the calculations are based. One of the main premises of the theory is that oxygen introduced into an aluminoborosilicate glass in the form of alkali-metal oxides is expended in the first instance for building of (AlO_4) tetrahedrons, and only the residue interacts with boron, converting it from triple to quadruple coordination.

The calculated and experimental values for the mean dispersion are also in good agreement. The data in the table show that the mean dispersion varies little. The variations of $n_F - n_C$ are very difficult to follow experimentally. They are revealed much more easily by calculation. The mean dispersion of glasses of Series I increases slightly at first, and then decreases. The maximum corresponds to 4-5% B_2O_3. The mean dispersion of

Optical Properties of Glasses of Series I-V

I. $(87 - x)\ SiO_2 \cdot 13Na_2O \cdot x B_2O_3$

x (molar %)		2	3	4	5	7	9	11	13	15	17	19	22
n_D	measured	1.4853	1.4885	1.4916	1.4943	1.4992	1.5031	1.5052	1.5073	1.5079	1.5047	1.5066	1.5042
	calculated	1.4870	1.4898	1.4927	1.4955	1.5012	1.5051	1.5069	1.5087	1.5101	1.5063	1.5066	1.5052
$(n_F - n_C) \cdot 10^5$	measured	776	774	778	779	779	775	779	780	778	764	768	770
	calculated	776	778	779	779	778	777	777	776	775	774	774	773

II. $(87 - x)\ SiO_2 \cdot 13Na_2O \cdot x Al_2O_3$

III. $(82 - x)\ SiO_2 \cdot 13Na_2O \cdot 5B_2O_3 \cdot x Al_2O_3$

x (molar %)		0	1	2	3	4	5	7	9	0	1	3	6	9
n_D	measured	—	1.4817	1.4830	1.4831	1.4848	1.4864	1.4880	1.4896	1.4943	1.4961	1.4974	1.4976	1.4963
	calculated	1.4813	1.4822	1.4832	1.4842	1.4851	1.4861	1.4879	1.4897	1.4955	1.4965	1.4983	1.4998	1.4985
$(n_F - n_C) \cdot 10^5$	measured	—	—	780	780	776	785	786	—	779	783	788	786	789
	calculated	772	774	775	777	779	781	784	788	779	780	782	785	789

IV. $(76 - x)\ SiO_2 \cdot 13Na_2O \cdot 11B_2O_3 \cdot x Al_2O_3$

V. $(70 - x)\ SiO_2 \cdot 13Na_2O \cdot 17B_2O_3 \cdot x Al_2O_3$

x (molar %)		0	1	3	6	9	0	1	3	6	9
n_D	measured	1.5052	1.5064	1.5041	1.5011	1.4976	1.5073	1.5031	1.5027	1.4989	1.4949
	calculated	1.5069	1.5066	1.5059	1.5004	1.4948	1.5063	1.5055	1.5030	1.4965	1.4932
$(n_F - n_C) \cdot 10^5$	measured	779	777	782	789	791	773	775	774	780	790
	calculated	777	778	780	783	786	774	775	778	781	784

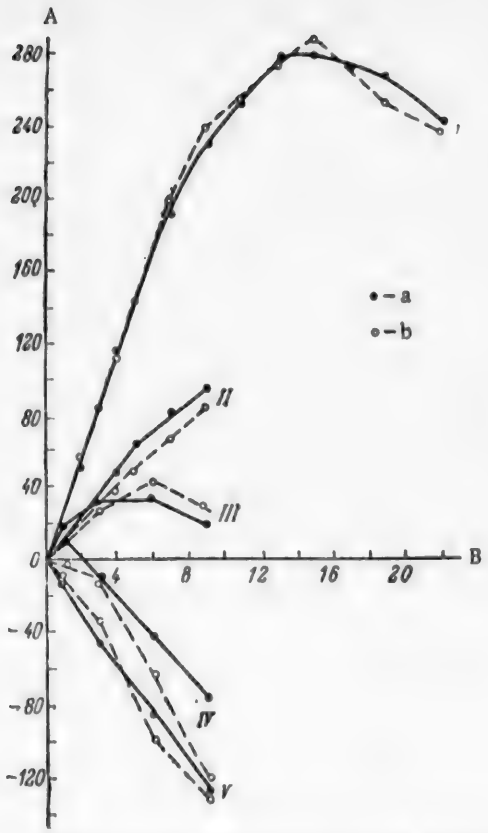

Variation of the refractive indices of silicate glasses on introduction of B_2O_3 (I) and Al_2O_3 (II, III, IV, V) instead of SiO_2.
A) Relative change of refractive index $\Delta n_D \cdot 10^4$, B) amount (in %) of B_2O_3 (I) or Al_2O_3 (II, III, IV, V). Data: a) Experimental, b) calculated.

the glasses of all the other series increases with replacement of SiO_2 by B_2O_3. However, in presence of B_2O_3 this effect is much weaker.

It must be stressed that our calculations of n_D and $n_F - n_C$ were based on statistical formulas and factors, derived for technical glasses. The agreement between the calculated and experimental values might be even better if, with the use of the same theoretical premises, correction factors for the system $Na_2O - Al_2O_3 - B_2O_3 - SiO_2$ were introduced into the calculation formulas.

The effect described above, consisting of a decrease of n_D of aluminoborosilicate glasses resulting from molar replacement of SiO_2 by Al_2O_3, is an exception to the general rules. It is an anomalous effect, as the title of this paper implies.

LITERATURE CITED

[1] A. A. Appen, J. Appl. Chem. 26, 9 (1953); 26, 569 (1953).•

[2] A. A. Appen, Travaux du IV Congress international du Verre. Paris, 36 (1956).

[3] A. A. Appen, Calculations of the Properties of Silicate Glasses [in Russian] (Industrial Construction Press, 1956).

[4] S. English, and W. E. S. Turner, J. Soc. Glass Technology 7, 155 (1923).

[5] W. E. S. Turner and F. Winks, J. Soc. Glass Technology 9, 389 (1925).

Received November 23, 1957.

• Original Russian pagination. See C. B. Translation.

INFLUENCE OF FRIT CRYSTALLIZATION ON THE PROPERTIES OF GROUND-COAT ENAMEL

G. N. Beliaev and N. F. Smakota

(The Dnepropetrovsk Institute of Chemical Technology)

It is stated in manuals of enameling technology [1-4] that the purpose of granulation of enamel melts is to facilitate the subsequent grinding of the frit in a ballmill. Enameling technicians hold the same views on the significance of the cooling of the melt.

In our studies of the interaction of boronless ground enamels at the steel boundary, it was decided to investigate the influence of the cooling rate of the enamel melt on the degree of crystallization of the frit and the quality of the enamel ground coat. We did not find any data in the literature on the influence of frit cooling conditions on enamel properties and the quality of the enameled goods. The following experiments were therefore carried out.

Production frit No 27 of the following chemical composition (%): SiO_2 – 59.4, Al_2O_3 – 2.5, Na_2O – 22.5, CaF_2 – 13.0, Fe_2O_3 – 2.0 and Co_2O_3 – 0.6 – was subjected to crystallization in a muffle furnace at 700° for 30, 60, 120, and 300 minutes. The melts, of different degrees of crystallization, were tested for fluidity, wetting of oxidized steel surfaces, and oxidation of steel during firing of the ground coats.

The fluidity was estimated from the length of a drop formed from a frit sample in 8 minutes on an enameled plate set at an angle of 45° in a muffle furnace heated to 850°. The contact angle θ was determined in a special apparatus [5] at 850° by the "sessile drop" method. The oxidation of steel during firing of the ground coat was estimated from the weight increase of the specimen [6].

Data on the influence of crystallization on frit fluidity are given below, while Figs. 1 and 2 represent the effects on contact angle and the oxidation of steel under the ground coat:

Duration of heat treatment (minutes)	0	30	60	120	300
Drop length (mm)	33	19	No spreading		

It follows from these results that with increase of the frit crystallization time the fluidity of the enamel melt decreases considerably, the oxidized steel is wetted less by the melt (the contact angle increases), and the oxidation rate of the steel under the enamel layer during firing increases.

For investigation of the effect of the degree of crystallization of the frit on the quality of the ground coat, trial enamelings of steel specimens by frits subjected to different heat treatments were carried out. Plates of O8KP steel were coated with slips made from ground experimental frits with additions of 45% water, 3% Glukhovo clay, and 1% borax.

Visual examination of the enameled specimens showed that the quality of the ground coat deteriorates with increase of frit crystallization time; the coatings become covered with numerous flaws and blisters rich in crystalline compounds of iron oxides.

The average ratings of the ground-coat quality for different crystallization times were: original frit, 3.5; after 30 minutes of crystallization, 2.7; 60 minutes, 2.2; 120 minutes, 2.0; 300 minutes, 2.0.

The purpose of the second series of experiments was to simulate production conditions in the laboratory; the following procedure was used.

Effect of Melt Cooling Conditions on the Properties of Ground-Coat Frits

Properties	Melt cooling method			
	in ice-cold water	in boiling water	in air	with furnace
Fluidity of frit (mm)	34	21	17	16
Contact angle (°C)	65	75	80	95
Oxidation of steel under the ground coat (mg/dm^2)	16.6	55.7	56.7	66.0

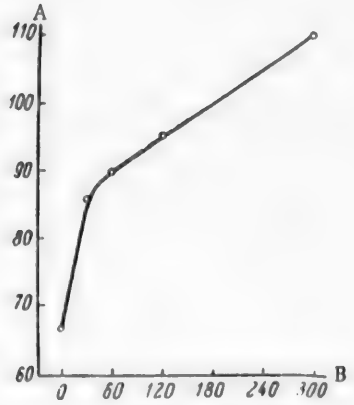

Fig. 1. Effect of frit crystallization time on the contact angle. A) Contact angle θ (in °), B) crystallization time (minutes).

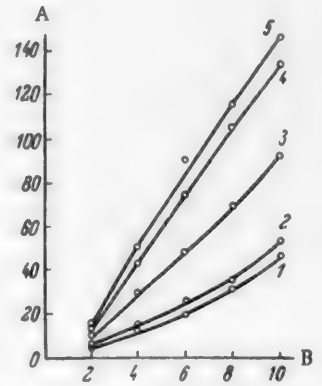

Fig. 2. Kinetics of steel oxidation under the ground coat in relation to the frit crystallization time. A) Weight increase (mg/dm^2), B) firing time (minutes). Crystallization time (minutes): 1) not crystallized, 2) 30, 3) 60, 4) 120, 5) 300.

Boronless ground-coat batch No. 27 was melted in a fireclay crucible in an electric furnace, the final temperature being 1180°. The melts were cooled at different rates in order to obtain products with different contents of glassy and crystalline phases, namely: in the first instance the melt was poured into ice-cold water; in the second, into boiling water; in the third, the melt was poured onto a fireclay plate and cooled in air; and in the fourth, the melt was cooled even more slowly (together with the furnace) in the crucible.

The results obtained with frits cooled at different rates are presented in the table.

These results demonstrate clearly that the more rapidly the melt is cooled, the better is the frit quality. The frit formed from a melt cooled in ice-cold water spreads and wets the steel surface much better when reheated than the frits which were cooled more slowly. This same frit gave much better results in trial enamelings and in determinations of the oxidation of steel during firing than frits of the same composition, but made by cooling of the melt in boiling water, in air, or in the furnace. The specimens coated with slip from the melt cooled in ice-cold water had bright, smooth coating free from noticeable faults or blisters.

Our experiments have evidently demonstrated for the first time that the cooling conditions of the enamel melt have a significant influence not only on the grinding properties of the frit, as is usually believed, but also on such important properties of the enamel coatings as fluidity, wetting of the solid surface, the oxidation of steel, and formation of blisters and faults during firing of the ground coat. The explanation is that the iron oxides formed during the first stages of firing react at different rates in the solid state with the crystalline and glassy components of the frit [6]. Our experiments and observations lead to the conclusion that the glassy phase reacts

better than the crystalline with the iron oxides. This is probably because a substance contains more internal energy in the glassy than in the crystalline state, and is thermodynamically unstable. Moreover, a crystallized frit not only reacts slowly with iron oxides when reheated and fired, but it softens slowly, wets the steel badly, and has low fluidity.

This leads to the important practical conclusion that enamel melts should be granulated in the works in such a way as to yield frits with the maximum contents of the glassy phase.

LITERATURE CITED

[1] L. Stuckert, Enamel Manufacture (Goskhimizdat, 1933) [Russian translation].

[2] N. N. Kholodilin, Enameling of Iron and Cast-Iron Goods (Industrial Construction Press, 1949). [In Russian]

[3] V. Ia. Lokshin, Technology of the Enameling of Metallurgical Articles (Russian State Local Ind. Press, 1955). [In Russian]

[4] A. Petzold, Email. Berlin (1955).

[5] K. P. Azarov, Proc. of Production and Technical Conference on Enameling (Metallurgy Press, 1956). [In Russian]

[6] G. I. Beliaev, Trans. Novocherkassk Polytech. Inst. 24 (38), (Industrial Construction Press, 1952).

Received December 30, 1957.

INVESTIGATION OF THE REACTION PRODUCTS OF CERTAIN ORGANOSILICON COMPOUNDS WITH AQUEOUS ALKALINE SOLUTIONS OF ALUMINATES, STANNATES, AND PLUMBITES BY MEANS OF INFRARED ABSORPTION SPECTROSCOPY

A. P. Kreshkov, Iu. Ia. Mikhailenko, L. V. Myshliaeva, and L. M. Khananashvili

It was shown in our previous paper [1] that certain organosilicon compounds react with aqueous alkaline aluminate solutions to form organic aluminosilicates. Our further investigations have shown that analogous compounds are formed in the interaction of organosilicon compounds with aqueous alkaline solutions of stannates and plumbites [2]. The products formed have a number of valuable technical properties: good adherence to glass, metals, asbestos, fabrics, and abrasives; the ability to form films on glass and metal which do not crack on heating; good resistance to acids and heat.

Moreover, the products formed from alkylalkoxy silances have good solubility in water, so that their solutions can be used as water-repellent impregnants for fabrics, paper, and constructional materials [3].

The course of the reactions and the composition and structure of these compounds were studied by means of chemical, physical, and physicochemical methods of analysis [2]. The most interesting results were obtained in studies of the reaction products by infrared absorption spectroscopy; such results, in conjunction with the results of chemical analysis, studies of microstructure, and x-ray analysis, shed some light on their structure.

EXPERIMENTAL

The investigation was performed in the region between 2 and 15μ, with the aid of the IKS-11 spectrophotometer and NaCl prisms.

Our solid reaction products were insoluble in the solvents generally used in infrared spectroscopy, while aqueous solutions could not be used because of their solvent action on the cells. The powder method was therefore used. The substances used were prepared by 3- or 4-fold reprecipitation by methyl alcohol from aqueous alkaline solutions. The compositions of the solid substances are given in the table.

For the spectrographic work, the powdered products were sifted through a No.100 sieve (10,000 holes/cm^2) and pressed in the form of tablets with KBr powder of the same fineness. The method of tablet preparation was described previously [4]. The ratio of KBr to the product was 10:1. The tablet weight was 250 mg. The tableting pressure was 7-8 tons/cm^2.

The literature contains no data on IR spectra for products having compositions analogous to ours. However, as their composition and properties are close to those of natural silicates, in some cases the results may be referred to definite structural groups. Infrared spectroscopic data on organosilicon compounds are also useful in interpretation of the spectra.

The absorption spectrum of Product 1 (Fig. 1) has the following maxima: 3.00 μ (3333 cm^{-1}), corresponding to the O – H bond in hydroaluminosilicates [5]; 9.6 μ (1042 cm^{-1}), for the Si – O bond [6]; 11.4 μ (878 cm^{-1}), for the Na – O bond [7], and 10.2 μ (982 cm^{-1}); this last maximum is characteristic of the Si – O – Al group in albite and anorthoclase – minerals of the sodium and calcium feldspar group [8]. A value close to this (10.14 μ) has been referred by others to the Al – O bond [9].

The following bonds can be identified in the absorption spectrum of Product 2 (Fig. 2): O – H 3.0 μ (3333 cm^{-1}), Si – O 9.6 μ (1042 cm^{-1}), Si – C 8.0 μ (1250 cm^{-1}) [6], Na – O 11.4 μ (878 cm^{-1}). The spectrum also

Compositions of the Solid Products

Product No.	Original organosilicon compound	Original inorganic compound	Composition of product (%)							Molar ratios		Notes
			Na_2O	SiO_2	Al_2O_3	PbO	SnO_2	C_2H_5O	C	metal : silicon, original	metal : silicon, in product	
1	Tetraethoxysilane	Aqueous sodium aluminate	21.04	44.00	33.60	—	—	1.36	—	1 : 2	0.45:1	Aqueous alkaline aluminate solution diluted with water in 1 : 4 ratio
2	Methyltriethoxysilane	The same	13.22	44.40	32.85	—	—	0.91	8.62	1 : 1	0.92:1	The same
3	Methoxypolysilane	" "	19.26	20.14	57.90	—	—	2.70	—	5 : 1	3.5 : 1	Without dilution
4	Tetraethoxysilane	Aqueous sodium plumbite	33.88	59.51	—	6.61	—	Traces	—	1 : 16	0.2 : 10	The same
5	The same	Aqueous sodium stannate	5.05	90.65	—	—	4.30	—	—	1 : 25	0.2 : 20	Aqueous alkaline stannate solution diluted with water in 1 : 1 ratio
6	Methyltriethoxysilane	Aqueous sodium stannate	6.02	90.54	—	—	3.44	—	—	1 : 25	0.2 : 25	The same

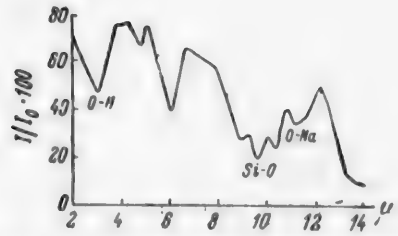

Fig. 1. Infrared absorption spectrum of the reaction product of tetraethoxysilane with aqueous alkaline aluminate solution (Al: Si = 1 : 2; aluminate solution: H_2O = 1 : 4).

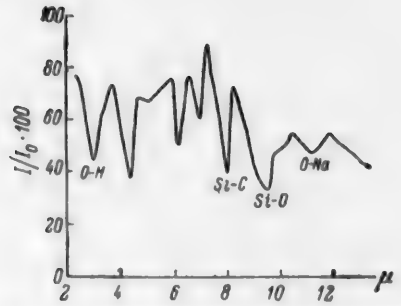

Fig. 2. Infrated absorption spectrum of the reaction product of methyltriethoxysilane with aqueous alkaline aluminate solution (Al: Si = 1 : 1; aluminate solution: H_2O = 4 : 1).

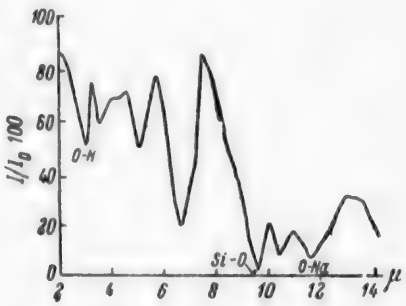

Fig. 3. Infrared absorption spectrum of the reaction product of methoxypolysiloxane with aqueous alkaline aluminate solution (Al: Si = 5 : 1).

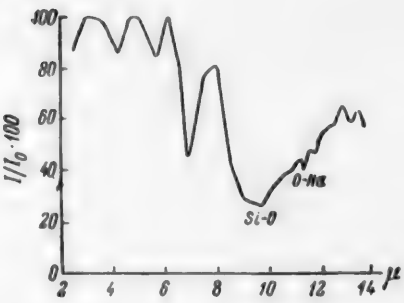

Fig. 4. Infrared absorption spectrum of the reaction product of tetraethoxysilane with aqueous alkaline plumbite solution (Pb: Si = 1 : 16).

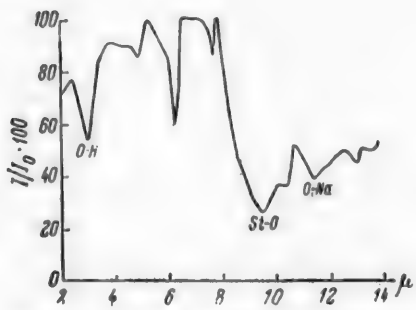

Fig. 5. Infrared absorption spectrum of the reaction product of tetraethoxysilane with aqueous alkaline stannate solution (Sn: Si = 1 : 25; stannate solution: H_2O = = 1 : 1).

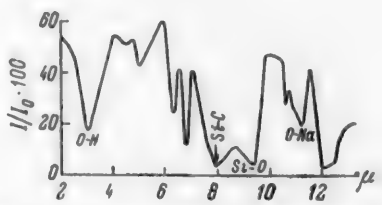

Fig. 6. Infrated absorption spectrum of the reaction product of methyltriethoxysilane with aqueous alkaline stannate solution (Sn: Si = 1 : 2; stannate solution: H_2O = 1 : 1).

has maxima at 4.4 μ (2275 cm^{-1}), 6.25 μ (1600 cm^{-1}), and others which were not identified.

The spectrum of Product 3 (Fig. 3) contains, in addition to absorption maxima for the Si – O, O – H, O – – Na bonds and the structural group of albite and anorthoclase, further maxima at about 3.5 μ (2856 cm^{-1}), 5.0 μ (2000 cm^{-1}), and 6.6 μ (1515 cm^{-1}).

The absorption spectrum of Product 4 (Fig. 4) has several maxima which also cannot be identified (5.7 μ, 13.2 μ, 6.8 μ); the maximum at 9.6 μ (1042 cm^{-1}) corresponds to the Si – O bond, and at 11.4 μ (878 cm^{-1}), to the Na – O bond.

The spectra of Products 5 (Fig. 5) and 6 (Fig. 6) have the same maxima, characterizing the O – H, Si – O, Na – O bonds. In addition to these three, the spectrum of Product 6 has a maximum at 8.0 μ (1250 cm^{-1}), corresponding to the Si – C bond.

The absorption bands for the Sn – O and Pb – O bonds are in the long-wave region on the spectrum (28-56 μ) [10], and therefore they cannot be identified in investigations of the region from 2 to 15 μ.

Thus, infrared spectroscopy reveals structural groupings characteristic of feldspars in products formed from alkaline aluminate solutions; the data for the products obtained from alkaline stannate and plumbite solutions reveal changes in the spectra of the original substances and the formation of a number of new maxima.

SUMMARY

1. The infrared absorption spectra of the reaction products of tetraalkoxysilanes and their derivatives with aqueous alkaline aluminate, stannate, and plumbite solutions have absorption maxima characteristic of O – H, Na – O, Si – O and Si – C bonds (the latter are found in the spectra of products based on alkylalkoxy silanes).

2. The reaction products of tetraethoxysilane and methoxypolysiloxane with aqueous alkaline sodium aluminate solution, which structurally are polyorganoaluminosiloxanes, gave absorption bands characteristic of aluminosilicates of the albite and anorthoclase type.

LITERATURE CITED

[1] L. M. Khananashvili, L. V. Myshliaeva, B. M. Mikhalev, and V. E. Shkol'nyi, J. Appl. Chem. 30, 2, 263 (1957).•

[2] A. P. Kreshkov, L. V. Myshliaeva, and L. M. Khananashvili, Trans. MKhTI 24, 333 (1957).

[3] A. P. Kreshkov, L. V. Myshliaeva, and L. M. Khananashvili. Authors' Certif. 111,485 (December 28, 1957). [In Russian]

[4] Iu. Ia. Mikhailenko and E. A. Kirichenko, Trans. MKhTI 23, 140 (1956).

[5] A. Buswell and N. Dudenbostel, J. Am. Chem. Soc. 63, 2554 (1941).

[6] A. P. Kreshkov, V. A. Bork, L. V. Myshliaeva, and G. D. Nessonova, Analysis of Organosilicon Compounds (Goskhimizdat, 1954). [In Russian]

[7] P. N. Ghosh and B. D. Catterjee, Z. Phys. 72, 542 (1931).

[8] G. S. Bachman, Glass Ind. 29, 435 (1948).

[9] G. A. Scott, J. Goloedson, S. E. Wiberlay, and W. H. Bauer, J. Phys. Chem. 58, 1, 61 (1954).

[10] M. Parodi, C. r. 204, 1111 (1937); 205, 906 (1937).

Received June 10, 1957.

• Original Russian pagination. See C. B. Translation.

ELECTRICAL CONDUCTIVITY OF THE SYSTEM NaOH – Na_2CO_3 – NaCl

A. F. Alabyshev, M. F. Lantratov, and L. I. Sokolova

(The V. I. Ul'ianov (Lenin) Electrotechnical Institute, Leningrad)

Electrical conductivity in the system NaOH – Na_2CO_3 – NaCl has been partially studied by Arndt and Ploetz [1]. They determined conductivity in the temperature range from 320 to 450° along lines of two sections of the composition diagram: the section with a constant content of sodium chloride (2.8 wt. %) and variable carbonate content (from 1.6 to 23.5 wt. %), and the section with a constant carbonate content (4.3 wt. %) and variable contents of sodium chloride (from 2.7 to 13.6 wt. %). By extrapolation to zero contents of sodium carbonate and chloride, Arndt and Ploetz found the conductivity of pure sodium hydroxide at 320-450° (see table).

We investigated the conductivity of the system NaOH – Na_2CO_3 – NaCl in the region of high caustic soda contents, with up to 20% of sodium carbonate and chloride by weight.

The apparatus used for the conductivity determinations was based on an improved alternating-current [2] bridge circuit (Fig. 1). The ZG-10 oscillator was used as the source of alternating current. The determinations were performed at a frequency of 3000 oscillations/second. The EO-7 electronic oscillograph was used for indication of bridge balance.

The rheochord AB consisted of two coils A and B, each with a bifilar winding consisting of 4.5 m of manganin wire, and a ruler with a manganin wire 1 m in length stretched along it.

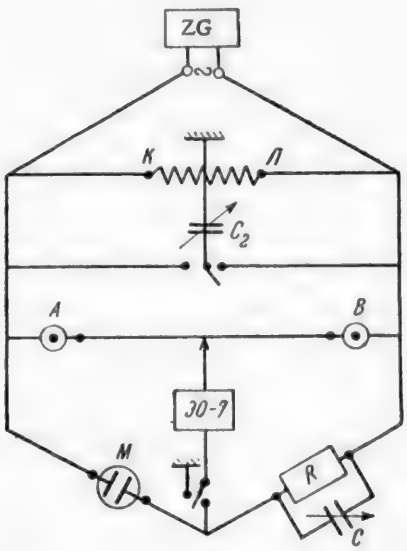

Fig. 1. Circuit of apparatus for conductivity measurements.

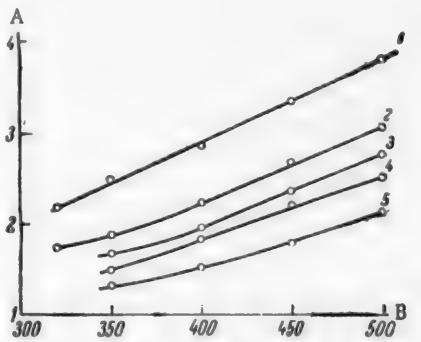

Fig. 2. The system NaOH – Na_2CO_3 – NaCl. Conductivity polytherms for NaOH – NaCl, mixtures containing 2% Na_2CO_3.
A) Conductivity (in $ohms^{-1} cm^{-1}$), B) temperature (°C). NaCl contents (wt. %): 1) pure NaOH, 2) 5, 3) 10, 4) 15, 5) 20.

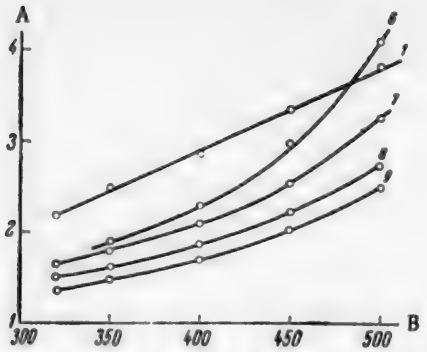

Fig. 3. The system NaOH – Na_2CO_3 – NaCl. Conductivity polytherms for the system NaOH – Na_2CO_3.
A) Conductivity (in $ohms^{-1} cm^{-1}$), B) temperature (°C). Na_2CO_3 contents (wt. %): 1) pure NaOH, 6) 5, 7) 10, 8) 15, 9) 20.

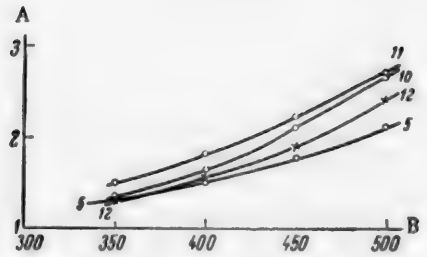

Fig. 4. The system NaOH – Na_2CO_3 – NaCl. Conductivity polytherms for constant NaCl content (20 wt. %).
A) Conductivity (in $ohms^{-1} cm^{-1}$), B) temperature (°C). Na_2CO_3 contents (wt. %): 5) 2, 10) 5, 11) 10, 12) 20.

Conductivity in the System NaOH – Na_2CO_3 – NaCl

Point No.	Composition (wt. %)			Temperature (°C)				
	NaOH	Na_2CO_3	NaCl	320	350	400	450	500
From [1]	100	—	—	2.12	2.38	2.82	3.27	—
1	100	—	—	2.18	2.48	2.87	3.36	3.93
2	93.0	2.0	5.0	1.75	1.87	2.227	2.68	3.06
3	88.0	2.0	10.0	—	1.69	1.96	2.37	2.76
4	83.0	2.0	15.0	—	1.51	1.836	2.19	2.51
5	78.0	2.0	20.0	—	1.32	1.525	1.800	2.13
6	95.0	5.0	0.0	—	1.887	2.307	2.98	(4.11)
7	90.0	10.0	0.0	1.65	1.80	2.10	2.55	3.13
8	85.0	15.0	0.0	1.50	1.62	1.87	2.22	2.74
9	80.0	20.0	0.0	1.35	1.485	1.70	2.03	2.49
10	75.0	5.0	20.0	—	1.35	1.65	2.13	2.67
11	70.0	10.0	20.0	—	1.50	1.82	2.23	2.71
12	60.0	20.0	20.0	—	1.30	1.55	1.90	2.44
13	90.0	5.0	5.0	1.50	1.70	2.10	2.60	—
14	80.0	10.0	10.0	1.30	1.48	1.85	2.33	—
15	70.0	20.0	10.0	—	1.433	1.70	2.10	2.67
16	85.0	5.0	10.0	1.36	1.53	1.87	2.17	—
17	80.0	5.0	15.0	—	1.47	1.69	1.98	2.44

The resistance box R was made from thick manganin wire. The resistance of the melts was measured to an accuracy of ± 0.005 Ω.

The variable capacitor C consisted of a cascade of ordinary variable capacitors used in radio technology.

All the circuit connections were made by means of special armored cable, the metallic sheath of which was grounded. The audiofrequency oscillator and oscillograph were also grounded. The vessel (crucible and central disk electrode) short circuited and the slider on the rheochord in the central position, R of the resistance box was zero.

A silver crucible 30 mm in diameter and 38 mm high was used as the vessel and also served as one of the electrodes. The second electrode was a silver disk, 8 mm in diameter, connected at the center to a silver wire

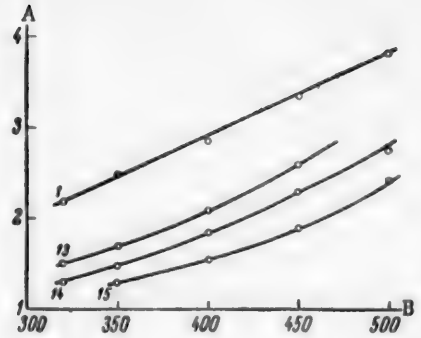

Fig. 5. The system NaOH – Na_2CO_3 – NaCl. Conductivity polytherms for constant ratio of Na_2CO_3 : NaCl = 1 (wt. %).
A) Conductivity (in $ohms^{-1} cm^{-1}$), B) temperature (°C). NaOH contents (wt. %): 1) pure NaOH, 13) 80, 14) 80, 15) 70.

1.2 mm in diameter and 180 mm long. The disk electrode was immersed in the melt to a depth of 2-3 mm. It was attached to a special stand which could be used for moving the electrode smoothly in the horizontal and vertical directions.

25 g of melt was put into the crucible. Each composition was weighed and its conductivity determined twice. The determinations were carried out with the temperature raised and lowered slowly (not over 5° per minute), and also at constant temperature. The carbonate content of the melt was checked by titrations of a sample by 0.1 N HCl solution.

The cell constant was determined from the conductivity of 30% sulfuric acid solution at 25°, and from the conductivities of fused $NaNO_3$, KNO_3, and NaOH. A temperature correction [1] was applied to the cell constant determined for 30% sulfuric acid solution. The values of the constant did not differ by more than 2-3%.

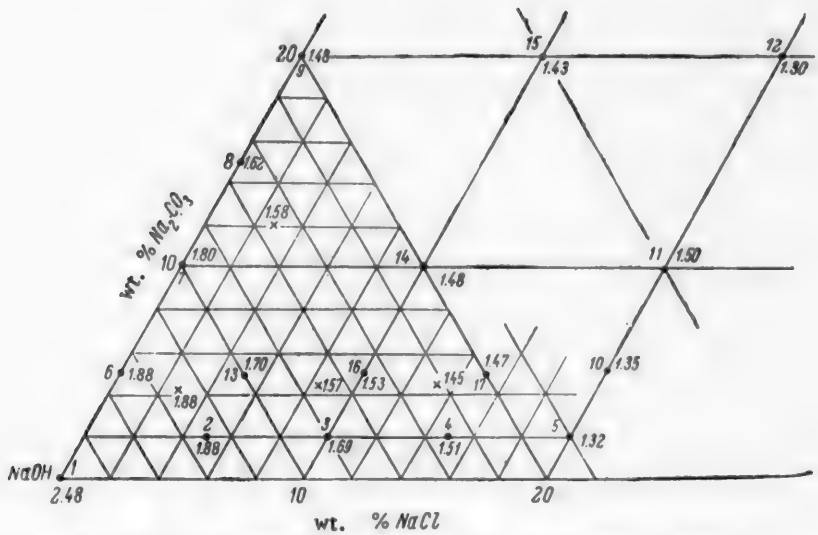

Fig. 6. The system NaOH – Na_2CO_3 – NaCl. Conductivity at 350°.

The temperature of the melts was measured by means of a chromel – alumel thermocouple enclosed in a silver casing. It was inserted in the crucible. The thermocouple was calibrated by the crystallization temperatures of $NaNO_3$, $LiNO_3$, $PbCl_2$, KCl, KCl, NaCl and KNO_3 [3].

The results of our conductivity determinations for pure NaOH and NaOH – Na_2CO_3 – NaCl, melts containing up to 20 wt. % of sodium chloride or carbonate are given in the table and Figs. 2-6. The data of Arndt and Ploetz [1] are also included in the table and Fig. 6.

The conductivity of pure NaOH is a linear function of temperature. Our values for the conductivity of pure NaOH are somewhat higher than those given previously [1]. Thus, our value for the conductivity of NaOH at 320° is 2.18 $ohms^{-1} cm^{-1}$, whereas Arndt and Ploetz give 2.21 $ohms^{-1} cm^{-1}$. As our sodium hydroxide contained only 0.3% of carbonate by weight (the Na_2CO_3 content of the hydroxide used by the earlier workers [1] was not less than 1.6% by weight), our extrapolation to zero contents of sodium chloride and carbonate is probably more reliable.

Fig. 2 shows that the conductivity of binary NaOH – NaCl melts is not a linear function of the temperature. This is probably due to changes in the viscosity and molecular state of the melts. The same is true for the system NaOH – Na_2CO_3 (Fig. 3). Comparison of Figs. 2 and 3 shows that additions of sodium chloride result in somewhat greater decreases in the conductivity of caustic soda than do corresponding additions of sodium carbonate. For example, a melt containing 20 wt. % NaCl and 80 wt. % NaOH (Point 5, see table) has a conductivity of 1.32 $ohms^{-1}$ cm^{-1} at 350°, whereas the conductivity of a melt containing 20 wt. % Na_2CO_3 and 80 wt. % NaOH (Point 9, see table) at the same temperature is 1.48 $ohms^{-1}$ cm^{-1}.

Fig. 6 represents a part of the concentration triangle with conductivity data at 350°. The data of Arndt and Ploetz are marked by crosses. Our results are in good agreement with theirs. We found somewhat higher conductivities in the composition region near Point 11.

LITERATURE CITED

[1] K. Arndt, and G. Ploetz, Z. Phys. Ch. 121, 439 (1926).

[2] V. P. Barzakovskii, Collected Papers on the Electrochemistry of Fused Salts (State Inst. Appl. Chem. 1940), 33. [In Russian]

[3] Technical Encyclopedia. Physical, Chemical, and Technological Data VI (1929). [In Russian]

Received March 21, 1958.

ELECTROCHEMICAL POLISHING OF ZINC IN SULFURIC ACID

G. P. Maltak

(Institute of General and Inorganic Chemistry, Academy of Science, Ukrainian SSR)

This paper is the second report on an experimental study performed in order to determine the possibility and conditions of anodic electrochemical polishing of zinc in sulfuric acid. The first part [1] contained an account of anodic passivation and electrochemical polishing of zinc in sulfuric acid solutions, observed with the aid of voltage – current curves. The present paper contains the results of determinations performed with current densities and electrolysis times which were constant for each individual experiment, but differed for different experiments.

In the light of the data on the sulfuric acid concentrations at which zinc was electrochemically polished during determinations of voltage – current curves, and of the characteristics of the latter [1], these experiments were performed in 5, 10, 20, 30, and 40% solutions of sulfuric acid, at anodic current densities of 50, 75, 100, and 125 amps/dm^2. The specimens, apparatus, and experimental conditions were the same as in the determinations of the voltage – current curves. The only difference was that the cathode was not zinc but copper of the same dimensions and shape. An auxiliary platinum electrode was used to bring the current strength to the necessary level in the experiment, so that when the current was switched over to the anode being polished its current density should at one be of the required value; this is important in experiments of brief duration.

Zinc was not polished in 40% sulfuric acid solution, not stirred, but if the solution was stirred it became polished at current densities of 50, 100, and 125 amps/dm^2 (the optimum was 100 amps/dm^2). Before the kick of the voltmeter corresponding to the limiting current zinc was not polished even under these last-named conditions, but the surface became bright immediately after the kick. The time required for the zinc surface to become not only bright but also smooth depended on the previous treatment. No traces of the coarse treatment used [1] remained after exposure at a current density of 100 amps/dm^2 for 10 minutes.

Similar results were obtained in 30% sulfuric acid solution. At current densities of 50-75 amps/dm^2 the zinc acquired noticeable luster if the solution was not stirred, but it became polished only in the stirred solution at current densities of 75, 100, and 125 amps/dm^2. At 50 amps/dm^2 in stirred 30% solution the zinc became black and pitted, in contrast to the effect observed in 40% solution. This is probably because the anodic passivation of zinc is less in 30% than in 40% sulfuric acid. The best specimens with the use of 30% acid were those treated at 100 amps/dm^2. Comparison of all the specimens treated in 40 and 30% acids under equivalent conditions showed that the latter were better.

The anodic passivation of zinc is still less in 20% sulfuric acid. The specimens became bright even in unstirred solution, but the leveling was slight, the vertical grooves were even intensified, and the surface was unsatisfactory. In the stirred solution, the zinc was etched at 50 amps/dm^2, and polished at 75, 100, and 125 dm^2. In 20% acid, however, the optimum current density was 125 amps/dm^2.

The results for 10% sulfuric acid are similar to those obtained under the same conditions in 20% acid, but the anodic passivation is still less. Thus, at current density of 75 amps/dm^2 and at the stirring rate used the zinc was polished in 10% acid after the kick of the voltmeter. If the stirring rate is increased, the galvanometer does not always give a kick, and in such experiments the zinc becomes coated with a black deposit.

Almost identical results were obtained for 5% acid. In the stirred solution zinc became polished at 75, 100, and 125 amps/dm^2.

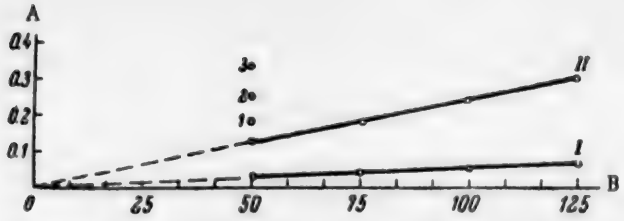

Fig. 1. Weight losses of zinc anodes in stirred and unstirred 5 to 40% sulfuric acid solutions, at different current densities and electrolysis times.
A) Weight loss of zinc anode (g), B) anodic current density (amps/dm^2). Electrolysis time: I) 1 minute (the weight losses were not determined at 50 amps/dm^2 in 5, 10, 20, and 30% solutions); II) 5 minutes (points at 50 amps/dm^2 not on the straight line correspond to the following sulfuric acid solutions; 1) 20%, not stirred, 2) 20%, stirred, 3) 30%, stirred.

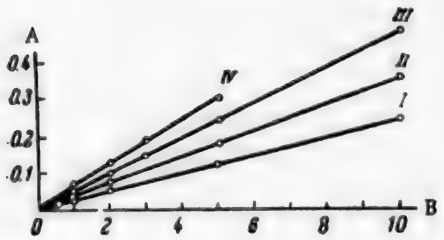

Fig. 2. Weight losses of zinc anodes, for different electrolysis times, in stirred and unstirred 5, 10, 20, 30, and 40% sulfuric acid solutions at different current densities.
A) Weight loss of zinc anode (g), B) electrolysis time (minutes). Anodic current densities (amps/dm^2): I) 50, II) 75, III) 100, IV) 125.

In all solutions (from 40 to 5%) zinc became polished only after the kick of the galvanometer, corresponding to the limiting current. Voltage – current curves for 1% sulfuric acid solution do not have any appreciable inflection. It was therefore of interest to carry out experiments on anodic treatment in 1% sulfuric acid solution. The solution was not stirred, and the experiments were performed at 100 and 125 amps/dm^2. After this treatment, most of the exposed surface was coated with a black deposit over an area shaped like a tongue, directed downward from the electrolyte – – air boundary but not reaching the bottom of the specimen, while a narrow strip (along the specimen edge), wider at the lower end was bright, and smooth if the solution was stirred.

It follows that zinc becomes electropolished when subjected to anodic dissolution in 5 to 40% sulfuric acid solutions, if these are stirred, at 18-20° and anodic current densities of 75, 100, and 125 amps/dm^2. Specimens treated in a stronger sulfuric acid solutions, 40 and 30%, were coated with a white deposit, while specimens polished in weaker solutions showed microscopic pitting.

The specimens were weighed for determination of the amount of zinc dissolved. At the current densities used (from 50 to 125 amps/dm^2), the weight loss of zinc anodes in 5 to 40% sulfuric acid solutions increases linearly with current density; if extrapolated to zero current density, the weight loss is zero (Fig. 1). Only in a few experiments at 50 amps/dm^2, indicated in Fig. 1, in which the galvanometer kick corresponding to the limiting current had not yet been observed, and in which therefore anodic dissolution was accompanied by chemical dissolution and the surface of the specimen therefore became black, the weight loss did not conform to this relationship, but was higher. In harmony with other observations, reported earlier, these results indicate that zinc is not dissolved chemically to any appreciable extent during electropolishing; it undergoes passivation, which does not increase with increasing current density.

These findings are consistent with the observed relationships between the amounts of zinc dissolved and the current efficiency, and the time of electrolysis. Fig. 2 shows that at a given current density the amount of zinc dissolved increases linearly with electrolysis time; when extrapolated to zero electrolysis time, the amount of zinc dissolved is also zero. The dependence of the current efficiency for zinc on the time of electrolysis is electrochemical polishing in 30 and 40% sulfuric acid is plotted in Fig. 3 (the curves for 20 and 10% sulfuric acid

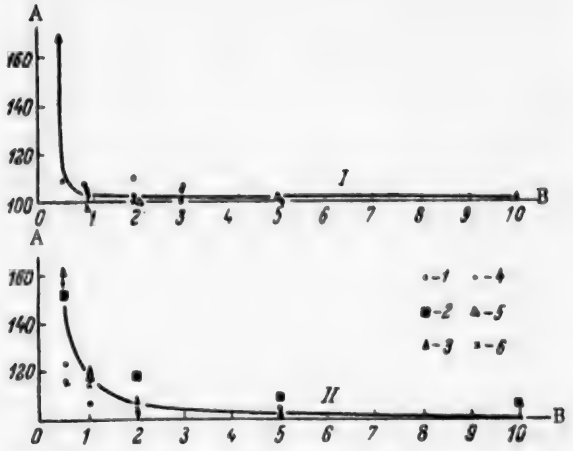

Fig. 3. Current efficiency in anodic dissolution of zinc in sulfuric acid solutions: 30% (I), and 40% (II), at different current densities and with different times of electrolysis.
A) Current efficiency for zinc (%), B) electrolysis time (minutes). Anodic current densities (amps/dm^2): 2, 3) 50; 1) 75; 4, 5) 100; 6) 125. 1, 2, 4, and 6) Stirred solutions; 3 and 5) not stirred.

almost coincide with these). It follows from this figure that at the concentration, current density, and other conditions necessary for electropolishing of zinc the current efficiency is higher than 100% in brief electrolysis, and tends to 100% with increase of the electrolysis time. The explanation of this result is that in brief electrolysis the weight loss of the specimen due to anodic dissolution is only a little more than the weight loss due to chemical dissolution before the kick of the voltmeter, while in prolonged electrolysis it is considerably greater. The current density used in these experiments was only slightly in excess of the limiting value, and therefore anodic liberation of oxygen and the proportion of the current expended for it were slight.

Thus, a whole series of facts indicates that in the electrochemical polishing of zinc in sulfuric acid the passivation is unstable, and is caused by a film which is unstable but which prevents zinc coming into direct contact with acid and undergoing chemical dissolution: the similarity (although with a certain hysteresis) of the ascending and the return voltage – – current curves, characterized by two ascents and a limiting current value terminating the first ascent; the cessation of chemical dissolution of zinc in sulfuric acid after the kick of the voltmeter; the 100% current efficiency, which is independent of the current density; and other facts.

Unstable anodic passivation and suppression of chemical dissolution are necessary conditions for electrochemical polishing of a metal in anodic dissolution. The voltage – current curve representing the anodic polarization of a metal in a solution suitable for its electrochemical polishing consists of two ascending branches joined by a "limiting current" plateau which terminates the first ascending branch, and the return voltage – current curve reproduces the curve determined at increasing current strength, but with some hysteresis. Anodic passivation, suppression of chemical dissolution, and hence electrochemical polishing, take place only under the conditions corresponding to the second ascending branch of the voltage – current curve. It is known that the current efficiency in electropolishing of metals may be below 100%, but the passivation remains unstable. It is probable that all factors which suppress chemical dissolution but do not lead to stable passivation and cessation of anodic dissolution of the metal should favor electrochemical polishing.

SUMMARY

Zinc becomes electropolished in the course of anodic dissolution in stirred solutions of 5 to 40% sulfuric acid, at 18-20° and current densities from 75 to 125 amps/dm^2.

LITERATURE CITED

[1] G. P. Maitak, J. Appl. Chem. 31, No 10, 1504 (1958). •

Received for the second time, May 30, 1958.

• Original Russian pagination. See C. B. Translation.

ELECTROLYSIS WITH A MERCURY CATHODE FLOWING OVER A VERTICAL METALLIC SURFACE

G. I. Volkov and E. I. Kus'kina

Despite the existence of a large number of patents relating to electrolytic cells with mercury cathodes flowing over vertical metallic surfaces, the literature contains hardly any publications dealing with studies of the performance of such cells. In 1904 Kettembeil and Carrier [1] published the results of their researches, and this is the only available literature reference on the subject. These authors concluded as the result of their investigations that rapidly-flowing mercury confers a vortex motion on the solution containing chlorine, and the reaction between chlorine and the amalgam results in a sharp drop of current efficiency, which does not exceed 50% in absence of a diaphragm. They found that if a diaphragm is used the current efficiency is at a maximum at current densities of 0.35-0.5 amp/ cm^2. They concluded that processes in which the mercury cathode moves rapidly hold little promise.

Kettembeil and Carrier's conclusion concerning the current-density optimum is dubious, because with a rapidly-moving amalgam cathode one can hardly expect considerable accumulation of the alkali metal at the cathode surface, which might be a cause of increased hydrogen discharge. Esin, Loshkarev, and Sofiiskii [2] succeeded in carrying out electrolysis with a streaming mercury cathode even at current densities of up to 0.9 amp/ cm^2 with high current efficiencies.

With regard to depolarization of the cathode by chlorine, the fraction of the current involved in this process should decrease with increase of current density. Therefore an increase of current efficiency should also be observed at higher current densities, and at sufficiently high current densities it might be possible to operate with satisfactory current efficiencies without the use of diaphragms. The present work was undertaken to verify this hypothesis.

EXPERIMENTAL

The cathode was made out of a smooth copper plate 2 mm thick and 20 x 260 mm in size, of the shape shown in Fig. 1. Pieces of ebonite with semicircular openings on the sides adjacent to the copper were attached to the flat sides of the plate at its constriction, as shown in Fig. 1. The cathode with its ebonite attachments was inserted in a glass tube in the lid of the electrolytic cell. Mercury was fed through this tube, and passed through the openings in the ebonite onto the copper plate. The current supply was connected to a ring of the copper plate, projecting from the tube.

A diagram of the cell is shown in Fig. 2.

The whole apparatus is shown schematically in Fig. 3. Amalgam passes from the cell 1 through the mercury seal 2 into the amalgam-decomposition vessel 3, packed with crushed graphite. Water is fed into the decomposition vessel from below from the header 4. The decomposed amalgam passes through the seal 5 into the receiver 6 of the air – vacuum elevator 7, and is fed through a header flask from the bottle 8 through the preheater 9.

The brine, together with chlorine, passes from the cell into the separator 10, where the chlorine is separated from the brine. Gas samples for analysis by means of the Orsat apparatus are taken from the separator 10. The cell circuit includes an ammeter and a shunted copper coulometer.

The experimental procedure was as follows: definite flow rates of the mercury and brine were established, and the current was switched on. After the flow water and temperature had been adjusted, the decomposition

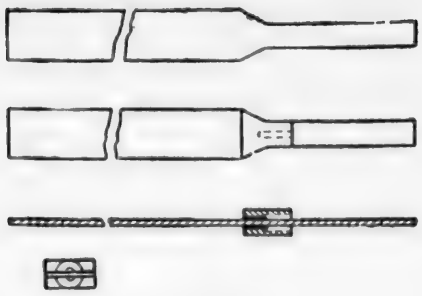

Fig. 1. Cathode design.

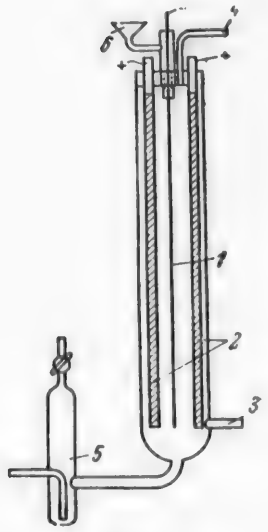

Fig. 2. Cell design. 1) Cathode, 2) graphite anodes, 10 mm away from the cathode, 3) brine inlet, 4) brine and chlorine outlet, 5) mercury seal to separate amalgam from brine, 6) funnel for supply of mercury to cathode.

vessel was rinsed out with a large volume of water, and the coulometer was switched in to start the experiment. The mercury flow rate was checked at 5-minute intervals during the experiment. At the end of the experiment, which lasted 30 minutes, the current was switched off, the decomposition vessel was rinsed out, and the collected alkali was titrated with acid for determination of the cathodic current efficiency. 3 determinations of the chlorine concentration and its hydrogen content were performed during the experiment. A saturated solution of common salt, prepared for electrolysis in diaphragm cells, was used in the experiments.

In attempts to ensure complete covering of the cathode by the flowing mercury it was found that this requires an excessively high mercury flow rate, as the stream of mercury does not readily reach the edge of the plate. The edges of the plate therefore had to be

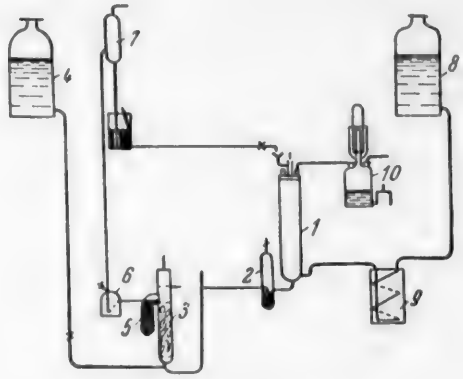

Fig. 3. Diagram of the apparatus.

covered by ebonite overlays on polyvinyl chloride lacquer. This decreased the width of the exposed part of the plate to 8 mm. It was then found that a mercury rate of 80-100 ml/minute was sufficient to cover the surface of the plate; at this mercury rate and at moderate current densities (when the cathode surface is still visible) no regions not covered by mercury were visible on the cathode. However, it was found in a series of experiments that the current efficiency fluctuated considerably under constant conditions; this was attributed to unequal distribution of the mercury between the two sides of the plate. One side of the cathode was therefore coated over with a cement material, and the anode on that side was disconnected.

Visual observations showed that 30 ml of mercury per minute is sufficient to cover the plate completely on one side. However, when the current is flowing the stream of amalgam becomes narrower because of the decrease in surface tension, and covering of the plate is disturbed. Tests of the hydrogen content of the chlorine showed that 50 ml of mercury per minute is sufficient to cover the cathode surface completely. This flow rate was used in experiments at various current densities, with a cell temperature of 55-57°.

The variations of the hydrogen content of the chlorine and current efficiency with current density are given below.

Current density (amps/cm^2)	1.45	1.45	1.0	1.0	0.6	0.6
Hydrogen content per 100 parts of chlorine (%)	1.6	1.5	1.5	1.5	2.6	2.3
Current efficiency (%)	94.5	94.7	90.3	89.3	85.7	84.9

These results refute the conclusion drawn by Kattembeil and Carrier that there is an optimum current efficiency as a function of current density in the 0.35-0.5 amp/cm^2 range. At a current density of 1-1.5 amps/cm^2 the current efficiency becomes high enough for electrolysis with a mercury cathode flowing over a vertical metallic surface, without the use of a diaphragm to separate the electrode compartments.

SUMMARY

A laboratory cell with a mercury cathode flowing over a vertical metallic surface was used to determine the dependence of current efficiency on current density in the electrolysis of common salt solution.

The current efficiency increases with current density in the current-density range investigated. At current densities of 1-1.5 amps/cm^2 the current efficiency reaches a value acceptable for practical purposes, without the use of a diaphragm between the electrodes.

LITERATURE CITED

[1] W. Kettembeil and C. F. Carrier, Z. Electroch. 10, 561 (1904).

[2] O. Esin, M. Loshkarev, and K. Sofiiskii, J. Phys. Chem. 10, 132 (1937).

Received November 10, 1957.

PREPARATION OF ETHYLENE GLYCOL DIACETATE IN PRESENCE OF CATION-EXCHANGE RESINS

N. S. Rabovskaia and V. N. Kucherovskaia

Many publications concerning the use of ion-exchange resins as catalysts in organic synthesis have recently appeared in the literature [1-7].

Ion-exchange resins have a number of advantages over the usual soluble catalysts. The most important advantages are: the catalysts may be used repeatedly, they have no corrosive action, the resins can be easily separated from the reaction products, the catalysts are selective, high yields are obtainable, and continuous processes may be used.

We desired to study the esterification of ethylene glycol by acetic acid in presence of cation-exchange resins, for preparation of the diester. Three cation exchangers were available: SG-1, KU-1, and KU-2; tests showed that their relative activity decreases in the following sequence: KU-2 > KU-1 > SG-1 (Fig. 1). KU-2 resin was used in our investigations.

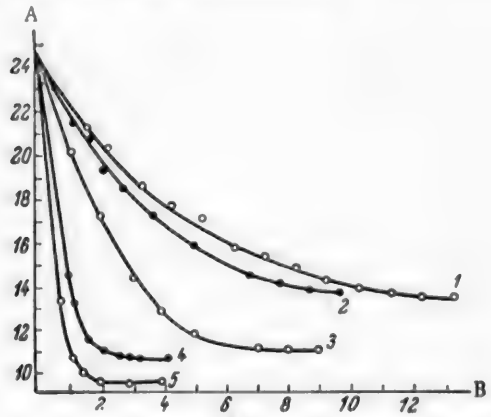

Fig. 1. Comparison of relative activities of SG-1, KU-1, and KU-2 resins and sulfuric acid in the esterification of ethylene glycol by acetic acid.
A) Amount of 0.5 N NaOH solution (ml), B) time (hours). 1) Without catalyst, 2) SG-1, 3) KU-1, 4) KU-2, 5) H_2SO_4.

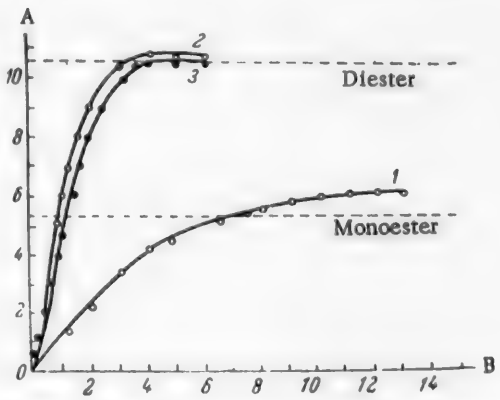

Fig. 2. Rate of water distillation in the esterification of ethylene glycol by acetic acid.
A) Amount of water (ml), B) time (hours). 1) Without catalyst, 2) with KU-2, 3) with H_2SO_4.

Preliminary experiments showed that the amount of catalyst used, above 0.5% on the weight of the reaction mixture, has virtually no effect on the process.

The results of a study of the esterification process in presence of KU-2, and in presence of sulfuric acid and also without catalyst, are plotted in Fig. 1.

In order to reach maximum yields of ester, the esterification of ethylene glycol by acetic acid was also performed in presence of benzene for removal of water by distillation. The rate of water evolution gave an indication of the reaction kinetics, and the total amount of water liberated showed the extent of the reaction. Fig. 2 shows that ethylene glycol diacetate is formed in presence of the cation exchanger or of sulfuric acid.

It should be noted that if the process is effected without removal of water the reaction rate is somewhat higher in presence of sulfuric acid than in presence of KU-2 (Fig. 1), but if water is distilled off the reaction rates almost coincide (Fig. 2).

The service life of KU-2 resin was determined by tests of its activity in a series of consecutive cycles. The activity of the same sample of KU-2 resin was not diminished after it had been used 9 times. There was some fall of activity after 10 cycles. The loss of activity was almost complete at the 11th cycle. It is interesting to note that the activity of this sample was restored completely after an interval of 6 days.

EXPERIMENTAL

Esterification without removal of water was performed in a 3-necked flask fitted with a reflux condenser, stirrer, and thermometer. The flask, containing 120 g of acetic acid (2 moles), 62 g of ethylene glycol (1 mole), and 1.6 g of KU-2 resin, was placed on a boiling water bath. Every 30 minutes 1 ml of the reaction mixture was removed, and the residual activity was determined by titration with 0.5 N NaOH solution. Esterification with distillation of water was performed in a 2-necked flask fitted with a Dean and Stark trap, a reflux condenser, and a thermometer. The flask contained 36 g of acetic acid (0.6 mole), 18.6 g of ethylene glycol (0.3 mole), 50 ml of benzene, and 1.6 g of KU-2 2 resin. The rate of collection of water in the trap was determined.

The 185-189° fraction, which corresponded to ethylene glycol diacetate, had $d^{20} = 1.1091$, $\eta^{15} = 1.4152$ and was immiscible with water in 1:1 and 1:3 ratios. (Literature data: b. p. 190.5° [8], $\eta^{15} = 1.4159$ [8], soluble in 7 volumes of water [9]).

The 178-185° fraction, corresponding to ethylene glycol monoacetate, had $d^{20} = 1.1082$, $\eta^{15} = 1.4210$; it became turbid when mixed with water in 1:1 ratio, but remained clear with water in 1:3 ratio; this shows that the monoester with a small admixture of diester had been formed. (Literature data: b. p. 180° [8], $\eta^{15} = 1.4225$ [8], miscible with water and alcohol [10]).

SUMMARY

Esterification of ethylene glycol by acetic acid in presence of KU-2 resin yields ethylene glycol diacetate. The esterification rate is 3-4 times the rate in absence of catalyst, and is equal to the rate in presence of sulfuric acid.

LITERATURE CITED

[1] M. J. Astle and B. Schalfer, J. Am. Chem. Soc. 77, 13, 3643 (1955).

[2] Vlastimil Ruzicka and Vladimir Medonos, Chem. Prumysl, 7, 268 (1956).

[3] Edouard Swistak C. r. 239, 12, 709 (1954).

[4] M. J. Astle and J. A. Zaslonsly, Ind. Eng. Ch. 46, 4, 787 (1954).

[5] J. Fodor, Acta Chim. Hungar. 10, 1/3, 141 (1956).

[6] T. R. E. Kressman, Manuf. Chem. XXVII, 11, 454 (1956).

[7] P. Mastagli, C. r. 242, 8, 1031 (1956).

[8] G. O. Curme and F. Johnston, Glycols (New York, 1952).

[9] A. Wurtz, Ann. Chim. Phys. 55, 3, 433 (1859).

[10] Atkinson, C. A. 109, 232, Beilst. II, 159, 141 (1920).

Received March 18, 1957.

BINARY COMPOUNDS OF GLUCOSE WITH MINERAL SALTS

V. I. Sharkov and V. Guzhavina

(The Leningrad Academy of Wood Technology)

In 1950 Lebedev and Liubin showed [1] that the binary compound of glucose and sodium chloride, of the composition: $(C_2H_{12}O_6)_2NaCl$ + water, which forms well-defined crystals, decomposes rapidly when mixed with a small amount of water, forming large crystals of glucose and a mother liquor containing part of the glucose and almost all the sodium chloride.

They made use of this fact in the production of crystalline glucose from strongly contaminated solutions, such as vegetable hydrolyzates [2]. Later this process was also used in the production of crystalline glucose from starch hydrolyzates.

By analogy with sodium chloride, other mineral salts capable of forming binary compounds with glucose might be expected to show similar behavior.

In addition to this binary compound of glucose and sodium chloride, other analogous compounds are known. For example, Stenhouse [2] concentrated a solution containing 1 mole of sodium bromide and 2 moles of glucose, and obtained a binary compound of the composition $(C_6H_{12}O_6)_2NaBr$. A similar compound was obtained by Hönig, who used a somewhat different method. A binary compound of glucose and sodium iodide: $(C_6H_{12}O_6)_2NaI$ + water, and a compound of glucose and potassium chloride [4]: $(C_6H_{12}O_6)_2KCl$ are also described in the literature. The specialized literature does not contain any information on the ability of these compounds to decompose with formation of crystalline glucose.

For investigation of this effect, we prepared a series of crystalline binary compounds of glucose with various mineral salts.

The binary compounds were prepared by slow dehydration, over sulfuric acid at 15°, of concentrated aqueous solutions containing 1 mole of mineral salt per 2 moles of glucose. The crystals formed were separated from the mother liquor on a porous plate, dried thoroughly first by means of filter paper and then in a drying oven at 60° to constant weight, and then analyzed quantitatively.

The glucose content of the crystals was determined by the Bertrand method, and the salt content (mainly the anion) was also determined. For example, in fluorides, chlorides, bromides, and iodides the anion was determined by titration with silver nitrate, sulfate was determined gravimetrically as $BaSO_4$, while in nitrates the cation was determined.

It should be noted that certain salts do not form crystalline binary compounds with glucose under the conditions of our experiments. These include NaF, KF, $CuCl_2$, MgF_2, CdF_2, CdI_2, SrF_2, $SrBr_2$, SrI_2, $CaCl_2$, CaF_2, K_2SO_4, $KAl(SO_4)_2$, $MgSO_4$, $CdSO_4$, $CaSO_4$, $KClO_4$, KIO_4, $Zn(NO_3)_2$, $KBrO_3$, K_2CrO_4, Na_2HPO_4, NaH_2PO_4, K_2HPO_4 and KH_2PO_4. Sodium acetate did not form a binary compound either.

The following salts formed binary compounds with glucose: NaCl, NaBr, NaI, KCl, KI, KBr, LiCl, LiBr, LiI, $SrCl_2$, $CdCl_2$, $CdBr_2$, $MgCl_2$, $BaCl_2$, $ZnSO_4$, Na_2SO_4, $NaNO_3$, KNO_3, $Ca(NO_3)_2$, $Mg(NO_3)_2$. Only the first four were known previously to this investigation.

Each binary compound was prepared three times, and each sample was analyzed.

The analytical data for the binary compounds, and their presumed structural formulas, are given in the table (the average values of triplicate analyses performed as stated above are given).

Analytical Data for Binary Compounds

Original salt	Found in the binary compound (%)			Presumed structural formula of binary compound	Contents calculated from the presumed formula (%)		
	glucose	salt	water		glucose	salt	water
NaCl	82.6	13.6	3.7	$(C_6H_{12}O_6)_2NaCl \cdot H_2O$	82.5	13.4	4.1
NaBr	78.2	21.4	0.3	$(C_6H_{12}O_6)_2NaBr$	77.8	22.1	0.0
NaI	70.5	29.8	0.0	$(C_6H_{12}O_6)_2NaI$	70.5	29.4	0.0
KCl	76.5	16.2	7.3	$(C_6H_{12}O_6)_2KCl \cdot 2H_2O$	76.5	15.8	7.6
KI	77.6	18.0	4.3	$(C_6H_{12}O_6)_4KI \cdot 2H_2O$	78.0	18.0	4.0
KBr	72.5	23.9	3.6	$(C_6H_{12}O_6)_2KBr \cdot H_2O$	72.4	23.9	3.6
LiCl	86.8	5.02	8.2	$(C_6H_{12}O_6)_4LiCl \cdot 4H_2O$	86.6	5.0	8.3
LiBr	85.3	10.5	4.2	$(C_6H_{12}O_6)_4LiBr \cdot 2H_2O$	85.4	10.3	4.2
LiI	80.8	15.1	4.0	$(C_6H_{12}O_6)_4LiI \cdot 2H_2O$	80.9	15.0	4.0
$SrCl_2$	80.3	8.9	10.8	$(C_6H_{12}O_6)_5SrCl_2 \cdot 11H_2O$	80.2	8.8	11.0
$CdCl_2$	68.7	14.1	17.2	$(C_6H_{12}O_6)_5CdCl_2 \cdot 12H_2O$	69.0	14.0	16.9
$CdBr_2$	60.7	38.0	1.2	$(C_6H_{12}O_6)_5CdBr_2 \cdot H_2O$	61.0	37.4	1.5
$MgCl_2$	76.1	8.9	14.9	$(C_6H_{12}O_6)_5MgCl_2 \cdot 9H_2O$	77.7	8.2	14.0
$BaCl_2$	60.1	36.7	3.1	$(C_6H_{12}O_6)_2BaCl_2 \cdot H_2O$	61.1	35.8	3.07
Na_2SO_4	75.2	19.8	4.9	$(C_6H_{12}O_6)_3Na_2SO_4 \cdot 2H_2O$	75.2	19.8	5.0
$ZnSO_4$	67.3	24.3	8.3	$(C_6H_{12}O_6)_52ZnSO_4 \cdot 6H_2O$	67.5	24.3	8.2
$NaNO_3$	85.0	13.2	1.7	$(C_6H_{12}O_6)_3NaNO_3 \cdot H_2O$	85.0	13.4	1.6
KNO_3	41.4	56.1	2.5	$(C_6H_{12}O_6)_25KNO_3 \cdot H_2O$	40.8	57.2	2.0
$Ca(NO_3)_2$	79.8	13.1	7.1	$(C_6H_{12}O_6)_5Ca(NO_3)_2 \cdot 5H_2O$	77.9	14.2	7.8
$Mg(NO_3)_2$	76.9	12.6	10.5	$(C_6H_{12}O_6)_5Mg(NO_3)_2 \cdot 7H_2O$	76.4	12.6	10.7

It follows from these results that Na halides, and some K halides, form binary compounds containing 2 molecules of glucose per 1 molecule of salt.

Lithium halides and potassium iodide form binary salts containing four glucose molecules. Cadmium chloride and bromide, magnesium chloride, zinc sulfate, and calcium and magnesium nitrates form binary compounds containing five glucose molecules.

Sodium sulfate and nitrate form binary compounds containg 3 glucose molecules, etc.

Binary compounds of glucose with NaCl, NaBr, NaI, $NaNO_3$ and KNO_3 form large, well-defined crystals. Of these, binary compounds with sodium halides form hexagonal and rhomboidal crystals. The crystals of $NaNO_3$ with glucose are pairs of 6-sided pyramids joined by their bases. The compound with KNO_3 forms long rods which increase in size rapidly. The compounds with KCl, KBr, and KI crystallize slowly, forming finely-crystalline precipitates consisting of druses and step-shaped pyramids.

Compounds with lithium salts form bulky precipitates consisting of fine crystals of indeterminate form. These crystals are very hygroscopic and deliquesce rapidly in air. The compounds with $CdCl_2$ and $CdBr_2$ crystallize readily in small regular plates. The compounds with Na_2SO_4, $ZnSO_4$, $Ca(NO_3)_2$ and $Mg(NO_3)_2$ readily form bulky precipitates consisting of crystalline acicular druses, difficult to separate from the mother liquor.

These results show that the compounds of greatest interest, with regard to a high tendency to crystallize and to form large crystals easily separated from the mother liquor, are binary compounds of glucose with NaCl, NaBr, NaI, $NaNO_3$ and to some extent also the compounds with cadmium chloride and bromide. The ability of sodium sulfate to form a well-crystallizing binary compound may also be used in the separation of glucose from low-grade sugar solutions.

The ability of these binary compounds to decompose in presence of water, with formation of glucose crystals, was tested by two methods: 1) microscopic estimation of the composition of the crystalline precipitate after decomposition of the binary compound by a small amount of water, and 2) chemical analysis of the precipitates for glucose and mineral salts.

In the experiments on the decomposition of the binary compounds, the crystals were ground in a mortar and

then mixed quickly with water in 1.5:1.0 ratio by weight at +15°. In all cases a fluid slurry was first formed, which thickened rapidly. Microscopic examination of the mass revealed numerous typical glucose crystals. After the mother liquor had been separated and the mass had been dried, chemical analysis showed it to consist of glucose with small amounts of mineral salt. For example, the binary compound of glucose with lithium chloride, containing 15.16% of the salt, yielded a crystalline precipitate containing only 0.4% of lithium chloride after such treatment.

The binary compound of glucose with potassium iodide yielded a precipitate in which the salt content fell from 18.03 to 3.3%. Similar results were obtained with all the other binary compounds. Thus, recrystallization of the binary compound, described by Lebedev and Liubin for the compound of glucose and sodium chloride, is a property common to many binary compounds of glucose with mineral salts. The selection of a particular salt for the production of crystalline glucose through its binary compounds may be based on the specific process requirements.

LITERATURE CITED

[1] N. V. Lebedev and B. O. Liubin, J. Appl. Chem. 23, 4, 409 (1950);* N. V. Lebedev, B. O. Liubin, and D. M. Khai, J. Appl. Chem. 23, 7 (1950).*

[2] V. I. Sharkov, Hydrolysis Ind. 3, 481 (1950).

[3] Stenhouse, Lieb. Ann. 129, 286.

[4] Tollens and Elsner, Brief Handbook of Carbothydrate Chemistry (GONTI, 1938), p. 225 [Russian translation].

Received May 15, 1957.

* Original Russian pagination. See C. B. Translation.

THERMOOXIDATIVE DECOMPOSITION OF BENZYLCELLULOSE

O. P. Koz'mina and V. I. Kurliankina

Benzylcellulose, like ethylcellulose, is oxidized by molecular oxygen, with evolution of benzaldehyde as the main reaction product; this was reported earlier [1]. The liquid products formed by the action of heat at 100° in oxygen contain 80-90% of benzaldehyde, while the rest contains benzyl alcohol, benzyl formate, water, and small amounts of benzoic and formic acids. Carboxyl and carbonyl groups are formed in the benzylcellulose molecule as the result of oxidation, and the molecular weight decreases.

Technical benzylcellulose (disubstituted), purified by means of exhaustive extraction in alcohol – benzene mixture (9:1), was used for the oxidation.

Composition of Liquid Oxidation Products of Benzylcellulose

Oxidation products of benzylcellulose	Contents (% of condensate wt.)	Characteristics
Benzaldehyde	86-90	Oil with almond odor, n_D^{20} = 1.5455; 2,4-dinitrophenylhydrazone, m. p. 236.5°; Condensation product with dimedon, m. p. 192°
Benzyl alcohol	2-3	m. p. of acid phthalate ester 104° (106° by literature data)
Benzyl formate	1-2	Saponification with formation of formic acid and benzyl alcohol
Formic acid	2-3	Lead salt, Pb content found 69.40%, $(HCO_2)_2$ Pb calculated 69.71%, reduction of Ag salts, oxidation by permanganate solution
Benzoic acid	0.5-1	m. p. 121°, etc.
Water	—	b. p. 100°, n_D^{20} = 1.3350

The experiments were performed at 100° (the benzylcellulose melted rapidly at higher temperatures) under conditions analogous to those in the oxidation of ethylcellulose [2], except that the apparatus was evacuated at intervals in order to remove high-boiling reaction products. The oxidation was slow, and ceased when the benzylcellulose melted. The intrinsic viscosity of benzylcellulose fell from 1.2 to 0.5-0.6, and the benzyl-group content decreased from 63.1 to 58-59%.

The liquid condensate of volatile oxidation products separated into two layers: a smaller aqueous layer containing a small amount of acids, and a larger oily layer. The oily substance was dissolved in ether and treated with aqueous sodium bicarbonate solution to extract acids; sodium bisulfite solution was used to bind the

benzaldehyde. The oil remaining in the ether after removal of acids and benzaldehyde consisted of benzyl formate and benzyl alcohol, which were identified.

LITERATURE CITED

[1] O. P. Koz'mina, V. I. Kurliankina, and E. N. Matveeva, Proc. Acad. Sci. USSR 114, 4, 789 (1957).*

[2] O. P. Koz'mina, and V. I. Kurliankina, J. Appl. Chem. 31, 4, 601 (1958).*

Received March 5, 1958.

* Original Russian pagination. See C. B. Translation.

STUDY OF THE COMPOSITION OF THE TURPENTINE AND THE PROPERTIES OF ROSIN FROM THE OLEORESIN OF THE SUDAK PINE (PINUS PITHYUSA VAR. STANKEWICZII SUK., PINUS STANKEWICZII FOM.)

I. I. Bardyshev and L. V. Roman

(The S. M. Kirov Belorussian Institute of Wood Technology)

The ancestor of the Stankewicz pine is considered to be an extinct pine species [1]. For example, it is close to a pine of the Tertiary period (Pinus sarmatica), the remains of which have been found in Sarmatian deposits of the Kerch peninsula. The Sudak pine has a wide crown and reached 25 meters in height. It grows in south Crimea near Sudak and near Cape Ai-Ya, in Massandra, Melas, and Kastro. It grows well and is not damaged by scale insects. It is extremely resistant to drought, and is more resistant to cold and tolerant of salt soils than Pinus halepensis. It yields valuable resinous wood and is suitable for tapping [2]. It is being successfully introduced by the Yalta Forestry Establishment into the forest culture of the lower zone, and it also grows well on the Black Sea shore in North Caucasus and in southern Central Asia. Trials by the Nikitskii Botanical Gardens showed that this is the most valuable species for decoration and afforestation of the shore zone of Southern Crimea [2].

TABLE 1

Physical Properties of Turpentine and Rosin Obtained from the Gum of Individual Trees

Tree No.	Weight of oleoresin (g)	Turpentine content (%)	Properties of turpentine		Rosin* $[\alpha]_D$
			n_D^{20}	α_D^{20}	
6	9.7	20.7	1.4678	+22.7	— 9.1
4	10.3	13.5	1.4680	—31.0	—13.8
12	8.1	12.8	1.4683	—	—10.6
10	15.6	20.1	1.4685	—22.3	—10.8
16	5.9	9.1	1.4689	—22.5	— 6.1
3	18.8	—	1.4692	—19.5	—21.5
14	121.7	29.5	1.4692	—13.9	—11.0
7	6.1	8.2	1.4696	—	—29.5
13	4.3	29.1	1.4698	+7.1	—16.1
2	11.8	32.4	1.4699	—	—29.9
8	10.4	4.8	1.4699	+18.5	— 4.6
11	10.4	3.0	1.4700	—	—18.1
17	8.8	18.8	1.4700	—15.6	—22.2
15	15.4	26.5	—	—	—26.1

*The specific rotation of rosin was determined in 2% alcoholic solutions in all cases.

No data are available in the literature on the composition of the turpentine and properties of rosin from the Sudak pine. There is only the work of Arbuzov et al. [3] on the composition of gum turpentine from a variety of this pine, Pinus pithyusa, which grows near the Black Sea shore in the Caucasus, around Sochi.

TABLE 2

Properties of Gum Rosin from Sudak Pine and Common Pine

Characteristics	Gum rosin from Sudak pine	GOST-55 specifications for 1st quality pine rosin
External appearance.	Clear glassy mass without visible inclusions	Clear glassy mass without visible inclusions
Color on standard scale.	x	x, ww, wg
Moisture content (%)	0.02	Not over 0.03
Ash content (%).	0.03	Not over 0.04
Mechanical impurities (%).	0.04	Not over 0.05
Softening point (°C)	69.1	Not below 68
Acid number	171	Not below 168
Unsaponifiable matter (%).	3.0	Not over 6.5

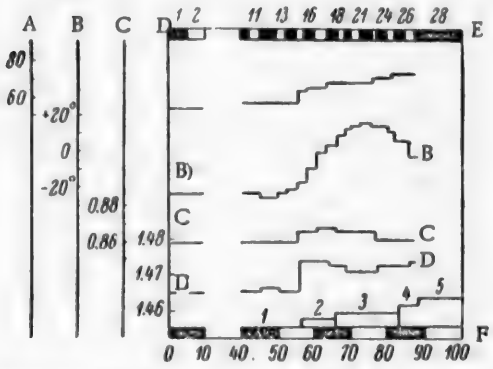

Properties of fractions obtained by distillation of turpentine.
A) b. p. at 20 mm (°C), B) d_4^{20}, C) n_D^{20}, D) α_D^{20}, E) numbers of fractions, F) % content of fraction. Zones: 1) α-pinene, 2) camphene (?), 3) β-pinene, 4) myrcene (?), 5) limonene (high-boiling fractions).

In view of the practical importance of cultivation of the Sudak pine [2], we considered it necessary to study the composition of the turpentine and the properties of the rosin obtained from this pine. Moreover, such study is of theoretical importance in our general series of investigations, performed over a period of many years [4], on the composition of turpentines from different conifers.

EXPERIMENTAL

The gum was obtained by tapping from a 25-year plantation of the Sudak pine in south Crimea, in the region of the Nikitskii Botanical Gardens. The tapping was carried out by the open method in August 1953. The gum was collected from the receiver 4 days after the start of tapping. The gum did not differ in external appearance from the gum of the common pine. Turpentine was distilled out of the gum with live steam. The turpentine content of the gum reached 32%. Table 1 contains data on the physical properties of turpentine and rosin samples obtained from the gum of individual trees. It follows from the data in Table 1 that the physical properties, and hence the chemical composition, vary considerably, as was found to be the case for other conifers [5-7].

The turpentine obtained from the gum of individual trees was combined and distilled in steam. After distillation, the combined sample of turpentine (38.8 g) had the following properties: n_D^{20} 1. 4700, d_4^{20} 0.8644, α-14.8°.

For isolation of individual components, the turpentine was fractionated through a column of 50 theoretical plates under residual pressure of 20 mm Hg, and reflux ratio 50-100. The distillation data are given in the diagram.

The composition of the turpentine is: a mixture of L-α-pinene and D-α-pinene (about 55%), L-β-pinene (about 10%), D-Δ^3-carene (about 18%), a mixture of L-limonene and dipentene (about 8%), and high-boiling fractions (about 10%). A sample of gum turpentine from P. pithyusa Strun., investigated by Arbuzov, consisted of a mixture of L-α-pinene with D-α-pinene (69.8%), D-Δ^3-carene (23.6%), an unknown component (1.5%), and high-boiling fractions (5.1-5.6%).

The physical properties of the fractions intermediate between α-pinene and β-pinene suggest that they may contain L-camphene, but we were not able to prove this chemically. The same applies to the presence of β-myrcene in the fractions between β-pinene and Δ^3-carene. The presence of the principal components in turpentine was confirmed by preparation of derivatives: α-pinene nitrosochloride of m. p. 103-104° (from Fractions 1-12), nopinic

acid of m. p. 126-127° (from Fractions 15-16), Δ^3-carene nitrosate of m. p. 146.5-147° (from Fractions 19-24), and dipentene tetrabromide of m. p. 124-125° (from Fractions 26-27).

The gum rosin from the Sudak pine (Table 2) differs very little in properties from gum rosin obtained from the common pine.

SUMMARY

1. Gum turpentine from the Sudak pine is analogous in chemical composition to gum turpentine from the common pine, and can be used for the same purposes. The principal components of the turpentine are α-pinene, β-pinene, Δ^3-carene, and limonene.

2. Gum rosin from the Sudak pine is analogous in properties to gum rosin from the common pine, and can be used for the same purposes.

LITERATURE CITED

[1] O. G. Kapper, Conifers (Moscow – Leningrad, State Wood and Paper Press, 1954). [In Russian]

[2] Trees and Bushes, Trans. Molotov Nikitskii State Botanical Gardens, Yalta (1939).

[3] B. A. Arbuzov, L. Bastanova, E. Ivanova, L. Kozlovskaia, A. Mal'tseva, and V. Fedorov, J. Appl. Chem. 5, 787 (1932).

[4] I. I. Bardyshev, Author's summary of Dissertation: Study of the Chemical Composition of Domestic Turpentines and Conversions of Some of their Components (Moscow, Inst. Org. Chem. Acad. Sci. USSR, 1952). [In Russian]

[5] I. I. Bardyshev and A. L. Piriatinskii, Proc. Acad. Sci. USSR 75 (1950).

[6] I. I. Bardyshev and K. V. Bardysheva, J. Appl. Chem. 25, 10, 1095 (1952). •

[7] I. I. Bardyshev and K. V. Bardysheva, J. Appl. Chem. 25, 12, 1231 (1952). •

Received July 15, 1957.

• Original Russian pagination. See C. B. Translation.

PREPARATION OF TOLUENE CONCENTRATES FROM PETROLEUM FRACTIONS BY LOW-TEMPERATURE DEHYDROGENATION OVER PLATINIZED CARBON

N. I. Shuikin, Kh. M. Minachev, I. L. Garanin, S. S. Novikov, and N. F. Kononov

Detailed analysis of the experimental data presented in the preceding paper [1] convinced us that platinized carbon can be extensively used as a catalyst, not only for aromatization of gasolines, but also for the production of concentrates of individual aromatic hydrocarbons. The results of experiments on the production of toluene concentrates in a pilot unit [1] are given below. Toluene was subsequently isolated from the concentrate by azeotropic distillation with methanol. The purified toluene fully conformed to GOST specifications.

EXPERIMENTAL

Catalyst preparation. The catalyst used in the experiments was 4% platinized carbon; the method of preparation and the equipment used were described previously [1].

Three catalyst samples were made. Sample No.2 was used in the aromatization of gasoline from Il'skii petroleum, and Samples Nos.3 and 4, in the aromatization of gasoline from Khadyzhensk petroleum.

Preparation of the raw material for aromatization. Straight-run gasolines from Il'skii and Khadyzhensk petroleums were used as the raw materials for aromatization. The straight-run gasolines were rectified in a batch unit in order to isolate the 89-112° fraction, destined for aromatization. This fraction was then purified by means of 3% oleum to remove sulfur compounds, and redistilled.

Rectification. Rectification was performed in a batch installation consisting of two independent units. Each unit contained a plate column of 50 theoretical plates, 40 m high and 2 m in diameter, a still 50 m^3 in capacity, a boiler with a heating surface of 50 m^2, a tubular dephlegmator with a cooling surface of 50 m^2, and other auxiliary equipment. The required 98-112° fraction went to purification, while the head fraction and residues were used in the production of high-grade gasolines.

The output of the rectification plant per cycle (32 hours) was 3.6 tons of the required 98-112° fractions, obtained in 15% yield. The 98-112° fraction had the following properties: n_D^{20} 1.4150, d_4^{20} 0.745 aromatic hydrocarbons 9%, sulfur 0.002-0.003%.

Aromatization of the 98-112° fraction from Il'skii petroleum. The apparatus used for the aromatization was described previously [1].

Selected data on the aromatization of the 98-112° fraction from Il'skii petroleum gasoline, in presence of Catalyst No.2, are presented in Table 1. These results show that 4% platinized carbon was effective for 75 days continuously; during this time the toluene content of the catalyzate (toluene concentrate) fell by only 6% (down to 23.8%) from the value at the initial stage of the process (29.8%). During this time 262.2 tons of gasoline was treated; this corresponds to a yield of about 40 kg of toluene concentrate per g of platinum.

Aromatization of the 98-112° fraction from Khadyzhensk petroleum. The results obtained in aromatization of the 98-112° fraction of petroleum showed that activated carbon containing 4% platinum can be used for aromatization for a long time without serious loss of activity, even if the original fraction has a moderate content of sulfur compounds. Threfore in subsequent trials the catalyst samples were used for aromatization of the 98-112° fraction of Khadyzhensk gasoline without previous removal of sulfur compounds. This fraction had an

TABLE 1

Results of Trials of Catalyst No.2 for Aromatization of the 98-112° Fraction Isolated from Il'skii Petroleum Gasoline

Time (hours)	Catalyzate		Gasoline rate (liters/hour)	Reactor temperature (°C)			
	n_D^{20}	toluene content (vol. %)		top of 1st pass	bottom of 1st pass	bottom of 2nd pass	top of 2nd pass
24	1.4285	29.8	225	273	300	298	301
144	1.4287	30.0	225	270	300	301	300
264	1.4280	29.2	225	280	300	301	302
384	1.4280	29.2	225	280	298	300	300
504	1.4275	28.7	225	285	305	305	306
624	1.4280	29.2	225	285	307	308	306
744	1.4290	30.2	225	285	307	308	309
864	1.4208	30.2	225	285	308	309	307
984	1.4286	29.8	225	290	307	307	308
1104	1.4282	29.4	225	285	308	308	308
1224	1.4284	29.7	225	285	308	309	310
1344	1.4272	28.0	225	280	308	308	308
1464	1.4270	28.0	175	275	308	308	308
1584	1.4263	26.3	175	280	313	311	312
1704	1.4263	26.3	175	291	318	318	320
1824	1.4243	23.8	175	282	319	318	319

TABLE 2

Results of Trials of Catalyst No.3 for Aromatization of the 98-112° Fraction Isolated from Khadyzhensk Petroleum Gasoline

Time (hours)	Catalyzate		Gasoline rate (liters/hour)	Reactor temperature (°C)		
	n_D^{20}	toluene content (vol. %)		top of 1st pass	bottom of 1st pass	top of 2nd pass
4	1.4370	39.0	225	270	287	285
124	1.4377	40.0	225	256	282	283
244	1.4360	37.5	225	255	302	297
364	1.4350	35.5	225	253	300	298
484	1.4330	32.5	210	247	301	300
604	1.4310	30.0	210	255	302	300
676	1.4304	29.5	200	260	289	300
796	1.4295	28.0	200	260	288	300
916	1.4280	27.0	210	262	300	305
1036	1.4274	26.5	210	260	300	310
1156	1.4260	26.0	210	260	300	308
1276	1.4260	25.5	210	260	300	307

average content of 10-12% aromatics and 0.012% sulfur, and had n_D^{20} 1.4189 and d_4^{20} 0.742. Each catalyst was used for more than 53 days, and retained high activity.

The results of trials with catalyst Samples Nos.3 and 4 are given in Tables 2 and 3.

TABLE 3

Results of Trials of Catalyst No 4 for Aromatization of the 98-112° Fraction Isolated from Khadyzhensk Petroleum Gasolines

Time (hours)	Catalyzate		Gasoline rate (liters/hour)	Reactor temperature (°C)		
	n_D^{20}	toluene content (vol. %)		top of 1st pass	bottom of 1st pass	top of 2nd pass
24	1.4416	—	300	250	290	300
100	1.4440	—	300	260	285	292
220	1.4418	41.6	265	255	286	290
440	—	—	245	250	292	295
580	1.4358	35.2	250	260	300	300
700	1.4348	34.5	220	250	300	300
820	—	—	200	260	295	300
940	—	—	200	250	298	305
1030	1.4322	31.6	200	260	300	304
1180	—	—	200	250	300	302
1300	—	—	200	265	302	305
1332	1.4312	30.0	200	250	300	306

SUMMARY

1. Toluene concentrate has been made for the first time on the pilot-plant scale by low-temperature catalytic dehydrogenation.

2. A catalyst consisting of 4% platinum on carbon has high activity and stability in the aromatization of the 98-112° fraction of gasoline from Il'skii petroleum. For example, after 75 hours of continuous service without regeneration the toluene content of the catalyzate fell by only 6% (from 29.8 to 23.8%).

3. Aromatization of the 98-112° fraction of Khadyzhensk petroleum, not treated to remove sulfur compounds, over two catalyst samples (Nos. 3 and 4) yielded toluene concentrates containing up to 40% toluene, and the catalyst remained active for more than 58 days.

4. Aromatization trials with desulfurized and undesulfurized 98-112° fractions over a catalyst consisting of 4% Pt on carbon showed that undesulfurized fractions may be used provided that the time of the catalyst run is reduced.

LITERATURE CITED

[1] N. I. Shuikin, Kh. M. Minachev, S. S. Novikov, N. F. Kononov, and I. L. Garanin, J. Appl. Chem. 31, 11, 1732 (1958).*

Received July 23, 1957.

* Original Russian pagination. See C. B. Translation.

SUBSCRIPTIONS CAN BE ACCEPTED FOR 1959

for a new journal of the Academy of Sciences USSR

"HIGH POLYMERS"

The journal "High Polymers" is the leading organ of the Academy of Sciences USSR in the field of physics and chemistry of polymers and monomers. It will be concerned with general questions of polymer theory, important in the development of production, conversion, and applications of polymer materials.

The journal will publish original theoretical researches and results of experimental work on high polymers, performed in the institutes and laboratories of the Academy of Sciences USSR, higher educational establishments, and industrial undertakings of our country. Both Soviet and foreign scientists are being invited to participate in the work of the journal.

The journal "High Polymers" is intended for scientific workers, research students, academic staffs, and workers in the scientific research institutes, laboratories, and industrial undertakings.

The annual subscription for 12 issues is 150 rubles.

The price of a single issue is 12 r. 50 k.

Subscriptions are accepted in city sections of "Soiuzpechat'," communications offices and departments, subscription offices, and by authorized agents in factories and plants, in scientific research institutes, teaching establishments, institutions and organizations.

Subscriptions are also accepted at the sections and stores of "Akademkniga" and by the "Akademkniga" office at:

Moscow, K-12, ul. Kuibysheva 8
"Akademkniga"

1760

SCIENTIST - TRANSLATORS WANTED

For over a decade, Consultants Bureau, Inc. has provided Western scientists with high quality cover-to-cover translations of Soviet scientific journals. Our unique contracts with the Soviet government are constantly revised to include more extensive coverage of technical activity in the USSR. In order to produce these journals at the high standards set down by both the Soviet and American governments, it is of prime importance to maintain a large staff of scientist-translators who can translate with precision in their specific scientific field. It is our strict policy to assign a translator only that material which is within his scope.

As part of our current and future* expansion programs, we have openings for a limited number of scientist-translators who can translate in the fields covered by the following journals:

Journal of General Chemistry

Antibiotics
Biochemistry
Bulletin of Experimental Biology and Medicine
Entomological Review
Microbiology
Pharmacology and Toxicology
Plant Physiology

Automation and Remote Control
Industrial Laboratory
Instruments and Experimental Techniques
Measurement Techniques

Czechoslovak Journal of Physics
Soviet Journal of Atomic Energy
Soviet Physics - Acoustics
Soviet Physics - Crystallography
Soviet Physics - Technical Physics

Our basic requirements are that the scientist-translator have a native command of English, a minimum degree of B.S. in his specific field, and a thorough knowledge of the contemporary technical terminology of his scientific discipline.

Translation may be done at home on a full or part-time basis.

For further information, please contact:

Translation Editor
CONSULTANTS BUREAU, INC.
227 West 17th Street
New York 11, New York

*We expect, in the near future, to initiate a program of translation from the growing amount of important Chinese scientific literature available. In preparation, we are accepting applications from Chinese to English translators.

the latest Soviet Research on...

- animal biochemistry
- antibiotics
- biophysics
- immunology
- industrial hygiene
- morphology
- oncology
- pathology
- pharmacology
- physiology
- plant biochemistry
- toxicology

NOW AVAILABLE ON SUBSCRIPTION

reports written by leading Soviet authorities . . .

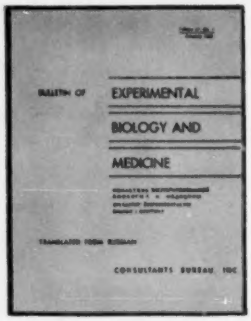

BULLETIN OF EXPERIMENTAL BIOLOGY AND MEDICINE (Byulleten' Eksperimental'noi Biologii i Meditsiny)

Important journal that features research reports, written by leading Soviet authorities, on *physiology, pathology, immunology, biophysics, pharmacology, oncology, morphology* and related fields. Translation is by special arrangement with the National Institutes of Health.

ANNUAL SUBSCRIPTION: 12 issues, $20.00
BACK ISSUES: 1956-1958 (12 issues per year) $20.00 per year

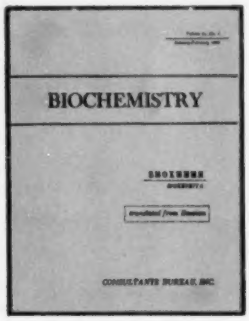

BIOCHEMISTRY (Biokhimiya)

The most comprehensive Soviet journal in this field. Each issue contains more than twenty articles on plant and animal biochemistry. Translation is by special arrangement with the National Institutes of Health.

ANNUAL SUBSCRIPTION: 6 issues, $20.00
BACK ISSUES: 1956-1958 (6 issues per year) $20.00 per year

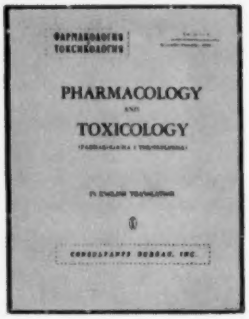

PHARMACOLOGY AND TOXICOLOGY (Farmakologiya i Toksikologiya)

This journal contains reports of the latest Soviet research on physiological effects of drugs, industrial hygiene, and related chemico-pharmacological-toxicological fields. The translation is published by special arrangement with the American pharmaceutical industry.

ANNUAL SUBSCRIPTION: 6 issues, $25.00
BACK ISSUES: 1957-1958 (6 issues per year) $25.00 per year

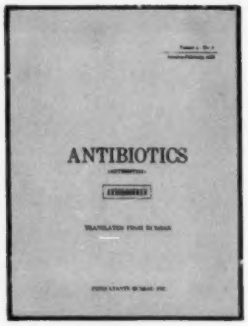

ANTIBIOTICS (Antibiotiki)

This outstanding new publication surveys the entire field with timely research reports by leading Soviet scientists. It is translated and published with the financial assistance of some leading U. S. companies.

ANNUAL SUBSCRIPTION: 6 issues, $25.00

(Add $5.00 for foreign mailings of current subscriptions)

COVER TO COVER TRANSLATIONS

c/b
CONSULTANTS BUREAU, INC.
227 WEST 17TH STREET, NEW YORK 11, N. Y.